

Box 29.2 COSMOLOGICAL REDSHIFT OF THE PRIMORDIAL RADIATION

As an important application of the redshift formula

$$\lambda/a = \text{constant} \quad (1)$$

[equation (29.10)], consider the radiation emerging from the hot big bang. Because it is initially in thermal equilibrium with matter, this primordial radiation initially has a Planck black-body spectrum. Subsequent interactions with matter cannot change the spectrum, because the matter remains in thermal equilibrium with the radiation so long as interactions are occurring. The cosmological redshift can and does change the spectrum, however. It was shown in exercise 22.17, using kinetic theory, that radiation with a Planck spectrum as viewed by one observer has a Planck spectrum as viewed by all observers; but the observed temperature is redshifted in precisely the same manner as the frequency of an individual photon is redshifted. Consequently, as seen by observers at rest

in the “fluid,” the temperature of the primordial radiation is redshifted

$$T \propto 1/a. \quad (2)$$

This is true after plasma recombination, when the radiation and matter are decoupled, as well as before recombination, when they are interacting. And it is true not only for the primordial photons but also for thermalized neutrinos and gravitons emerging from the hot big bang.

There is another way to derive the redshift equation (2). Combine the equation

$$\rho_r \propto T^4 \quad (3)$$

for the energy density of black-body radiation in terms of temperature, with the equation

$$\rho_r \propto (\text{volume})^{-4/3} \propto (a^3)^{-4/3} \propto a^{-4} \quad (4)$$

for the decrease of energy density with adiabatic expansion.

Box 29.3 USE OF REDSHIFT TO CHARACTERIZE DISTANCES AND TIME

Distance: When discussing objects within the Earth’s cluster of galaxies, astronomers typically describe distances in units of lightyears or parsecs. But when dealing with more distant objects (galaxies, quasars, etc.), astronomers find it more convenient to describe distance in terms of what is actually observed: redshift. For example, the statement “the galaxy 3C 295 is at a redshift of 0.4614” means that “3C 295 is at that distance from Earth [given by equation (29.16)] which corresponds to a redshift of $z = 0.4614$.“

Time: When discussing events that occurred during the last few 10^9 years, astronomers usually measure time in units of years. Example: “The solar system condensed out of interstellar gas 4.6×10^9 years ago” [see Wasserburg and Burnett (1968)]. But when dealing with events much nearer the beginning of the universe, all of which have

essentially the same age, of about 12×10^9 years, astronomers find it more convenient to describe time in terms of redshift. Example: “The primordial plasma recombined at a redshift of 1,000” means that “If a photon had been emitted at the time of plasma recombination, and had propagated freely ever since, it would have experienced a total redshift between then and now of $z = 1,000$.” Equivalently, since $1 + z = (a_0/a)$ [see equation (29.11)], “the plasma recombined when the universe was a factor of $1 + z \approx 1,000$ smaller than it is today.” [Application: In Figure 28.1, where the past evolution of the universe is summarized, one can freely replace the horizontal scale a/a_0 by $1/(1+z)$, and thereby see that primordial element formation occurred at a redshift of $z \approx 10^9$.) The conversion from redshift units to time units is strongly dependent on the parameters ρ_{mo} , ρ_{ro} , and k/a_0^2 [see §§27.10 and 27.11; also equation (29.15)].

of photons with 4-momenta \mathbf{p} . From the geodesic equation (or, for the reader who has studied chapter 25, from arguments about Killing vectors), show that

$$p_\chi \equiv \mathbf{p} \cdot (\partial/\partial\chi)$$

is conserved along the photon's world line. Use this fact, the fact that a photon's 4-momentum is null, $\mathbf{p} \cdot \mathbf{p} = 0$, and the equation $E = -\mathbf{p} \cdot \mathbf{u}$ for the energy measured by an observer with 4-velocity \mathbf{u} , to derive the redshift equation (29.11).

Exercise 29.3. REDSHIFT OF PARTICLE DE BROGLIE WAVELENGTHS

A particle of finite rest mass μ moves along a geodesic world line through the expanding cosmological fluid. Let

$$p \equiv (\mathbf{p} \cdot \mathbf{p})^{1/2} \equiv \frac{\mu v}{(1 - v^2)^{1/2}}$$

be the spatial 4-momentum of the particle as measured by observers at rest in the fluid. (The ordinary velocity they measure in their proper reference frames is v .) The associated "de Broglie wavelength" of the particle is $\lambda \equiv h/p$.

(a) Show that this de Broglie wavelength is redshifted in precisely the same manner as a photon wavelength:

$$\lambda/a = \text{constant.}$$

(b) Employing this result, show that, for the molecules of an ideal gas that fills the universe, their mean kinetic energy decreases in inverse proportion to a^2 when the gas is nonrelativistic and (like photon energies) in inverse proportion to a when the gas is highly relativistic.

§29.3. THE DISTANCE-REDSHIFT RELATION; MEASUREMENT OF THE HUBBLE CONSTANT

Equation (29.11) expresses the redshift in terms of the change in expansion factor between the event of emission and the event of reception. For "nearby" emitters (emitters at distances much less than $1/H_0$, the "Hubble length") it is more convenient to express the redshift in terms of the distance between the emitter and Earth. That distance ("present distance") is defined on the hypersurface of homogeneity that passes through Earth today, since that hypersurface agrees locally with the surface of simultaneity of the receiver today, and it is also, locally, a surface of simultaneity for any observer moving today with the "cosmological fluid."

Derivation of distance-redshift relation

The distance between emitter and observer today [the distance along the spatial geodesic of constant (t, θ, ϕ) connecting $(t_r, 0, \theta_e, \phi_e)$ and $(t_r, \chi_e, \theta_e, \phi_e)$] can be read directly from the line element (29.4):

$$\ell = a(t_r)(\chi_e - \chi_r) = a(t_r)\chi_e. \quad (29.12)$$

Using expression (29.9) for χ_e , one finds

$$\ell = a(t_r) \int_{t_e}^{t_r} a^{-1} dt. \quad (29.12')$$

In the recent past, $a(t)$ was given by

$$\begin{aligned} a(t) &= a(t_r) + (a_{,t})_{t_r}(t - t_r) + \frac{1}{2}(a_{,tt})_{t_r}(t - t_r)^2 + \dots \\ &= a(t_r)[1 + H_o(t - t_r) - \frac{1}{2}q_o H_o^2(t - t_r)^2 + \dots], \end{aligned} \quad (29.13)$$

where definitions (29.1) for the Hubble constant H_o and the deceleration parameter q_o have been used. Putting this expression into equation (29.12') and integrating, one finds for the distance the expression

$$\ell = (t_r - t_e) + \frac{1}{2}H_o(t_r - t_e)^2 + \dots$$

or, equivalently,

$$t_r - t_e = \ell - \frac{1}{2}H_o\ell^2 + \dots \quad (29.14)$$

The redshift [equation (29.11)] can be expressed as a power series in $t_r - t_e$ by using equation (29.13):

$$\begin{aligned} z &= \frac{a(t_r) - a(t_e)}{a(t_e)} = \frac{a(t_r)[H_o(t_r - t_e) + \frac{1}{2}q_o H_o^2(t_r - t_e)^2 + \dots]}{a(t_r)[1 - H_o(t_r - t_e) + \dots]} \\ &= H_o(t_r - t_e) + H_o^2\left(1 + \frac{1}{2}q_o\right)(t_r - t_e)^2 + \dots \end{aligned} \quad (29.15)$$

Combining this with equation (29.14) for $t_r - t_e$ in terms of ℓ , one finally obtains

$$z = H_o\ell + \frac{1}{2}(1 + q_o)(H_o\ell)^2 + O([H_o\ell]^3). \quad (29.16) \quad \text{Result for distance-redshift relation}$$

This is the “*distance-redshift relation*” for the standard big-bang model of the universe.

By comparing this distance-redshift relation with astronomical observations (see Box 29.4, which is best read after the next section), Allan Sandage (1972a) obtains a Hubble constant of

$$= 55 \pm 7 \text{ km sec}^{-1} \text{ Mpc}^{-1}; \quad (29.17)$$

i.e.,

$$H_o^{-1} = (18 \pm 2) \times 10^9 \text{ years}. \quad (29.18)$$

(Note: 1 Mpc \equiv one Megaparsec is 3.26×10^6 light years, or 3.08×10^{24} cm.) The uncertainty of $\pm 7 \text{ km sec}^{-1} \text{ Mpc}^{-1}$ quoted here is the “one-sigma” statistical uncertainty associated with the distance-redshift data. Systematic errors, not now understood, might be somewhat larger; but the true value of H_o almost certainly is within a factor 2 of Sandage’s value, $55 \text{ km sec}^{-1} \text{ Mpc}^{-1}$.

Measurement of Hubble constant H_o

Note that, if $\Lambda = 0$, then the “critical density” marking the dividing line between a “closed” universe and an “open” universe—i.e., between eventual recontraction and expansion forever—is

Value of critical density

$$\rho_{\text{crit}} = \frac{3}{8\pi} H_0^2 = 5 \times 10^{-30} \text{ g/cm}^3. \quad (29.19)$$

(As described in Box 29.1, $\rho > \rho_{\text{crit}} \iff$ “closed” \iff recontraction; $\rho < \rho_{\text{crit}} \iff$ “open” \iff expansion forever.) Comparison with the actual density will be delayed until §29.6.

The distance measurements are not accurate enough to yield useful information about the deceleration parameter, q_0 .

§29.4. THE MAGNITUDE-REDSHIFT RELATION; MEASUREMENT OF THE DECELERATION PARAMETER

Apparent magnitude defined

Information about q_0 is best obtained by comparing the apparent magnitudes of galaxies with their redshifts.

In astronomy one defines the apparent (bolometric) magnitude, m , of an object by the formula

$$\begin{aligned} m &= -2.5 \log_{10}(S/2.52 \times 10^{-5} \text{ erg cm}^{-2} \text{ sec}^{-1}) \\ &= -2.5 \log_{10} S + \text{constant}, \end{aligned} \quad (29.20)$$

Derivation of
magnitude-redshift relation

where S is the flux of energy (energy per unit time per unit area) that arrives at Earth from the object. [Of course, one cannot measure the flux over the entire wavelength range $0 < \lambda < \infty$; so one distinguishes various apparent magnitudes (m_U, m_B, m_V, \dots) corresponding to fluxes in various wavelength ranges (“U” \equiv “ultraviolet”; “B” \equiv “blue”; “V” \equiv “visual”). However, these subtleties are too far from gravitation physics to be treated here.]

Calculate the apparent magnitude for a galaxy of intrinsic luminosity L and redshift z . To simplify the calculation, put the emitter at the origin of the space coordinates ($\chi_e = 0$); and put the Earth at $(\chi_r, \theta_r, \phi_r)$. (Note the reversal of locations compared to redshift calculation of §29.2.) On Earth, place a photographic plate of area A perpendicular to the incoming light. Then at time t_r the plate is a tiny segment of a spherical two-dimensional surface ($t = t_r, \chi = \chi_r; \theta$ and ϕ vary) about the emitting galaxy. The total area of the 2-sphere surrounding the galaxy is

$$\mathcal{A} = 4\pi[a(t_r)\Sigma(\chi_r)]^2. \quad (29.21)$$

Therefore, the ratio of the area of the plate to the area of the 2-sphere is given by

$$\frac{A}{\mathcal{A}} = \frac{A}{4\pi[a(t_r)\Sigma(\chi_r)]^2}. \quad (29.22)$$

The plate catches a fraction A/\mathcal{A} of the energy that pours out through the 2-sphere.

If there were no redshift, the power crossing the entire 2-sphere at time t_r would be precisely the luminosity of the emitter at time t_e . However, the redshift modifies this result in two ways. (1) The energy of each photon that crosses the 2-sphere is smaller, as measured in the local Lorentz frame of the fluid there, than it was as measured by the emitter:

$$E_{\text{rec}}/E_{\text{em}} = \lambda_{\text{em}}/\lambda_{\text{rec}} = 1/(1+z). \quad (29.23)$$

(2) Two photons with the same θ and ϕ , which are separated by a time Δt_r as measured by an observer stationary with respect to the “cosmological fluid” at the 2-sphere, were separated by a shorter time Δt_e as measured by the emitter:

$$\Delta t_r/\Delta t_e = \lambda_r/\lambda_e = 1+z. \quad (29.24)$$

The luminosity, L , as measured at the source, is the sum of the energies $E_{\text{em}J}$ of the individual photons (labeled with the index J) emitted in a time interval Δt_e , divided by Δt_e :

$$L = (1/\Delta t_e) \sum_J E_{\text{em}J}. \quad (29.25)$$

The power that crosses the 2-sphere a time $t_r - t_e$ later, as measured by the fluid at the 2-sphere, is

$$P = (1/\Delta t_r) \sum_J E_{\text{rec}J}, \quad (29.26)$$

where the summation runs over the same set of photons.

Combining equations (29.23) to (29.26), one sees that the power crossing the 2-sphere is

$$P = L/(1+z)^2.$$

Of this, a fraction,

$$P_A = \frac{A}{\mathcal{A}} P = \frac{AL}{4\pi[(1+z)a(t_r)\Sigma(\chi_r)]^2},$$

crosses the photographic plate; so the flux measured at the Earth is

$$S = \frac{P_A}{A} = \frac{L}{4\pi R^2(1+z)^2}, \quad (29.27)$$

where R is the “radius of curvature” of the 2-sphere surrounding the emitter and passing through the receiver at the time of reception,

$$R \equiv a_o \Sigma(\chi_r - \chi_e) = \begin{cases} a_o \sinh(\chi_r - \chi_e) & \text{if } k = -1, \\ a_o[\chi_r - \chi_e] & \text{if } k = 0, \\ a_o \sin(\chi_r - \chi_e) & \text{if } k = +1 \end{cases} \quad (29.28)$$

[recall: χ_e is 0 according to the present conventions, and $a_o = a(t_r)$]. The corresponding apparent magnitude [equation (29.20)] is

$$m = +5 \log_{10}[(1+z)R] - 2.5 \log_{10}L + \text{constant}. \quad (29.29)$$

In order to relate the apparent magnitude to the redshift of the emitter, one must express the quantity R in terms of z . From equation (29.7) for the photon propagation (with sign reversed because positions of receiver and emitter have been reversed), one knows that

$$\chi_r - \chi_e = \int_{t_e}^{t_r} a^{-1} dt = \int_1^{a(t_r)/a(t_e)} \left[\frac{a}{a(t_r)} \right] \left[\frac{dt}{da} \right] d \left[\frac{a(t_r)}{a} \right], \quad (29.30)$$

and from equation (29.11) one knows that

$$z = a(t_r)/a(t_e) - 1.$$

Hence

$$\chi_r - \chi_e = \int_1^{1+z} \left[\frac{a}{a(t_r)} \right] \left[\frac{dt}{da} \right] d \left[\frac{a(t_r)}{a} \right]. \quad (29.31)$$

Equations (4) to (6) of Box 29.1, and (27.40), determine the function dt/da in terms of $a/a(t_r)$ and the constants H_o , q_o , σ_o . By inserting that result into equation (29.31) and integrating, one obtains $\chi_r - \chi_e$ in terms of the redshift z and the cosmological parameters H_o , q_o , σ_o :

$$\chi_r - \chi_e = |1 + q_o - 3\sigma_o|^{1/2} \int_1^{1+z} \frac{du}{[2\sigma_o u^3 + (1 + q_o - 3\sigma_o)u^2 + \sigma_o - q_o]^{1/2}}. \quad (29.32a)$$

The 2-sphere radius of curvature R is obtained by inserting this expression into the equation

$$R = \frac{H_o^{-1}}{|1 + q_o - 3\sigma_o|^{1/2}} \Sigma(\chi_r - \chi_e) \quad (29.32b)$$

[equation (29.28), with a_o evaluated by equation (5) of Box 29.1].

Equations (29.29) and (29.32) determine the apparent magnitude, m , in terms of redshift, z .

For the case of vanishing cosmological constant ($\sigma_o = q_o$; $\Lambda = 0$), the integral (29.32a) can be expressed in terms of elementary functions, yielding

$$\begin{aligned} R &= \frac{H_o^{-1}}{q_o^2(1+z)} [-q_o + 1 + q_o z + (q_o - 1)(2q_o z + 1)^{1/2}], \\ &\approx H_o^{-1} z \left[1 - \frac{1}{2}(1 + q_o)z + O(z^2) \right], \end{aligned} \quad (29.33)$$

so that

Result for magnitude-redshift relation

$$\begin{aligned} m &= 5 \log_{10} [1 - q_o + q_o z + (q_o - 1)(2q_o z + 1)^{1/2}] - 2.5 \log_{10} L + \text{const.} \\ &\approx 5 \log_{10} z + 1.086(1 - q_o)z + O(z^2) - 2.5 \log_{10} L + \text{const.} \end{aligned} \quad (29.34)$$

for $z \ll 1$.

(Note: the factor 1.086 is actually $2.5/\ln 10$.) A power-series solution for nonzero Λ (for $\sigma_o \neq q_o$) reveals a dependence on σ_o only at $O(z^2)$ and higher:

$$R \approx H_o^{-1}z \left[1 - \frac{1}{2}(1 + q_o)z + (\text{corrections of } O(z^2) \text{ depending on } \sigma_o \text{ and } q_o) \right], \quad (29.35a)$$

$$m \approx 5 \log_{10} z + 1.086(1 - q_o)z + O(z^2) - 2.5 \log_{10} L + \text{const.} \quad (29.35b)$$

Sheldon (1971) gives the exact solution for $\Lambda \neq 0$ in terms of the Weierstrass elliptic function. Refsdal *et al.* (1967) tabulate and plot the exact solution.

By comparing the theoretical magnitude-redshift relation (29.35b) with observations of the brightest galaxies in 82 clusters, Allan Sandage (1972a,c,d) obtains the following value for the deceleration parameter:

$$q_o = 1.0 \pm 0.5, \quad \text{if } \sigma_o = q_o \text{ (i.e. } \Lambda = 0\text{).} \quad (29.36)$$

(Note: 0.5 is the “one-sigma” uncertainty. Sandage estimates with 68 per cent confidence that $0.5 < q_o < 1.5$, and with 95 per cent confidence that $0 < q_o < 2$ —providing unknown evolutionary effects are negligible.) The observations leading to this result and the uncertainties due to evolutionary effects are described in Box 29.4. Box 29.5 gives a glimpse of Edwin Hubble, the man who laid the foundations for such cosmological measurements.

Measurement of deceleration parameter, q_o

(continued on page 794)

Box 29.4 MEASUREMENT OF HUBBLE CONSTANT AND DECELERATION PARAMETER

I. *Hubble Constant, H_o*

- A. *Objective:* To measure the constant H_o by comparing observational data with the distance-redshift relation

$$z = H_o \ell + \frac{1}{2}(1 + q_o)(H_o \ell)^2 + O([H_o \ell]^3).$$

Here ℓ is distance from Earth to source today; and z is redshift of source as measured at Earth.

- B. *Key Difficulty:* This distance-redshift relation does not apply to stars in our Galaxy: the Galaxy is gravitationally bound and therefore is impervious to the universal expansion. Nor does the distance-redshift relation apply to the separations between our Galaxy and nearby galaxies (the “local group”); gravitational attraction between our Galaxy and its neighbors is so great it perturbs their motions substantially away from universal expansion. Only on

Box 29.4 (continued)

scales large enough to include many galaxies (scales where each galaxy or cluster of galaxies can be thought of as a “grain of dust,” with the grains distributed roughly homogeneously)—only on such large scales should the distance-redshift relation hold with good accuracy. But it is very difficult to obtain reliable measurements of the distances ℓ to galaxies that are so far away!

- C. *Procedure by which H_o has been measured [Sandage and Tamman, as summarized in Sandage (1972a)]:*

1. Cepheid variables are pulsating stars with pulsation periods (as measured by oscillations in light output) that are very closely correlated with their luminosities L —or, equivalently, with their absolute (bolometric) magnitudes, M :

$$M \equiv \begin{cases} \text{apparent magnitude star would have were it at a} \\ \text{distance of 10 parsecs} = 32.6 \text{ light years} \end{cases} \quad (1)$$

$$= -2.5 \log_{10} (L/3.0 \times 10^{35} \text{ erg sec}^{-1})$$

[see equation (29.20).] By measurements within our Galaxy, astronomers have obtained the “period-luminosity relation” for cepheid variables.

2. Cepheid variables are clearly visible in galaxies as far away as ~ 4 Mpc (4 Megaparsecs $\equiv 4 \times 10^6$ parsecs). In each such galaxy one measures the periods of the cepheids; one then infers their absolute magnitudes M from the period-luminosity relation; one measures their apparent magnitudes m ; and one then calculates their distances ℓ from Earth using the relation

$$m - M = 5 \log_{10} (\ell/10 \text{ pc}). \quad (2)$$

By this means one obtains the distances ℓ to all galaxies within ~ 4 Mpc of our own. Unfortunately, such galaxies are too close to participate cleanly in the universal expansion. (They include only the “local group,” the “M81 group,” and the “south polar group.”) Thus, one must push the distance scale out still farther before attempting to measure H_o .

3. Galaxies of types Sc, Sd, Sm, and Ir within ~ 4 Mpc contain huge clouds of ionized hydrogen, which shine brightly in “H α light.” These clouds, called “H II regions,” exhibit a very tight correlation between diameter D of the H II region and luminosity L of the galaxy (or, equivalently, between D and absolute magnitude of galaxy, M). In fact, for a given galaxy luminosity L , the fractional spread in H II diameters is $\sigma(\Delta D/D) \approx 0.12$. Using (a) the distances (≤ 4 Mpc) to these galaxies as determined via cepheid variables, (b) the apparent magnitudes of the galaxies, and (c) the angular diameters of H II regions in the galaxies, one calculates

the actual H II diameters D and galaxy luminosities L , and thereby obtains the “diameter-luminosity relation” $D(L)$.

4. H II regions are large enough to be seen clearly in galaxies as far away as ~ 60 Mpc. By measuring the H II angular diameters $\alpha = D/\ell$ and galaxy apparent (bolometric) magnitudes

$$m = -2.5 \log_{10} \left(\frac{L/4\pi\ell^2}{2.52 \times 10^{-5} \text{ erg cm}^{-2} \text{ sec}^{-1}} \right), \quad (3)$$

and by combining with the diameter-luminosity relation, one obtains the distances ℓ to all galaxies of types Sc, Sd, Sm, and Ir which possess H II regions and lie within ~ 60 Mpc of Earth. Unfortunately, this is *still* not far enough away for local motions to be negligible compared with the universal expansion.

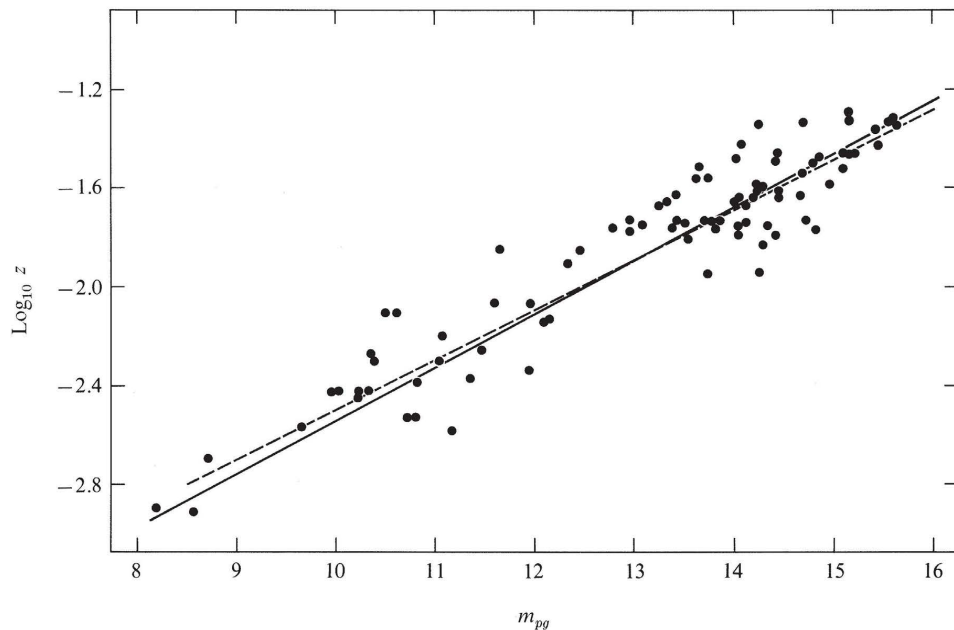
5. Within ~ 60 Mpc reside enough galaxies of type Sc I for one to discover that their luminosities (absolute magnitudes) are rather constant (difference in L from one Sc I galaxy to another $\lesssim 50$ per cent). Using the distances to such Sc I galaxies, as measured via H II regions, and using measurements of their apparent magnitudes, one calculates their universal absolute magnitude (measured photographically) to be $M_{pg} = -21.2$.



The Sc I galaxy M101 at a distance $\ell \sim 3$ Mpc from Earth, as photographed with the 200-inch telescope. (Courtesy of Hale Observatories)

Box 29.4 (continued)

6. One then examines all known Sc I galaxies with distances greater than ~ 70 Mpc. For each, one measures the apparent magnitude and compares it with the universal absolute magnitude to obtain the distance ℓ from Earth. And for each, one measures the redshift $z = \Delta\lambda/\lambda$ of the spectral lines. From the resulting redshift-distance relation—and taking into account the statistical uncertainties in all steps leading up to it—Sandage and Tamman (work carried out in 1965–1972) obtain the value $H_o = dz/d\ell = 55 \pm 7$ (km/sec) Mpc $^{-1} = 1/[(18 \pm 2) \times 10^9$ years]. [For a review see Sandage (1972a).] The quoted error is purely statistical. Systematic errors are surely larger—but they almost surely do not exceed a factor 2 [i.e., $30 < H_o < 110$ (km/sec) Mpc $^{-1}$].



Magnitude-redshift relation for Sc I galaxies at distances $\gtrsim 70$ Mpc. Solid line is a least-squares fit to the data; dotted line has the theoretical slope of 5. [From Sandage and Tamman.]

II. Deceleration Parameter, q_o .

- A. *Objective:* To measure the constant q_o by comparing observational data with the magnitude-redshift relation:

$$m = 5 \log_{10} z + 1.086(1 - q_o)z + O(z^2) - 2.5 \log_{10} L + \text{const.} \quad (4)$$

[Note: This relation is valid even if the cosmological constant is nonzero, i.e., even if $\sigma_o \neq q_o$. Dependence on σ_o occurs only at $O(z^2)$ and higher.]

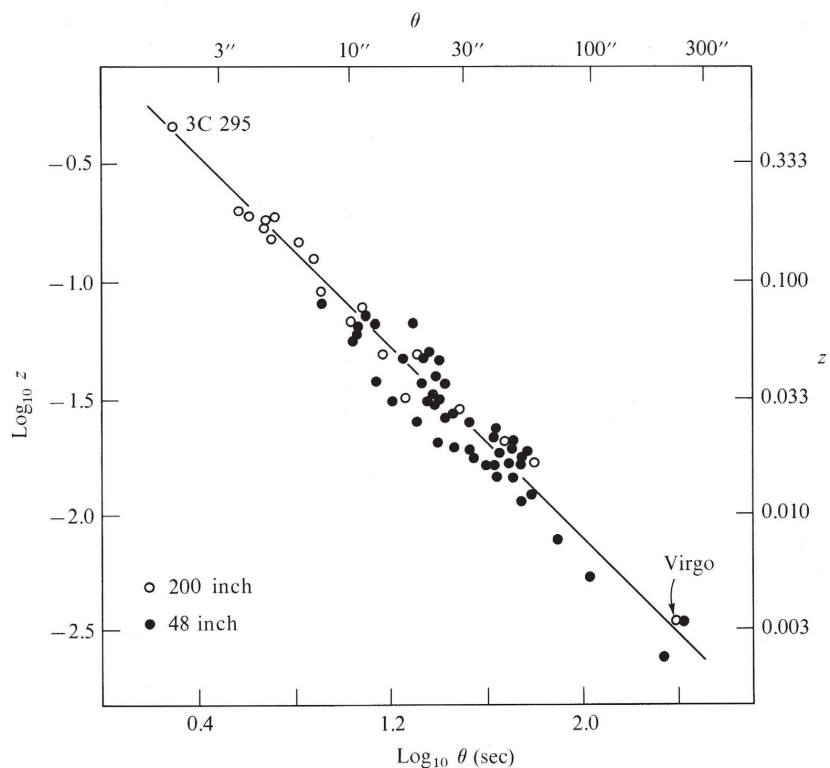
- B. *Key Difficulty:* One must use data for objects with the same absolute luminosity L (“standard candles”). But one cannot measure L at distances great enough for the effects of q_o to show up.
- C. *The Search for a Standard Candle:* One obvious choice for the standard candle would be Sc I galaxies, since they were found to all have nearly the same L (see above). But they are not bright enough to be seen at distances great enough for effects of q_o to show up. An alternative choice, quasars, are bright enough to be seen at very large redshifts (z as large as ~ 3). But their absolute luminosities have enormous scatter—or so one infers from the failure of quasars to fall on a straight line, even at small z , in the magnitude-redshift diagram. The best choice is the brightest type of object that has small scatter in L . Sandage (1972a,b,c) chooses the brightest galaxy in “recognized regular clusters of galaxies.” Such clusters are composed predominately of E-type galaxies, and the brightest members are remarkably similar from one cluster



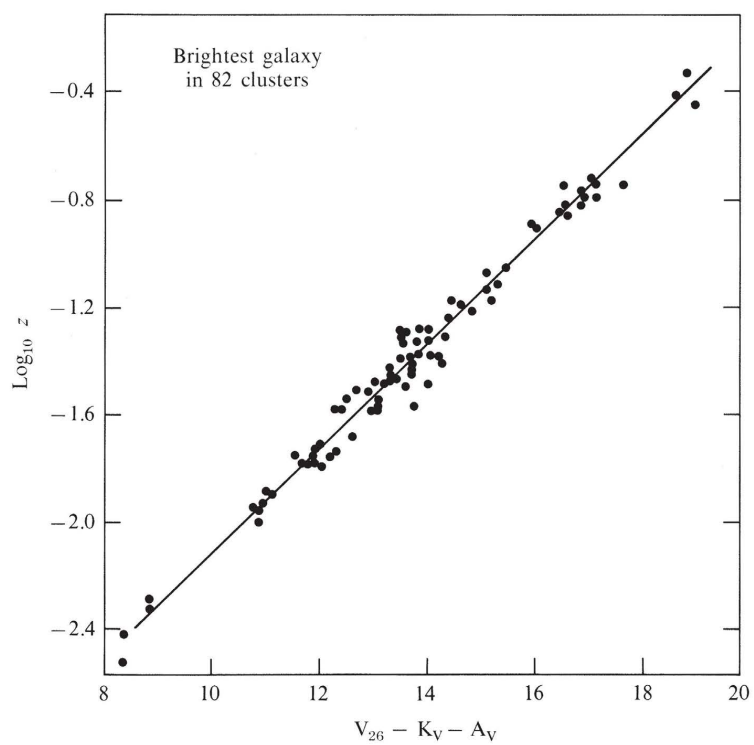
The E-type galaxy M87 at a distance $\ell \sim 11$ Mpc from Earth, as photographed with the 200-inch telescope. (Courtesy of Hale Observatories)

to another (scatter in L is ~ 25 per cent). The similarity shows up in their spectra and in the very precise straight lines they give when one plots angular diameter versus redshift (next page), or apparent magnitude versus redshift (next page), or angular diameter versus apparent magnitude.

Box 29.4 (continued)



Angular diameter versus redshift for brightest galaxy in recognized regular clusters. From Sandage (1972a,b). [These data are not sufficiently precise to yield useful information about q_o and σ_o ; but improvements in 1973 may bring the needed precision; see §29.5.]



Magnitude versus redshift for brightest galaxy in recognized regular clusters. $V_{26} - K_V - A_V$ is the apparent magnitude with certain corrections taken into account. The line plotted corresponds to $\sigma_o = q_o = 1$ (straight line of slope 5). From Sandage (1972a).

D. *Procedure by which q_0 has been measured [Sandage (1972a,c)]:*

1. Data on magnitude versus redshift have been gathered for the brightest galaxy in 82 recognized regular clusters (see above).
2. The data, when fitted with a straight line, show a slope of

$$dm/d \log_{10} z = 5.150 \pm 0.268 \text{ (rms)}, \quad (5)$$

by comparison with a theoretical slope of 5.

3. The data, when fitted to the theoretical relation

$$m = 5 \log_{10} z + 1.086(1 - q_0)z + O(z^2) + \text{const}, \quad (6)$$

[with the correct $O(z^2)$ and higher terms included; see equations (29.29), (29.32), and (29.34)] yield

$$\left. \begin{aligned} q_0 &= 1 \pm 0.5 \text{ (one-sigma)} \\ &= 1 \pm 1 \text{ (two-sigma)} \end{aligned} \right\} \text{ if } \sigma_0 = q_0(\Lambda = 0). \quad (7)$$

The data are inadequate to determine σ_0 and q_0 simultaneously. [The $O(z^2)$ terms, which depend on σ_0 , play a significant role in the fit to the data. For a graphical depiction of their theoretical effects see Figure 2 of Refsdal *et. al* (1967).]

E. *Evolutionary uncertainties*

1. Sandage's fit of data to theory assumes that the luminosities of his "standard candles" are constant in time. If, because of evolution of old stars and formation of new ones, his galaxies were to dim by 0.09 magnitudes per 10^9 years, then galaxies 10^9 light-years away, which one sees as they were 10^9 years ago, would be 0.09 magnitudes brighter intrinsically than identical nearby galaxies. Correction for this effect would lower the most probable value of q_0 from 1 to 0 [Sandage (1972c)].
2. Knowledge of the evolution of galaxies in 1972 is too rudimentary to confirm or rule out such an effect. [See references cited by Sandage (1972c).]

Box 29.5 EDWIN POWELL HUBBLE
November 20, 1889, Marshfield Missouri—
September 28, 1953, Pasadena, California



Edwin Hubble, at age 24, earned a law degree from Oxford University and began practicing law in Louisville, Kentucky. After a year of practice he became fed up and, in his own words, "chucked the law for astronomy, and I knew that even if I were second-rate or third-rate it was astronomy that mattered." He chose the University of Chicago and Yerkes Observatory as the site for his

astronomy education, and three years later (1917) completed a Ph.D. thesis on "Photographic Investigations of Faint Nebulae."

When Hubble entered astronomy, it was suspected that some nebulae lie outside the Galaxy, but the evidence was exceedingly weak. During the subsequent two decades, Hubble, more than anyone else, was responsible for opening to man's purview the extragalactic universe. Working with the 60-inch and 100-inch telescopes at Mount Wilson, Hubble developed irrefutable evidence of the extragalactic nature of spiral nebulae, elliptical nebulae, and irregular nebulae (now called galaxies). He devised the classification scheme for galaxies which is still in use today. He systematized the entire subject of extragalactic research: determining distance scales, luminosities, star densities, and the peculiar motion of our Galaxy; and obtaining extensive evidence that the laws of physics outside the Galaxy are the same as near Earth (in Hubble's words: "verifying the principle of the uniformity of nature"). He discovered and quantified the large-scale homogeneity of the universe. And—his greatest triumph of all!—he discovered the expansion of the universe.

The details of Hubble's pioneering work are best sketched in his own words:

"Extremely little is known of the nature of nebulae; and no classification has yet been suggested. . . . The agreement [between the velocity of escape from a spiral nebula and that from our galaxy] is such as to lend some color to the hypothesis that the spirals are stellar systems at distances to be measured often in millions of light years."

(1920; Ph.D. THESIS; PUBLICATION DELAYED 3 YEARS BY WORLD WAR I)

This box is based largely on the biography of Hubble by Mayall (1970).

"The present investigation [using Cepheid variables for the first time as an indicator of distances beyond the Magellanic clouds] identifies NGC 6822 as an isolated system of stars and nebulae of the same type as the Magellanic clouds, although somewhat smaller and much more distant. A consistent structure is thus reared on the foundation of the Cepheid criterion, in which the dimensions, luminosities, and densities, both of the system [NGC 6822] as a whole and its separate members, are of orders of magnitude which are thoroughly familiar. The distance is the only quantity of a new order. The principle of the uniformity of nature thus seems to rule undisturbed in this remote region of space."

(1925)

"Critical tests made with the 100-inch reflector, the highest resolving power available, show no difference between the photographic images of the so-called condensations in Messier 33 and the images of ordinary galactic stars. . . . The period-luminosity relation is conspicuous among the thirty-five Cepheids and indicates a distance about 8.1 times that of the Small Magellanic Cloud. Using Shapley's value for the latter, the distance of the spiral is about 263,000 parsecs."

(1926a)

"[To the present paper (1926b)] is prefaced a general classification of nebulae . . . the various types [of extragalactic nebulae] are homogeneously distributed over the sky. . . . The data are now available for deriving a value for the order of the density of space. This is accomplished by means of the formulae for the numbers of nebulae to a given limiting magnitude and for the distance in terms of the magnitude. [The result is]

$$\rho = 1.5 \times 10^{-31} \text{ grams per cubic centimeter.}$$

This must be considered as a lower limit, for loose material scattered between the systems is entirely ignored. The mean density of space can be used to determine the dimensions of the finite but boundless universe of general relativity . . .

$$R = \frac{c}{\sqrt{4\pi k}} \frac{1}{\sqrt{\rho}} = \dots = 2.7 \times 10^{10} \text{ parsecs.}"$$

(1926b)

"The data . . . indicate a linear correlation between distances and velocities [for extragalactic nebulae]. Two solutions have been made, one using the 24 nebulae individually, the other combining them into 9 groups according the proximity in direction and distance. The results are . . . 24 objects: $K = 465 \pm 50$ km/sec per 10^6 parsecs; 9 groups: $K = 513 \pm 60$ km/sec per 10^6 parsecs. . . . The outstanding feature, however, is the possibility that the velocity-distance relation may represent the de Sitter effect, and hence that numerical data may be introduced into discussions of the general curvature of space."

(1929)*

*Hubble's value of K (the "Hubble constant") was later revised downward by the work of Baade and Sandage; see section titled *The Hubble Time* in Box 27.1.

Box 29.5 (continued)

"The velocity-distance relation is re-examined with the aid of 40 new velocities. . . . The new data extend out to about eighteen times the distance available in the first formulation of the velocity-distance relation, but the form of the relation remains unchanged except for [Shapley's 10 per cent] revision of the unit of distance."

(1931), WITH M. L. HUMASON

"Many ways of producing such effects [redshifts in extragalactic nebulae] are known, but of them all, only one will produce large redshifts without introducing other effects which should be conspicuous but actually are not found. This one known permissible explanation interprets redshifts as due to actual motion away from the observer."

(1934a)

"We now have a hasty sketch of some of the general features of the observable region as a unit. The next step will be to follow the reconnaissance with a survey—to repeat carefully the explorations with an eye to accuracy and completeness. The program, with its emphasis on methods, will be a tedious series of successive approximations."

(1934b)

Most of the remainder of Hubble's career was dedicated to this "tedious series of successive approximations." Shortly before Hubble's death the 200-inch telescope went into operation at Palomar

Mountain; and Hubble's student, Alan Sandage, began using it in a continuation of Hubble's quest into the true nature of the universe. (See Box 29.4).

EXERCISES**Exercise 29.4. $m(z)$ DERIVED USING STATISTICAL PHYSICS**

Derive the magnitude-redshift relation using a statistical description of the photon distribution [cf. eq. (22.49) and associated discussion].

Exercise 29.5. DOPPLER SHIFT VERSUS COSMOLOGICAL REDSHIFT

(a) Consider, in flat spacetime, a galaxy moving away from the Earth with velocity v , and emitting light that is received at Earth. Let the distance between Earth and galaxy, as measured in the Earth's Lorentz frame at some specific moment of emission, be r ; and let the Doppler shift of the radiation when it is eventually received be $z = \Delta\lambda/\lambda$. Show that the flux of energy S received at the Earth is related to the galaxy's intrinsic luminosity L by

$$S = \frac{L}{4\pi r^2(1+z)^4}. \quad (29.37)$$

[Track-2 readers will find it most convenient to use the statistical formalism of equation (22.49).]

(b) Compare this formula for the flux with formula (29.27), where the redshift is of cosmological origin. Why is the number of factors of $1+z$ different for the two formulas? [Mathematical answer: equation (6.28a) of Ellis (1971).]

§29.5. SEARCH FOR "LENS EFFECT" OF THE UNIVERSE

Curved space should act as a lens of great focal length. The curving of light rays has little effect on the apparent size of nearby objects. However, distant galaxies—galaxies from a quarter of the way up to halfway around the universe—are expected to have greatly magnified angular diameters [Klauder, Wakano, Wheeler, and Willey (1959)]. To see a normal galaxy at such a distance by means of an optical telescope seems out of the question. However, radio telescopes resolve features in quasistellar sources and other radiogalaxies at redshifts of $z = 2$ or more. Moreover, paired radio telescopes at intercontinental distances (for example, Goldstone, California, and Woomera, Australia) resolve distant sources to better than $0''.001$ or 4.8×10^{-9} radians or 15 lightyears for an object at a distance of 3×10^9 lightyears (Euclidean geometry temporarily being assumed). A radio telescope in space paired with a radio telescope on earth will be able to do even better on angular resolution. Will one be able to find any fiducial distance characteristic of any one class of objects that will serve as a natural standard of length, for very great distances ($z = 2$ to $z = 3$) as well as for galaxies closer at hand? Perhaps not. However, it would seem unwise to discount this possibility, with all the advantages it would bring, in view of the demonstrated ability of skilled observers to find regularities elsewhere where one had no right to expect them in advance.

Let L denote the actual length of a fiducial element (if any be found) in a galaxy; and let $\delta\theta$ (radians!) denote the apparent length of the object, idealized as perpendicular to the line of sight, as seen by the observer. The ratio of these two quantities defines the "angle effective distance" of the source,

$$(\text{angle effective distance}) = r_{\text{aed}} = L/\delta\theta. \quad (29.38a)$$

In flat space and for objects with zero relative velocity, this distance is to be identified with the actual distance, r , to the source or with the actual time of flight, t , of light from source to observer. The situation is changed in an expanding universe.

To calculate the angle effective distance as a function of redshift, place the Earth (receiver) at $\chi_r = 0$; and place the object under study (emitter) at χ_e . Let the fiducial length L lie on the sphere at χ_e (perpendicular to line of sight), and let it run from θ_e to $\theta_e + \delta\theta$ [one end of fiducial element at $(\chi_e, \theta_e, \phi_e)$; other at $(\chi_e, \theta_e + \delta\theta, \phi_e)$]. Then

$$L = a(t_e)\Sigma(\chi_e)\delta\theta,$$

and

$$r_{\text{aed}} = a(t_e)\Sigma(\chi_e) = [a(t_r)\Sigma(\chi_e - \chi_r)]a(t_e)/a(t_r);$$

i.e. [see equation (29.28), with χ_r and χ_e reversed],

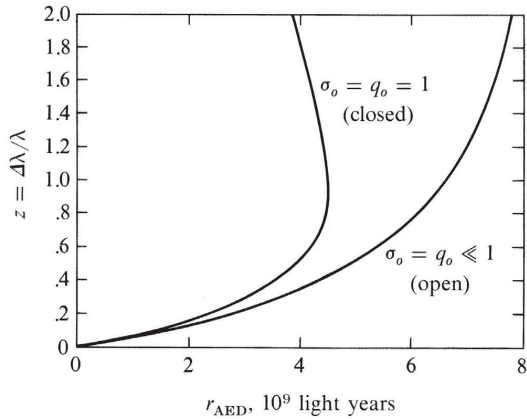
$$r_{\text{aed}} = R/(1 + z). \quad (29.38b)$$

Here R is given as a function of redshift of source, z , and cosmological parameters H_o, q_o, σ_o , by equations (29.32) in general, or by (29.33) if $A = 0$. [Equation (29.38b) is modified if the beam preferentially traverses regions of low mass density ("vacuum between the galaxies"); see equation (22.37) and Gunn (1967).]

The hope for a fiducial length
in distant objects

Angle effective distance
defined

Angle effective distance as
function of redshift

**Figure 29.2.**

Angle effective distance versus redshift for two typical cosmological models—one open ($0 < \sigma_0 = q_0 \ll 1$); the other closed ($\sigma_0 = q_0 = 1$); both with zero cosmological constant; both with $H_0^{-1} = 18 \times 10^9$ lyr.

Angle effective distance as a tool for determining whether universe is closed

Figure 29.2 shows angle effective distance as a function of redshift for a few selected choices of the relevant parameters. It is evident that the angle effective distance has a maximum for a redshift roughly of the order $z \sim 1$, provided that the universe is closed. However, there is a big difference if the universe is open (Figure 29.2). The rapid improvements taking place in radio astronomy make increasingly attractive the possibility it provides for testing whether the universe is closed, as Einstein argued it should be [Einstein (1950), pp. 107–108]. Moreover, even with optical telescopes, in 1973 one may be on the verge of measuring q_0 by studies of angle effective distance: preliminary studies [Sandage (1972b)] suggest that the optical size of the brightest E-type galaxies may be a usable fiducial length.

§29.6. DENSITY OF THE UNIVERSE TODAY

Measurements of mean mass density of universe:

- (1) luminous matter in galaxies

It is exceedingly difficult to measure the mean density ρ_{mo} of the universe today. A large amount of matter may be in forms that astronomers have not yet managed to observe (intergalactic matter, black holes, etc.). Therefore, the best one can do is to add up all the luminous matter in galaxies and regard the resulting number as a lower limit on ρ_{mo} . Even adding up the luminous matter is a difficult and risky task, so difficult that even today no analysis is more definitive than the classic work of Oort (1958). [See, however, the very detailed review of the problem in Chapter 4 of Peebles (1971)]. Oort's result is

$$\rho_{\text{luminous matter}} \sim (2 \times 10^{-31} \text{ g/cm}^3)(H_0/55 \text{ km sec}^{-1} \text{ Mpc}^{-1})^2, \quad (29.39)$$

corresponding to

$$\sigma_0 \gtrsim 0.02 \quad (\text{independent of the value of } H_0). \quad (29.40)$$

As an example (albeit an atypical one) of the danger inherent in any such estimate, Oort points to the Virgo cluster of galaxies. If the Virgo cluster is not gravitationally bound, then its $\sim 2,500$ galaxies will go flying apart, destroying any semblance of a cluster, in about one billion years. If it is gravitationally bound, then the mean velocity of its galaxies relative to each other, when combined with the virial theorem, yields an estimate of the cluster's total mass. That estimate is 25 times larger than the value one gets by Oort's method of adding up the luminous mass of the cluster.

Although one has no *definitive* evidence for or against large amounts of matter (enough to close the universe) in intergalactic space, one has tentative indirect limits:

(1) If $\Lambda = 0$ (in accord with Einstein), then $\sigma_o = q_o$; so Sandage's value of $q_o \lesssim 1$ —stretched to $q_o < 10$ under the most wild of assumptions about galaxy evolution—implies

$$\rho_{ig} < 10^{-28} \text{ g/cm}^3 \quad (\sigma_o = q_o < 10).$$

(2) matter in intergalactic space

(2) Gott and Gunn (1971) point out that, if the density of gas in intergalactic space were $\gtrsim 10^{-30}$ g/cm³ (i.e., if σ_o were $\gtrsim 0.1$), one would expect gas falling into the Coma cluster of galaxies to form a shock wave, which would emit large amounts of X-rays. From the current X-ray observations, one can place a limit on the amount of such infalling matter—and therefrom a limit

$$\rho_{ig} \lesssim 10^{-30} \text{ g/cm}^3 \quad (\sigma_o \lesssim 0.1)$$

on the density of gas in intergalactic space. But these limits, like others obtained in other ways [see Chapter 4 of Peebles (1971) for a review] are far from definitive; they depend too much on theoretical calculations to make one feel fully comfortable.

§29.7. SUMMARY OF PRESENT KNOWLEDGE ABOUT COSMOLOGICAL PARAMETERS

The best data available in 1973 [equations (29.18), (29.36), (29.40)] reveal

$$\begin{aligned} H_o^{-1} &= (18 \pm 2) \times 10^9 \text{ years}, \\ q_o &= 1 \pm 0.5 \text{ (one-sigma)} \quad \text{if } \sigma_o = q_o (\Lambda = 0), \\ \sigma_o &\gtrsim 0.02, \end{aligned} \tag{29.41}$$

Summary of observational parameters of universe

for the observational parameters of the universe. These numbers are inadequate to reveal whether the universe is closed or open, and whether it will continue to expand forever or will eventually slow to a halt and recontract.

If one is disappointed in this lack of knowledge, one can at least be consoled by the following. (1) There is excellent agreement between theory and observation for the linear (low- z) parts of the distance-redshift, magnitude-redshift, and angular diameter-redshift relations (Box 29.4). (2) There is remarkably good agreement between (a) the age of the universe (18 billion years if $q_o = \sigma_o \ll 1$; 12 billion years if $q_o = \sigma_o = \frac{1}{2}$) as calculated from the measured value of H_o ; (b) the ages of the

Some quantitative triumphs of cosmology

The bright prospects for observational cosmology

oldest stars ($\sim 10 \times 10^9$ years) as calculated by comparing the theory of stellar evolution with the properties of the observed stars; (c) the time (~ 9 billion years) since nucleosynthesis of the uranium, thorium, and plutonium atoms that one finds on Earth, as calculated from the measured relative abundances of various nucleides; and (d) the ages (4.6 billion years) of the oldest meteorites and oldest lunar rock samples, as calculated from measured relative abundances of other nucleides. For further detail see, e.g., Sandage (1968, 1970), Wasserburg *et al.* (1969), Wasserburg and Burnett (1968), and Fowler (1972). (3) Observations of the cosmic microwave radiation and measurements of helium abundance are now capable of giving direct information about physical processes in the universe at redshifts $z \gg 1$ (Chapter 28). (4) One may yet find “fiducial lengths” in radio sources, visible out to $z \gtrsim 1$, with which to measure q_o and σ_o by the angle-effective-distance method (§29.5). (5) The enigmas of the nature of quasars and of their peculiar distribution with redshift (great congregation at $z \sim 2$; absence at $z \gtrsim 3$) may yet be cracked and may yield, in the process, much new information about the origin of structure in the universe (Box 28.1). (6) The next decade may well bring as many great observational surprises, and corresponding new insights, as has the last decade.

EXERCISES

Exercise 29.6. SOURCE COUNTS

Suppose that one could find (which one cannot) a family of light or radio sources that (1) are all identical with intrinsic luminosities L , (2) are distributed uniformly throughout the universe, and (3) are born at the same rate as they die so that the number in a unit comoving coordinate volume is forever fixed.

(a) Show that the number of such sources $N(z)$ with redshifts less than z , as observed from Earth today, would be

$$N(z) = (\text{constant}) \cdot z^3 \left[1 - \frac{3}{2}(1 + q_o)z + O(z^2) \right]. \quad (29.42)$$

(b) Show that the number of sources $N(S)$ with fluxes greater than S as observed at Earth today would be

$$N(S) = (\text{constant}) \cdot \underbrace{\left(\frac{LH_o^2}{4\pi S} \right)^{3/2}}_{\substack{\uparrow \\ = z^2 + O(z^3)}} \left[1 - 3 \left(\frac{LH_o^2}{4\pi S} \right)^{1/2} + O \left(\frac{LH_o^2}{4\pi S} \right) \right] \quad (29.43)$$

\uparrow first-order correction
 \uparrow independent of q_o and σ_o

[Answer: See §15.7 of Robertson and Noonan (1968).]

Exercise 29.7. COSMIC-RAY DENSITY (Problem devised by Maarten Schmidt)

Suppose the universe has contained the same number of galaxies indefinitely into the past. Suppose further that the cosmic rays in the universe were created in galaxies and that a negligible fraction of them have been degraded or lost since formation. Derive an expression for the average density of energy in cosmic rays in the universe today in terms of: (1) the number density of galaxies, N_o , today; and (2) the nonconstant rate, dE/dz , at which the average galaxy created cosmic-ray energy during the past history of the universe. [At redshift z in range dz , the average galaxy liberates energy $(dE/dz) dz$ into cosmic rays.]

Exercise 29.8. FRACTION OF SKY COVERED BY GALAXIES

Assume that the redshifts of quasars are cosmological. Let the number of galaxies per unit physical volume in the universe today be N_0 , and assume that no galaxies have been created or destroyed since a redshift of ≥ 7 . Let D be the average angular diameter of a galaxy. Calculate the probability that the light from a quasar at redshift z , has passed through at least one intervening galaxy during its travel to Earth. [For a detailed discussion of this problem, see Wagoner (1967).]

CHAPTER 30

ANISOTROPIC AND INHOMOGENEOUS COSMOLOGIES

This chapter is entirely Track 2. The main text requires no special preparation, although Chapters 27–29 would be helpful.

Box 30.1 contains more technical sections: ideal preparation for it would be Chapters 4, 9–14, 21, and 27–29, plus §25.2; minimal preparation would be exercises 9.13, 9.14, and 25.2, Chapter 21 through §21.8, and §§27.8, 27.11, and 29.2.

Chapter 30 is not needed as preparation for any later chapter.

Motivation for studying inhomogeneous and anisotropic cosmologies: Why is universe so uniform?

§30.1. WHY IS THE UNIVERSE SO HOMOGENEOUS AND ISOTROPIC?

The last three chapters studied the Friedmann cosmological models and the relatively satisfactory picture they give of the universe and its evolution. This chapter describes less simplified cosmological models, and uses them to begin answering the question, “Why are the very simple Friedmann models satisfactory?” This question is intended to probe more deeply than the first, obvious answer—namely, that the models are satisfactory because they do not contradict observations. Accepting the agreement with observations, we want to understand *why the laws of physics should demand (rather than merely permit) a universe that is homogeneous and isotropic to high accuracy on large scales*. Because this question cannot be answered definitively in 1972, many readers will prefer to omit this chapter on the first reading and return to it only after they have surveyed the major results in other areas such as black holes (Chapter 33), gravitational waves (Chapters 35–37), and solar-system experiments (Chapter 40).

The approach described here to the question “Why is the universe so highly symmetric?” is to ask Einstein’s equations to describe what would have happened if the universe had started out highly irregular.

The first step in this approach is to ask what would have happened if the universe had started a little bit irregular. This problem can be tackled by analyzing small perturbations away from the high symmetry of the Friedmann models. Such an analysis is most fruitful in its discussion of the beginnings of galaxy formation, and

in its ability to relate small upper limits on the present-day anisotropy of the microwave background radiation to limits on density and temperature irregularities that might have existed ten billion years ago, when the radiation was emitted. These studies are described so well in the book by Zel'dovich and Novikov (1974) [see also Field (1973), Peebles (1969), Peebles and Yu (1970), Jones and Peebles (1972), and references cited therein] that we omit them here.

Another approach is to allow large deviations from the symmetry of the Friedmann universes, but to put the asymmetries into only a few degrees of freedom.

§30.2. THE KASNER MODEL FOR AN ANISOTROPIC UNIVERSE

The prototype for cosmological models with great asymmetry in a few degrees of freedom is the Kasner (1921a) metric,

$$ds^2 = -dt^2 + t^{2p_1} dx^2 + t^{2p_2} dy^2 + t^{2p_3} dz^2, \quad (30.1)$$

Kasner metric: an example of an anisotropic model universe

which was first studied as a cosmological model by Schücking and Heckmann (1958). In this metric the p_i are constants satisfying

$$p_1 + p_2 + p_3 = (p_1)^2 + (p_2)^2 + (p_3)^2 = 1. \quad (30.2)$$

Each $t = \text{constant}$ hypersurface of this cosmological model is a flat three-dimensional space. The world lines of constant x, y, z are timelike geodesics along which galaxies or other matter, treated as test particles, can be imagined to move. This model represents an expanding universe, since the volume element

$$\sqrt{-g} = \sqrt{{}^3g} = t$$

is constantly increasing. But it is an anisotropically expanding universe. The separation between two standard (constant x, y, z) observers is $t^{p_1} \Delta x$ if only their x -coordinates differ. Thus, distances parallel to the x -axis expand at one rate, $\ell_1 \propto t^{p_1}$, while those along the y -axis can expand at a different rate, $\ell_2 \propto t^{p_2}$. Most remarkable perhaps is the fact that along one of the axes distances contract rather than expand. This contraction shows up mathematically in the fact that equations (30.2) require one of the p 's, say p_1 , to be nonpositive:

$$-\frac{1}{3} \leq p_1 \leq 0. \quad (30.3)$$

As a consequence, in a universe of this sort, if black-body radiation were emitted at one time t and never subsequently scattered, later observers would see blue shifts near one pair of antipodes on the sky and red shifts in most other directions. In terms of this example, the fundamental cosmological question is why the Friedmann metrics should be a more accurate approximation to the real universe than is this Kasner metric.

Kasner model with matter becomes isotropic in “old age”

Anisotropy energy

Adiabatic cooling of anisotropy

§30.3. ADIABATIC COOLING OF ANISOTROPY

In seeking an answer, ask a question. Ask, in particular, what would become of a universe that starts out near $t = 0$ with a form described by the Kasner metric of equation (30.1). This metric is an exact solution of the vacuum Einstein equation $\mathbf{G} = 0$. It approximates a situation where the matter terms in the Einstein equations are negligible by comparison with typical non-zero components of the Riemann tensor. Schücking and Heckmann (1958) give solutions with matter included as a pressureless fluid. In this situation, the curvature of empty spacetime dominates both the geometry and the expansion rate at early times, $t \rightarrow 0$; but after some characteristic time t_m the matter terms become more important, and the metric reduces asymptotically to the homogeneous, isotropic model with $k = 0$.

This example illustrates the possibility that the universe might achieve a measure of isotropy and homogeneity in old age, even if it were born in a highly irregular state. Whether the symmetry of our universe can be explained along these lines is not yet clear in 1972. The model universe just mentioned is only a hint, especially since the critical parameter t_m can be given any value whatsoever.

The standard Einstein general-relativity physics of this model can be described in other language (Misner, 1968) by ascribing to the anisotropic motions of empty spacetime an “effective energy density” ρ_{aniso} , which enters the G_{00} component of the Einstein equation on an equal footing with the matter-energy density, and thereby helps to account for the expansion of the universe:

$$H^2 = \left(\frac{1}{3} \frac{d}{dt} \ln \sqrt{^{(3)}g} \right)^2 = \frac{8\pi}{3} (\rho_{\text{aniso}} + \rho_{\text{matter}}). \quad (30.4)$$

The anisotropy energy density is found to have an equation of state

$$\rho_{\text{aniso}} \propto {}^{(3)}g^{-1} = (\text{volume})^{-2},$$

while

$$\rho_{\text{matter}} \propto {}^{(3)}g^{-\gamma/2} = (\text{volume})^{-\gamma}.$$

For pressureless matter $\gamma = 1$; for a radiation fluid $\gamma = 4/3$; for a nonrelativistic ideal gas $\gamma = 5/3$.

This arrangement of the Einstein equation allows one to think of the anisotropy motions as being adiabatically cooled by the expansion of the universe, just as the thermal motions of an ideal gas would be. Since the adiabatic index for homogeneous anisotropy is $\gamma = 2$, the anisotropy will be the dominant source of “effective energy” in a highly compressed state, whereas the matter will dominate in an expanded state.

§30.4. VISCOUS DISSIPATION OF ANISTROPY

The model universe sketched above can be further elaborated by introducing dissipative mechanisms that convert anisotropy energy into thermal energy. Suppose that

such an anisotropic universe were filled at one time with thermal radiation. If the radiation were collisionless or nearly so, the quanta moving parallel to the contracting x -axis would get blueshifted and would develop an energy distribution corresponding to a high temperature. The quanta moving parallel to the other (expanding) axes would be redshifted to an energy distribution corresponding to a low temperature. Any collisions taking place between these two systems of particles would introduce a “thermal contact” between them, and would transfer energy from the hot system to the cold one, with a corresponding large production of entropy. This provides an irreversible dissipative process, which decreases ρ_{aniso} and increases $\rho_{\text{radiation}}$ relative to the values they would have had under conditions of adiabatic expansion. [For further details, see, e.g., Matzner and Misner (1972).]

It is possible that both the adiabatic cooling of anisotropy and the dissipation of anisotropy by its action on a gas of almost collisionless quanta have played significant roles in the evolution of our universe. In particular, neutrinos above 10^{10} K may have undergone sufficient ν - e scattering to have provided strong dissipation during the first few seconds of the life of the universe.

§30.5. PARTICLE CREATION IN AN ANISOTROPIC UNIVERSE

Adiabatic cooling and viscous dissipation might not be the chief destroyers of anisotropy in an expanding universe. More powerful still might be another highly dissipative process, which might occur at still earlier times, very near the initial “singularity.” This is a process of particle creation which was first treated by DeWitt (1953), then explored by Parker (1966 and 1969) for isotropic cosmologies and finally by Zel’dovich (1970) in the present context of anisotropic cosmologies. In this process one again turns to the Kasner metric for the simplest example, but now quantum-mechanical considerations enter the picture. One realizes that not only would real quanta propagating in different directions be subject to red shifts and blue shifts, but that virtual quanta must be considered as well. Vacuum fluctuations (zero-point oscillations) entail a certain minimum number of virtual quanta, which are subject to the redshifting and blueshifting action of the strong gravitational fields. Virtual quanta that are blueshifted sufficiently violently can materialize as real particles, thanks to their energy gain. In this context “sufficiently violently” means *not adiabatically*.

Creation of particles by
anisotropy of expansion

In an adiabatic expansion, the number of particles does not change, although the energy of each one does. This adiabatic limit is just the geometric-optics approximation to wave equations, which was discussed in §22.5. There one saw that, if spacetime were not flat on the scale of a wavelength, then the wave equation could not be replaced by a particle description with conserved particle numbers. Thus, the adiabatic limit (geometric-optics approximation) is violated in the conditions of high curvature near the singularity at the beginning of the universe.

By studying wave equations in the Kasner background metric, Zel’dovich and Starobinsky (1971) find quantitatively the consequences of the failure of the adia-

batic approximation near the singularity. Classically, the amplitudes of waves at frequencies comparable to the Hubble constant for any given epoch increase faster than a simple blue-shift calculation would imply (amplification through parametric resonance). Quantum-mechanically, the same amplification, applied to zero-point oscillations, leads to the creation of particle-antiparticle pairs. The calculations indicate that this effect is very strong at the characteristic time $t_q = \sqrt{G\hbar/c^5} \simeq 10^{-43}$ sec. (All calculations performed thus far are inadequate when the effect becomes strong, thus for $t \lesssim t_q$).

For the creation of massless particles, it is essential that an anisotropically expanding universe be postulated (except for scalar particles, for which particle creation occurs already in the Friedmann universe, *unless* the particle satisfies the conformal-invariant wave equation). The isotropic Friedmann universes are all conformally flat, so that solutions of the wave equation for a field of zero rest mass can be given in terms of solutions for flat-space wave equations where there is no particle creation. There is some particle creation even in the isotropic Friedmann universe when the particle has finite rest mass and low energy. However, the particle-creation process normally uses anisotropy energy as the energy supply that it converts into radiation energy.

Anisotropy might have created the matter content of our universe, damping itself out in the process

The pioneering work by Parker and Zel'dovich suggests that one should study in detail cosmological models in which the initial conditions are a singularity, and in which quantum effects near the time $t = t_q$ dissipate all anisotropies and simultaneously give rise to the matter content of the model. This program of research, which is in its infancy, seems to require extrapolating laws of physics down to the very natural looking but preposterously small dimension $\sqrt{G\hbar/c^5} \simeq 10^{-43}$ sec, or equivalently $\sqrt{G\hbar/c^3} \sim 10^{-33}$ cm.

§30.6. INHOMOGENEOUS COSMOLOGIES

Inhomogeneous cosmological models:

(1) with spherical symmetry

(2) with (rather symmetric) gravitational waves

(3) near a singularity, with few or no symmetries

The model universes considered above were all homogeneous although anisotropic. It is also crucial to study inhomogeneous cosmological models, in which the metric has a nontrivial dependence on the space coordinates. One class of such models is spherically symmetric universes, where the matter density, expansion rate, and all other locally measurable physical quantities have spherical symmetry about some preferred origin. Models of this sort were first considered by Lemaître (1933a,b), Tolman (1934b), and Datt (1938), and were also treated by Bondi in 1947. These models provide a means for studying density perturbations of large amplitude.

A recent tool is making it possible to study large-amplitude, spatially varying curvature perturbations of other symmetries; this tool is the Gowdy (1971, 1973) metrics. These metrics, which are exact solutions of the Einstein equations, represent closed universes with various topologies ($S^3, S^1 \times S^2, T^3$) containing gravitational waves. The wave form in these solutions is essentially arbitrary, but all the waves propagate along a single preferred direction and have a common polarization.

A rather different approach to understanding the behavior of inhomogeneous and anisotropic solutions of the Einstein equations has been developed by Khalatnikov,

Lifshitz, and their colleagues. Rather than truncate the Einstein theory by limiting attention to specialized situations where exact solutions can be obtained, they have sought to study the widest possible class of solutions, but to describe their behavior only in the immediate neighborhood of the singularity. These studies give a greatly enhanced significance to some of the exact solutions, by showing that phenomena found in them are in fact typical of much broader classes of solutions.

Thus, in the first large class of solutions studied [Lifshitz and Khalatnikov (1963)], it was found that near the singularity solutions containing matter showed no features not already found in the vacuum solutions. Furthermore, space derivatives in the Einstein equations became negligible near the singularity in these solutions, with the consequence that a metric of the Kasner form [equation (30.1)] described the local behavior of spacetime near the singularity, but with a different set of p_i values possible at each point of the singular hypersurface. Subsequently, broadened studies of solutions near a singularity [Belinsky and Khalatnikov (1970)] showed that the mixmaster universe [Misner (1969b); Belinsky, Khalatnikov, and Lifshitz (1970)] is a still better homogeneous prototype for singularity behavior than the Kasner metric.

§30.7. THE MIXMASTER UNIVERSE

The simplest example of a mixmaster universe is described in Box 30.1. It shows how, near the singularity, the Kasner exponents p_i can become functions of time. The result is most simply described in terms of the Khalatnikov-Lifshitz parameter u :

$$\begin{aligned} p_1 &= -u/(1 + u + u^2), \\ p_2 &= (1 + u)/(1 + u + u^2), \\ p_3 &= u(1 + u)/(1 + u + u^2). \end{aligned} \quad (30.5)$$

As one extrapolates backward in time toward the singularity, one finds that the expansion rates in the three principal directions correspond to those of the Kasner metric of equation (30.1), with p_i values corresponding to some fixed u parameter. In these mixmaster models, however, the metric is not independent of the space coordinates (the spacelike hypersurfaces can, for instance, have the same 3-sphere topology as the closed Friedmann universes).

The Kasner-like behavior at fixed u can persist through many decades of volume expansion before effects of the spatial derivatives of the metric come into play. The role then played by the space curvature is brief and decisive. The expansion is converted from a type corresponding to a parameter value $u = u_0$ to a type corresponding to the value $u = -u_0$ (which is equivalent, under a relabeling of the axes, to the value $u = u_0 - 1$). Extrapolating still farther back toward the singularity, one finds a previous period with $u = u_0 - 2$. Throughout an entire sequence $u = u_0, u_0 - 1, u_0 - 2, u_0 - 3, \dots$, with $u_0 \gg 1$, nearly the entire volume expansion is due to expansion in the 3-direction, whereas the 1- and 2-directions change very little, alternating at each step between expansion and contraction. Sufficiently far in the past, however, such a sequence leads to a value of u between 0 and 1. This value

Mixmaster universe:

- (1) "anisotropy oscillations" explained in terms of Kasner model

(2) as a prototype for generic behavior near singularities

Are there any other generic types of behavior near singularities?

can be interpreted as the starting point for another, similar sequence, through the transformation $u \rightarrow 1/u$, which interchanges the names of axes 2 and 3.

The extrapolation of the universe's evolution back toward the singularity at $t = 0$ therefore shows an extraordinarily complex behavior, in which similar but not precisely identical sequences of behavior are repeated infinitely many times. In terms of a time variable which is approximately $\log(\log t^{-1})$, these behaviors are quasi-periodic. In the generic example to which the Khalatnikov-Lifshitz methods lead, one has a metric whose asymptotic behavior near the singularity is at each point of the singular hypersurface described by a mixmaster-type behavior, but with the principal axes of expansion changing their directions as well as their roles (as characterized by the u parameter) at each step, and with the mixmaster parameters spatially variable. [For more details see Belinsky, Lifshitz, and Khalatnikov (1971), and Ryan (1971, 1972).]

It is not yet (1972) known whether there are important solutions or classes of solutions relevant to the cosmological problem, with asymptotic singularity behavior *not* described by the Khalatnikov-Lifshitz generic case. The difficulty in reaching a definitive assessment here is that Khalatnikov and Lifshitz use essentially local methods, confined to a single coordinate patch, whereas the desired assessment poses an essentially global question. The global approaches (described in Chapter 34) have not, however, provided any comparable description of the nature of the singularity whose necessity they prove. One attempt to bridge these differences in technique and content is the work by Eardley, Liang, and Sachs (1972).

(continued on page 815)

Box 30.1 THE MIXMASTER COSMOLOGY

The Mixmaster Cosmology is a valuable example. As described in §30.7, it shows a singularity behavior which illustrates most of the features of the most general examples known. In particular, it shows how properties of empty space reminiscent of an elastic solid become evident near the cosmological singularity.

The mathematical path to this example, as given in this box, also illustrates several important techniques in using the variational principles for the Einstein equations to elucidate the solution of these equations. The Mixmaster example can also be used to provide simple examples of superspace ideas and of quantum formulations of the laws of gravity [Misner (1972a)].

A Generalized Kasner Model

Two generalizations must be implemented in order to progress from the Kasner example (30.1) of a cosmological singularity to the Mixmaster example. The first is to allow a more general time-dependence while preserving some of the simplicity of the conditions (30.2) on the exponents p_i . Note that these exponents satisfy, e.g., $p_2 \equiv d \ln g_{22} / d \ln g$. Therefore one is led to parametrize the 3×3 spatial metric as

$$g_{ij} = e^{2\alpha}(e^{2\beta})_{ij} \quad (1)$$

or equivalently, $(\ln g)_{ij} = 2\alpha \delta_{ij} + 2\beta_{ij}$, where β_{ij} is a traceless 3×3 symmetric matrix, and the exponential is a matrix power series, so $\det e^{2\beta} = 1$ and

$$\sqrt{g} = e^{3\alpha}. \quad (2)$$

For the purposes of this paragraph only, define

$p_{ij} = d(\ln g)_{ij}/d \ln \det g$. Then from equations (1) and (2), one computes

$$p_{ij} = \frac{1}{3} [\delta_{ij} + (d\beta_{ij}/d\alpha)]; \quad (3)$$

so the one Kasner condition

$$1 = \sum_i p_i \equiv \text{trace } p_{ij} = 1 + \frac{1}{3} \text{trace } (d\beta/d\alpha)$$

is an identity in view of $\text{trace } \beta_{ij} = 0$. The second condition on the Kasner exponents is $\text{trace } (p^2) = 1$, and becomes $(d\beta_{ij}/d\alpha)^2 = 6$ by equation (3). This is not an identity, but a consequence of the Einstein equations in empty space. For the (Bianchi Type I) metric

$$ds^2 = -dt^2 + e^{2\alpha}(e^{2\beta})_{ij} dx^i dx^j, \quad (4)$$

and in the case when β_{ij} is diagonal, the Einstein equations are,

$$\left(\frac{d\alpha}{dt}\right)^2 = \frac{8\pi}{3} \left[T^{00} + \frac{1}{16\pi} (d\beta_{ij}/dt)^2 \right] \quad (5)$$

and

$$e^{-3\alpha} \frac{d}{dt} \left(e^{3\alpha} \frac{d\beta_{ij}}{dt} \right) = 8\pi \left(T_{ij} - \frac{1}{3} \delta_{ij} T_{kk} \right), \quad (6)$$

together with a redundant equation involving T_{kk} and the equation $T_{0k} = 0$. [The stress components here refer to an orthonormal frame with basis 1-forms $\omega^i = e^\alpha(e^\beta)_{ij} dx^j$.] From equation (5) one immediately derives

$$\rho_{\text{aniso(I)}} = (c^2/16\pi G)(d\beta_{ij}/dt)^2 \quad (7)$$

as a formula for the effectiveness of Type I anisotropy in contributing to the Hubble constant $H = d\alpha/dt$ on a basis comparable to matter energy, as in equation (30.4). Similarly, for equation (6) in the case of fluid matter (isotropic pressures), the stress terms vanish, and one obtains $\rho_{\text{aniso(I)}} e^{6\alpha} = \text{const.}$, as in the equation following (30.4). The Kasner condition $\sum p_i^2 = 1$ or $(d\beta_{ij}/d\alpha)^2 = 6$ follows from equation (5) whenever $T^{00} \ll \rho_{\text{aniso}}$.

In the diagonal case, β_{ij} has only two independ-

ent components, and it is convenient at times to define them explicitly by the parameterization

$$\begin{aligned} \beta_{11} &= \beta_+ + \sqrt{3}\beta_-, \\ \beta_{22} &= \beta_+ - \sqrt{3}\beta_-, \\ \beta_{33} &= -2\beta_+. \end{aligned} \quad (8)$$

For these the Kasner condition $(d\beta_{ij}/d\alpha)^2 = 6$ becomes

$$(d\beta_+/d\alpha)^2 + (d\beta_-/d\alpha)^2 = 1. \quad (9)$$

The β_\pm are related to the Kasner exponents p_i or the u parameter of equations (30.5) by

$$\begin{aligned} d\beta_+/d\alpha &= \frac{1}{2} (1 - 3p_3) \\ &= -1 + (3/2)(1 + u + u^2)^{-1} \\ d\beta_-/d\alpha &= \frac{1}{2} \sqrt{3}(p_1 - p_2) \\ &= -\frac{1}{2} \sqrt{3}(1 + 2u)(1 + u + u^2)^{-1}. \end{aligned} \quad (10)$$

Introducing Space Curvature

The first step in generalizing the Kasner metric has focused attention on the “velocity” $\beta' \equiv (d\beta_+/d\alpha, d\beta_-/d\alpha)$ which is a derivative of anisotropy with respect to expansion. The effects of matter or, as will soon appear, space curvature can change the magnitude $\|\beta'\|$ from the Kasner value of unity. The second step of generalization is to introduce space curvature. This one achieves in a simple example by retaining the metric components of equation (1), but employing them in a non-holonomic basis. Use the basis vectors introduced in exercises 9.13 and 9.14 on the rotation group $SO(3)$, whose dual 1-forms are

$$\begin{aligned} \sigma^1 &= \cos \psi d\theta + \sin \psi \sin \theta d\phi, \\ \sigma^2 &= \sin \psi d\theta - \cos \psi \sin \theta d\phi, \\ \sigma^3 &= d\psi + \cos \theta d\phi, \end{aligned} \quad (11)$$

to form the metric

$$ds^2 = -N^2 dt^2 + e^{2\alpha}(e^{2\beta})_{ij} \sigma^i \sigma^j, \quad (12)$$

where N , α , and β_{ij} are functions of t only. When

Box 30.1 (continued)

$\alpha = 0 = \beta_{ij}$, the three-dimensional space metric here reduces to the one studied in exercise 13.15, which is the metric of highest symmetry on the group space $SO(3)$. The simply connected covering space has the 3-sphere topology, and is obtained by extending the range of the Euler angle ψ to give it a 4π period [$SU(2)$ or spin $\frac{1}{2}$ covering of the rotation group]. With $N = 1$, $\frac{1}{2}a = e^\alpha$, and $\beta_{ij} = 0$, one obtains from equation (12) the same metric (in different coordinates) as that treated in exercise 14.4 and in Chapter 27 in discussions of the closed Friedmann cosmological model. A non-zero value for β_{ij} allows the 3-sphere to have a different circumference on great circles in each of 3 mutually orthogonal principal directions, thus destroying its isotropy but not its homogeneity.

Let us consider only the case with β_{ij} diagonal, as in equation (8). Then the T^{00} Einstein equation becomes (with $N = 1$ as a time-coordinate condition)

$$3(\dot{\alpha}^2 - \dot{\beta}_+^2 - \dot{\beta}_-^2) + \frac{1}{2}(^3R_{IX}) = 8\pi T^{00}, \quad (13)$$

where only the term

$${}^3R_{IX} = \frac{1}{2}e^{-2\alpha} \text{trace}(2e^{-2\beta} - e^{4\beta}) \quad (14)$$

is different from equation (5). This term [see equation (21.92)] is the scalar curvature of a three-dimensional slice, $t = \text{const}$ [which has symmetry properties known as “Bianchi Type IX” for the metric of equations (11) and (12)]. If equation (13) is interpreted in terms of an anisotropy energy density contributing, with T^{00} , to the volume expansion $\dot{\alpha}^2$, then there are not only kinetic energy terms $\dot{\beta}^2$ [as in equations (5) and (7)], but also a potential energy term. This term shows that negative scalar curvature, which can be produced by anisotropy ($\beta \neq 0$), is equivalent to a positive potential (or “internal”) energy, and suggests that empty space has properties with analogies to an elastic solid and resists shear strains. The more detailed analysis which follows shows that, near

the singularity, the scalar curvature is always negligible when positive.

Negative curvatures, however, arise in this closed universe from large shear (β) deformations near the singularity and become large enough to reverse one Kasner shear motion [u -value, etc.; equation (10)] and change it to another.

These conclusions and further details of the time-evolution of the “Mixmaster” metric (11, 12) require, in principle, the study of all the Einstein equations, not just equation (13) for T^{00} . As described in Chapter 21, however, this T^{00} constraint equation is central, and actually contains implicitly the full content of the Einstein equations when formulated properly.

Variational Principles

One adequate formulation, adopted here, involves treating equation (13) not as an energy equation (involving velocities), but as a Hamiltonian (involving momenta). Take the Einstein variational principle (21.15) in ADM form (21.95) and carry out the space integration, using

$$\int \sigma^1 \wedge \sigma^2 \wedge \sigma^3 = \int \sin \theta \, d\phi \wedge d\theta \wedge d\psi = (4\pi)^2,$$

to obtain the action integral in the form

$$I = (\pi) \int \left\{ \pi^{ij} dg_{ij} + Ne^{3\alpha} \left[{}^3R_{IX} + e^{-6\alpha} \left(\frac{1}{2}(\pi^\ell_\ell)^2 - \pi^{ik}\pi_{ik} \right) \right] dt \right\}. \quad (15)$$

When introducing the specific form (1) and (8) for g_{ij} , it is convenient also to parameterize the diagonal matrix π^i_k as follows:

$$\begin{aligned} p_\alpha &= (2\pi)\pi^k_k, \\ p^i_k &= (2\pi) \left(\pi^i_k - \frac{1}{3} \delta^i_k \pi^\ell_\ell \right), \end{aligned} \quad (16)$$

with

$$\begin{aligned} 6p^1_1 &= p_+ + p_- \sqrt{3}, \\ 6p^2_2 &= p_+ - p_- \sqrt{3}, \\ 6p^3_3 &= -2p_+ \end{aligned} \quad (17)$$

[see equation (8)]. The result is

$$\begin{aligned} I = & \int p_+ d\beta_+ + p_- d\beta_- + p_\alpha d\alpha \\ & - \frac{Ne^{-3\alpha}}{24\pi} [-p_\alpha^2 + p_+^2 + p_-^2 \\ & - 24\pi^2 e^{6\alpha} ({}^3R_{IX})] dt. \end{aligned}$$

This is cleaned up for further study as follows. Write

$${}^3R_{IX} = \frac{3}{2} e^{-2\alpha} (1 - V), \quad (18)$$

where

$$V = V(\beta) = \frac{1}{3} \text{trace} (1 - 2e^{-2\beta} + e^{4\beta}) \quad (19)$$

so $V(0) = 0$; and adjust the zero of α ($\alpha \rightarrow \alpha - \alpha_0$) so that $e^{2\alpha} \rightarrow (6\pi)^{-1} e^{2\alpha}$. Then the metric is

$$ds^2 = -N^2 dt^2 + (6\pi)^{-1} e^{2\alpha} (e^{2\beta})_{ij} \sigma^i \sigma^j, \quad (20)$$

and the variational integral is

$$\begin{aligned} I = & \int p_+ d\beta_+ + p_- d\beta_- + p_\alpha d\alpha \\ & - (3\pi/2)^{1/2} Ne^{-3\alpha} \mathcal{H} dt, \end{aligned} \quad (21)$$

with

$$2\mathcal{H} \equiv -p_\alpha^2 + p_+^2 + p_-^2 + e^{4\alpha} (V - 1). \quad (22)$$

One demands $\delta I = 0$ for arbitrary independent variations of p_\pm , p_α , β_\pm , α , N to obtain the Einstein equations. From varying N , one obtains the fundamental constraint equation $\mathcal{H} = 0$ [which would reduce to the vacuum version of equation (13) when the momenta are replaced by velocities (via equations obtained by varying the p 's) if the coordinate condition $N = 1$ were imposed.]

ADM Hamiltonian

The standard ADM prescription for reducing this variational principle to canonical (Hamiltonian) form is to choose one of the field variables or momenta as a time-coordinate, and solve the con-

straint for its conjugate Hamiltonian. Here an obvious and satisfactory choice is to set $t = \alpha$, and solve $\mathcal{H} = 0$ for

$$H_{ADM} = -p_\alpha = [p_+^2 + p_-^2 + e^{4\alpha} (V - 1)]^{1/2}. \quad (23)$$

The $\dot{\alpha}$ equation [vary p_α in equation (21)] is

$$\dot{\alpha} = -(3\pi/2)^{1/2} Ne^{-3\alpha} p_\alpha \quad (24)$$

and shows that the choice $\alpha = t$ (so $\dot{\alpha} = 1$) requires

$$N_{ADM} = (2/3\pi)^{1/2} e^{3\alpha} / H_{ADM}. \quad (25)$$

The reduced, canonical, variational principle which results when equation (23) is used to eliminate p_α reads $\delta I_{red} = 0$ with

$$I_{red} = \int p_+ d\beta_+ + p_- d\beta_- - H_{ADM} d\alpha \quad (26)$$

and must be supplemented by equation (25).

Super-Hamiltonian

A more convenient approach here is one more closely related to the Dirac Hamiltonian methods than those of ADM. Note, however, that one does not remove the arbitrariness in the lapse function by taking it to be some specified function $N(t)$ of the coordinates. Instead the procedure adopted here is to eliminate N from the variational principle (21) by choosing it (coordinate condition!) to be some chosen function of the field variables and momenta, $N = N(\alpha, \beta_\pm, p_\alpha, p_\pm)$. Any such choice, inserted in equation (21), leaves a variational integral in canonical Hamiltonian form. The content of this new variational principle becomes equivalent to the original one only when supplemented by the constraint

$$\mathcal{H} = 0, \quad (27)$$

which can no longer be derived from the variational principle. [The other Euler-Lagrange equations for these two principles differ only by terms proportional to \mathcal{H} , and thus are equivalent when

Box 30.1 (continued)

$\mathcal{K} = 0$ is imposed on the initial conditions.] The choice

$$N = (2/3\pi)^{1/2}e^{3\alpha} \quad (28)$$

is obvious and convenient. It makes \mathcal{K} become a super-Hamiltonian in the resulting variational principle

$$I = \int p_+ d\beta_+ + p_- d\beta_- + p_\alpha d\alpha - \mathcal{K} d\lambda, \quad (29)$$

where $t \equiv \lambda$ has been written to label the specific time-coordinate choice that equation (28) implies.

Mixmaster Dynamics

If matter terms with no additional degrees of freedom are included, the super-Hamiltonian in equation (29) is modified simply. For an example, choose

$$T^{\hat{0}\hat{0}} = -T^0_0 = (3/4)^2(\mu e^{-3\alpha} + \Gamma e^{-4\alpha}) \quad (30)$$

for the energy density of matter in a frame with time-axis $\mathbf{e}_{\hat{0}} = N^{-1}(\partial/\partial t)$. The two terms represent a nonrelativistic perfect fluid ($\rho \propto V^{-1}$) and a radiation fluid ($\rho \propto V^{-4/3}$), respectively, and lead to

$$2\mathcal{K} = -p_\alpha^2 + p_+^2 + p_-^2 + e^{4\alpha}(V - 1) + \mu e^{3\alpha} + \Gamma e^{2\alpha}. \quad (31)$$

This Hamiltonian, with its simple quadratic momentum dependence, differs in only two ways from the Hamiltonians of elementary mechanics, namely, (1) in the sign of the p_α^2 term and (2) in the detailed shape of the “potential” term as function of α and β_{\pm} , the study of which reduces to a study of the function $V(\beta)$. Hamilton’s equations, from varying α , β_{\pm} , p_α , and p_{\pm} in equation (29), yield

$$\frac{d^2\beta_{\pm}}{d\lambda^2} = -\frac{\partial\mathcal{K}}{\partial\beta_{\pm}} = -\frac{1}{2}e^{4\alpha}\frac{\partial V}{\partial\beta_{\pm}} \quad (32)$$

and

$$\frac{d^2\alpha}{d\lambda^2} = +\frac{\partial\mathcal{K}}{\partial\alpha} = 2e^{4\alpha}(V - 1) + \frac{3}{2}\mu e^{3\alpha} + \Gamma e^{2\alpha}. \quad (33)$$

Thus the sign of the p_α^2 term causes α to accelerate toward (rather than away from) higher values of the “potential” terms $e^{4\alpha}(V - 1) + \mu e^{3\alpha} + \Gamma e^{2\alpha}$. When $|V| \ll 1$ (small anisotropy), equation (33) is identical to its form in the isotropic Friedmann model, and allows a deceleration only when α is large enough that the positive curvature term ($-e^{4\alpha}$) dominates over matter ($\mu e^{3\alpha}$) and radiation ($\Gamma e^{2\alpha}$). Near the singularity ($\alpha \rightarrow -\infty$), the positive curvature term is always negligible compared to radiation and matter.

For studies of the singularity behavior, it is sufficient to study the simplified super-Hamiltonian

$$2\mathcal{K} \sim -p_\alpha^2 + p_+^2 + p_-^2 + e^{4\alpha}V(\beta), \quad (34)$$

since the other terms obviously vanish for $\alpha \rightarrow -\infty$. This form retains only the V term in ${}^3R_{IX} = \frac{3}{2}e^{-2\alpha}(1 - V)$, which dominates when the curvature of this closed universe becomes negative, $V \gg 1$. If the term in $V(\beta)$ were also negligible, then $\mathcal{K} = -p_\alpha^2 + p_+^2 + p_-^2$ would make each p_α, p_{\pm} constant, giving the Kasner behavior with

$$d\beta_{\pm}/d\alpha = p_{\pm}/p_\alpha = \text{const}$$

and $|d\beta/d\alpha|^2 = 1$ as expected (since matter and curvature have been neglected). To proceed further, a study of $V(\beta)$ is required, based on equations (19) and (8), and their immediate consequence:

$$V(\beta) = \frac{1}{3}e^{-8\beta_+} - \frac{4}{3}e^{-2\beta_+} \cosh 2\sqrt{3}\beta_- + 1 + \frac{2}{3}e^{4\beta_+}(\cosh 4\sqrt{3}\beta_- - 1). \quad (35)$$

One finds that $V(\beta)$ is a *positive definite* “potential well” which has the same symmetries as an equi-

lateral triangle in the $\beta_+ \beta_-$ plane. Near the origin, $\beta_{\pm} = 0$, the equipotentials are circles, since

$$V(\beta) = 8(\beta_+^2 + \beta_-^2) + 0(\beta^3). \quad (36)$$

For large β values, one finds

$$V(\beta) \sim \frac{1}{3} e^{-8\beta_+}, \quad \beta_+ \rightarrow -\infty, \quad (37)$$

and

$$V(\beta) \sim 1 + 16\beta_-^2 e^{4\beta_+}, \quad \begin{matrix} \beta_+ \rightarrow +\infty, \\ |\beta_-| \ll 1. \end{matrix} \quad (38)$$

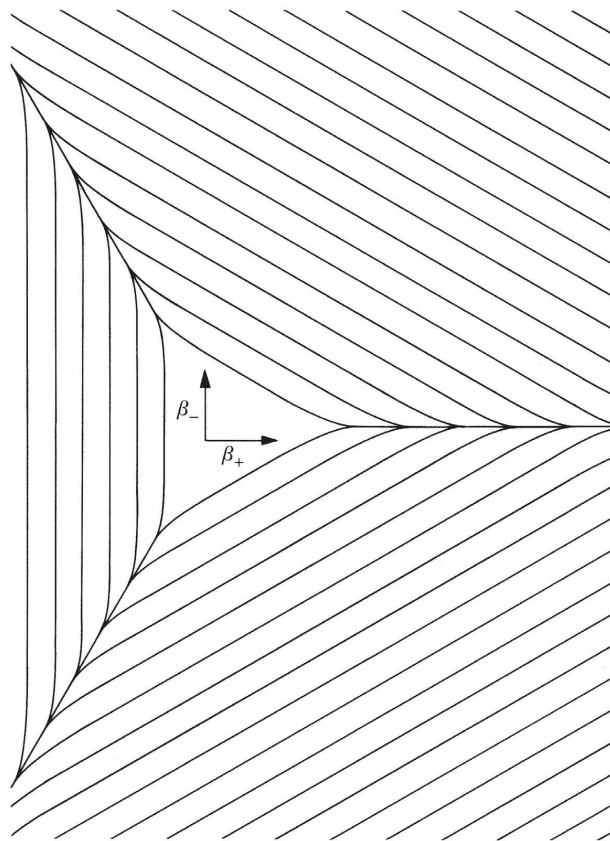
These two asymptotic forms, together with the triangular symmetry, give a complete asymptotic description of $V(\beta)$, as sketched in the figure, where on successive levels separated by $\Delta\beta = 1$, the potential V increases by a factor of $e^8 = 3 \times 10^3$.

"Bounce" Interrupts Kasner-like Steps Toward the Singularity

The dominant feature of the $V(\beta)$ potential is evidently its steep (exponential) triangular walls, with equation (37) representing the typical one for study. Under the influence of this potential wall, the evolution of this model universe is governed by the super-Hamiltonian

$$2\mathcal{H} \sim -p_{\alpha}^2 + p_+^2 + p_-^2 + \frac{1}{3} e^{4(\alpha - 2\beta_+)}. \quad (39)$$

If $\alpha \rightarrow -\infty$ with $d\beta_+/d\alpha > 1/2$ [recall $d\beta_+/d\alpha = \text{const.}$, $|d\beta/d\alpha| = 1$, when the last term in (39) is small], then the potential term grows and will eventually become large enough to influence the motion. A simple "Lorentz" transformation, suggested by the superspace metric (coefficients of the



Some equipotentials, $V(\beta) = \text{constant}$, are shown for the function defined in equation (35). Equipotentials near the origin of the β -plane are closed curves for $V < 1$ and are omitted here.

Box 30.1 (continued)

quadratic in the momenta) simplifies the computation further. Set

$$\bar{\beta}_+ = \left(\beta_+ - \frac{1}{2} \alpha \right) / \sqrt{3/4},$$

$$\bar{\alpha} = \left(\alpha - \frac{1}{2} \beta_+ \right) / \sqrt{3/4},$$

and find

$$2\mathcal{H} = -\bar{p}_\alpha^2 + \bar{p}_+^2 + p_-^2 + \frac{1}{3} \exp(-4\sqrt{3}\bar{\beta}_+). \quad (40)$$

For this super-Hamiltonian both \bar{p}_α and p_- are constants of motion, whereas the $\bar{\beta}_+$ -Hamiltonian, $\bar{p}_+^2 + \frac{1}{3}e^{-4\sqrt{3}\bar{\beta}_+}$, represents a simple bounce against a one-dimensional potential wall with the initial and final values of \bar{p}_+ different only in sign. The behavior of the anisotropy parameters β_\pm near the singularity thus consists of a simple Kasner step (where $d\beta_\pm/d\alpha = \text{const.}$, with the $d\beta_+/d\alpha \geq \frac{1}{2}$, or conditions equivalent by symmetry, satisfied relative to one of the three walls), followed by a bounce against that wall, beginning a new Kasner step with other Kasner parameters. [The most detailed description of this behavior and its relation to more general cosmological models can be found in Belinsky, Khalatnikov, and Lifshitz (1970)—see also the briefer report, Khalatnikov and Lifshitz (1970)—using quite different methods. For detailed developments by Hamiltonian methods, which supersede the partial Lagrangian methods of Misner (1969b), see Misner (1970, 1972a), and Ryan (1972a,b).]

Steady-State, Quasiperiodic Infinity of "Bounces" Approaching the Singularity

Some comprehensive features of the singularity behavior, involving many Kasner-like steps, can be exhibited by another transformation of the parameter space (superspace) of the metric field.

The transformation introduces a “radial” t -coordinate out from the origin of $\alpha\beta_\pm$ space, while respecting the metric properties of this superspace implied by the form of the super-Hamiltonian. Thus one defines (for any constant α_0)

$$\begin{aligned} \alpha_0 - \alpha &= e^t \cosh \xi, \\ \beta_+ &= e^t \sinh \xi \cos \phi, \\ \beta_- &= e^t \sinh \xi \sin \phi, \end{aligned} \quad (41)$$

and finds

$$2\mathcal{H} = e^{-2t} [(-p_t^2 + p_\xi^2 + p_\phi^2 \sinh^{-2}\xi) + e^{2t} e^{4\alpha} V]. \quad (42)$$

The advantage of this transformation is that in the limit $t \rightarrow \infty$ ($\alpha \rightarrow -\infty$, singularity) the potential terms become, in first approximation, independent of t . Thus equation (37) gives, for one potential wall,

$$\begin{aligned} e^{2t} e^{4\alpha} V &\sim \frac{1}{3} e^{2t} \exp \left[4\alpha_0 \right. \\ &\quad \left. - 8e^t \left(\sinh \xi \cos \phi + \frac{1}{2} \cosh \xi \right) \right]. \end{aligned} \quad (43)$$

For $t \rightarrow \infty$ this expression evidently tends to either zero or infinity, depending on the sign of the expression in parentheses. Therefore define the asymptotic potential walls by

$$\tanh \xi + \frac{1}{2} \sec \phi = 0 \quad (44)$$

in the sector $|\phi - \pi| < \pi/3$, and equivalent formulae in which ϕ is replaced by $\phi \pm (2\pi/3)$ for the other sides of the triangle. Consequently, an asymptotic approximation to the super-Hamiltonian is

$$2\mathcal{H} = e^{-2t} [-p_t^2 + p_\xi^2 + p_\phi^2 \sinh^{-2}\xi + V'(\xi, \phi)], \quad (45)$$

where $V'(\xi, \phi)$ vanishes inside the asymptotic walls (44) and equals $+\infty$ outside. Because the remaining t -dependence is a common factor in (45), a simple change of independent variable $e^{-2t} d\lambda = d\lambda'$ in equation (29)—equivalent to the choice

$$N = (2/3\pi)^{1/2} e^{-2t} \exp [3(\alpha_0 - e^t \cosh \xi)] \quad (46)$$

in place of equation (28)—gives a new super-Hamiltonian $\mathcal{H}' = e^{2t}\mathcal{H}$ with the variational integral

$$I = \int p_t dt + p_\xi d\xi + p_\phi d\phi - \mathcal{H}' d\lambda'. \quad (47)$$

In the asymptotic approximation where

$$2\mathcal{H}' = -p_t^2 + p_\xi^2 + p_\phi^2 \sinh^{-2}\xi + V(\xi, \phi), \quad (48)$$

one immediately sees that p_t is a constant of motion, and that the “bouncing” of the $\xi\phi$ values within the asymptotic potential walls is a stationary, quasi-periodic process in this time-coordinate λ' (or t , since $dt/d\lambda' = -p_t = \text{const}$). [More detailed studies based on this asymptotic super-Hamiltonian show that the motion is even ergodic, with $\xi\phi$ approaching arbitrarily close to any given value infinitely many times as $t \rightarrow \infty$; see Chitre (1972a).]

Summary

One has found the singularity behavior in this Mixmaster example to be extraordinarily active. In the simple Kasner singularity, two axes collapse, but the third is stretched in a simple tidal deformation accompanied by volume compression. But in the Mixmaster example, every such collapse attempt is defeated by the high negative curvature it implies. Or rather it is diverted to another attempt as compression continues inexorably, but the tidal deformations attempt first one configuration, then another, in an infinitely recurring probing of all possible configurations.

Speculations on Time and the Singularity

The cosmological singularity (in all examples where its character is not known to be unstable) involves infinite curvature and infinite density. One's abhorrence of such a theoretical prediction is particularly heightened by the correlative prediction that these infinities occurred at a finite proper time in the past, and would—if they

recur—occur again at some finite proper time in the future. The singularity prediction would be more tolerable if the infinite densities could be removed to the infinitely distant past. The universe could then, as now, find its natural state to be one of expansion, so every *finite* density will have been experienced at some suitably remote past time, but *infinite* density becomes a formal abstraction never realized in the course of evolution.

To push infinite curvature out of the finite past might be achieved in two ways. It is not known which, if either, works. One way is to change the physical laws which require the singularity, changing them perhaps only in obvious and desirable ways, such as stating the laws of gravity in a proper quantum language. Computations of quantum geometry are not yet definitive, however, and some (perhaps inadequate) approximations [Misner (1972a)] do not remove the singularity problem.

Another way to discard the singularity is to accept the mathematics of the classical Einstein equations, but reinterpret it in terms of an infinite past time. There are, of course, simple and utterly inadequate ways to do this by arbitrary coordinate transformations such as $t = \ln \tau$ which change a $\tau = 0$ singularity into one at $t = -\infty$. But an arbitrary coordinate is without significance. The problem is that the singularity occurs at a finite *proper* time in the past, and proper time is the most physically significant, most physically real time we know. It corresponds to the ticking of physical clocks and measures the natural rhythms of actual events. To reinterpret finite past time as infinite, one must attack proper time on precisely these grounds, and claim it is inadequately physical. On a local basis, where special relativity is valid, no challenge to the physical significance of proper time can succeed. It is on a more global scale that the physical primacy of proper time needs to be reviewed.

“The cosmological singularity occurred ten thousand million years ago.” In this statement, take time to mean the proper time along the world line of the solar system, ephemeris time. Then the statement would have a most direct physical sig-

Box 30.1 (continued)

nificance if it meant that the Earth had completed 10^{10} orbits about the sun since the beginning of the universe. But proper time is not that closely tied to actual physical phenomena. The statement merely implies that those 5×10^9 orbits which the earth may have actually accomplished give a standard of time which is to be extrapolated in prescribed ways, thus giving theoretical meaning to the other 5×10^9 years which are asserted to have preceeded the formation of the solar system.

A hardier standard clock changes the details of the argument, but not its qualitative conclusion. To interpret 10^{10} years in terms of SI (Système Internationale) seconds assigns a past history containing some 3×10^{27} oscillations of a hyperfine transition in neutral Cesium. But again the critical early ticks of the clock (needed to locate the singularity in time by actual physical events) are missing. The time needed for stellar nucleosynthesis to produce the first Cesium disqualifies this clock on historical grounds, and the still earlier high temperatures nearer the singularity would have ionized all Cesium even if this element had predated stars.

Thus proper time near the singularity is not a direct counting of simple and actual physical phenomena, but an elaborate mathematical extrapolation. Each actual clock has its "ticks" discounted by a suitable factor— 3×10^7 seconds per orbit from the Earth-sun system, 1.1×10^{-10} seconds per oscillation for the Cesium transition, etc. Since no single clock (because of its finite size and strength) is conceivable all the way back to the singularity, a statement about the proper time since the singularity involves the concept of an infinite sequence of successively smaller and sturdier clocks with their ticks then discounted and

added. "Finite proper time," then, need not imply that any finite sequence of events was possible. It may describe a necessarily infinite number of events ("ticks") in any physically conceivable history, converted by mathematics into a finite sum by the action of a non-local convergence factor, the "discount" applied to convert "ticks" into "proper time."

Here one has the conceptual inverse of Zeno's paradox. One rejects Zeno's suggestion that a single swing of a pendulum is infinitely complicated—being composed of a half period, plus a quarter period, plus 2^{-n} *ad infinitum*—because the terms in his infinite series are mathematical abstractions, not physically achieved discrete acts in a drama that must be played out. By a comparable standard, one should ignore as a mathematical abstraction the finite sum of the proper-time series for the age of the universe, if it can be proved that there must be an infinite number of discrete acts played out during its past history. In both cases, finiteness would be judged by counting the number of discrete ticks on realizable clocks, not by assessing the weight of unrealizable mathematical abstractions.

Whether the universe is infinitely old by this standard remains to be determined. The quantum influences, in particular, remain to be calculated. The decisive question is whether each present-epoch event is subject to the influence of infinitely many previous discrete events. In that case statistical assumptions (large numbers, random phases, etc.) could enter in stronger ways into theories of cosmology. The Mixmaster cosmological model does have an infinite past history in this sense, since each "bounce" from one Kasner-like motion to another is a recognizable cosmological event, of which infinitely many must be realized between any finite epoch and the singularity.

§30.8. HORIZONS AND THE ISOTROPY OF THE MICROWAVE BACKGROUND

The fundamental cosmological question—"Must a universe that is born chaotic necessarily become as homogeneous and isotropic as our universe is, and do so before life evolves?"—entails one further issue. This issue is *horizons*. As was discussed in §27.10, at any given epoch in the expansion of a Friedmann universe (e.g., the present epoch), there may be significant portions of the universe from which no light signal or other causally propagating influence will have yet reached Earth in the time available since the initial singularity. "If we should live so long," the question would arise, "will the new portions of the universe which first come into view during the next ten billion years look statistically identical to the neighboring portions which are already being seen?"

Horizons in a Friedmann universe

Observed isotropy of microwave radiation proves foundations for homogeneity were laid before universe became Friedmann-like

Fortunately, this question need not be posed only for the future. It can be asked as of some past time, and the answer then is yes. Microwave background radiation arrives at the earth from all directions in the sky with very nearly the same temperature. [The data of Boughn, Fram, and Partridge (1971) and of Conklin (1969) show $\Delta T/T \lesssim 0.004$.] The plasma that emitted the microwave radiation coming to earth from one direction in the sky had not been able, before the epoch of emission, to communicate causally with the plasma emitting the radiation that arrives from other directions. If one adopts a Friedmann model of the universe, then different sectors of the microwave sky are disjoint from each other in this sense if they are separated from each other by more than 30° , even if the microwaves were emitted as recently as $z = 7$. (The critical angle is much smaller if the microwaves were last scattered at $z = 1,000$.) From this, one concludes that the foundations for the homogeneity and isotropy of the universe were laid long before the universe became approximately Friedmann, for if statistical homogeneity and isotropy of the universe had not already been achieved at the longest wavelengths earlier, these horizon limitations would have prevented any further synchronization of conditions over large scales while the universe was in a nearly Friedmann state, and small amplitude (10%) deviations from isotropy should be observed now.

The mixmaster universe received its name from the hope that it could contribute to the solution of this problem. The very large u values that occur sporadically an infinite number of times near the singularity in a mixmaster universe give a geometry close to that of the Kasner model with $p_1 = 1$, $p_2 = p_3 = 0$. This model can be written in the form

$$ds^2 = e^{2\eta}(-d\eta^2 + dx^2) + dy^2 + dz^2, \quad (30.6)$$

What made the universe homogeneous and isotropic?

(1) Mixmaster oscillations?—probably not

where $\eta = \ln t$. If this metric is converted into a closed-universe model by interpreting x, y, z as angle coordinates each with period 4π , then one sees that a light ray can circumnavigate the universe in the x -direction in a time interval $\Delta\eta = 4\pi$, which corresponds to a volume expansion by a factor $\sqrt{-g_1}/\sqrt{-g_2} = e^{4\pi}$. Unfortunately, a quantitative analysis of the degree and frequency with which the mixmaster universe achieves this specific Kasner form suggests that the horizon breaking

(2) particle creation near singularity?

is inadequate to explain the present state of the universe [Doroshkevich, Lukash, and Novikov (1971); Chitre (1972)]. It may turn out that particle creation near the singularity can solve this horizon question, as well as provide for the dissipation of anisotropy. Hope is provided by the fact that particle creation, when described in purely classical terms, has some acausal appearances, even though it is a strictly causal process at the quantum level [Zel'dovich (1972)].

PART **VII**

GRAVITATIONAL COLLAPSE AND BLACK HOLES

Wherein the reader is transported to the land of black holes, and encounters colonies of static limits, ergospheres, and horizons—behind whose veils are hidden gaping, ferocious singularities.

CHAPTER 31

SCHWARZSCHILD GEOMETRY

§31.1. INEVITABILITY OF COLLAPSE FOR MASSIVE STARS

There is no equilibrium state at the endpoint of thermonuclear evolution for a star containing more than about twice the number of baryons in the sun ($A > A_{\max} \sim 2A_{\odot}$). This is one of the most surprising—and disturbing—consequences of the discussion in Chapter 24. Stated differently: A star with $A > A_{\max} \sim 2A_{\odot}$ must eject all but A_{\max} of its baryons—e.g., by nova or supernova explosions—before settling down into its final resting state; otherwise there will be no final resting state for it to settle down into.

What is the fate of a star that fails to eject its excess baryons before nearing the endpoint of thermonuclear evolution? For example, after a very massive supernova explosion, what will become of the collapsed degenerate-neutron core when it contains more than A_{\max} baryons? Such a supercritical mass cannot explode, since it is gravitationally bound and it has no more thermonuclear energy to release. Nor can it reach a static equilibrium state, since there exists no such state for so large a mass. There remains only one alternative; the supercritical mass must collapse through its “gravitational radius,” $r = 2M$, leaving behind a gravitating “black hole” in space.

The phenomenon of collapse through the gravitational radius, as described by classical general relativity, will be the subject of the next chapter. However, before tackling it, one must understand more fully than heretofore the Schwarzschild spacetime geometry, which surrounds black holes and collapsing stars as well as static stars.

This chapter will concern itself with two topics that, at first sight, appear to be disconnected. One is the fall of a test particle in a preexisting Schwarzschild geometry, which is regarded as static, but can also be visualized as all that remains of a star that underwent collapse some time ago. The second topic is the physical

This chapter, on Schwarzschild geometry, is key preparation for understanding gravitational collapse (next chapter) and black holes (following chapter)

character of this geometry, regarded in and by itself. For the exploration of this geometry, the test particle serves as the best of all explorers. But the test particle may also be regarded in another light. It can be viewed as a rag-tag johnny-come-lately piece of the matter of the falling star. Regarded in this way, it provides the simplest of all illustrations of an asymmetry in the distribution of mass of a collapsing star. That this asymmetry irons itself out will therefore give one some preliminary insight into how more complicated asymmetries also iron themselves out. In brief, the motion of the test particle and the dynamics of the Schwarzschild geometry (for this geometry will prove to be dynamic), two apparently different problems, have the happy ability to throw light on each other.

§31.2. THE NONSINGULARITY OF THE GRAVITATIONAL RADIUS

The Schwarzschild spacetime geometry

$$ds^2 = -\left(1 - \frac{2M}{r}\right)dt^2 + \frac{dr^2}{1 - 2M/r} + r^2(d\theta^2 + \sin^2\theta d\phi^2) \quad (31.1)$$

The Schwarzschild line element becomes singular at $r = 2M$ ("gravitational radius")

appears to behave badly near $r = 2M$; there g_{tt} becomes zero, and g_{rr} becomes infinite. However, one cannot be sure without careful study whether this pathology in the line element is due to a pathology in the spacetime geometry itself, or merely to a pathology of the (t, r, θ, ϕ) coordinate system near $r = 2M$. (As an example of a coordinate-induced pathology, consider the neighborhood of $\theta = 0$ on one of the invariant spheres, $t = \text{const}$ and $r = \text{const}$. There $g_{\phi\phi}$ becomes zero because the coordinate system behaves badly; however, the intrinsic, coordinate-independent geometry of the sphere is well-behaved there. For another example, see Figure 1.4.

The worrisome region of the Schwarzschild geometry, $r = 2M$, is called the "gravitational radius," or the "Schwarzschild radius," or the "Schwarzschild surface," or the "Schwarzschild horizon," or the "Schwarzschild sphere." It is also called the "Schwarzschild singularity" in some of the older literature; but that is a misnomer, since, as will be shown, the spacetime geometry is not singular there.

To determine whether the spacetime geometry is singular at the gravitational radius, send an explorer in from far away to chart it. For simplicity, let him fall freely and radially into the gravitational radius, carrying his orthonormal tetrad with him as he falls. His trajectory through spacetime ["parabolic orbit"; radial geodesic of metric (31.1)] is

$$\begin{aligned} \frac{\tau}{2M} &= -\frac{2}{3}\left(\frac{r}{2M}\right)^{3/2} + \text{constant}, \\ \frac{t}{2M} &= -\frac{2}{3}\left(\frac{r}{2M}\right)^{3/2} - 2\left(\frac{r}{2M}\right)^{1/2} + \ln \left| \frac{(r/2M)^{1/2} + 1}{(r/2M)^{1/2} - 1} \right| + \text{constant}. \end{aligned} \quad (31.2)$$

[See §25.5 and especially equation (25.38) for derivation and discussion.] One obtains the r coordinate of the explorer in terms of the proper time measured on a clock

he carries, $r(\tau)$, by inverting the first equation; one finds his r coordinate in terms of coordinate time, $r(t)$, by inverting the second equation.

Of all the features of the traveler's trajectory, one stands out most clearly and disturbingly: to reach the gravitational radius, $r = 2M$, requires a finite lapse of proper time, but an infinite lapse of coordinate time:

$$\begin{aligned} r/2M &= 1 - (\tau + \text{constant})/2M && \text{when near } r = 2M; \\ r/2M &= 1 + \text{constant} \times \exp(-t/2M) && \text{in limit as } t \rightarrow \infty. \end{aligned} \quad (31.3)$$

An infalling observer reaches $r = 2M$ in finite proper time but infinite coordinate time

(see Fig. 25.5.) Of course, proper time is the relevant quantity for the explorer's heart-beat and health. No coordinate system has the power to prevent him from reaching $r = 2M$. Only the coordinate-independent geometry of spacetime could possibly do that; and equation (31.3) shows it does not!

Let the explorer approach and reach $r = 2M$, then. What spacetime geometry does he measure there? Is it singular or nonsingular? Restated in terms of measurements, do infinite tidal gravitational forces tear the traveler apart and crush him as he approaches $r = 2M$, or does he feel only finite tidal forces which in principle his body can withstand?

The tidal forces felt by the explorer as he passes a given radius r are measured by the components of the Riemann curvature tensor with respect to his orthonormal frame there (equation of geodesic deviation). To calculate those curvature components at r , proceed in two steps. (1) Calculate the components, not in the traveler's frame, but rather in the "static" orthonormal frame

$$\boldsymbol{\omega}^{\hat{t}} = \left(1 - \frac{2M}{r}\right)^{1/2} \mathbf{d}t, \quad \boldsymbol{\omega}^{\hat{r}} = \frac{\mathbf{d}r}{(1 - 2M/r)^{1/2}}, \quad \boldsymbol{\omega}^{\hat{\theta}} = r \mathbf{d}\theta, \quad \boldsymbol{\omega}^{\hat{\phi}} = r \sin \theta \mathbf{d}\phi \quad (31.4a)$$

located at the event through which he is passing; the result [obtainable from equations (14.50) and (14.51) by setting $e^{2\Phi} = e^{-2\Lambda} = 1 - 2M/r$] is

$$\begin{aligned} R_{\hat{t}\hat{r}\hat{t}\hat{r}} &= \frac{-2M}{r^3}, & R_{\hat{t}\hat{\theta}\hat{t}\hat{\theta}} &= R_{\hat{t}\hat{\phi}\hat{t}\hat{\phi}} = \frac{M}{r^3}, \\ R_{\hat{\theta}\hat{\phi}\hat{\theta}\hat{\phi}} &= \frac{2M}{r^3}, & R_{\hat{r}\hat{\theta}\hat{r}\hat{\theta}} &= R_{\hat{r}\hat{\phi}\hat{r}\hat{\phi}} = \frac{-M}{r^3}; \end{aligned} \quad (31.4b)$$

all other $R_{\hat{\alpha}\hat{\beta}\hat{\gamma}\hat{\delta}}$ vanish except those obtainable from the above by symmetries of **Riemann**.

(2) Calculate the components in the explorer's frame by applying to the "static-frame" components (31.4b) the appropriate transformation—for $r > 2M$, a Lorentz boost in the $\mathbf{e}_{\hat{r}}$ direction with ordinary velocity $v^{\hat{r}}$; for $r < 2M$, not a "boost," but a transformation given by the standard boost formula (Box 2.4) with $v^{\hat{r}} > 1$. Here

$$v^{\hat{r}} = \frac{(g_{rr})^{1/2} dr}{(-g_{tt})^{1/2} dt} = \frac{dr/dt}{1 - 2M/r} = -\left(\frac{2M}{r}\right)^{1/2}. \quad (31.5)$$

The amazing result (a consequence of special algebraic properties of the Schwarzschild geometry, and somewhat analogous to what happens—or, rather, does not hap-

pen—to the components of the electromagnetic field, \mathbf{E} and \mathbf{B} , when they are both parallel to a boost) is this: all the components of **Riemann** are left completely unaffected by the boost. If $\mathbf{e}_{\hat{\rho}}$ is the traveler's radial basis vector, and $\mathbf{e}_{\hat{\tau}} = \mathbf{u}$ is his time basis vector, then

$$\begin{aligned} R_{\hat{\tau}\hat{\rho}\hat{\tau}\hat{\rho}} &= -2M/r^3, & R_{\hat{\tau}\hat{\theta}\hat{\tau}\hat{\theta}} &= R_{\hat{\tau}\hat{\phi}\hat{\tau}\hat{\phi}} = M/r^3, \\ R_{\hat{\theta}\hat{\phi}\hat{\theta}\hat{\phi}} &= 2M/r^3, & R_{\hat{\rho}\hat{\theta}\hat{\rho}\hat{\theta}} &= R_{\hat{\rho}\hat{\phi}\hat{\rho}\hat{\phi}} = -M/r^3. \end{aligned} \quad (31.6)$$

(See exercise 31.1.)

The infalling observer does not feel infinite tidal forces at $r = 2M$

Thus, the spacetime geometry is well behaved at $r = 2M$, but the coordinate system is pathological

The payoff of this calculation: according to equations (31.6), none of the components of **Riemann** in the explorer's orthonormal frame become infinite at the gravitational radius. The tidal forces the traveler feels as he approaches $r = 2M$ are finite; they do not tear him apart—at least not when the mass M is sufficiently great, because at $r = 2M$ the typical non-zero component $R_{\hat{\alpha}\hat{\beta}\hat{\gamma}\hat{\delta}}$ of the curvature tensor is of the order $1/M^2$. The gravitational radius is a perfectly well-behaved, nonsingular region of spacetime, and nothing there can prevent the explorer from falling on inward.

By contrast, deep inside the gravitational radius, at $r = 0$, the traveler must encounter infinite tidal forces, independently of the route he uses to reach there. One says that “ $r = 0$ is a physical singularity of spacetime.” To see this, one need only calculate from equation (31.4b) or (31.6) the “curvature invariant”:

$$I \equiv R_{\hat{\alpha}\hat{\beta}\hat{\gamma}\hat{\delta}} R^{\hat{\alpha}\hat{\beta}\hat{\gamma}\hat{\delta}} = 48M^2/r^6. \quad (31.7)$$

Box 31.1 THE “SCHWARZSCHILD SINGULARITY”: HISTORICAL REMARKS

Although Eddington (1924) was the first to construct a coordinate system that is nonsingular at $r = 2M$, he seems not to have recognized the significance of his result. Lemaître (1933c, especially p. 82) appears to have been the first to recognize that the so-called “Schwarzschild singularity” at $r = 2M$ is not a singularity. He wrote, “La singularité du champ de Schwarzschild est donc une singularité fictive, analogue à celle qui se présentait à l’horizon du centre dans la forme originale de l’univers de de Sitter”. He also provided a coordinate system to go through $r = 2M$. However, his coordinate system, like Eddington’s, covered only half of the Schwarzschild geometry:

regions I and II of Figure 31.3. Synge (1950) was the first to discover the incompleteness in the Eddington and Lemaître coordinate systems, and to provide coordinates that cover the entire geometry (regions I, II, III, IV of Figure 31.3). Fronsdal (1959), unaware of Synge’s work, rediscovered the global structure of the Schwarzschild geometry by means of embedding diagrams and calculations. The coordinate system that provides maximum insight into the Schwarzschild geometry is the one generally known as the Kruskal-Szekeres coordinate system. It was constructed independently by Kruskal (1960) and by Szekeres (1960).

In every local Lorentz frame this will be a sum of products of curvature components, and it will have the same value $48M^2/r^6$. Thus, in every local Lorentz frame, including the traveler's, **Riemann** will have one or more infinite components as $r \rightarrow 0$; i.e., tidal forces will become infinite.

At $r = 0$ the curvature is infinite

Exercise 31.1. TIDAL FORCES ON INFALLING EXPLORER

EXERCISE

- (a) Carry out the details of the derivation of the Riemann tensor components (31.6).
- (b) Calculate, roughly, the critical mass M_{crit} such that, if $M > M_{\text{crit}}$ the explorer's body (a human body made of normal flesh and bones) can withstand the tidal forces at $r = 2M$, but if $M < M_{\text{crit}}$ his body is mutilated by them. [Answer: $M_{\text{crit}} \sim 1000M_{\odot}$. Evidently, if $M \sim M_{\odot}$ the physicist should transform himself into an ant before taking the plunge! For details see §32.6.]

§31.3. BEHAVIOR OF SCHWARZSCHILD COORDINATES AT $r = 2M$

Since the spacetime geometry is well behaved at the gravitational radius, the singular behavior there of the Schwarzschild metric components, $g_{tt} = -(1 - 2M/r)$ and $g_{rr} = (1 - 2M/r)^{-1}$, must be due to a pathology there of the Schwarzschild coordinates t, r, θ, ϕ . Somehow one must find a way to get rid of that pathology—i.e., one must construct a new coordinate system from which the pathology is absent. Before doing this, it is helpful to understand better the precise nature of the pathology.

The most obvious pathology at $r = 2M$ is the reversal there of the roles of t and r as timelike and spacelike coordinates. In the region $r > 2M$, the t direction, $\partial/\partial t$, is timelike ($g_{tt} < 0$) and the r direction, $\partial/\partial r$, is spacelike ($g_{rr} > 0$); but in the region $r < 2M$, $\partial/\partial t$ is spacelike ($g_{tt} > 0$) and $\partial/\partial r$ is timelike ($g_{rr} < 0$).

What does it mean for r to “change in character from a spacelike coordinate to a timelike one”? The explorer in his jet-powered spaceship prior to arrival at $r = 2M$ always has the option to turn on his jets and change his motion from decreasing r (infall) to increasing r (escape). Quite the contrary is the situation when he has once allowed himself to fall inside $r = 2M$. Then the further decrease of r represents the passage of time. No command that the traveler can give to his jet engine will turn back time. That unseen power of the world which drags everyone forward willy-nilly from age twenty to forty and from forty to eighty also drags the rocket in from time coordinate $r = 2M$ to the later value of the time coordinate $r = 0$. No human act of will, no engine, no rocket, no force (see exercise 31.3) can make time stand still. As surely as cells die, as surely as the traveler's watch ticks away “the unforgiving minutes,” with equal certainty, and with never one halt along the way, r drops from $2M$ to 0.

At $r = 2M$, where r and t exchange roles as space and time coordinates, g_{tt} vanishes while g_{rr} is infinite. The vanishing of g_{tt} suggests that the surface $r = 2M$, which

Nature of the coordinate pathology at $r = 2M$:

- (1) t and r reverse roles as timelike and spacelike coordinates

- (2) the region $r = 2M$, $-\infty < t < +\infty$ is two-dimensional rather than three

appears to be three-dimensional in the Schwarzschild coordinate system ($-\infty < t < +\infty$, $0 < \theta < \pi$, $0 < \phi < 2\pi$) has zero volume and thus is actually only two-dimensional, or else is null; thus,

$$\int_{r=2M} |g_{tt}g_{\theta\theta}g_{\phi\phi}|^{1/2} dt d\theta d\phi = 0; \quad (31.8)$$

$$\int_{(r=2M, t=\text{const})} |g_{\theta\theta}g_{\phi\phi}|^{1/2} d\theta d\phi = 4\pi(2M)^2.$$

The divergence of g_{rr} at $r = 2M$ does *not* mean that $r = 2M$ is infinitely far from all other regions of spacetime. On the contrary, the proper distance from $r = 2M$ to a point with arbitrary r is

$$\int_{2M}^r |g_{rr}|^{1/2} dr = \begin{cases} [r(r - 2M)]^{1/2} + 2M \ln |(r/2M - 1)^{1/2} + (r/2M)^{1/2}| & \text{when } r > 2M, \\ -2M \cot^{-1}[r^{1/2}/(2M - r)^{1/2}] - [r(2M - r)]^{1/2} & \text{when } r < 2M, \end{cases} \quad (31.9)$$

which is finite for all $0 < r < \infty$.

Just how the region $r < 2M$ is physically connected to the region $r > 2M$ can be discovered by examining the radial geodesics of the Schwarzschild metric. Focus attention, for concreteness, on the trajectory of a test particle that gets ejected from the singularity at $r = 0$, flies radially outward through $r = 2M$, reaches a maximum radius r_{\max} (“top of orbit”) at proper time $\tau = 0$ and coordinate time $t = 0$, and then falls back down through $r = 2M$ to $r = 0$. The solution of the geodesic equation for such an orbit was derived in §25.5 and described in Figure 25.3. It has the “cycloid form” (with the parameter η running from $-\pi$ to $+\pi$),

$$r = \frac{1}{2} r_{\max}(1 + \cos \eta), \quad (31.10a)$$

$$\tau = (r_{\max}^3/8M)^{1/2}(\eta + \sin \eta), \quad (31.10b)$$

$$t = 2M \ln \left| \frac{(r_{\max}/2M - 1)^{1/2} + \tan(\eta/2)}{(r_{\max}/2M - 1)^{1/2} - \tan(\eta/2)} \right| + 2M \left(\frac{r_{\max}}{2M} - 1 \right)^{1/2} \left[\eta + \left(\frac{r_{\max}}{4M} \right)(\eta + \sin \eta) \right]. \quad (31.10c)$$

Figure 31.1 plots this orbit in the r , t -coordinate plane (curve $F-F'-F''$), along with several other types of radial geodesics.

- (3) radial geodesics reveal that the regions $r = 2M$, $t = \pm\infty$ are “finite” parts of spacetime

Every radial geodesic except a “set of geodesics of measure zero” crosses the gravitational radius at $t = +\infty$ (or at $t = -\infty$, or both), according to Figure 31.1 and the calculations behind that figure (exercises for the student! See Chapter 25). One therefore suspects that all the physics at $r = 2M$ is consigned to $t = \pm\infty$ by reason of some unhappiness in the choice of the Schwarzschild coordinates. A better coordinate system, one begins to believe, will take these two “points at infinity” and

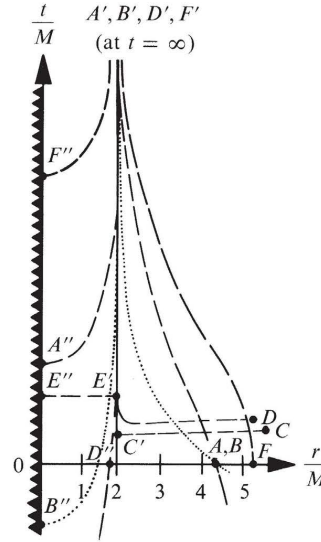


Figure 31.1.

Typical radial geodesics of the Schwarzschild geometry, as charted in Schwarzschild coordinates (schematic). $FF'F''$ [see equations (31.10)] is the timelike geodesic of a test particle that starts at rest at $r = 5.2M$ and falls straight in, arriving in a finite proper time at the singularity $r = 0$ (zig-zag marking). The unhappiness of the Schwarzschild coordinate system shows in two ways: (1) in the fact that t goes to ∞ partway through the motion; and (2) in the fact that t thereafter decreases as τ (not shown) continues to increase. The course of the same trajectory prior to $t = 0$ may be constructed by reflecting the diagram in the horizontal axis (“time inversion”). The time-reversed image of F'' marks the ejection of the test particle from the singularity. $AA'A''$ is a timelike geodesic which comes in from $r = +\infty$. $BB'B''$ is the null geodesic travelled by a photon that falls straight in (no summit; never at rest!). $DD'D''$ is a spacelike radial geodesic. So is CC' , but $E'E''$ is timelike. Neither of the latter two ever succeed in crossing $r = 2M$. (Unanswered questions about these geodesics will answer themselves in Figure 31.4, where the same world lines are charted in a “Kruskal-Szekeres diagram”).

Described mathematically via equation (31.10), the geodesic $F'' \text{ inverse } F' \text{ inverse } FF'F''$ starts with ejection at

$$r = 0 \text{ at } t = -2\pi M \left(\frac{r_{\max}}{2M} - 1 \right)^{1/2} \left(\frac{r_{\max}}{4M} + 1 \right), \quad \tau = -\frac{\pi}{2} \left(\frac{r_{\max}^3}{2M} \right)^{1/2};$$

it flies outward with increasing proper time τ , but decreasing coordinate time, t , until it reaches the gravitational radius

$$r = 2M \text{ at } t = -\infty, \quad \tau = -\left(\frac{r_{\max}^3}{8M} \right)^{1/2} \cos^{-1} \left(\frac{4M}{r_{\max}} - 1 \right) - r_{\max} \left(1 - \frac{2M}{r_{\max}} \right)^{1/2};$$

it then continues to fly on outward, but with coordinate time now increasing from $t = -\infty$, until it reaches its maximum radius

$$r = r_{\max} \text{ at } t = 0, \quad \tau = 0 \text{ (event } F \text{ in diagram);}$$

it then falls inward, with t continuing to increase, until it crosses the gravitational radius again

$$r = 2M \text{ at } t = +\infty, \quad \tau = +\left(\frac{r_{\max}^3}{8M} \right)^{1/2} \cos^{-1} \left(\frac{4M}{r_{\max}} - 1 \right) + r_{\max} \left(1 - \frac{2M}{r_{\max}} \right)^{1/2} \\ \text{(event } F' \text{ in diagram);}$$

and it finally falls on in with decreasing t (but, of course, still increasing τ) to

$$r = 0 \text{ at } t = +2\pi M \left(\frac{r_{\max}}{2M} - 1 \right)^{1/2} \left(\frac{r_{\max}}{4M} + 1 \right), \quad \tau = +\frac{\pi}{2} \left(\frac{r_{\max}^3}{2M} \right)^{1/2} \\ \text{(event } F'' \text{ in diagram).}$$

spread them out into a line in a new $(r_{\text{new}}, t_{\text{new}})$ -plane; and will squeeze the “line” ($r = 2M$, t from $-\infty$ to $+\infty$) into a single point in the $(r_{\text{new}}, t_{\text{new}})$ -plane. One is the more prepared to accept this tentative conclusion and act on it because one has already seen (equation 31.8) that the region covering the (θ, ϕ) 2-sphere at $r = 2M$, and extending from $t = -\infty$ to $t = +\infty$, has zero proper volume. What timelier indication could one want that the “line” $r = 2M$, $-\infty < t < \infty$, is actually a point?

§31.4. SEVERAL WELL-BEHAVED COORDINATE SYSTEMS

The well-behaved coordinate system that is easiest to visualize is one in which the radially moving test particles of equations (31.10) remain always at rest (“comoving coordinates”). Such coordinates were first used by Novikov (1963). Novikov attaches a specific value of his radial coordinate, R^* , to each test particle as it emerges from the singularity of infinite tidal forces at $r = 0$, and insists that the particle carry that value of R^* throughout its “cycloidal life”—up through $r = 2M$ to $r = r_{\text{max}}$, then back down through $r = 2M$ to $r = 0$. For definiteness, Novikov expresses the R^* value for each particle in terms of the peak point on its trajectory by

$$R^* = (r_{\text{max}}/2M - 1)^{1/2}. \quad (31.11)$$

As a time coordinate, Novikov uses proper time τ of the test particles, normalized so $\tau = 0$ at the peak of the orbit. Every particle in the swarm is ejected in such a manner that it arrives at the summit of its trajectory ($r = r_{\text{max}}$, $\tau = 0$) at one and the same value of the Schwarzschild coordinate time; namely, at $t = 0$.

Simple though they may be conceptually, the Novikov coordinates are related to the original Schwarzschild coordinates by a very complicated transformation: (1) combine equations (31.10b) and (31.11) to obtain $\eta(\tau, R^*)$; (2) combine $\eta(\tau, R^*)$ with (31.10a) and (31.11) to obtain $r(\tau, R^*)$; (3) combine $\eta(\tau, R^*)$ with (31.10c) and (31.11) to obtain $t(\tau, R^*)$. The resulting coordinate transformation, when applied to the Schwarzschild metric (31.1), yields the line element

(2) line element

$$ds^2 = -d\tau^2 + \left(\frac{R^{*2} + 1}{R^{*2}} \right) \left(\frac{\partial r}{\partial R^*} \right)^2 dR^{*2} + r^2(d\theta^2 + \sin^2\theta d\phi^2). \quad (31.12a)$$

(“Schwarzschild geometry in Novikov coordinates”.) Here r is no longer a radial coordinate; it is now a metric function $r(\tau, R^*)$ given implicitly by

$$\frac{\tau}{2M} = \pm (R^{*2} + 1) \left[\frac{r}{2M} - \frac{(r/2M)^2}{R^{*2} + 1} \right]^{1/2} + (R^{*2} + 1)^{3/2} \cos^{-1} \left[\left(\frac{r/2M}{R^{*2} + 1} \right)^{1/2} \right]. \quad (31.12b)$$

Figure 31.2 shows the locations of several key regions of Schwarzschild spacetime in this coordinate system. The existence of two distinct regions with $r = 0$ (singularities) and two distinct regions with $r \rightarrow \infty$ (asymptotically flat regions; recall that $4\pi r^2 = \text{surface area!}$) will be discussed in §31.5.

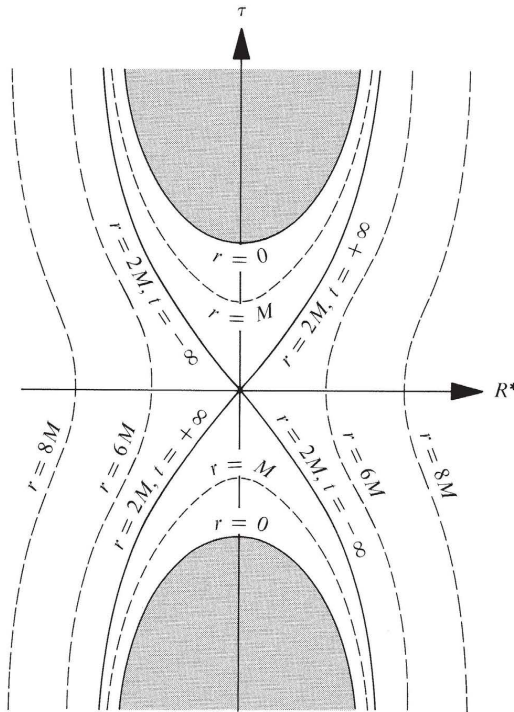


Figure 31.2.

The Novikov coordinate system for Schwarzschild spacetime (schematic). The dashed curves are curves of constant r (recall: $4\pi r^2 = \text{surface area about center of symmetry}$). The region shaded gray is not part of spacetime; it corresponds to $r < 0$, a region that cannot be reached because of the singularity of spacetime at $r = 0$. Notice that the “line” ($r = 2M$, $-\infty < t < +\infty$) of the Schwarzschild coordinate diagram (Figure 31.1) has been compressed into a point here, in accordance with the discussion at the end of §31.3.

Although Novikov’s coordinate system is very simple conceptually, the mathematical expressions for the metric components in it are rather unwieldy. Simpler, more usable expressions have been obtained in a different coordinate system (“Kruskal-Szekeres coordinates”) by Kruskal (1960), and independently by Szekeres (1960).

Kruskal and Szekeres use a dimensionless radial coordinate u and a dimensionless time coordinate v related to the Schwarzschild r and t by

$$\left. \begin{array}{l} u = (r/2M - 1)^{1/2} e^{r/4M} \cosh(t/4M) \\ v = (r/2M - 1)^{1/2} e^{r/4M} \sinh(t/4M) \end{array} \right\} \text{when } r > 2M, \quad (31.13a)$$

$$\left. \begin{array}{l} u = (1 - r/2M)^{1/2} e^{r/4M} \sinh(t/4M) \\ v = (1 - r/2M)^{1/2} e^{r/4M} \cosh(t/4M) \end{array} \right\} \text{when } r < 2M. \quad (31.13b)$$

Kruskal-Szekeres coordinates

(Motivation for introducing such coordinates is given in Box 31.2.) By making this change of coordinates in the Schwarzschild metric (31.1), one obtains the following line element:

$$ds^2 = (32M^3/r)e^{-r/2M}(-dv^2 + du^2) + r^2(d\theta^2 + \sin^2\theta d\phi^2) \quad (31.14a)$$

(“Schwarzschild geometry in Kruskal-Szekeres coordinates”). Here r is to be regarded as a function of u and v defined implicitly by

$$(r/2M - 1)e^{r/2M} = u^2 - v^2 \quad (31.14b)$$

[cf. equations (31.13)].

(continued on page 833)

Box 31.2 MOTIVATION FOR KRUSKAL-SZEKERES COORDINATES***A. EDDINGTON-FINKELSTEIN COORDINATES**

The motivation for the Kruskal-Szekeres system begins by introducing a different coordinate system, first devised by Eddington (1924) and rediscovered by Finkelstein (1958). Eddington and Finkelstein use as the foundation of their coordinate system, not freely falling particles as did Novikov, but freely falling photons. More particularly, they introduce coordinates \tilde{U} and \tilde{V} , which are labels for outgoing and ingoing, radial, null geodesics. The geodesics are given by

$$ds^2 = 0 = -(1 - 2M/r) dt^2 + (1 - 2M/r)^{-1} dr^2.$$

Equivalently, outgoing geodesics are given by $\tilde{U} = \text{const}$, where

$$\tilde{U} \equiv t - r^*; \quad (1a)$$

and ingoing geodesics are given by $\tilde{V} = \text{const}$, where

$$\tilde{V} \equiv t + r^*. \quad (1b)$$

Here r^* is the “tortoise coordinate” of §25.5 and Figure 25.4:

$$r^* \equiv r + 2M \ln |r/2M - 1|. \quad (1c)$$

Ingoing Eddington-Finkelstein Coordinates—Adopt r and \tilde{V} as coordinates in place of r and t

The Schwarzschild metric becomes.

$$ds^2 = -(1 - 2M/r) d\tilde{V}^2 + 2 d\tilde{V} dr + r^2 d\Omega^2. \quad (2)$$

The radial light cone, $ds^2 = 0$, has one leg

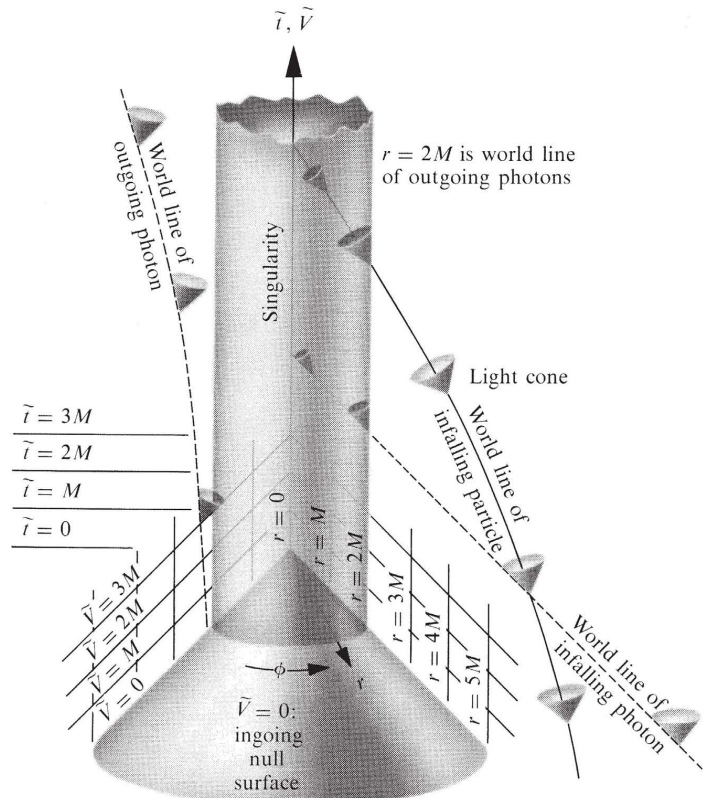
$$d\tilde{V}/dr = 0, \quad (3a)$$

and the other leg

$$\frac{d\tilde{V}}{dr} = \frac{2}{1 - 2M/r}. \quad (3b)$$

From this, and this alone, one can infer all features of the drawing.

*This box is based on Misner (1969a).



Ingoing Eddington-Finkelstein coordinates (one rotational degree of freedom is suppressed; i.e., θ is set equal to $\pi/2$). Surfaces of constant \tilde{V} , being ingoing null surfaces, are plotted on a 45-degree slant, just as they would be in flat spacetime. Equivalently, surfaces of constant

$$\tilde{t} \equiv \tilde{V} - r = t + 2M \ln |r/2M - 1|$$

are plotted as horizontal surfaces.

Outgoing Eddington-Finkelstein Coordinates—Adopt r and \tilde{U} as coordinates in place of r and t

The Schwarzschild metric becomes

$$ds^2 = -(1 - 2M/r) d\tilde{U}^2 - 2 d\tilde{U} dr + r^2 d\Omega^2. \quad (4)$$

Box 31.2 (continued)

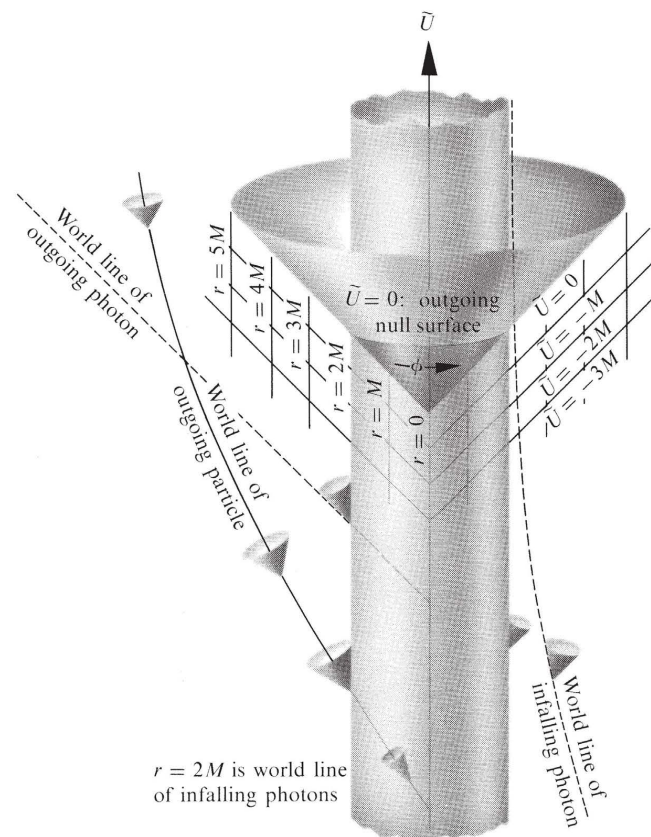
The radial light cone, $ds^2 = 0$, has one leg

$$d\tilde{U}/dr = 0, \quad (5a)$$

and the other leg

$$\frac{d\tilde{U}}{dr} = -\frac{2}{1-2M/r}. \quad (5b)$$

From this, and this alone, one can infer all features of the drawing.



Outgoing Eddington-Finkelstein coordinates (one rotational degree of freedom is suppressed). (Surfaces of constant \tilde{U} , being outgoing null surfaces, are plotted on a 45-degree slant, just as they would be in flat spacetime.)

Notice that both Eddington-Finkelstein coordinate systems are better behaved at the gravitational radius than is the Schwarzschild coordinate system; but they are not *fully* well-behaved. The outgoing coordinates $(\tilde{U}, r, \theta, \phi)$ describe in a non-pathological manner the ejection of particles outward from $r = 0$ through $r = 2M$; but their description of infall through $r = 2M$ has the same pathology as the description given by Schwarzschild coordinates (Figure 31.1). Similarly, the ingoing coordinates $(\tilde{V}, r, \theta, \phi)$ describe well the infall of a particle through $r = 2M$, but they give a pathological description of outgoing trajectories. Moreover, the contrast between the two diagrams seems paradoxical: in one the gravitational radius is made up of world lines of outgoing photons; in the other it is made up of world lines of ingoing photons! To resolve the paradox, one must seek another, better-behaved coordinate system. [But *note*: because the ingoing Eddington-Finkelstein coordinates describe infall so well, they are used extensively in discussions of gravitational collapse (Chapter 32) and black holes (Chapters 33 and 34).]

B. TRANSITION FROM EDDINGTON-FINKELSTEIN TO KRUSKAL-SZEKERES

Perhaps one would obtain a fully well-behaved coordinate system by dropping r from view and using \tilde{U} , \tilde{V} , as the two coordinates in the radial-time plane. The resulting coordinate system is related to Schwarzschild coordinates by [see equations (1)]

$$\tilde{V} - \tilde{U} = 2r^*, \quad (6a)$$

$$\tilde{V} + \tilde{U} = 2t; \quad (6b)$$

and the line element in terms of the new coordinates reads

$$ds^2 = -(1 - 2M/r) d\tilde{U} d\tilde{V} + r^2(d\theta^2 + \sin^2\theta d\phi^2). \quad (7)$$

Contrary to one's hopes, this coordinate system is pathological at $r = 2M$.

Second thoughts about the construction reveal the trouble: the surfaces $\tilde{U} =$ constant (outgoing null surfaces) used in constructing it are geometrically well-defined, as are the surfaces $\tilde{V} =$ constant (ingoing null surfaces); but the way of labeling them is not. Any relabeling, $\tilde{u} = F(\tilde{U})$ and $\tilde{v} = G(\tilde{V})$, will leave the surfaces unchanged physically. What one needs is a relabeling that will get rid of the singular factor $1 - 2M/r$ in the line element (7). A successful relabeling is suggested by the equation

$$\exp[(\tilde{V} - \tilde{U})/4M] = \exp(r^*/2M) = (r/2M - 1) \exp(r/2M), \quad (8)$$

Box 31.2 (continued)

which follows from equations (6a) and (1c). Experimenting with this relation quickly reveals that the relabeling

$$\tilde{u} \equiv -e^{-\tilde{v}/4M} = -(r/2M - 1)^{1/2} e^{r/4M} e^{-t/4M}, \quad (9a)$$

$$\tilde{v} \equiv e^{+\tilde{v}/4M} = (r/2M - 1)^{1/2} e^{r/4M} e^{t/4M}, \quad (9b)$$

will remove the offending $1 - 2M/r$ from the metric coefficients. In terms of these new coordinates, the line element reads

$$ds^2 = -(32M^3/r)e^{-r/2M} d\tilde{v} d\tilde{u} + r^2(d\theta^2 + \sin^2\theta d\phi^2). \quad (10a)$$

Here r is still defined by $4\pi r^2 = \text{surface area}$, but it must be regarded as a function of \tilde{v} and \tilde{u} :

$$(r/2M - 1)e^{r/2M} = -\tilde{u}\tilde{v}. \quad (10b)$$

One can readily verify that this equation determines r uniquely (recall: $r > 0!$) in terms of the product $\tilde{u}\tilde{v}$ [details in Misner (1969a)].

The coordinates, \tilde{u}, \tilde{v} , which label the ingoing and outgoing null surfaces, are null coordinates; i.e.,

$$\partial/\partial\tilde{u} \cdot \partial/\partial\tilde{u} = g_{\tilde{u}\tilde{u}} = 0, \quad \partial/\partial\tilde{v} \cdot \partial/\partial\tilde{v} = g_{\tilde{v}\tilde{v}} = 0$$

[see equation (10a)]. If one is not accustomed to working with null coordinates, it is helpful to replace \tilde{u} and \tilde{v} by spacelike and timelike coordinates, u and v (Kruskal-Szekeres coordinates!) defined by

$$u \equiv \frac{1}{2}(\tilde{v} - \tilde{u}) = (r/2M - 1)^{1/2} e^{r/4M} \cosh(t/4M), \quad (11a)$$

$$v \equiv \frac{1}{2}(\tilde{v} + \tilde{u}) = (r/2M - 1)^{1/2} e^{r/4M} \sinh(t/4M), \quad (11b)$$

so that

$$dv^2 - du^2 = d\tilde{v} d\tilde{u}. \quad (12)$$

In terms of these coordinates, the line element has the Kruskal form (31.14), which is fully well-behaved at the gravitational radius.

Although the Kruskal-Szekeres line element is well behaved at $r = 2M$, the transformation (11) from Schwarzschild to Kruskal-Szekeres is not; it becomes meaningless (u and v “imaginary”) when one moves from $r > 2M$ to $r < 2M$. Of course, this is a manifestation of the pathologies of Schwarzschild coordinates. By trial and error, one readily finds a new transformation, to replace (11) at $r < 2M$, leading from Schwarzschild to Kruskal-Szekeres coordinates:

$$u = (1 - r/2M)^{1/2} e^{r/4M} \sinh(t/4M), \quad (11c)$$

$$v = (1 - r/2M)^{1/2} e^{r/4M} \cosh(t/4M). \quad (11d)$$

§31.5. RELATIONSHIP BETWEEN KRUSKAL-SZEKERES COORDINATES AND SCHWARZSCHILD COORDINATES

In the Kruskal-Szekeres coordinate system, the singularity $r = 0$ is located at $v^2 - u^2 = 1$. Thus there are actually *two* singularities, not one; both

$$v = +(1 + u^2)^{1/2} \text{ and } v = -(1 + u^2)^{1/2} \text{ correspond to } r = 0! \quad (31.15)$$

Kruskal-Szekeres coordinates reveal that Schwarzschild spacetime has two “ $r = 0$ singularities” and two “ $r \rightarrow \infty$ exterior regions”

This is not the only surprise that lies hidden in the Kruskal-Szekeres line element (31.14). Notice also that $r \gg 2M$ (the region of spacetime far outside the gravitational radius) is given by $u^2 \gg v^2$. Thus there are actually *two* exterior regions*; both

$$u \gg +|v| \text{ and } u \ll -|v| \text{ correspond to } r \gg 2M! \quad (31.16)$$

How can this be? When the geometry is charted in Schwarzschild coordinates, it contains one singularity and one exterior region; but when expressed in Kruskal-Szekeres coordinates, it shows two of each. The answer must be that the Schwarzschild coordinates cover only part of the spacetime manifold; they must be only a local coordinate patch on the full manifold. Somehow, by means of the coordinate transformation that leads to Kruskal-Szekeres coordinates, one has analytically extended the limited Schwarzschild solution for the metric to cover all (or more nearly all) of the manifold.

To understand this covering more clearly, transform back from Kruskal-Szekeres coordinates to Schwarzschild coordinates (see Figure 31.3). The transformation equations, as written down in (31.13) were valid only for the quadrants $u > |v|$ [equation (31.13a)] and $v > |u|$ [equation (31.13b)] of Kruskal coordinates. Denote these quadrants by the numerals I and II; and denote the other quadrants by III and IV (see Figure 31.3). In the other quadrants, one can also transform the Kruskal-Szekeres line element (31.14) into the Schwarzschild line element (31.1); but slightly different transformation equations are needed. One easily verifies that the following sets of transformations work:

$$(I) \begin{cases} u = (r/2M - 1)^{1/2} e^{r/4M} \cosh(t/4M) \\ v = (r/2M - 1)^{1/2} e^{r/4M} \sinh(t/4M) \end{cases}, \quad (31.17a)$$

$$(II) \begin{cases} u = (1 - r/2M)^{1/2} e^{r/4M} \sinh(t/4M) \\ v = (1 - r/2M)^{1/2} e^{r/4M} \cosh(t/4M) \end{cases}, \quad (31.17b)$$

$$(III) \begin{cases} u = -(r/2M - 1)^{1/2} e^{r/4M} \cosh(t/4M) \\ v = -(r/2M - 1)^{1/2} e^{r/4M} \sinh(t/4M) \end{cases}, \quad (31.17c)$$

$$(IV) \begin{cases} u = -(1 - r/2M)^{1/2} e^{r/4M} \sinh(t/4M) \\ v = -(1 - r/2M)^{1/2} e^{r/4M} \cosh(t/4M) \end{cases}. \quad (31.17d)$$

Transformation between Schwarzschild coordinates and Kruskal-Szekeres coordinates

*The global structure of the Schwarzschild geometry, including the existence of two singularities and two exterior regions, was first discovered by Synge (1950). See Box 31.1.

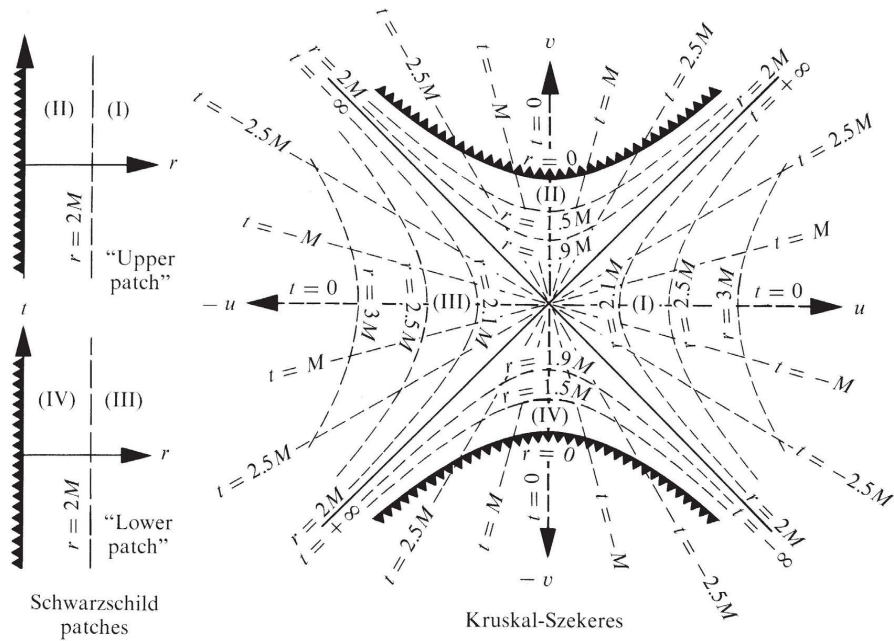


Figure 31.3.

The transformation of the Schwarzschild vacuum geometry between Schwarzschild and Kruskal-Szekeres coordinates. Two Schwarzschild coordinate patches I, II, and III, IV (illustrated in the upper and lower portions of Figure 31.5.a) are required to cover the complete Schwarzschild geometry, whereas a single Kruskal-Szekeres coordinate system suffices. The Schwarzschild geometry consists of four regions I, II, III, IV. Regions I and III represent two distinct, but identical, asymptotically flat universes in which $r > 2M$; while regions II and IV are two identical, but time-reversed, regions in which physical singularities ($r = 0$) evolve. The transformation laws that relate the Schwarzschild and Kruskal-Szekeres coordinate systems to each other are given by equations (31.17) and (31.18). In the Kruskal-Szekeres u,v -plane, curves of constant r are hyperbolae with asymptotes $u = \pm v$, while curves of constant t are straight lines through the origin.

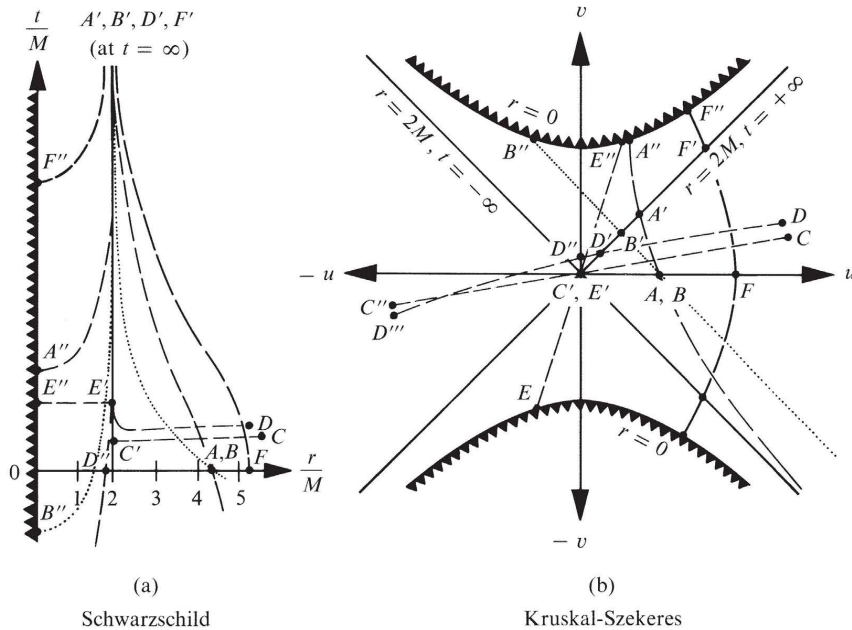
The inverse transformations are

$$(r/2M - 1)e^{r/2M} = u^2 - v^2 \text{ in I, II, III, IV;} \quad (31.18a)$$

$$t = \begin{cases} 4M \tanh^{-1}(v/u) & \text{in I and III,} \\ 4M \tanh^{-1}(u/v) & \text{in II and IV.} \end{cases} \quad (31.18b)$$

Two Schwarzschild coordinate patches are required to cover all of spacetime

These coordinate transformations are exhibited graphically in Figure 31.3. Notice that two Schwarzschild coordinate patches, I, II, and III, IV, are required to cover the entire Schwarzschild geometry; but a single Kruskal coordinate system suffices. Schwarzschild patch I, II, is divided into two regions—region I, which is outside the gravitational radius ($r > 2M$), and region II, which is inside the gravitational radius ($r < 2M$). Similarly, Schwarzschild patch III, IV, consists of an exterior region (III) and an interior region (IV).

**Figure 31.4.**

(a) Typical radial timelike (A, E, F), lightlike (B), and spacelike (C, D) geodesics of the Schwarzschild geometry, as seen in the Schwarzschild coordinate system (schematic only). This is a reproduction of Figure 31.1.

(b) The same geodesics, as seen in the Kruskal-Szekeres coordinate system, and as extended either to infinite length or to the singularity of infinite curvature at $r = 0$ (schematic only).

Equations (31.18) reveal that the regions of constant r (constant surface area) are hyperbolae with asymptotes $u = \pm v$ in the Kruskal-Szekeres diagram, and that regions of constant t are straight lines through the origin.

Several radial geodesics of the complete Schwarzschild geometry are depicted in the Kruskal-Szekeres coordinate system in Figure 31.4. Notice how much more reasonable the geodesic curves look in Kruskal-Szekeres coordinates than in Schwarzschild coordinates. Notice also that *radial, lightlike geodesics (paths of radial light rays) are 45-degree lines in the Kruskal-Szekeres coordinate system*. This can be seen from the Kruskal-Szekeres line element (31.14), for which $du = \pm dv$ guarantees $ds = 0$. Because of this 45-degree property, the radial light cone in a Kruskal-Szekeres diagram has the same form as in the space-time diagram of special relativity. Any radial curve that points “generally upward” (i.e., makes an angle of less than 45 degrees with the vertical, v , axis) is timelike; and curves that point “generally outward” are spacelike. This property enables a Kruskal-Szekeres diagram to exhibit easily the causality relation between one event in spacetime and another (see exercises 31.2 to 31.4).

Properties of the
Kruskal-Szekeres coordinate
system

EXERCISES**Exercise 31.2. NONRADIAL LIGHT CONES**

Show that the world line of a photon traveling nonradially makes an angle less than 45 degrees with the vertical v -axis of a Kruskal-Szekeres coordinate diagram. From this, infer that particles with finite rest mass, traveling nonradially or radially, must always move “generally upward” (angle less than 45 degrees with vertical v -axis).

Exercise 31.3. THE CRACK OF DOOM

Use a Kruskal diagram to show the following.

- (a) If a man allows himself to fall through the gravitational radius $r = 2M$, there is no way whatsoever for him to avoid hitting (and being killed in) the singularity at $r = 0$.
- (b) Once a man has fallen inward through $r = 2M$, there is no way whatsoever that he can send messages out to his friends at $r > 2M$, but he can still receive messages from them (e.g., by radio waves, or laser beam, or infalling “CARE packages”).

Exercise 31.4. HOW LONG TO LIVE?

Show that once a man falling inward reaches the gravitational radius, no matter what he does subsequently (no matter in what directions, how long, and how hard he blasts his rocket engines), he will be pulled into the singularity and killed in a proper time of

$$\tau < \tau_{\max} = \pi M = 1.54 \times 10^{-5}(M/M_{\odot}) \text{ seconds.} \quad (31.19)$$

[Hint: The trajectory of longest proper time lapse must be a geodesic. Use the mathematical tools of Chapter 25 to show that the geodesic of longest proper time lapse between $r = 2M$ and $r = 0$ is the radial geodesic (31.10a), with $r_{\max} = 2M$, for which the time lapse is πM .]

Exercise 31.5. EDDINGTON-FINKELSTEIN AND KRUSKAL-SZEKERES COMPARED

Use coordinate diagrams to compare the ingoing and outgoing Eddington-Finkelstein coordinates of Box 31.2 with the Kruskal-Szekeres coordinates. Pattern the comparison after that between Schwarzschild and Kruskal-Szekeres in Figures 31.3 and 31.4.

Exercise 31.6. ANOTHER COORDINATE SYSTEM

Construct a coordinate diagram for the $\tilde{U}, \tilde{V}, \theta, \phi$ coordinate system of Box 31.2 [equations (6) and (7)]. Show such features as (1) the relationship to Schwarzschild and to Kruskal-Szekeres coordinates; (2) the location of $r = 2M$; and (3) radial geodesics.

§31.6. DYNAMICS OF THE SCHWARZSCHILD GEOMETRY

What does the Schwarzschild geometry look like? This question is most readily answered by means of embedding diagrams analogous to those for an equilibrium star (§23.8; Figure 23.1; and end of Box 23.2) and for Friedmann universes of positive and negative spatial curvature [equations (27.23) and (27.24) and Box 27.2].

Examine, first, the geometry of the spacelike hypersurface $v = 0$, which extends from $u = +\infty$ ($r = \infty$) into $u = 0$ ($r = 2M$) and then out to $u = -\infty$ ($r = \infty$). In Schwarzschild coordinates this surface is a slice of constant time, $t = 0$ [see equation (31.18b)]; it is precisely the surface for which an embedding diagram was calculated in equation (23.34b). The embedded surface, with one degree of rotational freedom suppressed, is described by the paraboloid of revolution

$$\bar{r} = 2M + \bar{z}^2/8M \quad (31.20)$$

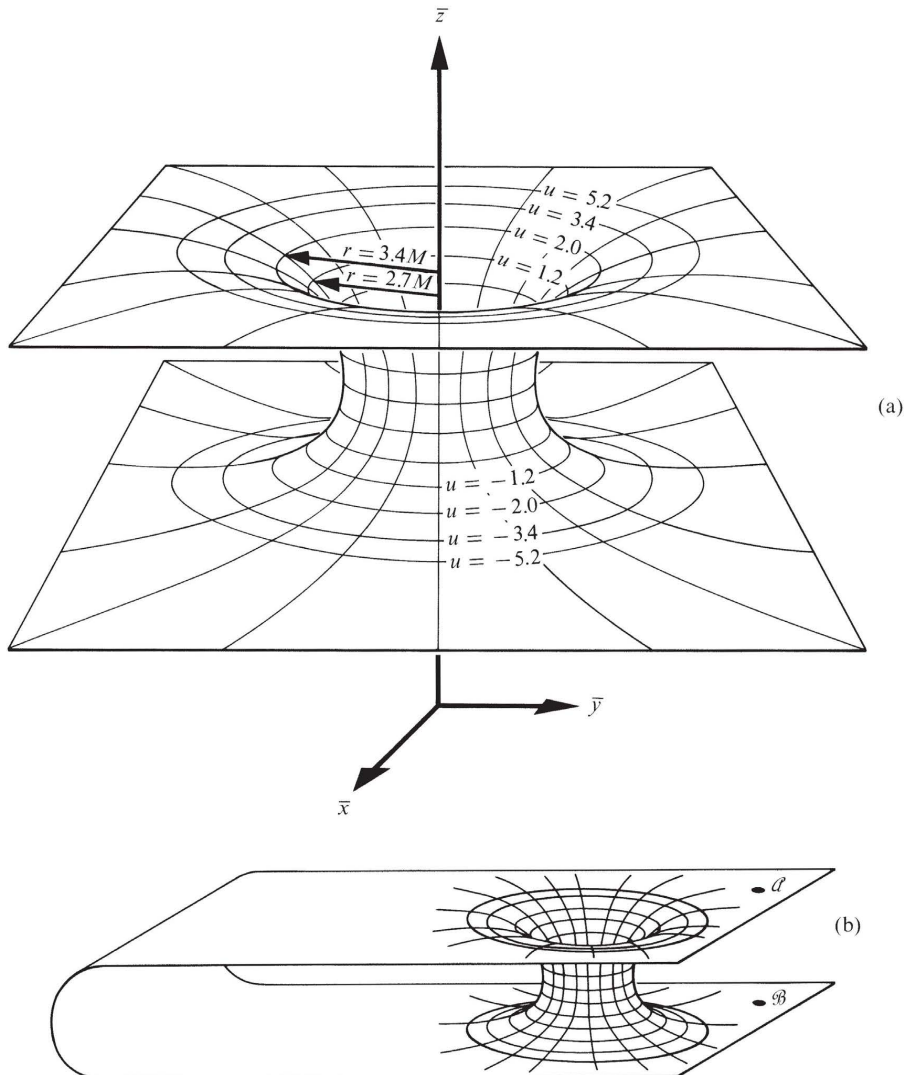


Figure 31.5.

(a) The Schwarzschild space geometry at the “moment of time” $t = v = 0$, with one degree of rotational freedom suppressed ($\theta = \pi/2$). To restore that rotational freedom and obtain the full Schwarzschild 3-geometry, one mentally replaces the circles of constant $\bar{r} = (\bar{x}^2 + \bar{y}^2)^{1/2}$ with spherical surfaces of area $4\pi\bar{r}^2$. Note that the resultant 3-geometry becomes flat (Euclidean) far from the throat of the bridge in both directions (both “universes”).

(b) An embedding of the Schwarzschild space geometry at “time” $t = v = 0$, which is geometrically identical to the embedding (a), but which is topologically different. Einstein’s field equations fix the local geometry of spacetime, but they do not fix its topology; see the discussion at end of Box 27.2. Here the Schwarzschild “wormhole” connects two distant regions of a single, asymptotically flat universe. For a discussion of issues of causality associated with this choice of topology, see Fuller and Wheeler (1962).

in the flat Euclidean space with metric

$$d\sigma^2 = d\bar{r}^2 + d\bar{z}^2 + \bar{r}^2 d\bar{\phi}^2. \quad (31.21)$$

(See Figure 31.5.)

Notice from the embedding diagram of Figure 31.5,a, that the Schwarzschild

The 3-surface $v = t = 0$ is a “wormhole” connecting two asymptotically flat universes, or two different regions of one universe

Schwarzschild geometry is dynamic in regions $r < 2M$

Time evolution of the wormhole: creation; expansion; recontraction; and pinch-off

Communication through the wormhole is impossible: it pinches off too fast

geometry on the spacelike hypersurface $t = \text{const}$ consists of a bridge or “wormhole” connecting two distinct, but identical, asymptotically flat universes. This bridge is sometimes called the “Einstein-Rosen bridge” and sometimes the “Schwarzschild throat” or the “Schwarzschild wormhole.” If one so wishes, one can change the topology of the Schwarzschild geometry by connecting the two asymptotically flat universes together in a region distant from the Schwarzschild throat [Fuller and Wheeler (1962); Fig. 31.5b]. The single, unique universe then becomes multiply connected, with the Schwarzschild throat providing one spacelike path from point \mathcal{A} to point \mathcal{B} , and the nearly flat universe providing another. For concreteness, focus attention on the interpretation of the Schwarzschild geometry, not in terms of Wheeler’s multiply connected single universe, but rather in terms of the Einstein-Rosen double universe of Figure 31.5,a.

One is usually accustomed to think of the Schwarzschild geometry as static. However, the static “time translations,” $t \rightarrow t + \Delta t$, which leave the Schwarzschild geometry unchanged, are time translations in the strict sense of the words only in regions I and III of the Schwarzschild geometry. In regions II and IV, $t \rightarrow t + \Delta t$ is a spacelike motion, not a timelike motion (see Fig. 31.3). Consequently, a spacelike hypersurface, such as the surface $t = \text{const}$ of Figure 31.5,a, which extends from region I through $u = v = 0$ into region III, is *not* static. As this spacelike hypersurface is pushed forward in time (in the $+v$ direction of the Kruskal diagram), it enters region II, and its geometry begins to change.

In order to examine the time-development of the Schwarzschild geometry, one needs a sequence of embedding diagrams, each corresponding to the geometry of a spacelike hypersurface to the future of the preceding one. But how are the hypersurfaces to be chosen? In Newtonian theory or special relativity, one chooses hypersurfaces of constant time. But in dynamic regions of curved spacetime, no naturally preferred time coordinate exists. This situation forces one to make a totally *arbitrary* choice of hypersurfaces to use in visualizing the time-development of geometry, and to keep in mind how very arbitrary that choice was.

Figure 31.6 uses two very different choices of hypersurfaces to depict the time-development of the Schwarzschild geometry. (Still other choices are shown in Figure 21.4.) Notice that the precise geometry of the evolving bridge depends on the arbitrary choice of spacelike hypersurfaces, but that the qualitative nature of the evolution is independent of the choice of hypersurfaces. Qualitatively speaking, the two asymptotically flat universes begin disconnected, with each one containing a singularity of infinite curvature ($r = 0$). As the two universes evolve in time, their singularities join each other and form a nonsingular bridge. The bridge enlarges, until it reaches a maximum radius at the throat of $r = 2M$ (maximum circumference of $4\pi M$; maximum surface area of $16\pi M^2$). It then contracts and pinches off, leaving the two universes disconnected and containing singularities ($r = 0$) once again. The formation, expansion, and collapse of the bridge occur so rapidly, that no particle or light ray can pass across the bridge from the faraway region of the one universe to the faraway region of the other without getting caught and crushed in the throat as it pinches off. (To verify this, examine the Kruskal-Szekeres diagram of Figure 31.3, where radial light rays move along 45-degree lines.)

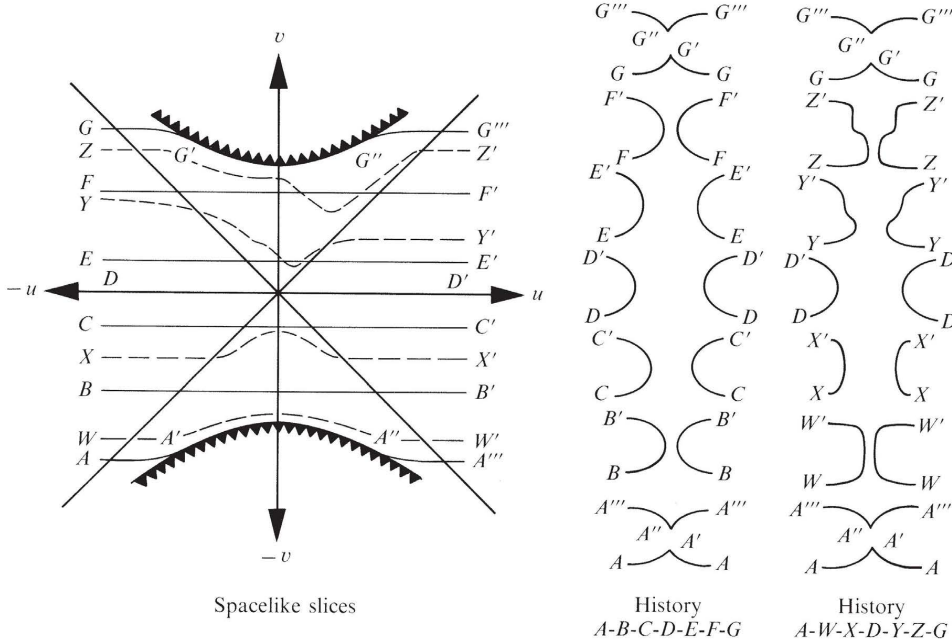


Figure 31.6.

Dynamical evolution of the Einstein-Rosen bridge of the vacuum Schwarzschild geometry (schematic). Shown here are two sequences of embedding diagrams corresponding to two different ways of viewing the evolution of the bridge—History $A-B-C-D-E-F-G$, and History $A-W-X-D-Y-Z-G$. The embedding diagrams are skeletonized in that each diagram must be rotated about the appropriate vertical axis in order to become two-dimensional surfaces analogous to Figure 31.5,a. [Notice that the hypersurfaces of which embedding diagrams are given intersect the singularity only tangentially. Hypersurfaces that intersect the singularity at a finite angle in the u,v -plane are not shown because they cannot be embedded in a Euclidean space. Instead, a Minkowski space (indefinite metric) must be used, at least near $r = 0$. For an example of an embedding in Minkowski space, see the discussion of a universe with constant negative spatial curvature in equations (27.23) and (27.24) and Box 27.2C.] Figure 21.4 exhibits embedding diagrams for other spacelike slices in the Schwarzschild geometry.

From the Kruskal-Szekeres diagram and the 45-degree nature of its radial light rays, one sees that any particle that ever finds itself in region IV of spacetime must have been “created” in the earlier singularity; and any particle that ever falls into region II is doomed to be crushed in the later singularity. Only particles that stay forever in one of the asymptotically flat universes I or III, outside the gravitational radius ($r > 2M$), are forever safe from the singularities.

Some investigators, disturbed by the singularities at $r = 0$ or by the “double-universe” nature of the Schwarzschild geometry, have proposed modifications of its topology. One proposal is that the earlier and later singularities be identified with each other, so that a particle which falls into the singularity of region II, instead of being destroyed, will suddenly reemerge, being ejected, from the singularity of region IV. One cannot overstate the objections to this viewpoint: the region $r = 0$ is a physical singularity of infinite tidal gravitation forces and infinite Riemann curvature. Any particle that falls into that singularity must be destroyed by those

Creation and destruction in the singularities

Nonviable proposals for modifying the topology of Schwarzschild spacetime

forces. Any attempt to extrapolate its fate through the singularity using Einstein's field equations must fail; the equations lose their predictive power in the face of infinite curvature. Consequently, to postulate that the particle reemerges from the earlier singularity is to make up an *ad hoc* mathematical rule, one unrelated to physics. It is conceivable, but few believe it true, that any object of finite mass will modify the geometry of the singularity as it approaches $r = 0$ to such an extent that it can pass through and reemerge. However, whether such a speculation is correct must be answered not by *ad hoc* rules, but by concrete, difficult computations within the framework of general relativity theory (see Chapter 34).

A second proposal for modifying the topology of the Schwarzschild geometry is this: one should avoid the existence of two different asymptotically flat universes by identifying each point (v, u, θ, ϕ) with its opposite point $(-v, -u, \theta, \phi)$ in the Kruskal-Szekeres coordinate system. Two objections to this proposal are: (1) it produces a sort of "conical" singularity (absence of local Lorentz frames) at $(v, u) = (0, 0)$, i.e., at the neck of the bridge at its moment of maximum expansion; and (2) it leads to causality violations in which a man can meet himself going backward in time.

One good way for the reader to become conversant with the basic features of the Schwarzschild geometry is to reread §§31.1–31.4 carefully, reinterpreting everything said there in terms of the Kruskal-Szekeres diagram.

EXERCISES

Exercise 31.7. SCHWARZSCHILD METRIC IN ISOTROPIC COORDINATES

- (a) Show that, rewritten in the isotropic coordinates of Exercise 23.1, the Schwarzschild metric reads

$$ds^2 = -\left(\frac{1 - M/2\bar{r}}{1 + M/2\bar{r}}\right)^2 dt^2 + \left(1 + \frac{M}{2\bar{r}}\right)^4 [d\bar{r}^2 + \bar{r}^2(d\theta^2 + \sin^2\theta d\phi^2)]; \quad (31.22)$$

and derive the transformation

$$r = \bar{r}(1 + M/2\bar{r})^2 \quad (31.23)$$

between the two radial coordinates.

- (b) Which regions of spacetime (I, II, III, IV; see Figure 31.3) are covered by the isotropic coordinate patch, and which are not?
(c) Calculate and construct an embedding diagram for the spacelike hypersurface $t = 0$, $0 < \bar{r} < \infty$.
(d) Find a coordinate transformation that interchanges the region near $\bar{r} = 0$ with the region near $\bar{r} = \infty$, while leaving the metric coefficients in their original form.

Exercise 31.8. REISSNER-NORDSTRÖM GEOMETRY

- (a) Solve the Einstein field equations for a spherically symmetric, static gravitational field

$$ds^2 = -e^{2\Phi(r)} dt^2 + e^{2A(r)} dr^2 + r^2(d\theta^2 + \sin^2\theta d\phi^2),$$

with no matter present, but with a radial electric field $\mathbf{B} = 0$, $\mathbf{E} = f(r)\mathbf{e}_r$ in the static orthonormal frame

$$\omega^{\hat{t}} = e^\phi \mathbf{d}t, \quad \omega^{\hat{r}} = e^A \mathbf{d}r, \quad \omega^{\hat{\theta}} = r \mathbf{d}\theta, \quad \omega^{\hat{\phi}} = r \sin \theta \mathbf{d}\phi.$$

Use as a source in the Einstein field equations the stress-energy of the electric field. [Answer:

$$\mathbf{E} = (Q/r^2)\mathbf{e}_r, \quad (31.24a)$$

$$ds^2 = -\left(1 - \frac{2M}{r} + \frac{Q^2}{r^2}\right)dt^2 + \left(1 - \frac{2M}{r} + \frac{Q^2}{r^2}\right)^{-1}dr^2 + r^2(d\theta^2 + \sin^2\theta d\phi^2). \quad (31.24b)$$

This is called the “Reissner (1916)-Nordstrøm (1918) metric”.]

(b) Show that the constant Q is the total charge as measured by a distant observer ($r \gg 2M$ and $r \gg Q$), who uses a Gaussian flux integral, or who studies the coulomb-force-dominated orbits of test charges with charge-to-mass ratio $e/\mu \gg M/Q$. What is the charge-to-mass ratio, in dimensionless units, for an electron? Show that the constant M is the total mass as measured by a distant observer using the Keplerian orbits of electrically neutral particles.

(c) Show that for $Q > M$, the Reissner-Nordstrøm coordinate system is well-behaved from $r = \infty$ down to $r = 0$, where there is a physical singularity and infinite tidal forces.

(d) Explore the nature of the spacetime geometry for $Q < M$, using all the techniques of this chapter (coordinate transformations, Kruskal-like coordinates, studies of particle orbits, embedding diagrams, etc.).

[*Solution:* see Graves and Brill (1960); also Fig. 34.4 of this book.]

(e) Similarly explore the spacetime geometry for $Q = M$. [*Solution:* see Carter (1966b).]

(f) For the case of a large ratio of charge to mass [$Q > M$ as in part (c)], show that the region near $r = 0$ is unphysical. More precisely, show that any spherically symmetric distribution of charged stressed matter that gives rise to the fields (31.24) outside its boundary must modify these fields for $r < r_0 = Q^2/2M$. [Hint: Study the quantity $m(r)$ defined in equations (23.18) and (32.22h), noting its values deduced from equation (31.24), on the one hand, and from the appropriate Einstein equation within the matter distribution, on the other hand. See Figure 26 of Misner (1969a) for a similar argument.]

CHAPTER 32

GRAVITATIONAL COLLAPSE

Now, here, you see, it takes all the running you can do, to keep in the same place. If you want to get somewhere else, you must run twice as fast as that.

The Red Queen, in *Through the Looking Glass*,
LEWIS CARROLL (1871)

§32.1. RELEVANCE OF SCHWARZSCHILD GEOMETRY

The story that unfolded in the preceding chapter was fantastic! One began with the innocuous looking Schwarzschild line element

$$ds^2 = -\left(1 - \frac{2M}{r}\right)dt^2 + \frac{dr^2}{1 - 2M/r} + r^2(d\theta^2 + \sin^2\theta d\phi^2), \quad (32.1)$$

which was derived originally as the external field of a static star. One asked what happens if the star is absent; i.e., one probed the nature of the Schwarzschild geometry when no star is present to generate it. One might have expected the geometry to be that of a point mass sitting at $r = 0$. But it was not. It turned out to represent a “wormhole” connecting two asymptotically flat universes. Moreover, the wormhole was dynamic. It was created by the “joining together” of two “ $r = 0$ ” singularities, one in each universe; it expanded to a maximum circumference of $4\pi M$; it then recontracted and pinched off, leaving the two universes disconnected once again, each with its own “ $r = 0$ ” singularity.

The roles and relevance of the Schwarzschild geometry

As a solution to Einstein’s field equations, this expanding and recontracting wormhole must be taken seriously. It is an exact solution; and it is one of the simplest of all exact solutions. But there is no reason whatsoever to believe that such wormholes exist in the real universe! They can exist only if the expanding universe, $\sim 10 \times 10^9$ years ago, was “born” with the necessary initial conditions—with “ $r = 0$ ”

Schwarzschild singularities ready and waiting to blossom forth into wormholes. There is no reason at all to believe in such pathological initial conditions!

Why, then, was so much time and effort spent in Chapter 31 on understanding the Schwarzschild geometry? (1) Because it illustrates clearly the highly non-Euclidean character of spacetime geometry when gravity becomes strong; (2) because it illustrates many of the techniques one can use to analyze strong gravitational fields; and most importantly (3) because, when appropriately truncated, it is the spacetime geometry of a black hole and of a collapsing star—as well as of a wormhole.

This chapter explores the role of the Schwarzschild geometry in gravitational collapse; the next chapter explores its role in black-hole physics.

§32.2. BIRKHOFF'S THEOREM

That the Schwarzschild geometry is relevant to gravitational collapse follows from *Birkhoff's (1923) theorem*: *Let the geometry of a given region of spacetime (1) be spherically symmetric, and (2) be a solution to the Einstein field equations in vacuum. Then that geometry is necessarily a piece of the Schwarzschild geometry.* The external field of any electrically neutral, spherical star satisfies the conditions of Birkhoff's theorem, whether the star is static, vibrating, or collapsing. Therefore the external field must be a piece of the Schwarzschild geometry.

Birkhoff's theorem is easily understood on physical grounds. Consider an equilibrium configuration that is unstable against gravitational collapse and that, like all equilibrium configurations (see §23.6), has the Schwarzschild geometry as its external gravitational field. Perturb this equilibrium configuration in a spherically symmetric way, so that it begins to collapse radially. The perturbation and subsequent collapse cannot affect the external gravitational field so long as exact spherical symmetry is maintained. Just as Maxwell's laws prohibit monopole electromagnetic waves, so Einstein's laws prohibit monopole gravitational waves. There is no possible way for any gravitational influence of the radial collapse to propagate outward.

Not only is Birkhoff's theorem easy to understand, but it is also fairly easy to prove. Consider a spherical region of spacetime. Spherical symmetry alone is sufficient to guarantee that conditions (i), (ii), and (iii) of Box 23.3 are satisfied, and thus to guarantee that one can introduce Schwarzschild coordinates

$$ds^2 = -e^{2\Phi} dt^2 + e^{2A} dr^2 + r^2(d\theta^2 + \sin^2\theta d\phi^2), \\ \Phi = \Phi(t, r), \text{ and } A = A(t, r). \quad (32.2)$$

[See Box 23.3 for proof; and notice that: (1) for generality one must allow $g_{tt} = -e^{2\Phi}$ and $g_{rr} = e^{2A}$ to be positive or negative (no constraint on sign!); (2) at events where the gradient of the “circumference function” r is zero or null, Schwarzschild coordinates cannot be introduced. The special case $(\nabla r)^2 = 0$ is treated in exercise 32.1.]

The uniqueness of the
Schwarzschild geometry:
Birkhoff's theorem

The physics underlying
Birkhoff's theorem

Proof of Birkhoff's theorem

Impose Einstein's vacuum field equation on the metric (32.2), using the orthonormal components of the Einstein tensor as derived in exercise 14.16:

$$G_{\hat{t}\hat{t}} = r^{-2}(1 - e^{-2A}) + 2(\Lambda_{,r}/r)e^{-2A} = 0, \quad (32.3a)$$

$$G_{\hat{t}\hat{r}} = G_{\hat{r}\hat{t}} = 2(\Lambda_{,t}/r)e^{-(A+\Phi)} = 0, \quad (32.3b)$$

$$G_{\hat{r}\hat{r}} = 2(\Phi_{,r}/r)e^{-2A} + r^{-2}(e^{-2A} - 1) = 0, \quad (32.3c)$$

$$\begin{aligned} G_{\hat{\theta}\hat{\theta}} = G_{\hat{\phi}\hat{\phi}} = & +(\Phi_{,rr} + \Phi_{,r}^2 - \Phi_{,r}\Lambda_{,r} + \Phi_{,r}/r - \Lambda_{,r}/r)e^{-2A} \\ & - (\Lambda_{,tt} + \Lambda_{,t}^2 - \Lambda_{,t}\Phi_{,t})e^{-2\Phi} = 0. \end{aligned} \quad (32.3d)$$

Equation (32.3b) guarantees that Λ is a function of r only, and equation (32.3a) then guarantees that Λ has the same form as for the Schwarzschild metric:

$$\Lambda = -\frac{1}{2} \ln |1 - 2M/r|. \quad (32.4a)$$

Equations (32.3c,d) then become two equivalent equations for $\Phi(t, r)$ —equivalent by virtue of the Bianchi identity, $\nabla \cdot \mathbf{G} = 0$ —whose solution is

$$\Phi = \frac{1}{2} \ln |1 - 2M/r| + f(t). \quad (32.4b)$$

Here f is an arbitrary function. Put expressions (32.4) into the line element (32.2); thereby obtain

$$ds^2 = -e^{2f(t)} \left(1 - \frac{2M}{r}\right) dt^2 + \frac{dr^2}{1 - 2M/r} + r^2(d\theta^2 + \sin^2\theta d\phi^2).$$

Then redefine the time coordinate

$$t_{\text{new}} = \int e^{f(t)} dt,$$

and thereby bring the line element into the Schwarzschild form

$$ds^2 = -\left(1 - \frac{2M}{r}\right) dt^2 + \frac{dr^2}{1 - 2M/r} + r^2(d\theta^2 + \sin^2\theta d\phi^2).$$

Conclusion: When the spacetime surrounding any object has spherical symmetry and is free of charge, mass, and all fields other than gravity, then one can introduce coordinates in which the metric is that of Schwarzschild. Conclusion restated in coordinate-free language: the geometry of any spherically symmetric vacuum region of spacetime is a piece of the Schwarzschild geometry (Birkhoff's theorem). Q.E.D.

EXERCISE

Exercise 32.1. UNIQUENESS OF REISSNER-NORDSTRÖM GEOMETRY [Track 2]

Prove the following generalization of Birkhoff's theorem. Let the geometry of a given region of spacetime (1) be spherically symmetric, and (2) be a solution to the Einstein field equations

with an electromagnetic field as source. Then that geometry is necessarily a piece of the Reissner-Nordström geometry [equation (31.24b)] with electric and magnetic fields, as measured in the standard static orthonormal frames

$$\mathbf{E} = (Q_e/r^2)\mathbf{e}_r, \quad \mathbf{B} = (Q_m/r^2)\mathbf{e}_r, \quad Q = (Q_e^2 + Q_m^2)^{1/2}.$$

[*Hints:* (1) First consider regions of spacetime in which $(\nabla r)^2 \neq 0$, using the same methods as the text uses for Birkhoff's theorem. The result is the Reissner-Nordström solution. (2) Any region of dimensionality less than four, in which $(\nabla r)^2 = 0$ (e.g., the Schwarzschild radius), can be treated as the join between four-dimensional regions with $(\nabla r)^2 \neq 0$. Moreover, the geometry of such a region is determined uniquely by the geometry of the adjoining four-dimensional regions (“junction conditions”; §21.13). Since the adjoining regions are necessarily Reissner-Nordström (step 1), then so are such “sandwiched” regions. (3) Next consider four-dimensional regions in which $\nabla r = dr$ is null and nonzero. Show that in such regions there exist coordinate systems with

$$ds^2 = -2\Psi dr dt + r^2(d\theta^2 + \sin^2\theta d\phi^2),$$

where $\Psi = \Psi(r, t)$. Show further that the Ricci tensor for this line element has an orthonormalized component

$$R_{\hat{\theta}\hat{\theta}} = 1/r^2,$$

whereas the stress-energy tensor for a spherically symmetric electromagnetic field has

$$8\pi T_{\hat{\theta}\hat{\theta}} = 8\pi \left(T_{\hat{\theta}\hat{\theta}} - \frac{1}{2}g_{\hat{\theta}\hat{\theta}}T \right) = Q^2/r^4, \quad Q = \text{const.}$$

These quantities, $R_{\hat{\theta}\hat{\theta}}$ and $8\pi T_{\hat{\theta}\hat{\theta}}$, must be equal (Einstein's field equation) but cannot be because of their different r -dependence. Thus, an electromagnetic field cannot generate regions with $dr \neq 0$, $dr \cdot dr = 0$. (4) Finally, consider four-dimensional regions in which $dr = 0$. Denote the constant value of r by a , and show that any event can be chosen as the origin of a locally well-behaved coordinate system with

$$ds^2 = a^2(-d\tilde{\tau}^2 + e^{2\lambda} dz^2 + d\theta^2 + \sin^2\theta d\phi^2), \\ \lambda = \lambda(\tilde{\tau}, z), \quad \lambda(\tilde{\tau} = 0, z) = 0, \quad \dot{\lambda}(\tilde{\tau} = 0, z) = 0.$$

[Novikov-type coordinate system; see §31.4.] Show that, in the associated orthonormal frame, spherical symmetry demands

$$\mathbf{E} = (Q_e/a^2)\mathbf{e}_z, \quad \mathbf{B} = (Q_m/a^2)\mathbf{e}_z, \quad Q \equiv (Q_e^2 + Q_m^2)^{1/2},$$

and that the Einstein field equations then require $Q = a$ and $e^\lambda = \cos \tilde{\tau}$, so that

$$ds^2 = Q^2(-d\tilde{\tau}^2 + \cos^2 \tilde{\tau} dz^2 + d\theta^2 + \sin^2\theta d\phi^2).$$

(5) This solution of the field equations [sometimes called the “Bertotti (1959)-Robinson (1959a) Electromagnetic Universe,” and explored in this coordinate system by Lindquist (1960)] is actually the throat of the Reissner-Nordström solution for the special case $Q = M$. Verify this claim by performing the following coordinate transformation on the Reissner-Nordström throat region [equation (31.24b) with $Q = M$ and $|r - Q| \ll Q$]:

$$r - Q = Qe^{-z} \cos \tilde{\tau}, \quad t = Qe^z \tan \tilde{\tau}.$$

(6) Thus, each possible case leads either to no solution at all, or to a segment of the Reissner-Nordström geometry. Q.E.D.] Note: The missing case, $(\nabla r)^2 = 0$, in the text's proof of Birkhoff's theorem, is resolved by noting that, for $Q = 0$, steps (3) and (4) above lead to no solutions at all. We thank G. F. R. Ellis for pointing out the omission of the case $(\nabla r)^2 = 0$ in the preliminary version of this book.

§32.3. EXTERIOR GEOMETRY OF A COLLAPSING STAR

Consider a star that is momentarily static, but will subsequently begin to collapse. Its space geometry at the initial moment of Schwarzschild coordinate time, $t = 0$, has two parts: in the exterior, vacuum region ($r > R > 2M$), it is the Schwarzschild geometry (Birkhoff's theorem!); but in the star's interior, it is some other, totally different geometry. Whatever the interior geometry may be, it has an embedding diagram at time $t = 0$ which is qualitatively like that of Figure 23.1. (For discussion and proof of this, see §23.8.) Notice that the star's space geometry is obtained by discarding the lower universe of the full Schwarzschild geometry (Figure 31.5,a), and replacing it with a smooth "bowl" on which the matter of the star is contained.

To follow the subsequent collapse of this star in the Schwarzschild coordinate system, or in the Kruskal-Szekeres coordinate system, or in an ingoing Eddington-Finkelstein coordinate system, one can similarly discard that part of the coordinate diagram which lies inside the star's surface, and keep only the exterior Schwarzschild region. (See Figure 32.1.) In place of the discarded interior Schwarzschild region, one must introduce some other coordinate system, line element, and diagram that correctly describe the interior of the collapsing star.

From truncated coordinate diagrams (such as Figures 32.1,a,b,c), one can readily discover and understand the various peculiar features of collapse through the gravitational radius.

Gravitational collapse
analyzed by examining the
star's exterior, Schwarzschild
geometry

The gravitational radius as a
point of no return, and the
"crushing" at $r = 0$

(1) No matter how stiff may be the matter of which a (spherical) star is made, once its surface has collapsed within the gravitational radius, the star will continue to collapse until its surface gets crushed in the singularity at $r = 0$. This one discovers by recalling that the star's surface cannot move faster than the speed of light, so its world line must always make an angle of less than 45 degrees with the v -axis of the Kruskal-Szekeres diagram.

(2) No signal (e.g., photon) emitted from the star's surface after it collapses inside the gravitational radius can ever escape to an external observer. Rather, all signals emitted from inside the gravitational radius get caught and destroyed by the collapse of the surrounding geometry into the singularity at $r = 0$ as space "pinches off" around the star.

(3) Consequently, an external observer can never see the star after it passes the gravitational radius; and he can never see the singularity that terminates its collapse—unless he chooses to fall through the gravitational radius himself and pay the price of death for the knowledge gained.

Does this mean that the collapsing star instantaneously and completely disappears from external view as it reaches the gravitational radius? No, not according to the analysis depicted in Figure 31.1c: Place an astrophysicist on the surface of a collapsing star, and have him send a series of uniformly spaced signals to a distant astronomer, at rest at $r \gg 2M$, to inform him of the progress of the collapse. These signals propagate along null lines in the spacetime diagram of Figure 31.1c. The signals originate on the world line of the stellar surface, and they are received by the distant astronomer when they intersect his world line, $r = \text{constant} \gg M$. As the star collapses closer and closer to its gravitational radius, $R = 2M$, the signals, which are sent at equally spaced intervals according to the astrophysicist's clock, are received by the astronomer at more and more widely spaced intervals. The astronomer does not receive a signal emitted just before the gravitational radius is reached until after an infinite amount of time has elapsed; and he never receives signals emitted after the gravitational radius has been passed. Those signals, like the astrophysicist who sends them, after brief runs get caught and destroyed by the collapsing geometry in the singularity, at $r = 0$. It is not only the star that collapses. The geometry around the star collapses.

Hence, to the distant astronomer, the collapsing star appears to slow down as it approaches its gravitational radius: light from the star becomes more and more red-shifted. Clocks on the star appear to run more and more slowly. It takes an infinite time for the star to reach its gravitational radius; and, as seen by the distant astronomer, the star never gets beyond there.

The optical appearance of a collapsing star was first analyzed mathematically, giving main attention to radially propagating photons, by J. R. Oppenheimer and H. Snyder (1939). More recently a number of workers have reexamined the problem [see, e.g., Podurets (1964), Ames and Thorne (1968) and Jaffe (1969)]. The most important quantitative results of these studies are as follows. In the late stages of collapse, when the distant astronomer sees the star to be very near its gravitational radius, he observes its total luminosity to decay exponentially in time

$$L \propto \exp\left(-\frac{2}{3\sqrt{3}} \frac{t}{2M}\right). \quad (32.5)$$

Simultaneously, photons that travel to him along radial trajectories arrive with exponentially increasing redshifts

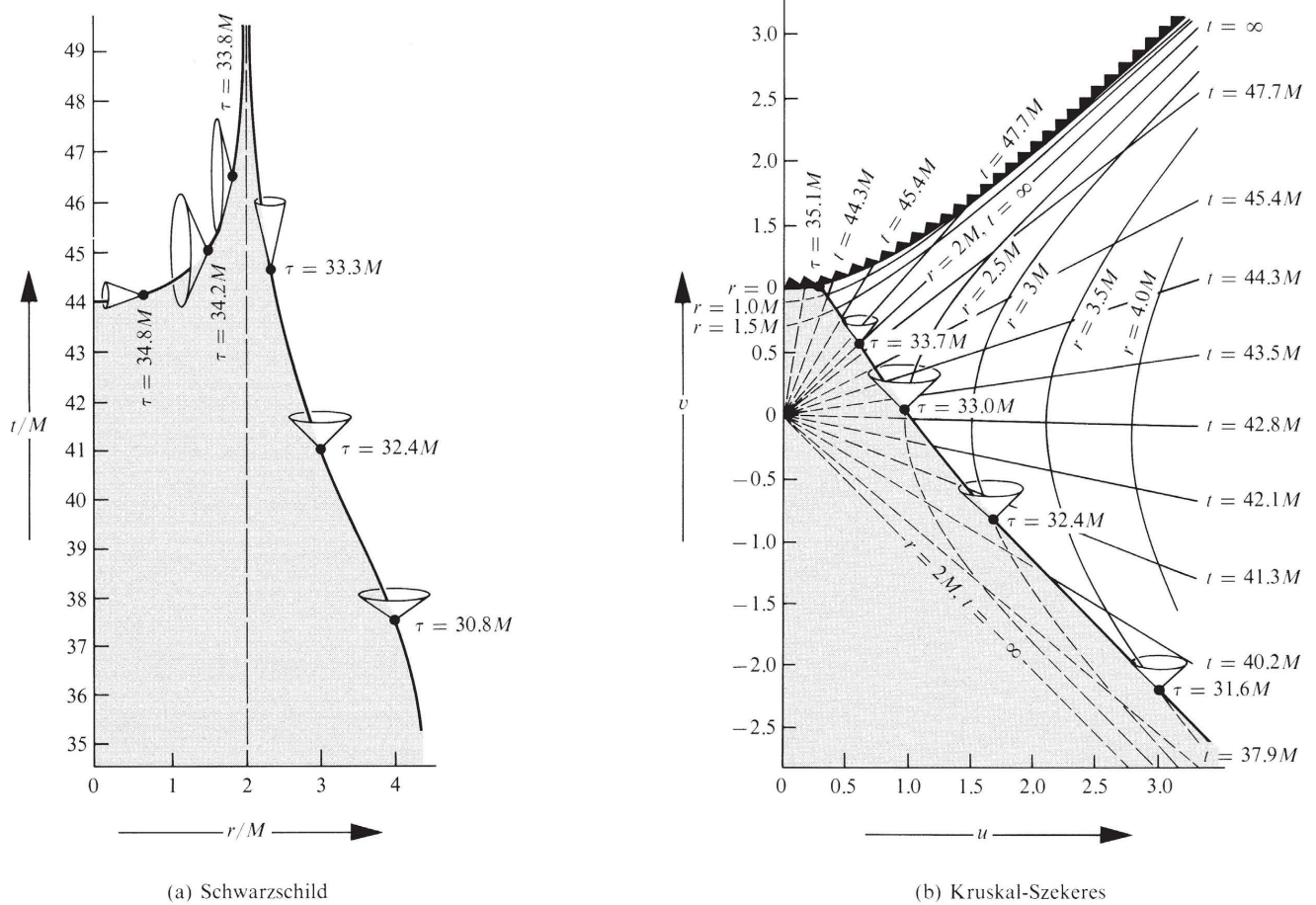
$$z = \Delta\lambda/\lambda \propto e^{t/4M}. \quad (32.6)$$

However, the light from the star is dominated in these late stages, not by photons flying along radial trajectories from near the gravitational radius, but by photons that were deposited by the star in unstable circular orbits as its surface passed through $r = 3M$ (see §25.6 and Box 25.7). As time passes, these photons gradually leak out the diffuse spherical shell of trapped photons at $r = 3M$ and fly off to the distant observer, who measures them to have redshift $z \approx 2$. Consequently, in the late stages of collapse the star's spectral lines are broadened enormously, but they are brightest at redshift $z \approx 2$.

The redshift of signals emitted just before passage through the gravitational radius

Optical appearance of the collapsing star

(continued on page 850)

**Figure 32.1.**

The free-fall collapse of a star of initial radius $R_i = 10 M$ as depicted alternatively in (a) Schwarzschild coordinates, (b) Kruskal-Szekeres coordinates, and (c) ingoing Eddington-Finkelstein coordinates (see Box 31.2). The region of spacetime inside the collapsing star is grey, that outside it is white. Only the geometry of the exterior region is that of Schwarzschild. The curve separating the grey and white regions is the geodesic world line of the surface of the collapsing star (equations [31.10] or [32.10] with $r_{\max} = R_i = 10 M$). This world line is parameterized by proper time, τ , as measured by an observer who sits on the surface of the star; the radial light cones, as calculated from $ds^2 = 0$, are attached to it.

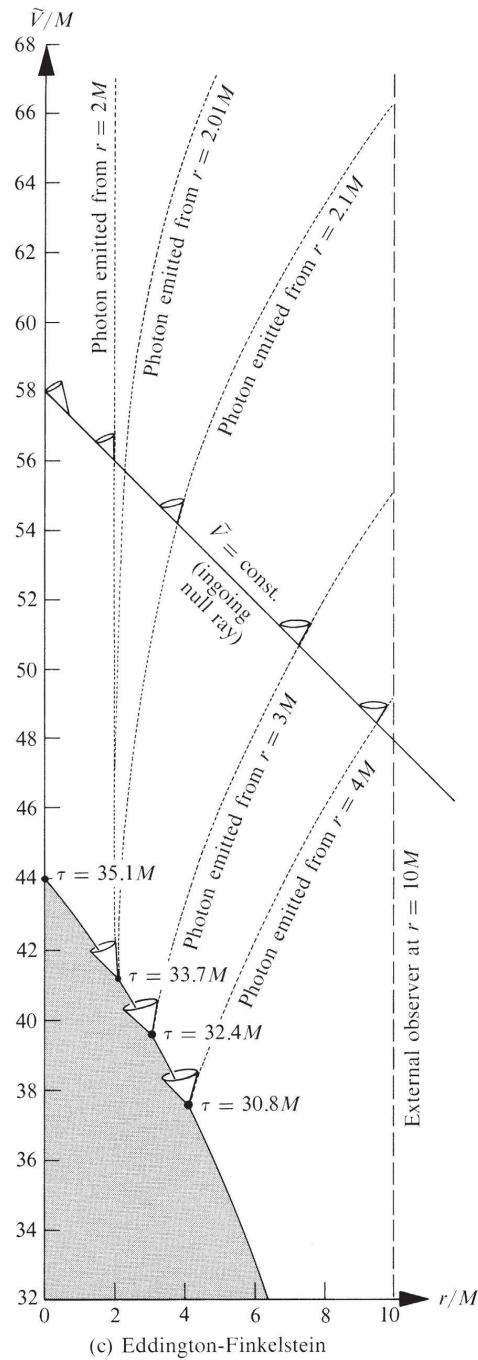
Notice that, although the shapes of the light cones are not all the same relative to Schwarzschild coordinates or relative to Eddington-Finkelstein coordinates, they are all the same relative to Kruskal-Szekeres coordinates. This is because light rays travel along 45-degree lines in the u,v -plane ($dv = \pm du$), but they travel along curved paths in the r,t -plane and r,\tilde{V} -plane.

The Kruskal-Szekeres spacetime diagram shown here is related to the Schwarzschild diagram by equations (31.13) plus a translation of Schwarzschild time: $t \rightarrow t + 42.8 M$. The Eddington-Finkelstein diagram is related to the Schwarzschild diagram by

$$\tilde{V} = t + r^* = t + r + 2 M \ln |r/2 M - 1|$$

(see Box 31.2).

It is evident from these diagrams that the free-fall collapse is characterized by a constantly diminishing radius, which drops from $R = 10 M$ to $R = 0$ in a finite and short comoving proper time interval, $\Delta\tau = 35.1 M$. The point $R = 0$ and the entire region $r = 0$ outside the star make up a physical “singularity” at which infinite tidal gravitational forces—according to classical, unquantized general relativity—can and do crush matter to infinite density (see end of §31.2; also §32.6).



(c) Eddington-Finkelstein

The Eddington-Finkelstein diagram depicts a series of photons emitted radially from the surface of the collapsing star, and received by an observer at $r = R_{\text{initial}} = 10 M$. The observer eventually receives all photons emitted radially from outside the gravitational radius; all photons emitted after the star passes through its gravitational radius eventually get pulled into the singularity at $r = 0$; and any photon emitted radially at the gravitational radius stays at the gravitational radius forever.

Non-free-fall collapse is similar to the collapse depicted here. When pressure gradients are present, only the detailed shape of the world line of the star's surface changes.

Notice how short is the characteristic e -folding time for the decay of luminosity and for the radial redshift:

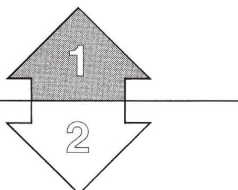
$$\begin{aligned}\tau_{\text{char}} &= 2M \approx 1 \times 10^{-5}(M/M_{\odot}) \text{ sec} \\ &= \left(\begin{array}{l} \text{light-travel time across a flat-space} \\ \text{distance equal to the gravitational radius} \end{array} \right).\end{aligned}\quad (32.7)$$

Here M_{\odot} denotes one solar mass.

EXERCISE

Exercise 32.2. REDSHIFTS DURING COLLAPSE

- (a) Let a radio transmitter on the surface of a collapsing spherical star emit monochromatic waves of wavelength λ_e ; and let a distant observer, at the same θ, ϕ , as the transmitter, receive the waves. Show that at late times the wavelength received varies as



$$\lambda_{\text{rec}}/\lambda_{\text{em}} \propto e^{t/4M} \quad (32.8a)$$

[equation (32.6)], where t is proper time as measured by the distant observer.

- (b) [Track 2] Use kinetic theory for the outgoing photons (conservation of density in phase space: Liouville's theorem; §22.6) to show that the energy flux of the radiation received (ergs/cm² sec) varies as

$$F \propto e^{-t/M}. \quad (32.8b)$$

The rest of this chapter is Track 2. No previous Track-2 material is needed as preparation for it, but it is needed as preparation for (1) the Track-2 part of Chapter 33 (black holes), and (2) Chapter 34 (singularities and global methods).

- (c) Suppose that nuclear reactions at the center of the collapsing star generate neutrinos of energy E_e , and that these neutrinos flow freely outward (negligible absorption in star). Show that the energy of the neutrinos received by a distant observer decreases at late times as

$$E_{\text{rec}}/E_e \propto e^{-t/4M}. \quad (32.9a)$$

- (d) Show that the flux of neutrino energy dies out at late times as

$$F \propto e^{-t/2M}. \quad (32.9b)$$

- (e) Explain in elementary terms why the decay laws (32.8a) and (32.9a) for energy are the same, but the decay laws (32.8b) and (32.9b) for energy flux are different.

- (f) Let a collapsing star emit photons from its surface at the black-body rate

$$\frac{dN}{d\tau} = \left(1.5 \times 10^{11} \frac{\text{photons}}{\text{cm}^2 \text{ sec K}^3} \right) \times \left(\frac{\text{surface area}}{\text{of star}} \right) \times \left(\frac{\text{temperature}}{\text{of surface}} \right)^3.$$

Let a distant observer count the photons as they pass through his sphere of radius $r \gg M$. Let him begin his count (time $t = 0$) when he sees (via photons traveling radially outward) the center of the star's surface pass through the radius $r = 3M$. Show that, in order of magnitude, the time he and his associates must wait, until the last photon that will ever get out has reached them, is

$$t = (M/M_{\odot})[8 \times 10^{-4} + 5 \times 10^{-5} \log_{10}(T_{11}M/M_{\odot})] \text{ seconds}, \quad (32.9c)$$

where T_{11} is the star's surface temperature in units of 10^{11} K.

§32.4. COLLAPSE OF A STAR WITH UNIFORM DENSITY AND ZERO PRESSURE

When one turns attention to the interior of a collapsing star and to the precise world line that its surface follows in the Schwarzschild geometry, one encounters rather complicated mathematics. The simplest case to treat is that of a “star” with uniform density and zero pressure; and, indeed, until recently that was the only case which had been treated in detail. The original—and very complete—analysis of the collapse of such a uniform-density “ball of dust” was given in the classic paper of Oppenheimer and Snyder (1939). More recently, other workers have discussed it from slightly different points of view and using different coordinate systems. The approach taken here was devised by Beckedorff and Misner (1962).

Because no pressure gradients are present to deflect their motion, the particles on the surface of any ball of dust must move along radial geodesics in the exterior Schwarzschild geometry. For a ball that begins at rest with finite radius, $R = R_i$, at time $t = 0$, the subsequent geodesic motion of its surface is given by equations (31.10):

$$R = (R_i/2)(1 + \cos \eta), \quad (32.10a)$$

$$t = 2M \ln \left| \frac{(R_i/2M - 1)^{1/2} + \tan(\eta/2)}{(R_i/2M - 1)^{1/2} - \tan(\eta/2)} \right| + 2M(R_i/2M - 1)^{1/2}[\eta + (R_i/4M)(\eta + \sin \eta)]. \quad (32.10b)$$

The collapse, from rest, of a uniform-density ball of “dust”:

- (1) world line of ball's surface in exterior Schwarzschild coordinates

Here R is the Schwarzschild radial coordinate (i.e., $4\pi R^2$ is the star's surface area) at Schwarzschild time t . This world line is plotted in Figure 32.1 for $R_i = 10M$, in terms of Schwarzschild coordinates, Kruskal-Szekeres coordinates, and Eddington-Finkelstein coordinates. The proper time read by a clock on the surface of the collapsing star is given by equation (31.10b):

$$\tau = (R_i^3/8M)^{1/2}(\eta + \sin \eta). \quad (32.10c)$$

Note that the collapse begins when the parameter η is zero ($R = R_i$, $t = \tau = 0$); and it terminates at the singularity ($R = 0$, $\eta = \pi$) after a lapse of proper time, as measured on any test particle falling with the dust, equal to

$$\Delta\tau = \pi(R_i^3/8M)^{1/2}.$$

It is interesting, though coincidental, that this is precisely the time-lapse required for free-fall collapse to infinite density in Newtonian theory [see equation (25.27'), Figure 25.3, and associated discussion].

What is the behavior of the interior of the ball of dust as it collapses? A variety of different interiors for pressureless dust can be conceived (exercise 32.8). But here attention focuses on the simplest of them: an interior that is homogeneous and isotropic everywhere, except at the surface—i.e., an interior locally identical to a dust-filled Friedmann cosmological model (Box 27.1). Is the Friedmann interior to be “open” ($k = -1$), “flat” ($k = 0$), or “closed” ($k = +1$)? Only the closed case

- (2) interior of ball is identical to a portion of a closed Friedmann universe

is appropriate, since one has already demanded [equation (32.10)] that the star be at rest initially (initial rate of change of density equals zero; “moment of maximum expansion”).

Using comoving hyperspherical coordinates, χ, θ, ϕ , for the star’s interior, and putting the origin of coordinates at the star’s center, one can write the line element in the interior in the familiar Friedmann form

$$ds^2 = -d\tau^2 + a^2(\tau)[d\chi^2 + \sin^2\chi(d\theta^2 + \sin^2\theta d\phi^2)]. \quad (32.11)$$

Here $a(\tau)$ is given by the familiar cycloidal relation,

$$\begin{aligned} a &= \frac{1}{2}a_m(1 + \cos\eta), \\ \tau &= \frac{1}{2}a_m(\eta + \sin\eta); \end{aligned} \quad (32.12)$$

and the density is given by

$$\rho = (3a_m/8\pi)a^{-3} = (3/8\pi a_m^2)\left[\frac{1}{2}(1 + \cos\eta)\right]^{-3} \quad (32.13)$$

[see equations (1), (9), (4), and (5) of Box 27.1, with η replaced by $\eta + \pi$].

There is one possible difficulty with this interior solution. In the cosmological case, the solution was homogeneous and isotropic everywhere. Here homogeneity and isotropy are broken at the star’s surface—which lies at some radius

$$\chi = \chi_0 \quad (32.14)$$

for all τ , as measured in terms of the hyperspherical polar angle χ , a comoving coordinate (first picture in Box 27.2). At that surface (i.e., three-dimensional world tube enclosing the star’s fluid) the interior Friedmann geometry must match smoothly onto the exterior Schwarzschild geometry. If the match cannot be achieved, then the Friedmann line element (32.11) cannot represent the interior of a collapsing star. An example of a case in which the matching could not be achieved is an interior of uniform and nonzero pressure, as well as uniform density. In that case there would be an infinite pressure gradient at the star’s surface, which would blow off the outer layers of the star, and would send a rarefaction wave propagating inward toward its center. The uniform distribution of density and pressure would quickly be destroyed.

For the case of zero pressure, the match is possible. As a partial verification of the match, one can examine the separate and independent predictions made by the interior and exterior solutions for the star’s circumference, $C = 2\pi R$, as a function of proper time τ at the star’s surface. The external Schwarzschild solution predicts the cycloidal relation,

$$\begin{aligned} C &= 2\pi R = 2\pi(R_i/2)(1 + \cos\eta), \\ \tau &= (R_i^3/8M)^{1/2}(\eta + \sin\eta) \end{aligned} \quad (32.15)$$

[equations (32.10)]. The interior Friedmann solution predicts a similar cycloidal relation:

- (3) the join between Friedmann interior and Schwarzschild exterior

$$C = 2\pi R = 2\pi a \sin \chi_0 = 2\pi \left(\frac{1}{2} a_m \sin \chi_0 \right) (1 + \cos \eta),$$

$$\tau = \frac{1}{2} a_m (\eta + \sin \eta). \quad (32.16)$$

The two predictions agree perfectly for all time if and only if

$$R_i = a_m \sin \chi_0, \quad (32.17a)$$

$$M = \frac{1}{2} a_m \sin^3 \chi_0. \quad (32.17b)$$

A more complete verification of the match is given in exercise 32.4.

For further insight into this idealized model of gravitational collapse, see Box 32.1.

Exercise 32.3. EMBEDDING DIAGRAMS AND PHOTON PROPAGATION FOR COLLAPSING STAR

Verify in detail the features of homogeneous collapse described in Box 32.1.

Exercise 32.4. MATCH OF FRIEDMANN INTERIOR TO SCHWARZSCHILD EXTERIOR

The Einstein field equations are satisfied on a star's surface if and only if the intrinsic and extrinsic geometries of the surface's three-dimensional world tube are the same, whether measured on its interior or on its exterior (see §21.13 for proof and discussion). Verify that for the collapsing star discussed above, the intrinsic and extrinsic geometries match at the join between the Friedmann interior and the Schwarzschild exterior. [Hints: (a) Use η, θ, ϕ , as coordinates on the world tube of the star's surface, and show that the intrinsic geometry has the same line element

$$ds^2 = a^2(\eta) [-d\eta^2 + \sin^2 \chi_0 (d\theta^2 + \sin^2 \theta d\phi^2)], \quad (32.18a)$$

whether measured in the Schwarzschild exterior or in the Friedmann interior. (b) Show that the extrinsic curvature of the world tube has the same components

$$K_{\eta\eta} = K_{\eta\theta} = K_{\eta\phi} = K_{\theta\phi} = 0, \quad (32.18b)$$

$$K_{\theta\theta} = K_{\phi\phi}/\sin^2 \theta = -a(\eta) \sin \chi_0 \cos \chi_0,$$

whether measured in the Schwarzschild exterior or in the Friedmann interior.]

Exercise 32.5. STARS THAT COLLAPSE FROM INFINITY

(a) Patch together a truncated Schwarzschild geometry and the geometry of a truncated “flat” ($k = 0$), dust-filled Friedmann universe to obtain a model of a star that collapses from rest at an infinite initial radius. [Hint: The world line of the star's surface in the Schwarzschild geometry is given by equations (31.2).]

(b) Similarly patch together a truncated Schwarzschild geometry and the geometry of a truncated “open” ($k = -1$), dust-filled Friedmann universe to obtain a star which collapses from infinity with finite initial inward velocity.

EXERCISES

(continued on page 857)

**Box 32.1 AN IDEALIZED COLLAPSING STAR
WITH FRIEDMANN INTERIOR
AND SCHWARZSCHILD EXTERIOR**

(See §32.4 and exercises 32.3 and 32.4
for justification of the results
described here.)

Initial State

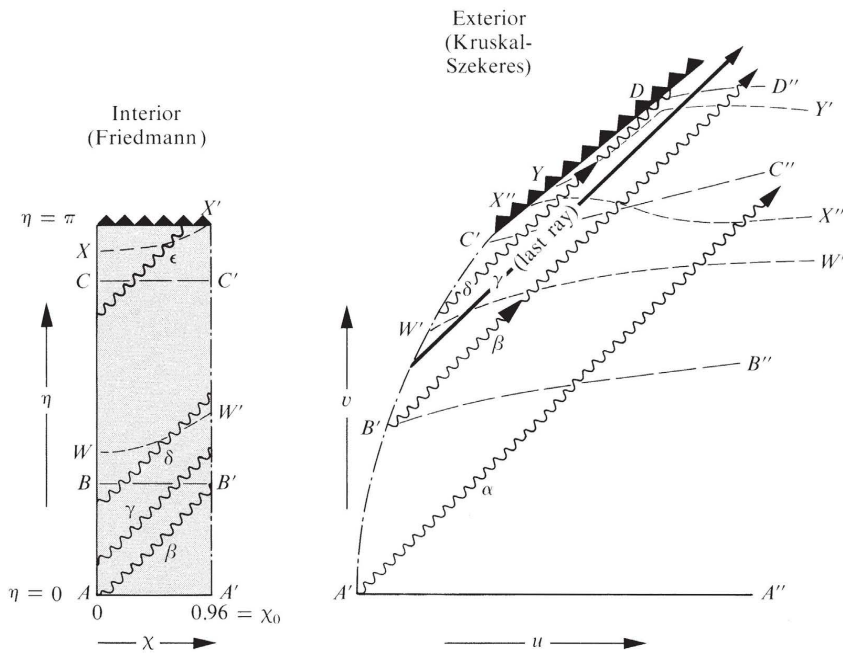
(1) Take a Friedmann universe of radius $a = a_m$ at its moment of maximum expansion, $\eta = 0$; and slice off and discard the region $\chi_0 < \chi \leq \pi$, where χ_0 is some angle less than $\pi/2$. (2) Take a Schwarzschild geometry of mass $M = (a_m/2) \sin^3 \chi_0$ at the moment $t = 0$; and slice off and discard the region $r < R_i = a_m \sin \chi_0$. (3) Glue the remaining pieces of Friedmann and Schwarzschild geometry together smoothly along their cut surfaces. The resultant object will be a momentarily static star of uniform density $\rho_i = 3/(8\pi a_m^2)$, of mass $M = (a_m/2) \sin^3 \chi_0$, and of radius $R_i = a_m \sin \chi_0$.

Subsequent Evolution

Release this star from its initial state, and let it collapse in accord with Einstein's field equations. The interior, truncated Friedmann universe and the exterior, truncated Schwarzschild geometry will evolve just as though they had never been cut up and patched together; and this evolution will preserve the smoothness of the match between interior and exterior!

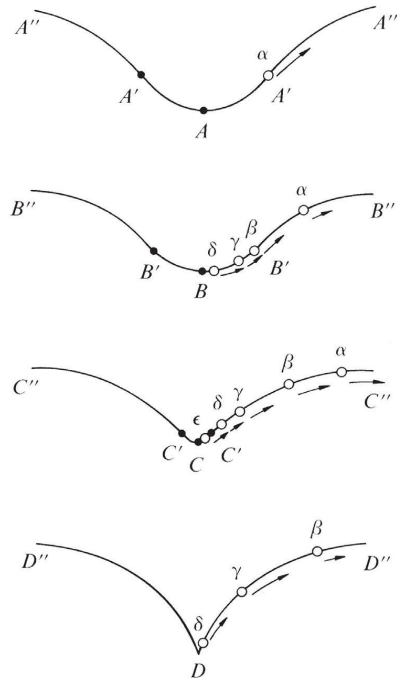
Details of the Collapse

Probe the details of the collapse using sequences of embedding diagrams (histories $ABCD$ and $AWXY$), and using photons that propagate radially outward (photons $\alpha, \beta, \gamma, \delta, \epsilon$). The example shown here has $\chi_0 = 0.96$ and $R_i/M = 2/\sin^2 \chi_0 = 3$.



History of Collapse as Probed by Hypersurfaces ABCD:

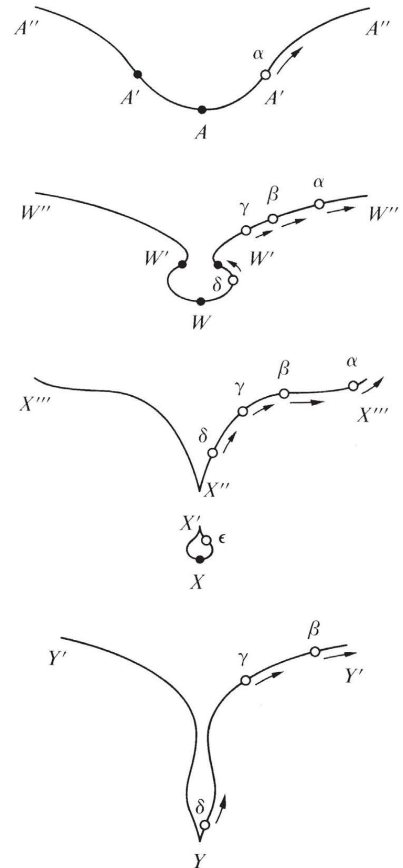
- (1) Initial configuration, $A - A' - A''$, is that constructed by cutting and sewing at times $\eta = t = 0$.
- (2) Each subsequent configuration has as its interior a slice of constant Friedmann time η .
- (3) The interior remains always a spherical cup of half-angle χ_0 ; but it contracts from radius $R = R_i = a_m \sin \chi_0$ to $R = 0$ as time increases.
- (4) The matter in the star is all crushed simultaneously to infinite density when R reaches zero, and the external Schwarzschild "funnel" develops a cusp-like singularity at that point.
- (5) As time increases further, this cusp pulls the region $r < 2M$ of the funnel into $r = 0$ so fast that the outward-traveling photon δ is gobbled up and crushed.



These embedding diagrams must be rotated about the vertical axes in order to become 2-dimensional surfaces analogous to Figure 23.1.

Box 32.1 (continued)**History as Probed by Hypersurfaces AWXY**

- (1) Initial configuration, $A - A' - A''$, is again that constructed by cutting and sewing at $\eta = t = 0$.
- (2) Subsequent hypersurfaces are very different from $\eta = \text{const}$.
- (3) As time passes, a neck develops in the geometry just outside the surface of the star.
- (4) This neck becomes tighter and tighter and then pinches off, leaving the star completely isolated from the rest of the universe, and leaving a deadly cusp-like singularity in the exterior geometry where the star used to be.
- (5) The isolated star, in its own little closed universe, continues to contract until it is crushed to infinite density, while the external geometry begins to develop another neck and the cusp quickly gobbles up photon δ .



The extreme difference between histories $ABCD$ and $AWXY$ dramatizes the “many-fingered time” of general relativity. The hypersurface on which one explores the geometry can be pushed ahead faster in time in one region, at the option of the party of explorers. Thus whether one region of the star collapses first, or another, or the entire star collapses simultaneously, is a function both of the spacetime geometry and of the choice of slicing. The party of explorers has this choice of slicing at their own control, and thus they themselves to this extent govern what kind of spacelike slices they will see as their exploration moves forward in time. The spacetime geometry that they slice, however, is in no way theirs to control or to change. To the extent that their masses are negligible and they serve merely as test objects, they have no influence whatsoever on the spacetime. It was fixed completely by the specification of the initial conditions for the collapse. In brief, spacetime is four-dimensional and slices are only three-dimensional (and in the pictures here look only two-dimensional or one-dimensional). Any one set of slices captures only a one-sided view of the whole story. To see the entire picture one must either examine the dynamics of the geometry as it reveals itself in varied choices of the slicing or become accustomed to visualizing the spacetime geometry as a whole.

§32.5. SPHERICALLY SYMMETRIC COLLAPSE WITH INTERNAL PRESSURE FORCES

So far as the external gravitational field is concerned, the only difference between a freely collapsing star and a collapsing, spherically symmetric star with internal pressure is this: that the surfaces of the two stars move along different world lines in the exterior Schwarzschild geometry. Because the exterior geometry is the same in both cases, *the qualitative aspects of free-fall collapse as described in the last section can be carried over directly to the case of nonnegligible internal pressure.*

An important and fascinating question to ask is this: can large internal pressures in any way prevent a collapsing star from being crushed to infinite density by infinite tidal gravitational forces? From the Kruskal-Szekeres diagram of Figure 32.1,b, it is evident that, once a star has passed inside its gravitational radius ($R < 2M$), no internal pressures, regardless of how large they may be, can prevent the star's surface from being crushed in a singularity. The surface must move along a time-like world line, and all such world lines inside $r = 2M$ hit $r = 0$. Although there is no such theorem now available, one can reasonably conjecture that, if the surface of a spherical configuration is crushed in the $r = 0$ singularity, the entire interior must also be crushed.

The details of the interior dynamics of a spherically symmetric collapsing star with pressure are not so well-understood as the exterior Schwarzschild dynamics. However, major advances in one's understanding of the interior dynamics are now being made by means of numerical computations and analytic analyses [see Misner (1969a) for a review]. In these computations and analyses, no new features (at least, no unexpected ones) have been encountered beyond those that occurred in the simple uniform-density, free-fall collapse of the last section.

Spherical collapse with pressure is qualitatively the same as without pressure

Exercise 32.6. GENERAL SPHERICAL COLLAPSE: METRIC IN COMOVING COORDINATES

EXERCISES

Consider an inhomogeneous star with pressure, undergoing spherical collapse. Spherical symmetry alone is enough to guarantee the existence of a Schwarzschild coordinate system (t, r, θ, ϕ) throughout the interior and exterior of the star [see equation (32.2) and preceding discussion]. Label each spherical shell of the star by a parameter a , which tells how many baryons are contained interior to that shell. Then $r(a, t)$ is the world line of the shell with label a . The expression for these world lines can be inverted to obtain $a(t, r)$, the number of baryons interior to radius r at time t . Show that there exists a new time coordinate $\tilde{t}(t, r)$, such that the line element (32.2), rewritten in the coordinates $(\tilde{t}, a, \theta, \phi)$, has the form

$$ds^2 = -e^{2\tilde{\Phi}} d\tilde{t}^2 + \left[\frac{(\partial r/\partial a)\tilde{t} da}{\Gamma} \right]^2 + r^2 d\Omega^2, \quad (32.19a)$$

$$\tilde{\Phi} = \tilde{\Phi}(\tilde{t}, a), \quad r = r(\tilde{t}, a), \quad \Gamma = \Gamma(\tilde{t}, a). \quad (32.19b)$$

These are “comoving, synchronous coordinates” for the stellar interior.

Exercise 32.7. ADIABATIC SPHERICAL COLLAPSE: EQUATIONS OF EVOLUTION [Misner and Sharp (1964)]

Describe the interior of a collapsing star by the comoving, synchronous metric (32.19), by the number density of baryons n , by the total density of mass-energy ρ , and by the pressure p . The 4-velocity of the star's fluid is

$$\mathbf{u} = e^{-\tilde{\Phi}} \partial/\partial \tilde{t}, \quad (32.20)$$

since the fluid is at rest in the coordinate system. Let a dot denote a proper time derivative as seen by the fluid—e.g.,

$$\dot{n} \equiv \mathbf{u}[n] = e^{-\tilde{\Phi}} (\partial n / \partial \tilde{t})_a;$$

and let a prime denote a partial derivative with respect to baryon number,—e.g.

$$n' \equiv (\partial n / \partial a)_{\tilde{t}}.$$

Denote by U the rate of change of $(1/2\pi) \times (\text{circumference of shell})$, as measured by a man riding in a given shell:

$$U \equiv \dot{r}; \quad (32.21a)$$

and denote by $m(\tilde{t}, a)$ the “total mass-energy interior to shell a at time \tilde{t} :

$$m(\tilde{t}, a) \equiv \int_0^a 4\pi r^2 \rho(\tilde{t}, a) r' da. \quad (32.21b)$$

(See Box 23.1 for discussion of this method of localizing mass-energy.) Assume that the collapse is adiabatic (no energy flow between adjacent shells; stress-energy tensor entirely that of a perfect fluid).

(a) Show that the equations of collapse [baryon conservation, (22.3); local energy conservation, (22.11a); Euler equation, (22.13); and Einstein field equations (ex. 14.16)] can be reduced to the following eight equations for the eight functions $\tilde{\Phi}$, Γ , r , n , ρ , p , U , m :

$$\dot{r} = U \quad (\text{dynamic equation for } r); \quad (32.22a)$$

$$\frac{(nr^2)'}{nr^2} = -\frac{U'}{r'} \quad (\text{dynamic equation for } n); \quad (32.22b)$$

$$\frac{\dot{\rho}}{\rho + p} = \frac{\dot{n}}{n}, \quad \begin{matrix} \text{except at a shock front, where adiabaticity} \\ \text{breaks down (dynamic equation for } \rho\text{)}; \end{matrix} \quad (32.22c)$$

$$\dot{U} = -\frac{\Gamma^2}{\rho + p} \frac{p'}{r'} - \frac{m + 4\pi r^3 p}{r^2} \quad (\text{dynamic equation for } U); \quad (32.22d)$$

$$p = p(n, \rho) \quad (\text{equation of state}); \quad (32.22e)$$

$$\tilde{\Phi}' = -p' / (\rho + p), \quad \tilde{\Phi} = 0 \text{ at star's surface} \quad (\text{source equation for } \tilde{\Phi}); \quad (32.22f)$$

$$m' = 4\pi r^2 \rho r', \quad m = 0 \text{ at } a = 0, \quad (\text{source equation for } m); \quad (32.22g)$$

$$\Gamma = \text{sign}(r')(1 + U^2 - 2m/r)^{1/2} \quad (\text{algebraic equation for } \Gamma). \quad (32.22h)$$

(b) The preceding equations are in a form useful for numerical calculations. [For particular numerical solutions and for the handling of shocks, see May and White (1966).] For analytic work it is often useful to replace (32.22b) by

$$n = \Gamma / (4\pi r^2 r'), \quad (32.22b')$$

and (32.22d) by

$$\dot{m} = -4\pi r^2 p U. \quad (32.22d')$$

Derive these equations.

(c) Explain why equations (32.22g) and (32.22d') justify the remarks made in Box 23.1 about localizability of energy.

Exercise 32.8. ANALYTIC SOLUTIONS FOR PRESSURE-FREE COLLAPSE

[Tolman (1934b); Datt (1938)]

Show that the general solution to equations (32.22) in the case of zero pressure can be generated as follows.

(a) Specify the mass inside shell a , $m(a)$; by equation (32.22d'), with $p = 0$, it will not change with time \tilde{t} .

(b) Assume that all the dust particles have rest masses μ that depend upon radius, $\mu(a)$; so

$$\rho = \mu n. \quad (32.23a)$$

(c) Calculate Γ from the equation

$$\Gamma = m'/\mu; \quad (32.23b)$$

it will be independent of \tilde{t} .

(d) Specify an initial distribution of circumference $2\pi r$ as function of a , and solve the dynamic equation

$$\left(\frac{\partial r}{\partial \tilde{t}}\right)^2 - \frac{2m(a)}{r} = \Gamma^2(a) - 1 \quad (32.23c)$$

to obtain the subsequent evolution of $r(\tilde{t}, a)$. Notice that this equation has identically the same form as in Newtonian theory!

(e) Calculate the remaining quantities of interest from the algebraic equations

$$ds^2 = -d\tilde{t}^2 + (r' da/\Gamma)^2 + r^2 d\Omega^2, \quad (32.23d)$$

$$\rho = \mu n = m'/(4\pi r^2 r'), \quad (32.23e)$$

$$\tilde{\Phi} = 0, \quad U = \partial r / \partial \tilde{t}. \quad (32.23f)$$

[Note: In this solution, successive ‘‘shells’’ may pass through each other, producing a surface of infinite density as they do ($r' \rightarrow 0$ where $m' \neq 0$), since there is no pressure built up to stop shell crossing. When this happens, the coordinate system becomes pathological (a no longer increases monotonically outward), but spacetime remains well-behaved. The surface of infinite density (1) produces negligible tidal forces on neighboring dust particles; and (2) like the surface layers of §21.13, it is an idealization that gets smeared down to finite density by finite pressure.]

Exercise 32.9. COLLAPSE WITH UNIFORM DENSITY

Recover the Friedmann-Schwarzschild solution for collapse with uniform density and zero pressure by specifying appropriate forms for $m(a)$ and $r(a)$ in the prescription of exercise 32.8. In the interior of the star, give the dust particles nonzero rest masses, $\mu = \text{constant} \neq 0$; in the exterior give them zero rest masses, $\mu = 0$ (“imaginary dust particles” in vacuum). Reduce the resulting metric (32.23d) to that of Friedmann inside the star, and to that of Novikov for the Schwarzschild geometry outside the star [equations (31.12)].

§32.6. THE FATE OF A MAN WHO FALLS INTO THE SINGULARITY AT $r = 0$

The effect of tidal forces on the body of a man falling into the $r = 0$ singularity:

Consider the plight of an experimental astrophysicist who stands on the surface of a freely falling star as it collapses to $R = 0$.

As the collapse proceeds toward $R = 0$, the various parts of the astrophysicist's body experience different gravitational forces. His feet, which are on the surface of the star, are attracted toward the star's center by an infinitely mounting gravitational force; while his head, which is farther away, is accelerated downward by a somewhat smaller, though ever rising force. The difference between the two accelerations (tidal force) mounts higher and higher as the collapse proceeds, finally becoming infinite as R reaches zero. The astrophysicist's body, which cannot withstand such extreme forces, suffers unlimited stretching between head and foot as R drops to zero.

But this is not all. Simultaneous with this head-to-foot stretching, the astrophysicist is pulled by the gravitational field into regions of spacetime with ever-decreasing circumferential area, $4\pi r^2$. In order to accomplish this, tidal gravitational forces must compress the astrophysicist on all sides as they stretch him from head to foot. The circumferential compression is actually more extreme than the longitudinal stretching; so the astrophysicist, in the limit $R \rightarrow 0$, is crushed to zero volume and indefinitely extended length.

The above discussion can be put on a mathematical footing as follows.

There are three stages in the killing of the astrophysicist: (1) the early stage, when his body successfully resists the tidal forces; (2) the intermediate stage, when it is gradually succumbing; and (3) the final stage, when it has been completely overwhelmed.

Stage 1: body resists deformation; stresses build up

During the early stage, one can analyze the tidal forces by means of the equation of geodesic deviation, evaluated in the astrophysicist's orthonormal frame $\mathbf{w}^\hat{\tau}$, $\mathbf{w}^\hat{\rho}$, $\mathbf{w}^\hat{\phi}$ (see §31.2). In this frame, the nonvanishing components of the Riemann curvature tensor are given by equations (31.6):

$$\begin{aligned} R_{\hat{\tau}\hat{\rho}\hat{\tau}\hat{\rho}} &= -2M/r^3, & R_{\hat{\tau}\hat{\theta}\hat{\tau}\hat{\theta}} &= R_{\hat{\tau}\hat{\phi}\hat{\tau}\hat{\phi}} = M/r^3, \\ R_{\hat{\theta}\hat{\phi}\hat{\theta}\hat{\phi}} &= 2M/r^3, & R_{\hat{\rho}\hat{\theta}\hat{\rho}\hat{\theta}} &= R_{\hat{\rho}\hat{\phi}\hat{\rho}\hat{\phi}} = -M/r^3. \end{aligned} \quad (32.24a)$$

The equation of geodesic deviation says that two *freely moving* particles, momentarily at rest in the astrophysicist's local inertial frame, and separated by the 3-vector

$$\boldsymbol{\xi} = \xi^{\hat{j}} \mathbf{e}_{\hat{j}},$$

must accelerate apart with a relative acceleration given by

$$\begin{aligned} D^2 \boldsymbol{\xi} / d\tau^2 &= -R_{\hat{\tau}\hat{k}\hat{\tau}\hat{k}}^{\hat{j}} \boldsymbol{\xi}^{\hat{k}} = -R_{\hat{j}\hat{\tau}\hat{k}\hat{\tau}} \boldsymbol{\xi}^{\hat{k}} \\ &= -R_{\hat{\tau}\hat{j}\hat{k}} \boldsymbol{\xi}^{\hat{k}}. \end{aligned}$$

Using the components (32.24a) of the curvature tensor, one sees that

$$\begin{aligned} D^2\xi^{\hat{\rho}}/d\tau^2 &= +(2M/r^3)\xi^{\hat{\rho}}, \\ D^2\xi^{\hat{\theta}}/d\tau^2 &= -(M/r^3)\xi^{\hat{\theta}}, \\ D^2\xi^{\hat{\phi}}/d\tau^2 &= -(M/r^3)\xi^{\hat{\phi}}. \end{aligned} \quad (32.24b)$$

To apply these equations to the astrophysicist's body, idealize it (for simplicity) as a homogeneous rectangular box of mass $\mu \approx 165$ pounds ≈ 75 kg, of length $\ell \approx 70$ inches ≈ 1.8 m in the $\mathbf{e}_{\hat{\rho}}$ direction, and of width and depth $w \approx 10$ inches ≈ 0.2 m in the $\mathbf{e}_{\hat{\theta}}$ and $\mathbf{e}_{\hat{\phi}}$ directions. Then calculate the stresses that must be set up in this idealized body to prevent its particles from moving along diverging (and converging) geodesics.

From the form of equations (32.24), it is evident that the principal directions of the stress will be $\mathbf{e}_{\hat{\rho}}$, $\mathbf{e}_{\hat{\theta}}$, and $\mathbf{e}_{\hat{\phi}}$ (i.e., in the $\mathbf{e}_{\hat{\rho}}$, $\mathbf{e}_{\hat{\theta}}$, $\mathbf{e}_{\hat{\phi}}$ basis, the stress tensor will be diagonal). The longitudinal component of the stress, at the astrophysicist's center of mass, can be evaluated as follows. A volume element of his body with mass $d\mu$, located at a height h above the center of mass (distance h measured along $\mathbf{e}_{\hat{\rho}}$ direction) would accelerate with $a = (2M/r^3)h$ away from the center of mass, if it were allowed to move freely. To prevent this acceleration, the astrophysicist's muscles must exert a force

$$dF = a d\mu = (2M/r^3)h d\mu.$$

This force contributes to the stress across the horizontal plane ($\mathbf{e}_{\hat{\theta}} \wedge \mathbf{e}_{\hat{\phi}}$ plane) through the center of mass. The total force across that plane is the sum of the forces on all mass elements above it (which is also equal to the sum of the forces on the mass elements below it):

$$\begin{aligned} F &= \int_{(\text{region above plane})} a d\mu = \int_0^{\ell/2} \left(\frac{2Mh}{r^3} \right) \left(\frac{\mu}{\ell w^2} \right) (w^2 dh) \\ &= \frac{1}{4} \frac{\mu M \ell}{r^3}. \end{aligned}$$

The stress is this force divided by the cross-sectional area w^2 , with a minus sign because it is a tension rather than a pressure:

$$T_{\hat{\rho}\hat{\rho}} = -\frac{1}{4} \frac{\mu M \ell}{w^2 r^3} \approx -1.1 \times 10^{15} \frac{M/M_{\odot}}{(r/1 \text{ km})^3} \frac{\text{dynes}}{\text{cm}^2}. \quad (32.25a)$$

The components of the stress in the $\mathbf{e}_{\hat{\theta}}$ and $\mathbf{e}_{\hat{\phi}}$ directions at the center of mass are, similarly,

$$T_{\hat{\theta}\hat{\theta}} = T_{\hat{\phi}\hat{\phi}} = +\frac{1}{8} \frac{\mu M}{\ell r^3} \approx +0.7 \times 10^{13} \frac{M/M_{\odot}}{(r/1 \text{ km})^3} \frac{\text{dynes}}{\text{cm}^2}. \quad (32.25b)$$

(Recall that one atmosphere of pressure is 1.01×10^6 dynes/cm².)

Stage 2: body gives way;
man dies

Stage 3: body gets crushed
and distended

The human body cannot withstand a tension or pressure of $\gtrsim 100$ atmospheres $\approx 10^8$ dynes/cm² without breaking. Consequently, an astrophysicist on a freely collapsing star of one solar mass will be killed by tidal forces when the star's radius is $R \sim 200$ km $\gg 2M \approx 3$ km.

By the time the star is much smaller than its gravitational radius, the baryons of the astrophysicist's body are moving along geodesics; his muscles and bones have completely given way. In this final stage of collapse, the timelike geodesics are curves along which the Schwarzschild "time"-coordinate, t , is almost constant [*cf.* the narrowing down of the light cones near $r = 0$ in Figure 32.1,a; also equation (31.2) in the limit $r \ll 2M$]. The astrophysicist's feet touch the star's surface at one value of t —say $t = t_f$ —while his head moves along the curve $t = t_h > t_f$. Consequently, the length of the astrophysicist's body increases according to the formula

$$\ell_{\text{astroph}} = [g_{tt}(R)]^{1/2}[t_h - t_f] = [2M/R]^{1/2}[t_h - t_f] \propto R^{-1/2} \propto (\tau_{\text{collapse}} - \tau)^{-1/3}. \quad (32.26a)$$

Here $\tau = [-\int^R g_{rr}^{1/2} dr + \text{constant}]$ is proper time as it would be measured by the astrophysicist if he were still alive, and τ_{collapse} is the time at which he hits $r = 0$. The gravitational field also constrains the baryons of the astrophysicist's body to fall along world lines of constant θ and ϕ during the final stages of collapse. Consequently, his cross-sectional area decreases according to the law

$$\mathcal{A}_{\text{astroph}} = [g_{\theta\theta}(R)g_{\phi\phi}(R)]^{1/2} \Delta\theta \Delta\phi \propto R^2 \propto (\tau_{\text{collapse}} - \tau)^{4/3}. \quad (32.26b)$$

By combining equations (32.26a,b), one sees that the volume of the astrophysicist's body decreases, during the last few moments of collapse, according to the law

$$\mathcal{V}_{\text{astroph}} = \ell_{\text{astroph}} \mathcal{A}_{\text{astroph}} \propto R^{3/2} \propto (\tau_{\text{collapse}} - \tau). \quad (32.26c)$$

This crushing of matter to infinite density by infinitely large tidal gravitational forces can occur not only on the surface of the collapsing star, but also at any other point along the $r = 0$ singularity outside the surface of the star. Hence, any foolish rocketeer who ventures below the radius $r = 2M$ of the external gravitational field is doomed to destruction.

For further discussion of spacetime singularities, and of the possibility that quantum gravitational effects might force a reconsideration of the singularities predicted by classical gravitation theory, see Chapter 30, §34.6, and Chapter 44.

§32.7. REALISTIC GRAVITATIONAL COLLAPSE— AN OVERVIEW

Review of spherical collapse

Instability, implosion, horizon, and singularity; these are the key stages in the spherical collapse of any star. *Instability:* The star, having exhausted its nuclear fuel, and having contracted slowly inward, begins to squeeze its pressure-sustaining electrons or photons onto its atomic nuclei; this softens the equation of state, which induces an instability [see, e.g., §§10.15 and 11.4 of Zel'dovich and Novikov (1971)]

for details]. *Implosion:* Within a fraction of a second the instability develops into a full-scale implosion; for realistic density distributions, the stellar core falls rapidly inward on itself, and the outer envelopes trail along behind [see, e.g., the numerical calculations of Colgate and White (1966), Arnett (1966, 1967), May and White (1966), and Ivanova, Imsheenik, and Nadezhin (1969)]. *Horizon:* In the idealized spherical case, the star's surface falls through its gravitational radius ("horizon"; end of communication with the exterior; point of no return). From the star's vantage point this happens after a finite, short lapse of proper time. But from an external vantage point the star requires infinite time to reach the horizon, though it becomes black exponentially rapidly in the process [e-folding time $\sim M \sim 10^{-5}(M/M_\odot)$ sec]. The result is a "black hole", whose boundary is the horizon (gravitational radius), and whose interior can never communicate with the exterior. *Singularity:* From the star's interior vantage point, within a short proper time interval $\Delta\tau \sim M \sim 10^{-5}(M/M_\odot)$ sec after passing through the horizon, a singularity is reached (zero radius, infinite density, infinite tidal gravitational forces).

Does this basic picture—instability, implosion, horizon, singularity—have any relevance for real stars? Might complications such as rotation, nonsphericity, magnetic fields, and neutrino fluxes alter the qualitative picture? No, not for small initial perturbations from sphericity. Perturbation theory analyses described in Box 32.2 and exercise 32.10 show that *realistic, almost-spherically symmetric collapse, like idealized collapse, is characterized by instability, implosion, horizon;* and Penrose (1965b; see §34.6) proves that *some type of singularity then follows.*

Highly nonspherical collapse is more poorly understood, of course. Nevertheless, a number of detailed calculations and precise theorems point with some confidence to two conclusions: (1) *horizons (probably) form when and only when a mass M gets compacted into a region whose circumference in EVERY direction is $\mathcal{C} \lesssim 4\pi M$* (Box 32.3); (2) *the external gravitational field of a horizon (black hole), after all the "dust" and gravitational waves have cleared away, is almost certainly the Kerr-Newman generalization of the Schwarzschild geometry* (Chapter 33). *If so, then the external field is determined uniquely by the mass, charge, and angular momentum that went "down the hole."* (This nearly proved theorem carries the colloquial title "A black hole has no hair.")

The interior of the horizon, and the endpoint (if any) of the collapse are very poorly understood today. The various possibilities will be reviewed in Chapter 34. That a singularity occurs one can state with much certainty, thanks to theorems of Penrose, Hawking, and Geroch. But whether all, only some, or none of the collapsing matter and fields ultimately encounter the singularity one does not know.

Summary of 1972
knowledge about realistic,
nonspherical collapse:

(1) horizon

(2) black hole

(3) singularity

Exercise 32.10. PRICE'S THEOREM FOR A SCALAR FIELD

[See Price (1971, 1972a), also Thorne (1972),
for more details than are presented here.]

EXERCISES

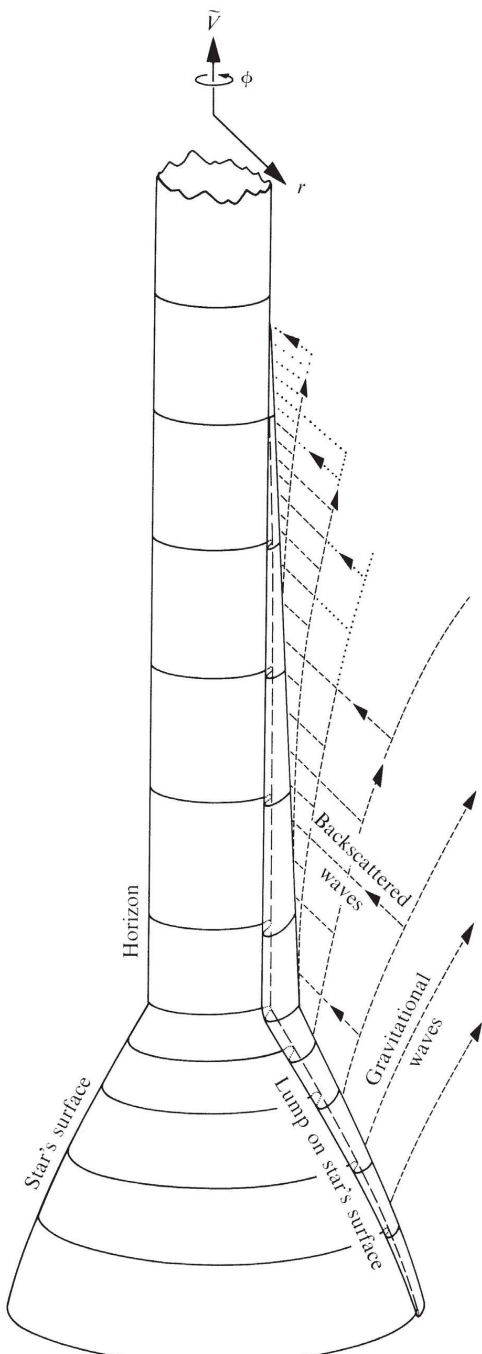
A collapsing spherical star, with an arbitrary nonspherical "scalar charge distribution," generates an external scalar field Φ . The vacuum field equation for Φ is $\square\Phi = \Phi_{;\alpha}^\alpha = 0$. Ignore the back-reaction of the field's stress-energy on the geometry of spacetime.

(continued on page 868)

Box 32.2 COLLAPSE WITH SMALL NON-SPHERICAL PERTURBATIONS
 [based on detailed calculations by Richard H. Price (1971, 1972a,b)].

A. Density Perturbations

1. When star begins to collapse, it possesses a small nonspherical “lump” in its density distribution.
2. As collapse proceeds, lump grows larger and larger [instability of collapse against small perturbations—a phenomenon well known in Newtonian theory; see, e.g., Hunter (1967); Lin, Mestel, and Shu (1965)].
3. The growing lump radiates gravitational waves.
4. Waves of short wavelength ($\lambda \ll M$), emitted from near horizon ($r - 2M \lesssim M$), partly propagate to infinity and partly get backscattered by the “background” Schwarzschild curvature of spacetime. Backscattered waves propagate into horizon (surface of black hole; gravitational radius) formed by collapsing star.
5. Waves of long wavelength ($\lambda \gg M$), emitted from near horizon ($r - 2M \lesssim M$), get fully backscattered by spacetime curvature; they never reach out beyond $r \sim 3M$; they end up propagating “down the hole.”
6. Is lump on star still there as star plunges through horizon, and does star thereby create a deformed (lumpy) horizon? Yes, according to calculations.
7. But external observers can only learn about existence of “final lump” by examining deformation (quadrupole moment) in final gravitational field. That final deformation in field does not and cannot propagate outward with infinite speed (no instantaneous “action at a distance”). It propagates with speed of light, in form of gravitational waves with near-infinite wavelength (infinite redshift from edge of horizon to any external radius). Deformation in final field, like any other wave of long wavelength, gets fully backscattered by curvature of spacetime at $r \lesssim 3M$; it cannot reach external observers. External observers can never learn of existence



Collapse depicted in ingoing
 Eddington-Finkelstein coordinates

of final lump. *Final external field is perfectly spherical, lump-free, Schwarzschild geometry!*

8. Even in region of backscatter ($2M < r \leq 3M$), final external field is lump-free. Backscattered waves, carrying information about existence of final lump, interfere destructively with outgoing waves carrying same information. Result is destruction of all deformation in external field and in horizon!
9. Final black hole is a Schwarzschild black hole!

B. Perturbations in Angular Momentum

1. When star begins to collapse, it possesses a small, nonzero intrinsic angular momentum (“spin”) \mathbf{S} .
2. As collapse proceeds, \mathbf{S} is conserved (except for a tiny, negligible change due to angular momentum carried off by waves; that change is proportional to square of amplitude of waves, i.e., to square of amplitude of perturbations in star, i.e., to S^2).
3. Consequently, external field always and everywhere carries imprint of angular momentum \mathbf{S} (on imprints, see Chapter 19). There is no need for that imprint to propagate outward from near horizon. Moreover, it could not so propagate even if it tried, because of the conservation law for \mathbf{S} (absence of dipole gravitational waves; see §§36.1 and 36.10).
4. Hence, the final external field is that of an undeformed, slowly rotating black hole:

$$ds^2 = - \left(1 - \frac{2M}{r} \right) dt^2 + \underbrace{\frac{dr^2}{1 - 2M/r} + r^2 d\Omega^2}_{\text{Schwarzschild geometry}} - \underbrace{\left(\frac{4S \sin \theta}{r^2} \right) (r \sin \theta d\phi) dt}_{\text{rotational imprint, see exercise 26.1; also Chapter 19.}}$$

Here the polar axis has been oriented along \mathbf{S} .

C. Perturbations in Electromagnetic Field

1. Star possesses a magnetic field generated by currents in its interior, and an electric field due to an arbitrary internal charge distribution; and electromagnetic radiation is emitted by its hot matter. For simplicity, \mathbf{S} is assumed zero.
2. Evolution of external electromagnetic field is similar to evolution of perturbations in external gravitational field. Distant observer can never learn “final” values of changeable quantities (magnetic dipole moment, electric dipole moment, quadrupole moments, . . .). Final values try to propagate out from horizon, carried by electromagnetic waves of near-infinite wavelength. But they cannot get out: spacetime curvature reflects them back down the hole; and they superpose destructively with their outgoing counterparts, to produce zero net field.
3. By contrast with all other quantities, which are changeable, the electric monopole moment (total flux of electric field; equal to 4π times total electric charge) is conserved. It never changes from before star collapses, through the collapse stage, into the quiescent black-hole stage.
4. Hence, the final external electromagnetic field is a spherically symmetric coulomb field

$$\begin{aligned} \mathbf{E} &= (Q/r^2)\mathbf{e}_r \\ \mathbf{B} &= 0 \end{aligned} \quad \left. \begin{array}{l} \text{as measured by static} \\ \text{observer } (r, \theta, \phi, \text{ constant}) \end{array} \right\}$$

and the final spacetime geometry is that of Reissner and Nordstrøm (charged black hole; see exercises 31.8 and 32.1):

$$ds^2 = - \left(1 - \frac{2M}{r} + \frac{Q^2}{r^2} \right) dt^2 + \frac{dr^2}{(1 - 2M/r + Q^2/r^2)} + r^2 d\Omega^2.$$

Box 32.2 (continued)**D. Generalization; Price's Theorem**

1. Let the star generate a “zero-rest-mass, integer-spin field.” [“Zero rest mass” refers to the quantized particles associated with the classical field. Classically it means the field has a Coulomb-law ($1/r$) fall off at large distances. The spin also is a property of the quantized particles; classically it is most easily visualized as describing the symmetries of a monochromatic plane wave under rotations about the direction of propagation; see §35.6. A scalar field has spin zero; an electromagnetic field has spin one; Einstein’s gravitational field has spin two; Of such fields, only gravitational ($s = 2$) and electromagnetic ($s = 1$) are known to exist in the real universe. See, e.g., Dirac (1936), Gårding (1945), Bargmann and Wigner (1948), Penrose (1965a), for further discussion.]
2. Let the spin- s field be sufficiently weak that its stress-energy perturbs the star’s external, Schwarzschild geometry only very slightly.
3. Resolve the external field into spherical harmonics (scalar spherical harmonics for $s = 0$; vector spherical harmonics for $s = 1$; tensor spherical harmonics for $s \geq 2$); and label the spherical harmonics by the usual integer ℓ ($\ell = 0$ for monopole; $\ell = 1$ for dipole; $\ell = 2$ for quadrupole; etc.).
4. All multipole fields with $\ell < s$ are conserved during the collapse (theorem from classical radiation theory). A scalar field ($s = 0$) conserves

nothing. The electromagnetic field ($s = 1$) conserves only its monopole parts (electric Coulomb field, and vanishing magnetic Coulomb field). The gravitational field ($s = 2$) conserves its monopole part (with imprint equal to mass), and its dipole parts (with imprints measuring the angular momentum, and the standard gravitational dipole moment—which vanishes if coordinate system is centered on star).

5. For $\ell \geq s$, and only for $\ell \geq s$, radiation is possible (scalar waves can have any multipolarity; electromagnetic waves must be dipole and higher; gravitational waves must be quadrupole and higher; see §36.1).
6. Price’s theorem states that, as the nearly spherical star collapses to form a black hole, all things that can be radiated (all multipoles $\ell \geq s$) get radiated completely away—in part “off to infinity”; in part “down the hole” (“what is permitted is compulsory”). The final field is characterized completely by its conserved quantities (multipole moments with $\ell < s$).
7. For proof of Price’s theorem in the case of a scalar field, see exercise 32.10.

E. Generalization to Nonclassical Fields

See Hartle (1971, 1972) and Teitelboim (1972b,c) for neutrino fields; Bekenstein (1972a,b) and Teitelboim (1972a) for pion fields.

Box 32.3 COLLAPSE IN ONE AND TWO DIMENSIONS

A. The Question

To produce a black hole (horizon from which nothing can emerge), must one compact matter strongly in all three spatial dimensions, to circumferences $\mathcal{C} \lesssim 4\pi M$ (quasispherical compaction); or is it sufficient to compact only in one or two dimensions?

B. The Answer for One Dimension

Consider, as an example readily generalized, the gravitational collapse of a spheroid of dust (zero pressure). Let the spheroid be highly Newtonian ($r \gg 2M$) in its initial, momentary state of rest; and let it be slightly flattened (oblate). In Newtonian theory, any homogeneous, nonrotating spheroid of dust remains homogeneous as it collapses; but its deformations grow [see, e.g., Lin, Mestel, and Shu (1965) for details]. Hence, the spheroid of interest implodes to form a pancake of infinite density but finite mass per unit surface area. The final kinetic energy of the dust particles is roughly equal to their final potential energy:

$$\frac{1}{2} v^2 \sim \frac{M}{(\mathcal{C}/2\pi)}$$

M = mass of spheroid,

\mathcal{C} = circumference of final pancake.

Consequently, so long as $\mathcal{C}/2\pi \gg 2M$, the collapse velocities remain much smaller than light, and the gravitational energy remains much smaller than the rest mass-energy. This means that for $\mathcal{C}/2\pi \gg 2M$, the Newtonian analysis is an excellent approximation to general relativity all the way down to the pancake endpoint. Hence, *no horizon can form*, hardly any gravitational waves are emitted, and the whole story is exceedingly simple and fully Newtonian. However, since the pancake endpoint is not a singularity of spacetime (see the remarks at end of exercise 32.8), the evolution can proceed beyond it; and as \mathcal{C} contracts to $\lesssim 4\pi M$, the evolu-

tion will become very complicated and highly relativistic (see the “collapse, pursuit, and plunge scenario” of Figure 24.3).

C. The Answer for Two Dimensions

Consider, as an example *not* so readily generalized, the gravitational collapse of a homogeneous prolate spheroid of dust, initially highly Newtonian. Such a spheroid collapses to form a thin “thread” or “spindle” [see Lin, Mestel, and Shu (1965)]. Assume that the spheroid is still Newtonian when its threadlike state is reached. It then has a length ℓ , a mass per unit length $\lambda = M/\ell \ll 1$, and a rapidly contracting equatorial radius $R \ll \ell$. Subsequently, each segment of the thread collapses radially as though it were part of an infinite cylinder. [Ignore the instability of breakup into “beads”; see, e.g., Hunter (1967), Chandrasekhar (1968).] The radial collapse velocity approaches the speed of light and the gravitational energy approaches the rest mass-energy only when the thread has become exceedingly thin, $R \leq R_{\text{crit}} \sim \ell \exp(-1/4\lambda)$. At this stage, relativistic deviations from Newtonian collapse come into play. Thorne (1972) and Morgan and Thorne (1973) have analyzed the relativistic effects using an idealized infinite-cylinder model. The results are very different from either the spherical case or the pancake case. The collapsing cylinder emits a large flux of gravitational waves; but they are powerless to halt the collapse. *The collapse proceeds inward to a thread-like singularity, without the creation of any horizon (no black hole!).*

D. Objection to the Answer, a Reply, and a Conjecture

One can object that the collapses of both pancake and cylinder can be halted short of their endpoints, especially that of the pancake. As the thickness of

Box 32.3 (continued)

the pancake approaches zero, the vertical pull of gravity remains finite, but the pressure gradient caused by any finite pressure goes to infinity. Hence, pressure halts the collapse. Subsequently the rim of the pancake contracts toward the relativistic regime $\mathcal{C}/2\pi \lesssim 2M$. In the collapse of a cylinder according to Newtonian theory, with a pressure-density relation $p \propto \rho^\gamma$, the gravitational acceleration a_g and pressure-buoyancy acceleration a_p vary as

$$a_g = -2\lambda/R, \quad a_p \sim \rho^{-1}(p/R) \propto \rho^{\gamma-1}/R.$$

Hence, for $\gamma > 1$ (the most common realistic case) pressure halts the collapse, but for $\gamma < 1$ it does

not. Whether this is true also after the relativistic domain is reached, one does not yet know.

Actually, the ability of pressure to halt the collapse is of no importance to the issue of black holes and horizons. The important thing is that *in oblate collapse with final circumference $\mathcal{C} \gg 4\pi M$, and also in prolate collapse with final thread length $\ell \gg 2M$, no horizons are created*. This, coupled with the omnipresent horizons in nearly spherical collapse (Box 32.2) suggests the following conjecture [Thorne (1972)]: *Black holes with horizons form when and only when a mass M gets compacted into a region whose circumference in EVERY direction is $\mathcal{C} \lesssim 4\pi M$.* (Like most conjectures, this one is sufficiently vague to leave room for many different mathematical formulations!)

(a) Resolve the external field into scalar spherical harmonics, using Schwarzschild coordinates for the external Schwarzschild geometry:

$$\Phi = \sum_{\ell} \frac{1}{r} \Psi_{\ell}(t, r) Y_{lm}(\theta, \phi). \quad (32.27a)$$

Show that the vacuum field equation reduces to

$$-\Psi_{\ell,tt} + \Psi_{\ell,r^*r^*} = \left(1 - \frac{2M}{r}\right) \left(\frac{2M}{r^3} + \frac{\ell(\ell+1)}{r^2}\right) \Psi_{\ell}, \quad (32.27b)$$

where r^* is the “tortoise coordinate” of §25.5 and Figure 25.4:

$$r^* = r + 2M \ln(r/2M - 1). \quad (32.27c)$$

Notice that (32.27b) is a flat-space, one-dimensional wave equation with effective potential

$$V_{\text{eff}}(r) = \left(1 - \frac{2M}{r}\right) \left(\frac{2M}{r^3} + \frac{\ell(\ell+1)}{r^2}\right). \quad (32.27d)$$

Part of this effective potential [$\ell(\ell+1)/r^2$] is the “centrifugal barrier,” and part [$2M/r$] is due to the curvature of spacetime. Notice the similarity of this effective potential for scalar waves, to the effective potentials for particles and photons moving in the Schwarzschild geometry,

$$\begin{aligned} (\tilde{V}^2)_{\text{particles}} &= (1 - 2M/r)(1 + \tilde{L}^2/r^2), \\ (B^{-2})_{\text{photons}} &= (1 - 2M/r)r^{-2} \end{aligned}$$

(Boxes 25.6 and 25.7). The scalar-wave potential, like the photon potential, is positive for all $r > 2M$. It rises, from 0 at $r = 2M$, to a barrier summit; then falls back to 0 at $r = \infty$.

(b) Show that *there exist no physically acceptable, static scalar-wave* perturbations of a Schwarzschild black hole. [More precisely, show that all static solutions to equation (32.27b) become infinite at either the horizon ($r = 2M, r^* = -\infty$) or at radial infinity.] This suggests that somehow the black hole formed by collapse must divest itself of the star's external scalar field before it can settle down into a quiescent state.

(c) The general solution to the wave equation (32.27b) can be written in terms of a Fourier transform. For waves that begin near the horizon, propagate outward, and are partially transmitted and partially reflected ("rightward-propagating waves"), show that the general solution is

$$\Psi_l(t, r^*) = \int_{-\infty}^{\infty} A(k) R_k^l(r^*) e^{-ikt} dk, \quad (32.28a)$$

where

$$d^2 R_k^l / dr^{*2} = [-k^2 + V_{\text{eff}}(r)] R_k^l, \quad (32.28b)$$

$$R_k^l = e^{ikr^*} + \Gamma_k^{(R)} e^{-ikr^*} \quad \text{as } r^* \rightarrow -\infty,$$

$$R_k^l = T_k^{(R)} e^{ikr^*} \quad \text{as } r^* \rightarrow \infty. \quad (32.28c)$$

Show that the "reflection and transmission coefficients for rightward-propagating waves," $\Gamma_k^{(R)}$ and $T_k^{(R)}$, have the following asymptotic forms for $|k| \ll 1/M$ (short wave number; long wavelength):

$$\Gamma_k^{(R)} = -1 + \alpha 2Mik, \quad T_k^{(R)} = \underbrace{\frac{\beta}{(2\ell - 1)!!} (2Mik)^{\ell + 1}}_{\substack{\uparrow \\ \text{no transmission} \\ \text{in limit } k \rightarrow 0; \text{ see} \\ \text{Box 32.2}}} \quad (32.28d)$$

↑

[produces complete reflection and complete destructive interference in limit $k \rightarrow 0$; see Box 32.2 for detailed discussion of consequences]

where α and β are constants of order unity. Give a similar analysis for waves that impinge on a Schwarzschild black hole from outside ("leftward-propagating waves").

(d) Show that, as the star collapses into the horizon, the world line of its surface in (t, r^*) coordinates is

$$r^* = R^*(t) \equiv -t - R_0^* \exp(-t/2M) + \text{const.}, \quad (32.29a)$$

where R_0^* is related to the magnitude a of the surface's 4-acceleration ($a > 0$ for outward 4-acceleration) by

$$R_0^* = (8M/e) \left\{ 1 + 16Ma \left[Ma + \left(M^2a^2 + \frac{1}{8} \right)^{1/2} \right] \right\}. \quad (32.29b)$$

Thus, the world line of the surface appears to become null near the horizon ($t + r^* \equiv \tilde{V} = \text{constant}$); of course, this is due to pathology of the coordinate system there. Show, further, that the scalar field on the star's surface ($\tilde{V} = \text{constant}$) must vary as

$$\Psi_l = Q_{l0} + Q_{l1} e^{-\tilde{U}/4M}, \quad \tilde{U} \equiv t - r^*. \quad (32.29c)$$

when the star is approaching the horizon ($t \rightarrow \infty, r^* \rightarrow -\infty, \tilde{U} \rightarrow \infty$), in order that the rate of change of Ψ_l be finite as measured on the star's surface. Notice that Q_{l0} is the "final value" of the scalar field on the star's surface. It can be regarded as an outgoing wave with zero wave number (infinite wavelength); and, consequently, *it gets completely and*

destructively reflected by the effective potential [see equation (32.28d); also Box 32.2]. Conclusion: All multipoles of the scalar field die out at finite r^* as $t \rightarrow \infty$. (Price's theorem for a scalar field.) For a more detailed analysis, including the rates at which the multipoles die out, see Price (1971, 1972a) or Thorne (1972).

Exercise 32.11. NEWMAN-PENROSE “CONSTANTS”

[See Press and Bardeen (1971), Bardeen and Press (1972), and Piir (1971) for more details than are presented here.]

Wheeler (1955) showed that Maxwell's equations for an ℓ -pole electromagnetic field residing in the Schwarzschild geometry can be reduced to the wave equation

$$-\Psi_{\ell,tt} + \Psi_{\ell,r^*r^*} = \left(1 - \frac{2M}{r}\right) \frac{\ell(\ell+1)}{r^2} \Psi_{\ell} \quad (32.30)$$

[electromagnetic analogue of (32.27b)]. After this equation has been solved, the components of the electromagnetic field can be obtained by applying certain differential operators to $\Psi_{\ell}(t, r^*) Y_{lm}(\theta, \phi)$.

(a) Show that the general solution to the electromagnetic wave equation (32.30) for dipole ($\ell = 1$) fields, with outgoing-wave boundary conditions at $r^* \rightarrow +\infty$, has the form

$$\Psi_1 = f_0(\tilde{U}) + \frac{f_1(\tilde{U})}{r} + \frac{f_2(\tilde{U})}{r^2} + \dots, \quad (32.31a)$$

where

$\tilde{U} = t - r^*$ is “retarded time”, and

$$f'_1 = f_0, \quad f'_2 = 0, \quad \dots, \quad f'_n = -\frac{(n+1)(n-2)}{2n} f_{n-1} + (n-2)M f_{n-2}. \quad (32.31b)$$

When spacetime is flat ($M = 0$), this solution becomes

$$\Psi_1 = f'_1(\tilde{U}) + f_1(\tilde{U})/r. \quad (32.31N)$$

[The $1/r$ fall-off of the radiation field $f'_1(\tilde{U})$ has been factored out of Ψ_1 ; see the scalar-wave function (32.27a).] The terms $f'_2(\tilde{U})/r^2 + \dots$, which are absent in flat spacetime, are attributable to backscatter of the outgoing waves by the curvature of spacetime. They are sometimes called the “tail” of the waves.

(b) Show that the general static dipole field has the form (32.31a) with

$$(f_0)_{\text{static}} = 0; \quad (f_1)_{\text{static}} \equiv D = \text{dipole moment}; \quad (32.32)$$

$$(f_2)_{\text{static}} = \frac{3}{2} MD; \dots$$

(c) Consider a star (not a black hole!) with a dipole field that is initially static. At time $t = 0$, let the star suddenly change its dipole moment to a new static value D' . Equations (32.31b) demand that f_2 be conserved [“Newman-Penrose (1965) constant”]. Hence, f_2 will always exhibit a value, $\frac{3}{2}MD$, corresponding to the old dipole moment; it can never change to $\frac{3}{2}MD'$. This is a manifestation of the tail of the waves that are generated by the sudden change in dipole moment. To understand this tail effect more clearly, and to discover an important flaw in the above result, evaluate the solution (32.31) for retarded time $\tilde{U} > 0$, using the assumptions

- (1) field has static form (32.32) for $\tilde{U} < 0$,
- (2) $f_1 = D'$ for $\tilde{U} > 0$.

Put the answer in the form

$$\Psi_1 = \underbrace{\frac{D'}{r} + \frac{\frac{3}{2}MD}{r^2}}_{\text{new static solution}} + \sum_{n=3}^{\infty} \frac{2M(D' - D)(-1)^{n+1}(n+1)\tilde{U}^{n-2}}{(2r)^n} + O\left(\frac{M^2}{r^3}, \frac{M^2\tilde{U}}{r^4}\right). \quad (32.34)$$

(The terms neglected are small compared to those kept for all \tilde{U}/r , so long as $r \gg M$.) Evidently, so long as the series converges the Newman-Penrose “constant” (coefficient of $1/r^2$) remembers the old D value and is conserved, as claimed above. Show, however, that the series diverges for $\tilde{U} > 2r$ —i.e., it diverges inside a sphere that moves outward with asymptotically $\frac{1}{3}$ the speed of light. Thus, *the Newman-Penrose “constant” is well-defined and conserved only outside the “ $\frac{1}{3}$ -speed-of-light cone.”*

(d) Sum the series in (32.34) to obtain a solution valid even for $\tilde{U} > 2r$:

$$\begin{aligned} \Psi &= \underbrace{\frac{D'}{r} + \frac{3}{2}\frac{MD'}{r^2}}_{\text{new static solution}} - \underbrace{\frac{2M(D' - D)}{r} \frac{(\tilde{U} + 3r)}{(\tilde{U} + 2r)^2}}_{\text{“tail term”}} + O\left(\frac{M^2}{r^3}\right) \\ &= \text{the series (32.34) for } \tilde{U} < 2r \text{ (domain of convergence of that series)} \\ &= \frac{D'}{r} + \frac{3}{2}\frac{MD'}{r^2} + O\left(\frac{M}{\tilde{U}r}, \frac{M^2}{r^3}\right) \quad \text{for } \tilde{U} \gg r \gg M. \end{aligned} \quad (32.35)$$

From this result conclude that *at fixed r and late times the electromagnetic field becomes asymptotically static, and the Newman-Penrose “constant” assumes the new value $\frac{3}{2}MD'$ appropriate to the new dipole moment.*

CHAPTER 33

BLACK HOLES

A luminous star, of the same density as the Earth, and whose diameter should be two hundred and fifty times larger than that of the Sun, would not, in consequence of its attraction, allow any of its rays to arrive at us; it is therefore possible that the largest luminous bodies in the universe may, through this cause, be invisible.

P. S. LAPLACE (1798)

A dialog explaining why black holes deserve their name

§33.1. WHY “BLACK HOLE”?

Sagredus. What is all this talk about “black holes”? When an external observer watches a star collapse, he sees it implode with ever-increasing speed, until the relativistic stage is reached. Then it appears to slow down and become “frozen,” just outside its horizon (gravitational radius). However long the observer waits, he never sees the star proceed further. How can one reasonably give the name “black hole” to such a frozen object, which never disappears from sight?

Salvatius. Let us take the name “black hole” apart. Consider first the blackness. Surely nothing can be blacker than a black hole. The very redshift that makes the collapsing star appear to freeze also makes it darken and become black. In the continuum approximation, where one ignores the discreteness of photons, the intensity of the radiation received by distant observers decreases exponentially as time passes, $L \propto \exp(-t/3\sqrt{3}M)$, with an exceedingly short e -folding time

$$\tau = 3\sqrt{3}M = (2.6 \times 10^{-5} \text{ sec})(M/M_{\odot}).$$

Within a fraction of a second, the star is essentially black. Discreteness of photons makes it even blacker. The number of photons emitted before the star crosses its horizon is finite, so the exponential decay cannot continue

For a more detailed exposition of the foundations of “black-hole physics,” see DeWitt and DeWitt (1973).

forever. Eventually—only $10^{-3}(M/M_\odot)$ seconds after the star begins to dim (see exercise 32.2)—the last photon that will ever get out reaches the distant observers. Thereafter nothing emerges. The star is not merely “essentially black”; it is “*absolutely black*.”

Sagredus. Agreed. But it is the word “hole” that concerns me, not “black.” How can one possibly regard the name “hole” as appropriate for an object that hovers forever just outside its horizon. True, absence of light makes the object invisible. But couldn’t one always see it by shining a flashlight onto its surface? And couldn’t one always fly down to its surface in a rocket ship and scoop up a few of the star’s baryons? After all, as seen from outside the baryons at its surface will never, never, never manage to fall into the horizon!

Salvatius. Your argument *sounds* persuasive. To test its validity, examine the collapse of a spherically symmetric system, using the ingoing Eddington-Finkelstein diagram of Figure 33.1. Let a family of external observers shine their flashlights onto the star’s surface, as you have suggested. Let the surface of the star be carefully silvered so it reflects back all light that reaches it. Initially (low down in the spacetime diagram of Figure 33.1) the ingoing light beams

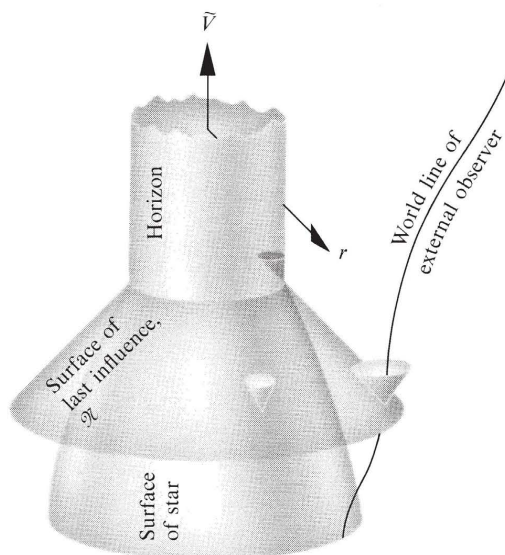


Figure 33.1.

Spherical gravitational collapse of a star to form a black hole, as viewed in ingoing Eddington-Finkelstein coordinates. The “surface of last influence,” \mathcal{R} , is an ingoing null surface that intersects the horizon in coincidence with the surface of the collapsing star. After an external observer, moving forward in time, has passed through the surface of last influence, he cannot interact with and influence the star before it plunges through the horizon. Thus, one can think of the surface of last influence as the “birthpoint” of the black hole. Before passing through this surface, the external observer can say his flashlight is probing the shape of a collapsing star; afterwards, he can regard his signals as probes of a black hole. For further discussion, see text.

reach the star's surface and are reflected back to the flashlights with no difficulty. But there is a critical point—an ingoing radial null surface \mathcal{N} —beyond which reflection is impossible. Photons emitted inward along \mathcal{N} reach the star just as it is passing through its horizon. After reflection these photons fly “outward” along the horizon, remaining forever at $r = 2M$. Other photons, emitted inward after the flashlight has passed through \mathcal{N} , reach the surface of the star and are reflected only after the star is inside its horizon. Such photons can never return to the shining flashlights. Once inside the horizon, they can never escape. Thus, the total number of photons returned is finite and is subject to the same blackness decay law as is the intrinsic luminosity of the star. Moreover, *if the observers do not turn on their flashlights until after they pass through the null surface \mathcal{N} , they can never receive back any reflected photons!* Evidently, flashlights are of no help in seeing the “frozen star.”

Sagredus. I cannot escape the logic of your argument. Nevertheless, seeing is not the only means of interacting with the frozen star. I have already suggested swooping down in a rocket ship and stealing a few baryons from its surface. Similarly, one might let matter fall radially inward onto the frozen star. When the matter hits the star's surface, its great kinetic energy of infall will be converted into heat and into outpouring radiation.

Salvatius. Thus it might seem at first sight. But examine again Figure 33.1. No swooping rocket ship and no infalling matter can move inward faster than a light ray. Thus, if the decision to swoop is made after the ship passes through the surface \mathcal{N} , the rocket ship has no possibility of reaching the star before it plunges through the horizon; the rocket and pilot cannot touch the star, sweep up baryons, and return to tell their tale. Similarly, infalling matter to the future of \mathcal{N} can never hit the star's surface before passing through the horizon. The surface \mathcal{N} is, in effect, a “surface of last influence.” Once anybody or anything has passed through \mathcal{N} , he or it has no possibility whatever of influencing or interacting with the star in any way before it plunges through the horizon. *Thus, from a “causal” or “interaction” standpoint, the collapsing star becomes a hole in space at the surface \mathcal{N} .* This hole is not black at first. Radiation from the collapsing star still emerges after \mathcal{N} because of finite light-propagation times, just as radiation still reaches us today from the hot big-bang explosion of the universe. But if an observer at radius $r \gg 2M$ waits for a time $2r$ after passing through \mathcal{N} (time for \mathcal{N} to reach horizon, plus time for rays emitted at $R \sim 3M$ to get back to observer), then he will see the newly formed hole begin to turn black; and within a time $\Delta t \sim (10^{-3} \text{ seconds})(M/M_\odot)$ thereafter, it will be completely black.

Sagredus. You have convinced me. For all practical purposes the phrase “black hole” is an excellent description. The alternative phrases “frozen star” and “collapsed star,” which I find in the pre-1969 physics literature, emphasize an optical-illusion aspect of the phenomenon. Attention must be directed away from the star that created the black hole, because beyond the surface of last influence one has no means to interact with that star. The star is irrelevant

to the subsequent physics and astrophysics. Only the horizon and its external spacetime geometry are relevant for the future. Let us agree to call that horizon the “surface of a black hole,” and its external geometry the “gravitational field of the black hole.”

Salvatius. Agreed.

§33.2. THE GRAVITATIONAL AND ELECTROMAGNETIC FIELDS OF A BLACK HOLE

The collapse of an electrically neutral star endowed with spherical symmetry produces a spherical black hole with external gravitational field described by the Schwarzschild line element

$$ds^2 = -(1 - 2M/r) dt^2 + \frac{dr^2}{1 - 2M/r} + r^2(d\theta^2 + \sin^2\theta d\phi^2). \quad (33.1)$$

The surface of the black hole, i.e., the horizon, is located at $r = 2M$ = (gravitational radius). Only the region on and outside the black hole’s surface, $r \geq 2M$, is relevant to external observers. Events inside the horizon can never influence the exterior.

The gravitational collapse of a realistic star (nonspherical, collapse with small but nonzero net charge of one sign or the other) produces a black hole somewhat different from the simple Schwarzschild hole. For collapse with small charge and small asymmetries, perturbation-theory calculations (Box 32.2) predict a final black hole with external field determined entirely by the mass M , charge Q , and intrinsic angular momentum S of the collapsing star. For fully relativistic collapse, with large asymmetries and possibly a large charge, the final black hole (if one forms) is also characterized uniquely by M , Q , and S . This is the conclusion that strongly suggests itself in 1972 from a set of powerful theorems described in Box 33.1.

The structure of a black hole is determined uniquely by its mass M , charge Q , and intrinsic angular momentum, S

Heuristic explanation of the $M\text{-}Q\text{-}S$ uniqueness

Why M , Q , and S should be the complete governors of the final external field of the black hole, one can understand heuristically as follows. Of all quantities intrinsic to any isolated source of gravity and electromagnetism, only M , Q , and S possess (and are defined in terms of) *unique, conserved imprints* in the distant external fields of the source (conserved Gaussian flux integrals; see Box 19.1 and §20.2). When a star collapses to form a black hole, its distant external fields are forced to maintain unchanged the imprints of M , Q , and S . In effect, M , Q , and S provide anchors or constraints on the forms of the fields. Initially other constraints are produced by the distributions of mass, momentum, stress, charge, and current inside the star. But ultimately the star plunges through a horizon, cutting itself off causally from the external universe. (The nonpropagation of long-wavelength waves through curved spacetime plays a key role in this cutoff; see Box 32.2.) Subsequently, the only anchors remaining for the external fields are the conserved imprints of M , Q , and S . Consequently, the external fields quickly settle down into unique shapes corresponding to the given M , Q , and S . Of course, the settling down involves dynamic changes of the fields and an associated outflow of gravitational and electro-

Box 33.1 A BLACK HOLE HAS NO “HAIR”

The following theorems come close to proving that *the external gravitational and electromagnetic fields of a stationary black hole (a black hole that has settled down into its “final” state) are determined uniquely by the hole’s mass M , charge Q , and intrinsic angular momentum S* —i.e., the black hole can have no “hair” (no other independent characteristics). For a detailed review, see Carter (1973).

- I. Stephen Hawking (1971b, 1972a): A stationary black hole must have a horizon with spherical topology; and it must either be static (zero angular momentum), or axially symmetric, or both.
- II. Werner Israel (1967a, 1968): Any *static* black hole with event horizon of spherical topology has external fields determined uniquely by its mass M and charge Q ; moreover, those external fields are the Schwarzschild solution if $Q = 0$, and the Reissner-Nordström solution (exercises 31.8 and 32.1) if $Q \neq 0$ (both special cases of Kerr-Newman; see §33.2).
- III. Brandon Carter (1970): “All uncharged, stationary, axially symmetric black holes with event horizons of spherical topology fall into disjoint families not deformable into each other. The black holes in each family have external gravitational fields determined uniquely by two parameters: the mass M and the angular momentum S .” (Note: the “Kerr solutions”—i.e., “Kerr-Newman” with $Q = 0$ —form one such family; it is very likely that there are no others, but this has not been proved as of December 1972. It is also likely that Carter’s theorem can be extended to the case with charge; but this has also not yet been done.)

IV. Conclusions made by combining all three theorems:

- (a) All stationary black holes are axially symmetric.
- (b) All static (nonrotating) black holes are characterized uniquely by M and Q , and have the Reissner-Nordström form.
- (c) All uncharged, rotating black holes fall into distinct and disjoint families, with each black hole in a given family characterized uniquely by M and S . The Kerr solutions form one such family. There may well be no other family.

V. Remarks and Caveats:

- (a) The above statements of the theorems are all somewhat heuristic. Each theorem makes several highly technical assumptions, not stated here, about the global properties of spacetime. These assumptions seem physically reasonable and innocuous, but they might not be.
- (b) Progress in black-hole physics is so rapid that, by the time this book is published, there may well exist theorems more powerful than the above, which really prove that “a black hole has no hair.”
- (c) For insight into the techniques of “global geometry” used in proving the above theorems and others like them, see Chapter 34; for greater detail see the forthcoming book by Hawking and Ellis (1973).
- (d) For analyses which show that a black hole cannot exert any weak-interaction forces caused by the leptons which have gone down it, see Hartle (1971, 1972) and Teitelboim (1972b,c). For similar analyses which show absence of strong-interaction forces from baryons that have gone down the hole, see Bekenstein (1972a,b) and Teitelboim (1972a).

magnetic waves. And, of course, the outflowing waves carry off mass and angular momentum (but not charge), thereby leaving M and S changed. And, of course, the external fields must then readjust themselves to the new M and S . But the process will quickly converge, producing a black hole with specific final values of M , Q , and S and with external fields determined uniquely by those values.

The problem of calculating the external fields for given M , Q , and S and their given imprints, is analogous to the problem of Plateau—to calculate the shape of a soap film anchored to a wire of given shape.* One calculates the shape of the soap film by seeking a surface of minimum area spanning the bent wire. The condition of minimum area leads to a differential equation describing the soap film, which must be solved subject to the constraint imposed by the shape of the wire.

To calculate the external fields of a black hole, one can extremize the “action integral” $\int(\mathcal{R} + \mathcal{L})\sqrt{-g}d^4x$ for interacting gravitational and electromagnetic fields (see Chapter 21) subject to the anchored-down imprints of M , Q , and S at radial infinity, and subject to the existence of a physically nonsingular horizon (no infinite curvature at horizon!). Extremizing the action is equivalent to solving the coupled Einstein-Maxwell field equations subject to the constraints imprinted by M , Q , and S , and the existence of the horizon. The derivation of the solution and the proof of its uniqueness are much too complex to be given here. (See references cited in Box 33.1.) However, the solution turns out to be the “*Kerr-Newman geometry*” and its associated electromagnetic field.†

Written in the t, r, θ, ϕ coordinates of Boyer and Lindquist (1967) (generalization of Schwarzschild coordinates), the Kerr-Newman geometry has the form

$$ds^2 = -\frac{\Delta}{\rho^2}[dt - a \sin^2\theta d\phi]^2 + \frac{\sin^2\theta}{\rho^2} [(r^2 + a^2)d\phi - a dt]^2 + \frac{\rho^2}{\Delta} dr^2 + \rho^2 d\theta^2, \quad (33.2)$$

(1) metric (“Kerr-Newman geometry”)

where

$$\Delta \equiv r^2 - 2Mr + a^2 + Q^2, \quad (33.3a)$$

$$\rho^2 \equiv r^2 + a^2 \cos^2\theta, \quad (33.3b)$$

$$a \equiv S/M \equiv \text{angular momentum per unit mass}. \quad (33.4)$$

The corresponding electromagnetic field tensor, written as a 2-form (recall: $\mathbf{dx}^\alpha \wedge \mathbf{dx}^\beta \equiv \mathbf{dx}^\alpha \otimes \mathbf{dx}^\beta - \mathbf{dx}^\beta \otimes \mathbf{dx}^\alpha$) is

$$\mathbf{F} = Q\rho^{-4}(r^2 - a^2 \cos^2\theta) \mathbf{dr} \wedge [\mathbf{dt} - a \sin^2\theta \mathbf{d}\phi] + 2Q\rho^{-4}ar \cos\theta \sin\theta \mathbf{d}\theta \wedge [(r^2 + a^2) \mathbf{d}\phi - a \mathbf{dt}]. \quad (33.5)$$

(2) electromagnetic field

*On the problem of Plateau see, e.g., Courant (1937), Darboux (1941), or p. 157 of Lipman Bers (1952).

†The uncharged ($Q = 0$) version was first found as a solution to Einstein’s vacuum field equations by Kerr (1963). The charged generalization was first found as a solution to the Einstein-Maxwell field equations by Newman, Couch, Chinnapared, Exton, Prakash, and Torrence (1965). Only later was the connection to black holes discovered; see Box 33.1.

Variational principle for black-hole structure

Details of black-hole structure:

Expressions (33.2) for the metric and (33.5) for the electromagnetic field are sufficiently long to be somewhat frightening. Therefore, it is helpful to develop some qualitative insight into them and into their implications before attempting detailed computations with them. Boxes 33.2, 33.3, and 33.4 develop qualitative insight by presenting, without derivation, a summary of the key features of the Kerr-Newman geometry and a summary of the physics and astrophysics of black holes. The remainder of this chapter is a Track-2 justification and derivation of some, but not all, of the results cited in Boxes 33.2–33.4.

(continued on page 891)

Box 33.2 KERR-NEWMAN GEOMETRY AND ELECTROMAGNETIC FIELD

I. Equations for metric and electromagnetic field

A. Parameters appearing in equations:

M = mass, Q = charge, $a \equiv S/M$ = angular momentum per unit mass, all as measured by their standard imprints on the distant fields.

B. Constraint on parameters:

The Kerr-Newman geometry has a horizon, and therefore describes a black hole, if and only if $M^2 \geq Q^2 + a^2$. It seems likely that in any collapsing body which violates this constraint, centrifugal forces and/or electrostatic repulsion will halt the collapse before a size $\sim M$ is reached; see equation (33.56).

C. Limiting cases:

- | | |
|-------------------|---|
| $Q = 0$, | Kerr (1963) geometry; |
| $S = 0$, | Reissner-Nordstrøm geometry and electromagnetic field
(exercises 31.8 and 32.1); |
| $Q = S = 0$, | Schwarzschild geometry; |
| $M^2 = Q^2 + a^2$ | “Extreme Kerr-Newman geometry.” |

D. Boyer-Lindquist (1967) coordinates (t, r, θ, ϕ —generalization of Schwarzschild coordinates; black hole rotates in ϕ direction):

$$ds^2 = -(\Delta/\rho^2)[dt - a \sin^2\theta d\phi]^2 + (\sin^2\theta/\rho^2)[(r^2 + a^2)d\phi - a dt]^2 + (\rho^2/\Delta)dr^2 + \rho^2 d\theta^2; \quad (1)$$

$$\Delta \equiv r^2 - 2Mr + a^2 + Q^2, \quad \rho^2 \equiv r^2 + a^2 \cos^2\theta. \quad (2)$$

$$\mathbf{F} = Q\rho^{-4}(r^2 - a^2 \cos^2\theta) \mathbf{dr} \wedge [\mathbf{dt} - a \sin^2\theta \mathbf{d}\phi] + 2Q\rho^{-4}ar \cos\theta \sin\theta \mathbf{d}\theta \wedge [(r^2 + a^2) \mathbf{d}\phi - a \mathbf{dt}]. \quad (3)$$

E. Kerr coordinates [$\tilde{V}, r, \theta, \tilde{\phi}$ —generalization of ingoing Eddington-Finkelstein coordinates; $(\tilde{V}, \theta, \tilde{\phi}) = \text{constant}$ is an ingoing, “radial,” null geodesic; black hole rotates in $\tilde{\phi}$ direction]:

Relationship to Boyer-Lindquist:

$$\begin{aligned}\mathbf{d}\tilde{V} &= \mathbf{dt} + (r^2 + a^2)(\mathbf{dr}/\Delta), \\ \mathbf{d}\tilde{\phi} &= \mathbf{d}\phi + a(\mathbf{dr}/\Delta).\end{aligned}\quad (4)$$

$$\begin{aligned}ds^2 &= -[1 - \rho^{-2}(2Mr - Q^2)] d\tilde{V}^2 + 2 dr d\tilde{V} + \rho^2 d\theta^2 \\ &\quad + \rho^{-2}[(r^2 + a^2)^2 - \Delta a^2 \sin^2\theta] \sin^2\theta d\tilde{\phi}^2 - 2a \sin^2\theta d\tilde{\phi} dr \\ &\quad - 2ap^{-2}(2Mr - Q^2) \sin^2\theta d\tilde{\phi} d\tilde{V}.\end{aligned}\quad (5)$$

$$\begin{aligned}\mathbf{F} &= Q\rho^{-4}[(r^2 - a^2 \cos^2\theta) \mathbf{dr} \wedge \mathbf{d}\tilde{V} - 2a^2 r \cos\theta \sin\theta \mathbf{d}\theta \wedge \mathbf{d}\tilde{V} \\ &\quad - a \sin^2\theta(r^2 - a^2 \cos^2\theta) \mathbf{dr} \wedge \mathbf{d}\tilde{\phi} + 2ar(r^2 + a^2) \cos\theta \sin\theta \mathbf{d}\theta \wedge \mathbf{d}\tilde{\phi}].\end{aligned}\quad (6)$$

II. Properties of spacetime geometry

A. Symmetries (§33.4):

The metric coefficients in Boyer-Lindquist coordinates are independent of t and ϕ , and in Kerr coordinates are independent of \tilde{V} and $\tilde{\phi}$. Thus the spacetime geometry is “time-independent” (stationary) and axially symmetric. The “Killing vectors” (§25.2) associated with these two symmetries are $(\partial/\partial t)_{r,\theta,\phi} = (\partial/\partial \tilde{V})_{r,\theta,\tilde{\phi}}$ and $(\partial/\partial \phi)_{t,r,\theta} = (\partial/\partial \tilde{\phi})_{\tilde{V},r,\theta}$.

B. Dragging of inertial frames and static limit (§33.4):

1. The “dragging of inertial frames” by the black hole’s angular momentum produces a precession of gyroscopes relative to distant stars. By this precession one defines and measures the angular momentum of the black hole (see §§19.2 and 19.3).

2. The dragging becomes more and more extreme the nearer one approaches the horizon of the black hole. Before the horizon is reached, at a surface described by

$$\begin{aligned}r &= r_0(\theta) \\ &\equiv M + \sqrt{M^2 - Q^2 - a^2 \cos^2\theta},\end{aligned}\quad (7)$$

the dragging becomes so extreme that no observer can possibly remain at rest there (i.e., be “static”) relative to the distant stars. At and inside this surface

(called the “*static limit*”), all observers with fixed r and θ must orbit the black hole in the same direction in which the hole rotates:

$$\begin{aligned}\Omega &\equiv d\phi/dt \\ &> \frac{a \sin\theta - \sqrt{\Delta}}{(r^2 + a^2) \sin\theta - \sqrt{\Delta} a \sin^2\theta} \\ &(\geq 0 \text{ for } a = S/M > 0 \text{ and } r \leq r_0).\end{aligned}$$

No matter how hard an observer, at fixed (r, θ) inside the static limit, blasts his rocket engines, he can never halt his angular motion relative to the distant stars.

3. The mathematical foundation for the above statement is this: world lines of the form $(r, \theta, \phi) = \text{constant}$ [tangent vector $\propto \partial/\partial t$ = “Killing vector in time direction”] change from being timelike outside the static limit to being spacelike inside it. Therefore, on and inside the static limit, no observer can remain at rest.

C. Horizon (§33.4):

1. The horizon is located at

$$r = r_+ \equiv M + \sqrt{M^2 - Q^2 - a^2}. \quad (8)$$

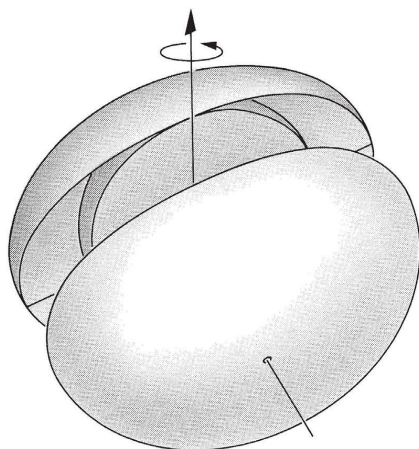
2. As with the Schwarzschild horizon of a nonrotating black hole, so also here, particles and photons can fall inward through the horizon; but no particle or

Box 33.2 (continued)

- photon can emerge outward through it.
3. The horizon is “generated” by outgoing null geodesics (outgoing photon world lines).

D. Ergosphere (§33.4):

1. The “ergosphere” is the region of space-time between the horizon and the static limit. It plays a fundamental role in the physics of black holes (Box 33.3; §33.7).
2. The static limit and the horizon touch at the point where they are cut by the axis of rotation of the black hole ($\theta = 0, \pi$); they are well-separated elsewhere with the static limit outside the horizon, unless $a = 0$ (no rotation). When $a = 0$, the static limit and horizon coincide; there is no dragging of inertial frames; there is no ergosphere.



Qualitative representation of horizon, ergosphere, and static limit [adapted from Ruffini and Wheeler (1971b)].

E. Singularity in Boyer-Lindquist coordinates:

1. For a nonrotating black hole, the Schwarzschild coordinates become singular at the horizon. One manifestation

of the singularity is the infinite amount of coordinate time required for any particle or photon to fall inward through the horizon, $t \rightarrow \infty$ as $r \rightarrow 2M$. One way to remove the singularity (Eddington-Finkelstein way) is to replace t by a null coordinate

$$\tilde{V} = t + r + 2M \ln |r/2M - 1|$$

attached to infalling photons [so $(\partial/\partial r)_{\tilde{V}, \theta, \phi}$ is vector tangent to photon world lines].

2. For a rotating black hole, the Boyer-Lindquist coordinates, being generalizations of the Schwarzschild coordinates, are also singular at the horizon. It requires an infinite coordinate time for any particle or photon to fall inward through the horizon, $t \rightarrow \infty$ as $r \rightarrow r_+$. But that is not all. The dragging of inertial frames forces particles and photons near the horizon to orbit the black hole with $\Omega \equiv d\phi/dt > 0$. Consequently, for a particle falling through the horizon ($r \rightarrow r_+$), just as $t \rightarrow \infty$, so also $\phi \rightarrow \infty$ (infinite twisting of world lines around horizon).
3. To remove the coordinate singularity, one must perform an infinite compression of coordinate time, and an infinite untwisting in the neighborhood of the horizon. Kerr coordinates achieve this by replacing t with a null coordinate \tilde{V} , and ϕ with an untwisted angular coordinate $\tilde{\phi}$:

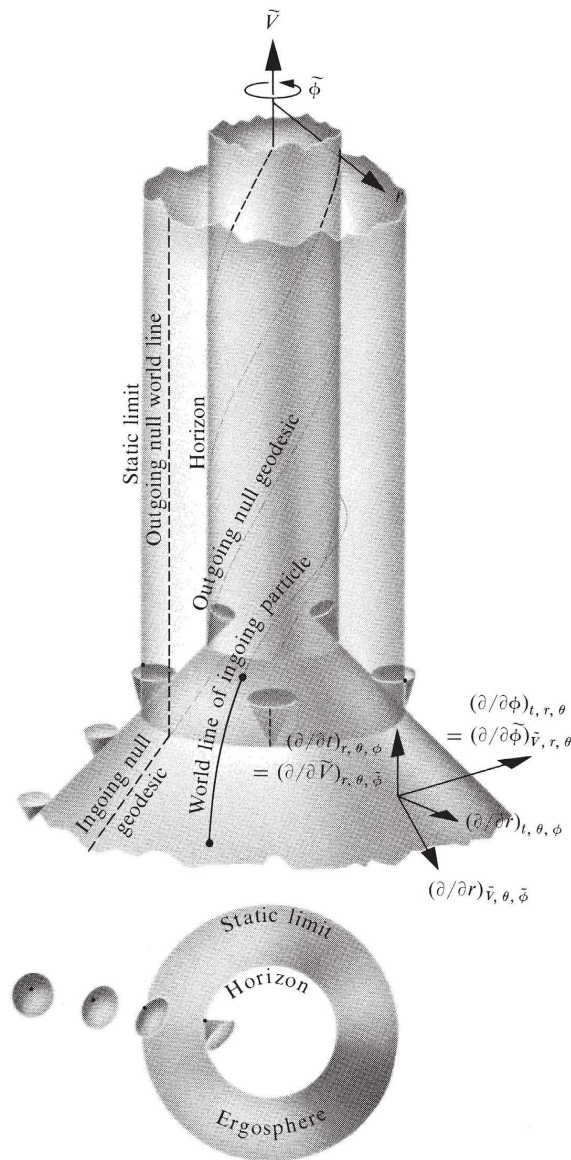
$$\begin{aligned}\mathbf{d}\tilde{V} &= \mathbf{d}t + (r^2 + a^2)(\mathbf{d}r/\Delta), \\ \mathbf{d}\tilde{\phi} &= \mathbf{d}\phi + a(\mathbf{d}r/\Delta).\end{aligned}$$

Both of the new coordinates are attached to the world lines of a particular family of infalling photons; $(\partial/\partial r)_{\tilde{V}, \theta, \tilde{\phi}}$ is the field of vectors tangent to the world lines of this family of photons (ingoing principal null congruence; §33.6).

F. Spacetime diagram:

1. A spacetime diagram in Kerr coordinates looks much like an Eddington-Finkelstein diagram for the Schwarzschild geometry. In both cases, one plots the surfaces of constant \tilde{V} not as horizontal planes, but as “backward light cones” (“45-degree surfaces”), because they are generated by the world lines of ingoing photons. Equivalently, one plots surfaces of constant $\tilde{t} \equiv \tilde{V} - r$ as horizontal planes.
2. The key differences between a Kerr diagram and an Eddington-Finkelstein diagram are: (a) Because the Kerr-Newman geometry is not spherical, a Kerr diagram with one rotational degree of freedom suppressed loses information about the geometry. Kerr diagrams are usually made for the equatorial “plane,” $\theta = \pi/2$. (b) Just as the horizon pulls the light cones inward, so the dragging of inertial frames tilts the light cones in the direction of increasing $\tilde{\phi}$, for $a > 0$ and $r = \text{constant}$. (c) The *ingoing* edge of a light cone ($dr/d\tilde{V} = -\infty$) does *not* tilt toward increasing $\tilde{\phi}$; the transformation from Boyer-Lindquist coordinates to Kerr coordinates untwists the tilt with decreasing r , which would otherwise be produced by “frame dragging.”
3. The shapes of the light cones reveal the special features of the static limit and horizon. At the static limit, a vertical world line [$[r, \theta, \tilde{\phi}]$ constant; $(\partial/\partial\tilde{V})_{r,\theta,\tilde{\phi}} = (\partial/\partial t)_{r,\theta,\phi}$ = tangent vector] lies on the light cone. At the horizon the light cones tilt fully inward, except for a single line of tangency to the horizon. Notice that the line of tangency has $d\tilde{\phi}/d\tilde{V} = a/(r_+^2 + a^2) \neq 0$. Equivalently, the outgoing null geodesics, which generate the horizon, twist about it (“barber-pole-twist”)—yet another manifestation of the dragging of inertial frames.

Kerr diagram for equatorial slice ($\theta = \pi/2$) through the spacetime of an “extreme Kerr” black hole ($Q = 0, a = M$).

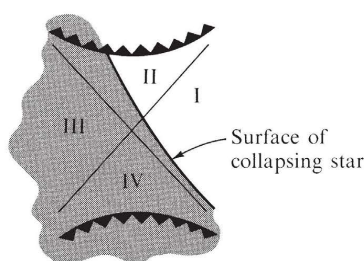


View from above showing the shapes of the light cones as a function of radius

Box 33.2 (continued)

4. The Kerr diagram, like the Eddington-Finkelstein diagram, describes infall through the horizon in a faithful, non-singular way.
 5. [The term “Kerr diagram” is a misnomer. Kerr has not published such diagrams himself, though nowadays others construct such diagrams using his coordinate system. Penrose is the originator and greatest exploiter of such diagrams (see, e.g., Penrose, 1969). But several other types of diagrams bear Penrose’s name, so it would be confusing to name them all after him.]
- G. Maximal analytic extension of Kerr-Newman geometry:
1. When one abstracts the Schwarzschild geometry away from all sources (Chapter 31), one discovers that it describes an expanding and recontracting bridge, connecting two different universes. But in the context of black holes, only half of the Schwarzschild geometry (regions I and II) is relevant. The other half (regions III and IV) gets fully replaced by the interior of the star that collapsed to form the black hole. Because only a

2. Similarly, when one abstracts the Kerr-Newman geometry away from all sources, one discovers that it describes a much larger, and more complex space-time manifold than one might ever have suspected. This “maximum analytic extension” of the Kerr-Newman geometry has been analyzed in detail by Boyer and Lindquist (1967) and by Carter (1966a, 1968a). But it is totally irrelevant to the subject of black holes, for two reasons. First, as with Schwarzschild, the star that collapsed to form the black hole replaces most of the inward extension of the Kerr-Newman manifold. Second, even outside the star, the Kerr-Newman geometry does not properly represent the true geometry at early times. At early times the star has not got far down the road to collapse. Gravitational moments of the star arise from mountains or prominences or turbulence or other particularities that have not yet gone into the meat grinder. The geometry departs from flatness (1) by a term that varies for large distances as mass divided by distance, and (2) by another term that varies as angular momentum divided by the square of the distance and multiplied by a spherical harmonic of order one, but also (3) by higher-order terms proportional to higher-order mass moments multiplied by higher spherical harmonics. These higher-order terms normally will deviate at early times from the corresponding terms in the mathematical analysis of the Kerr-Newman geometry—though the deviations will die out as time passes. For a system endowed with spherical symmetry, no such higher-order terms do occur or can occur. Therefore the geometry outside is



part of the Schwarzschild geometry comes into play, ingoing Eddington-Finkelstein coordinates—which describe I and II well, but III and IV badly—are well-suited to black-hole physics.

Schwarzschild in character at all stages of the collapse. However, when the system lacks spherical symmetry, the geometry outside initially departs from Kerr-Newman character. *Only well after the collapse occurs (asymptotic future), and in the region at and outside the horizon, is the Kerr-Newman geometry a faithful descriptor of a black hole.* This region is described in a nonsingular manner by Kerr coordinates and Kerr diagrams; and it is the only region that this book will explore.

H. Test-particle orbits

See §§33.5–33.8 and Box 33.5.

III. Properties of electromagnetic field (§33.3):

- A. Far from the black hole, where spacetime is nearly flat, in the usual spherical orthonormal frame ($\omega^t = dt$, $\omega^r = dr$, $\omega^\theta = r d\theta$, $\omega^\phi = r \sin \theta d\phi$), the electric and magnetic fields have dominant components

$$E_r = \frac{Q}{r^2};$$

$$B_\theta = \frac{2Qa}{r^3} \cos \theta, B_\phi = \frac{Qa}{r^3} \sin \theta.$$

These reveal that

Q = charge of black hole,

$\mathcal{M} \equiv Qa$ = magnetic dipole moment of black hole.

- B. Notice that the gyromagnetic ratio, $\gamma \equiv (\text{magnetic moment})/(\text{angular momentum})$, is equal to $Q/M = (\text{charge}/\text{mass})$, just as for an electron!
- C. Notice that the value of the magnetic moment, like all other features of the black hole, is determined uniquely by the hole's mass, charge, and angular momentum: $\mathcal{M} = QS/M$. This illustrates the theorem (Box 33.1) that a black hole has no “hair.”
- D. Other electric and magnetic moments are nonzero, but are determined uniquely by M , S , and Q .
- E. Near the black hole, the curvature of spacetime deforms the electric and magnetic fields produced by the charged, rotating black hole. For a mathematical description of this deformed field, see Cohen and Wald (1971); for a diagrammatic representation, Hanni and Ruffini (1973).

Box 33.3 THE ASTROPHYSICS OF BLACK HOLES

Black holes in nature should participate in astrophysical processes that are as varied as those for stars. By searching for observable phenomena associated with these processes, astronomers have a good chance of discovering the first black hole sometime during the 1970's. This box lists some possible astrophysical processes, and a few relevant references.

I. Mechanisms of Formation

- A. “Direct, in isolation”: A massive star ($M \geq 3M_\odot$) collapses, almost spherically, producing a collapsed neutron-star core that is too massive to support itself against gravity. Gravity pulls the core inward, producing a horizon and black hole. [May

Box 33.3 (continued)

- and White (1966, 1967); Chapter 32 of this book.]
- B. “Indirect, in isolation”: “Collapse, pursuit, and plunge scenario” depicted in Figure 24.3 [Ruffini and Wheeler (1971b).]
 - C. “In the thick of things”: Stars collected into a dense cluster (e.g., the nucleus of a galaxy) exchange energy. Some acquire energy and move out into a halo. Others lose energy and make a more compact cluster. This process of segregation continues. The cluster becomes so compact that collisions ensue and gas is driven off. The gas moves toward the center of the gravitational potential well. Out of it new stars form. The process continues. Eventually star-star collisions may become sufficiently energetic and inelastic that the centers of the colliding stars coalesce. In this way supermassive objects may be built up and may evolve. Ultimately (1) many “small” stars may collapse to form “small” black holes ($M \sim M_{\odot}$); (2) one or more supermassive stars may collapse to form huge black holes ($M \sim 10^4 M_{\odot}$ to $10^9 M_{\odot}$); (3) the entire conglomerate of stars and gas and holes may become so dense that it collapses to form a single gigantic hole. [Sanders (1970), Spitzer (1971), Lynden-Bell (1967, 1969), Colgate (1967), §§24.5, 24.6, 25.7 of this book.]
 - D. “Primordially”: Perturbations in the initial density distribution of the expanding universe may produce collapse, resulting in “primordial black holes.” Those holes would subsequently grow by accretion of radiation and matter. By today all such holes might have grown into enormous objects [$M \sim 10^{17} M_{\odot}$; Zel'dovich and Novikov (1966)]; but some of them might have avoided such growth and might be as small as 10^{-5} grams [Hawking (1971a)].
- II. How many black holes are there in our galaxy today?
- Peebles (1972) has given an excellent review of this issue and of prospects for finding black holes in the near future. He says “a good fraction of the mass of the disc of our galaxy was deposited [long ago] in stars capable of collapsing to black holes. . . . The indication is that the galaxy’s disk may contain on the order of 10^9 black holes.”
- III. “Live” black holes versus “dead” black holes
- A. A Schwarzschild black hole is “dead” in the sense that one can never extract from it any of its mass-energy. One aspect of this “deadness”—the fact that a Schwarzschild black hole is stable against small perturbations—is essential (1) to the identification of a black hole with the ultimate “ground state” of a large mass, and (2) to any assertion that general relativity theory predicts the possible existence of black holes. [For a proof of stability see Vishveshwara (1970). The problem was formulated, and most of the necessary techniques developed, by Regge and Wheeler (1957), with essential contributions also by Zerilli (1970a).] Thus a small pulse of gravitational (or other) radiation impinging on a Schwarzschild black hole does not initiate a transition of the black hole into a very different object or state.
 - B. A Kerr-Newman black hole—which is rotating or charged or both—is not dead. The rotational and electromagnetic contributions to the mass-energy *can* be extracted. (See §§33.7 and 33.8 for mathematical details.) Thus, such black holes are “live”; they can inject energy into their surroundings. By a suitable arrangement of external apparatus, one can trigger an exponentially growing energy release [Press and Teukolsky (1972).] But for a perturbed

black hole in isolation, the release is always “controlled” and damped; i.e., Kerr black holes are stable in any classical context [Press and Teukolsky (1973)].

- C. Most objects (massive stars; galactic nuclei; ...) that can collapse to form black holes have so much angular momentum that the holes they produce should be “very live” (a nearly equal to M ; S nearly equal to M^2). [Bardeen (1970a).]
- D. By contrast, it is quite probable (but far from certain) that no black hole in the universe has substantial charge—i.e., that all black holes have $Q \ll M$. A black hole with $Q \sim M$ (say, $Q > 0$ for concreteness) would exert attractive electrostatic forces on electrons, and repulsive electrostatic forces on protons, that are larger than the hole’s gravitational pull by the factor

$$\frac{(\text{electrostatic force})}{(\text{gravitational force})} = \frac{eQ}{\mu M} \sim \frac{e}{\mu} \sim 10^{20}.$$

Here e is the electron charge and μ is the electron (or proton) mass. Such huge differential forces are likely to pull in enough charge from outside the hole to neutralize it.

- E. But one has learned from the “unipolar induction process” for neutron stars [Goldreich and Julian (1968)] that charge neutralization can sometimes be circumvented. Whether any black-hole process can possibly prevent neutralization one does not know in 1972.

IV. Interaction of a black hole with its environment

- A. Gravitational pull: A black hole exerts a gravitational pull on surrounding matter and stars. The pull is indistinguishable, at radii $r \gg M$, from the pull of a star with the same mass.
- B. Accretion and emission of x -rays and γ -rays: Gas surrounding a black hole gets

pulled inward and is heated by adiabatic compression, by shock waves, by turbulence, by viscosity, etc. Before it reaches the horizon, the gas may become so hot that it emits a large flux of x -rays and perhaps even γ -rays. Thus, accreting matter can convert a black hole into a glowing “white” body [for a review of the literature, see Novikov and Thorne (1973)]. Accretion from a nonrotating gas cloud tends to decrease the angular momentum of a black hole [preferential accretion of particles with “negative” angular momentum; Doroshkevich (1966), Godfrey (1970a)]. But the gas surrounding a hole is likely to be rotating in the same direction as the hole itself, and to maintain $S \sim M^2$ [more precisely, $S \approx 0.998M^2$; Thorne (1973b)].

- C. A lump of matter (an “asteroid” or a “planet” or a star) falling into a black hole should emit a burst of gravitational waves as it falls. The total energy radiated is $E \sim 0.01\mu(\mu/M)$, where μ is the mass of the object. [Zerilli (1970b); Davis, Ruffini, Press, and Price (1971); Figure 36.2 of this book.]
- D. An object in a stable orbit around a black hole should spiral slowly inward because of loss of energy through gravitational radiation, until it reaches the most tightly bound, stable circular orbit. It should then fall quickly into the hole, emitting a “last-gasp burst” of waves. The total energy radiated during the slow inward spiral is equal to the binding energy of the last stable circular orbit:

$$E_{\text{radiated}} = \mu - E_{\text{last orbit}}$$

$$= \begin{cases} 0.0572\mu & \text{for Schwarzschild hole,} \\ 0.4235\mu & \text{for Kerr hole with} \\ & S = M^2, Q = 0. \end{cases}$$

Here μ is the rest mass of the captured object. [Box 33.5.] The total energy in the last-gasp burst is $E \sim 0.01\mu(\mu/M)$ if $\mu \ll M$. [Fig. 36.2.]

Box 33.3 (continued)

- E. When matter falls down a black hole, it can excite the hole's external spacetime geometry into vibration. The vibrations are gradually converted into gravitational waves, some of which escape, others go down the hole. [Press (1971), Goebel (1972).] These vibrations are analogous to an “incipient gravitational geon” [Wheeler (1962); Christodoulou (1971)]—except that for a vibrating black hole the background Kerr geometry holds the vibration energy together (prevents it from propagating away immediately), whereas in a geon it is curvature produced by the “vibration energy” itself that prevents disruption.
- F. By a non-Newtonian, induction-zone (i.e., nonradiative) gravitational interaction, a black hole gradually transfers its angular momentum to any non-axially-symmetric, nearby distribution of matter or fields. [Hawking (1972a); Ipser (1971), Press (1972), Hawking and Hartle (1972).]
- G. A star or planet falling into a large black hole will get torn apart by tidal gravitational forces. If the tearing occurs near but outside the horizon, it may eject a blob of stellar matter that goes out with relativistic velocity (“tube-of-toothpaste effect”). Moreover, the outgoing jet may extract a substantial amount of rotational energy from the hole's ergosphere—i.e., the hole might throw it off with a rest mass plus kinetic energy in excess of the rest mass of the original infalling object. [Wheeler (1971d); §§33.7 and 33.8.]
- H. The magnetic field lines of a charged black hole may be anchored to surrounding plasma, may get wound up as the hole rotates, and may shake, twitch, and excite the plasma.

V. Collisions between black holes

- A. Two black holes can collide and coalesce; but there is no way to blast a black hole apart into several black holes [Hawking (1972a); exercise 34.4].
- B. When two black holes collide and coalesce, the surface area of the final black hole must exceed the sum of the surface areas of the two initial black holes (“second law of black-hole dynamics”; Hawking (1971a,b); Box 33.4; §34.5). This constraint places an upper limit on the amount of gravitational radiation emitted in the collision. For example, if all three holes are of the Schwarzschild variety and the two initial holes have equal masses $M/2$, then

$$4\pi(2M_{\text{final}})^2 \geq 4\pi[2(M/2)]^2 + 4\pi[2(M/2)]^2, \\ M_{\text{final}} \geq M/\sqrt{2},$$

so the energy radiated is

$$E_{\text{radiated}} \leq M - M/\sqrt{2} = 0.293M.$$

VI. Where and how to search for a black hole [For a detailed review, see Peebles (1971)]:

- A. When it forms, by the burst or bursts of gravitational radiation given off during formation [Figure 24.3].
- B. In a binary star system: black-hole component optically invisible, but may emit x-rays and γ -rays due to accretion; visible component shows telltale Doppler shifts [Hoyle, Fowler, Burbidge, and Burbidge (1964); Zel'dovich and Guseynov (1965); Trimble and Thorne (1969); Pringle and Rees (1972); Shakura and Sunyaev (1973)]. The velocity of the visible component and the period give information on the mass of the invisible component. If

mass of this invisible component is four solar masses or more, it cannot be an ordinary star, because an ordinary star of that mass would have $(4)^3 = 64$ times the luminosity of the sun. Neither can it be a white dwarf or a neutron star because either object, so heavy, would instantly collapse to a black hole. Therefore, it is attractive—though not necessarily compelling [see Trimble and Thorne (1969)]—to identify the invisible object as a black hole.

- C. [But one must not expect to see any noticeable gravitational lens action from a black hole in a binary system: if it taxed the abilities of astronomers for decades to see the black disc of Mercury, 4,800 km in diameter, swim across the great face of the sun, little hope there is to see a black hole with an effective radius of only ~ 3 km, enormously more remote, occult a companion star. Significant lens action requires that the lens (black hole) be separated by a normal interstellar distance from the star it focuses; whence the impact parameter of the focused rays is more than a stellar radius, so the lens action is not more than that of a normal star. Moreover,

even with 10^9 black holes in the galaxy, only one per year would pass directly between the Earth and a more distant star, and produce significant lens action (Refsdal, 1964). Chance of watching the right spot on the sky at the right time with a sufficiently strong telescope: nil!]

- D. At the center of a globular cluster, where a black hole may settle down, attract normal stars to its vicinity, and thereby produce a cusp in the distribution of light from the cluster. [Cameron and Truran (1971), Peebles (1971).]
- E. In the nucleus of a galaxy, including even the Milky Way, where a single huge black hole ($M \sim 10^4$ to $10^8 M_\odot$) might sit as an end-product of earlier activity of the galactic nucleus. Such a hole will emit gravitational waves, light, and radio waves as it accretes matter. Much of the light may be converted into infrared radiation by surrounding dust. The black hole may also produce jets and other nuclear activity. [Lynden-Bell (1969), Lynden-Bell and Rees (1971), Wheeler (1971d), Peebles (1971).]

Box 33.4 THE LAWS OF BLACK-HOLE DYNAMICS

The black-hole processes described in Box 33.3 are governed by the standard laws of physics: general relativity, plus Maxwell electrodynamics, plus hydrodynamic, quantum mechanical, and other laws for the physics of matter and radiation. From these standard laws of physics, one can derive certain “rules” or “constraints,” which all black-hole processes must satisfy. Those rules have a power, elegance, and simplicity that rival and resemble the power, elegance, and simplicity of the laws of thermodynamics. Therefore, they have been given the analogous name “the laws of black-hole dynamics” (Israel 1971). This box states two of the laws of black-hole

Box 33.4 (continued)

dynamics and some of their ramifications. Two additional laws, not discussed here, have been formulated by Bardeen, Carter, and Hawking (1973).

I. The First and Second Laws of Black-Hole Dynamics.

A. *The first law.*

1. Like the first law of thermodynamics, the first law of black-hole dynamics is the standard law of conservation of total energy, supplemented by the laws of conservation of total momentum, angular momentum, and charge. For detailed discussions of these conservation laws, see Box 19.1 and Chapter 20.
2. Specialized to the case where matter falls down a black hole and gravitational waves pour out, the first law takes the form depicted and discussed near the end of Box 19.1.
3. Specialized to the case of infalling electric charge, the first law says that the total charge Q of a black hole, as measured by the electric flux emerging from it, changes by an amount equal to the total charge that falls down the hole,

$$\Delta Q = q_{\text{that falls in}}.$$

4. Specialized to the case where two black holes collide and coalesce (example given in Box 33.3), the first law says: (a) Let \mathbf{P}_1 and \mathbf{P}_2 be the 4-momenta of the two black holes as measured gravitationally, when they are so well-separated that they have negligible influence on each other. (\mathbf{P}_1 and \mathbf{P}_2 are 4-vectors in the surrounding asymptotically flat spacetime.) Similarly, let \mathbf{J}_1 and \mathbf{J}_2 be their total angular-momentum tensors (not intrinsic angular-momentum vectors!) relative to some arbitrarily chosen origin of coordinates, \mathcal{P}_0 , in the surrounding asymptotically flat spacetime (\mathbf{J}_1 and \mathbf{J}_2 contain orbital angular momentum, as well as intrinsic angular momentum; see Box 5.6.). (b) Let \mathbf{P}_3 and \mathbf{J}_3 be the similar total 4-momentum and angular momentum of the final black hole. (c) Let \mathbf{P}_r and \mathbf{J}_r be the total 4-momentum and angular momentum radiated as gravitational waves during the collision and coalescence. *Then*

$$\mathbf{P}_3 = \mathbf{P}_1 + \mathbf{P}_2 - \mathbf{P}_r \quad \mathbf{J}_3 = \mathbf{J}_1 + \mathbf{J}_2 - \mathbf{J}_r.$$

[Note: to calculate the mass and intrinsic angular momentum of the final black hole from a knowledge of \mathbf{P}_3 and \mathbf{J}_3 , follow the prescription of Box 5.6. In that prescription, the world line of the final black hole is that world line, in the distant asymptotically Lorentz coordinates, on which the hole's distant spherical field is centered.]

- B. *The second law* [expounded and applied by Hawking (1971b, 1972a)].

When anything falls down a black hole, or when several black holes collide and coalesce or collide and scatter, or in any other process whatsoever involving black holes, *the sum of the surface areas* (or squares of “irreducible masses”—see equation 3 below) *of all black holes involved can never decrease.* (See §34.5 for proof.) This is the second law of black-hole dynamics.

II. Reversible and Irreversible Transformations; Irreducible Mass

[Christodoulou (1970); Christodoulou and Ruffini (1971)—results derived independently of and simultaneously with Hawking’s discovery of the second law.]

- A. Consider a single Kerr-Newman black hole interacting with surrounding matter and fields. Its surface area, at any moment of time, is given in terms of its momentary mass M , charge Q , and intrinsic angular momentum per unit mass $a \equiv S/M$ by

$$A = 4\pi[r_+^2 + a^2] = 4\pi[(M + \sqrt{M^2 - Q^2 - a^2})^2 + a^2] \quad (1)$$

(exercise 33.12). Interaction with matter and fields may change M , Q , and a in various ways; M can even be decreased—i.e., energy can be extracted from the black hole! [Penrose (1969); §33.7.] But whatever may be the changes, they can never reduce the surface area A . Moreover, if any change in M , Q , and a ever increases the surface area, no future process can ever reduce it back to its initial value.

- B. Thus, one can classify black-hole processes into two groups.

1. *Reversible transformations* change M , Q , or a or any set thereof, while leaving the surface area fixed. They can be reversed, bringing the black hole back to its original state.
2. *Irreversible transformations* change M , Q , or a or any set thereof, and increase the surface area in the process. Such a transformation can never be reversed. The black hole can never be brought back to its original state after an irreversible transformation.

- C. Examples of reversible transformations and of irreversible transformations induced by infalling particles are presented in §§33.7 and 33.8.

- D. The reversible extraction of charge and angular momentum from a black hole (decrease in Q and a holding A fixed) necessarily reduces the black hole’s mass (energy extraction!). By the time all charge and angular momentum have been removed, the mass has dropped to a final “irreducible value” of

$$M_{\text{ir}} = (A/16\pi)^{1/2} = \left(\begin{array}{l} \text{mass of Schwarzschild} \\ \text{black hole of surface area } A \end{array} \right). \quad (2)$$

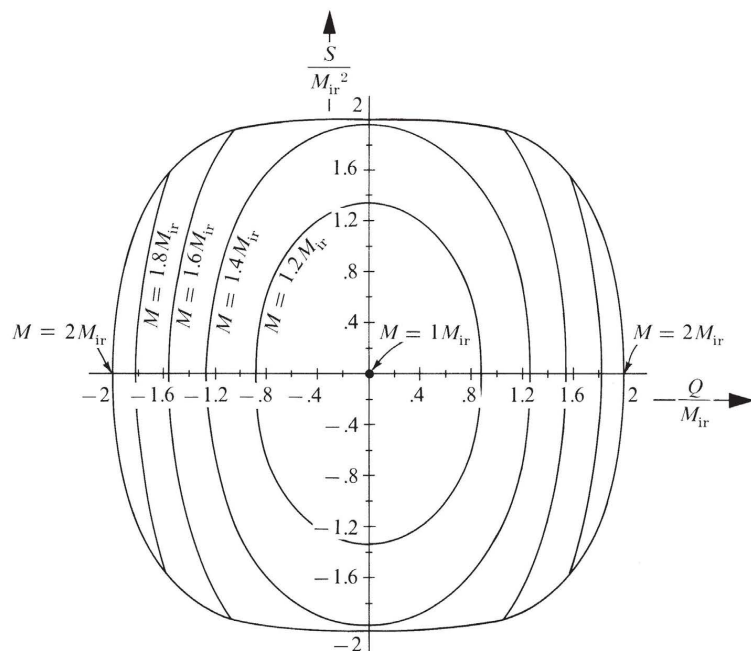
Box 33.4 (continued)

- E. Expressed in terms of this final, irreducible mass, the initial mass-energy of the black hole (with charge Q and intrinsic angular momentum S) is

$$M^2 = \left(M_{\text{ir}} + \frac{Q^2}{4M_{\text{ir}}} \right)^2 + \frac{S^2}{4M_{\text{ir}}^2} \quad (3)$$

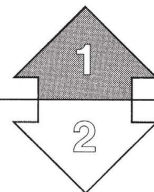
[This formula, derived by Christodoulou and Ruffini, may be obtained by combining equations (1), (2), and $S = Ma$.]

- F. Thus, *one can regard the total mass-energy of a black hole as made up of an irreducible mass, an electromagnetic mass-energy, and a rotational energy. But one must resist the temptation to think of these contributions as adding linearly. On the contrary, they combine in a way [equation (3)] analogous to the way rest mass and linear momentum combine to give energy, $E^2 = m^2 + \mathbf{p}^2$.*
- G. Contours of constant M/M_{ir} are depicted below in the “charge-angular momentum plane.” Black holes can exist only in the interior of the region depicted ($Q^2 + a^2 \leq M^2$). [Diagram adapted from Christodoulou (1971).]



H. Since a black hole's irreducible mass is proportional to the square root of its surface area, one can restate the second law of black-hole dynamics as follows:

In black-hole processes the sum of the squares of the irreducible masses of all black holes involved can never decrease.



§33.3. MASS, ANGULAR MOMENTUM, CHARGE, AND MAGNETIC MOMENT

It is instructive to verify that the constants M , Q , and a , which appear in equations (33.2)–(33.5) for the Kerr-Newman geometry and electromagnetic field, are actually the black hole's mass, charge, and angular momentum per unit mass, as claimed above.

Mass and angular momentum are defined by their imprints on the spacetime geometry far from the black hole. Therefore, to calculate the mass and angular momentum, one can expand the line element (33.2) in powers of $1/r$ and examine the leading terms:

$$\begin{aligned} ds^2 = & - \left[1 - \frac{2M}{r} + O\left(\frac{1}{r^2}\right) \right] dt^2 - \left[\frac{4aM}{r} \sin^2\theta + O\left(\frac{1}{r^2}\right) \right] dt d\phi \\ & + \left[1 + O\left(\frac{1}{r}\right) \right] [dr^2 + r^2(d\theta^2 + \sin^2\theta d\phi^2)]. \end{aligned} \quad (33.6)$$

The examination is facilitated by transforming to asymptotically Lorentz coordinates— $x = r \sin\theta \cos\phi$, $y = r \sin\theta \sin\phi$, $z = r \cos\theta$:

$$\begin{aligned} ds^2 = & - \left[1 - \frac{2M}{r} + O\left(\frac{1}{r^2}\right) \right] dt^2 - \left[\frac{4aM}{r^3} + O\left(\frac{1}{r^4}\right) \right] [x dy - y dx] \\ & + \left[1 + O\left(\frac{1}{r}\right) \right] [dx^2 + dy^2 + dz^2]. \end{aligned} \quad (33.6')$$

Direct comparison with the “standard form” [equation (19.13)] of the metric far from a stationary rotating source reveals that (1) the parameter M is, indeed, the mass of the black hole; and (2) the intrinsic angular momentum vector of the black hole is

$$\mathbf{s} = (aM) \partial/\partial z = (aM) \cdot \left(\begin{array}{l} \text{unit vector pointing along polar axis} \\ \text{of Boyer-Lindquist coordinates} \end{array} \right). \quad (33.7)$$

The charge is defined for the black hole, as for any source, by a Gaussian flux integral of its electric field over a closed surface surrounding the hole. The electric

The rest of this chapter is Track 2. To be prepared for it, one needs to have covered the Track-2 part of Chapter 32 (gravitational collapse). In reading it, one will be helped greatly by Chapter 25 (orbits in Schwarzschild geometry). The rest of this chapter is needed as preparation for Chapter 34 (singularities and global methods).

The metric far outside a black hole: imprints of mass and angular momentum

The electromagnetic field far outside a black hole:

(1) electric field

field in the asymptotic rest frame of the black hole has as its orthonormal components

$$\begin{aligned} E_{\hat{r}} &= E_r = F_{rt} = Q/r^2 + O(1/r^3), \\ E_{\hat{\theta}} &= E_\theta/r = F_{\theta t}/r = O(1/r^4), \\ E_{\hat{\phi}} &= E_\phi/r \sin \theta = F_{\phi t}/r \sin \theta = 0. \end{aligned} \quad (33.8)$$

Hence, the electric field is purely radial with a Gaussian flux integral of $4\pi Q$, which reveals Q to be the black hole's charge.

A similar calculation of the dominant components of the magnetic field reveals

(2) magnetic field

$$\begin{aligned} B_{\hat{r}} &= F_{\theta\hat{\phi}} = \frac{F_{\theta\phi}}{r^2 \sin \theta} = 2 \frac{Qa}{r^3} \cos \theta + O\left(\frac{1}{r^4}\right), \\ B_{\hat{\theta}} &= F_{\phi\hat{r}} = \frac{F_{\phi r}}{r \sin \theta} = \frac{Qa}{r^3} \sin \theta + O\left(\frac{1}{r^4}\right), \\ B_{\hat{\phi}} &= F_{\hat{r}\hat{\theta}} = \frac{F_{r\theta}}{r} = 0. \end{aligned} \quad (33.9)$$

This is a dipole magnetic field, and from it one immediately reads off the value

(3) magnetic dipole moment

$$\mathcal{M} = Qa = \underbrace{(Q/M)S}_{\substack{\text{charge/mass} \\ \text{“gyromagnetic ratio”}}} \times (\text{angular momentum}) \quad (33.10)$$

Nonspherical shape of hole's geometry

for the magnetic moment of the black hole.

Just as the rotation of the black hole produces a magnetic field, so it also produces nonspherical deformations in the gravitational field of the black hole [see Hernandez (1967) for quantitative discussion]. But those deformations, like the magnetic moment, are *not* freely specifiable. They are determined uniquely by the mass, charge, and angular momentum of the black hole.

§33.4. SYMMETRIES AND FRAME DRAGGING

The metric components (33.2) of a Kerr-Newman black hole are independent of the Boyer-Lindquist time coordinate t and angular coordinate ϕ . This means (see §25.2) that

Killing vectors for the Kerr-Newman geometry

$$\xi_{(t)} \equiv (\partial/\partial t)_{r,\theta,\phi} \text{ and } \xi_{(\phi)} \equiv (\partial/\partial \phi)_{t,r,\theta} \quad (33.11)$$

are Killing vectors associated with the stationarity (time-translation invariance) and axial symmetry of the black hole. The scalar products of these Killing vectors with themselves and each other are

$$\xi_{(t)} \cdot \xi_{(t)} = g_{tt} = -\left(\frac{\Delta - a^2 \sin^2 \theta}{\rho^2}\right) = -\left(1 - \frac{2Mr - Q^2}{\rho^2}\right), \quad (33.12a)$$

$$\xi_{(t)} \cdot \xi_{(\phi)} = g_{t\phi} = \frac{a \sin^2 \theta (\Delta - r^2 - a^2)}{\rho^2} = -\frac{(2Mr - Q^2)a \sin^2 \theta}{\rho^2}, \quad (33.12b)$$

$$\xi_{(\phi)} \cdot \xi_{(\phi)} = g_{\phi\phi} = \frac{[(r^2 + a^2)^2 - \Delta a^2 \sin^2 \theta] \sin^2 \theta}{\rho^2}. \quad (33.12c)$$

Since Killing vectors are geometric properties of spacetime, with existence independent of any and all coordinate systems, their scalar products also have coordinate-free meaning. It so happens (not by chance, but by careful choice of coordinates!) that the Boyer-Lindquist metric components g_{tt} , $g_{t\phi}$, and $g_{\phi\phi}$ are equal to these coordinate-independent scalar products. Thus g_{tt} , $g_{t\phi}$, and $g_{\phi\phi}$ can be thought of as three scalar fields which embody information about the symmetries of spacetime. By contrast, the metric coefficients $g_{rr} = \rho^2/\Delta$ and $g_{\theta\theta} = \rho^2$ carry no information at all about the symmetries.* They depend, for their existence and values, on the specific Boyer-Lindquist choice of coordinates.

Any observer who moves along a world line of constant (r, θ) with uniform angular velocity sees an unchanging spacetime geometry in his neighborhood. Hence, such an observer can be thought of as “stationary” relative to the local geometry. If and only if his angular velocity is zero, that is, if and only if he moves along a world line of constant (r, θ, ϕ) , will he also be “static” relative to the black hole’s asymptotic Lorentz frame (i.e., relative to the “distant stars”).

The precise definition of “angular velocity relative to the asymptotic rest frame”—or simply “angular velocity”—is

$$\Omega \equiv \frac{d\phi}{dt} = \frac{d\phi/d\tau}{dt/d\tau} = \frac{u^\phi}{u^t} \quad (33.13a)$$

(see exercise 33.2). In terms of Ω , the Killing vectors, and the scalar products of Killing vectors, the 4-velocity of a stationary observer is

$$\begin{aligned} \mathbf{u} &= u^t(\partial/\partial t + \Omega\partial/\partial\phi) = \frac{\xi_{(t)} + \Omega\xi_{(\phi)}}{|\xi_{(t)} + \Omega\xi_{(\phi)}|} \\ &= \frac{\xi_{(t)} + \Omega\xi_{(\phi)}}{(-g_{tt} - 2\Omega g_{t\phi} - \Omega^2 g_{\phi\phi})^{1/2}}. \end{aligned} \quad (33.13b)$$

A stationary observer is static if and only if Ω vanishes.

The stationary observers at given r, θ cannot have any and every angular velocity. Only those values of Ω are allowed for which the 4-velocity \mathbf{u} lies inside the future light cone—i.e., for which

$$(\xi_{(t)} + \Omega\xi_{(\phi)})^2 = g_{tt} + 2\Omega g_{t\phi} + \Omega^2 g_{\phi\phi} < 0.$$

*This is not quite true. Kerr-Newman spacetime possesses, in addition to its two Killing vectors, also a “Killing tensor” which is closely linked to the Boyer-Lindquist coordinates r and θ . See Walker and Penrose (1970); also §33.5.

Stationary observers

Static observers

Angular velocity and
4-velocity of a stationary
observer

Frame dragging, static limit, and ergosphere

Thus, the angular velocities of stationary observers are constrained by

$$\Omega_{\min} < \Omega < \Omega_{\max}, \quad (33.14)$$

where

$$\Omega_{\min} = \omega - \sqrt{\omega^2 - g_{tt}/g_{\phi\phi}}, \quad (33.15a)$$

$$\Omega_{\max} = \omega + \sqrt{\omega^2 - g_{tt}/g_{\phi\phi}} \quad (33.15b)$$

$$\omega \equiv \frac{1}{2}(\Omega_{\min} + \Omega_{\max}) = -\frac{g_{\phi t}}{g_{\phi\phi}} = \frac{(2Mr - Q^2)a}{(r^2 + a^2)^2 - 4a^2 \sin^2\theta}, \quad (33.16)$$

and it is assumed that $S/M = a > 0$. The following features of these limits are noteworthy. (1) Far from the black hole, one has $r\Omega_{\min} = -1$ and $r\Omega_{\max} = +1$, corresponding to the standard limits imposed by the speed of light in flat spacetime. (2) With decreasing radius, Ω_{\min} increases (“dragging of inertial frames”). Finally, when g_{tt} reaches zero, i.e., at

$$r = r_0(\theta) \equiv M + \sqrt{M^2 - Q^2 - a^2 \cos^2\theta}, \quad (33.17)$$

Ω_{\min} becomes zero. At and inside this surface, all stationary observers must orbit the black hole with positive angular velocity. Thus, *static observers exist outside and only outside $r = r_0(\theta)$* . For this reason $r = r_0(\theta)$ is called the “static limit”; see Box 33.2. (3) As one moves through the static limit into the “ergosphere,” one sees the allowed range of angular velocities become ever more positive (ever more “frame dragging”). At the same time, one sees the allowed range narrow down, until finally, at the horizon

$$r = r_+ \equiv M + \sqrt{M^2 - Q^2 - a^2}, \quad (33.18)$$

the limits Ω_{\min} and Ω_{\max} coalesce ($\omega^2 = g_{tt}/g_{\phi\phi}$). Thus, at the horizon there are no stationary observers. All timelike world lines point inward. There is no escape from the black hole’s “pull.”

Further features of stationary observers and “frame dragging” are explored in the exercises.

EXERCISES

Exercise 33.1. KERR DESCRIPTION OF KILLING VECTORS

(a) Use the transformation law from Boyer-Lindquist coordinates to Kerr coordinates [equation (4) of Box 33.2] to show that

$$\xi_{(t)} \equiv (\partial/\partial t)_{r,\theta,\phi} = (\partial/\partial \tilde{V})_{r,\theta,\tilde{\phi}}, \quad (33.19a)$$

$$\xi_{(\phi)} \equiv (\partial/\partial \phi)_{t,r,\theta} = (\partial/\partial \tilde{\phi})_{\tilde{V},r,\theta}. \quad (33.19b)$$

Verify explicitly by examining metric components that

$$g_{\tilde{V}\tilde{V}} = g_{tt}, \quad g_{\tilde{V}\tilde{\phi}} = g_{t\phi}, \quad g_{\tilde{\phi}\tilde{\phi}} = g_{\phi\phi}, \quad (33.19c)$$

in accordance with equations (33.19a,b).

(b) Show that for a stationary observer (world line of constant r, θ), the angular velocity expressed in terms of Kerr coordinates is

$$\Omega \equiv d\phi/dt = d\tilde{\phi}/d\tilde{V} = u^{\tilde{\phi}}/u^{\tilde{V}},$$

so that the entire discussion of stationary observers in terms of Kerr coordinates is identical to the discussion in terms of Boyer-Lindquist coordinates. Differences between the coordinate systems show up only when one moves along world lines of changing r . Reconcile this fact with the fact that both coordinate systems use the *same* coordinates (r, θ) but different time and azimuthal coordinates (t, ϕ) versus $(\tilde{V}, \tilde{\phi})$.

Exercise 33.2. OBSERVATIONS OF ANGULAR VELOCITY

An observer, far from a black hole and at rest in the hole's asymptotic Lorentz frame, watches (with his eyes) as a particle moves along a stationary (nongeodesic) orbit near the black hole. Let $\Omega = d\phi/dt$ be the particle's angular velocity, as defined and discussed above. The distant observer uses his stopwatch to measure the time required for the particle to make one complete circuit around the black hole (one complete circuit relative to the distant observer himself; i.e., relative to the hole's asymptotic Lorentz frame).

(a) Show that the circuit time measured is $2\pi/\Omega$. Thus, Ω can be regarded as the particle's "angular velocity as measured from infinity."

(b) Let the observer moving with the particle measure its circuit time relative to the asymptotic Lorentz frame, using his eyes and a stopwatch he carries. Show that his answer for the circuit time must be

$$\Delta\tau = \frac{2\pi}{\Omega} \underbrace{(-g_{tt} - 2\Omega g_{t\phi} - \Omega^2 g_{\phi\phi})^{1/2}}_{\substack{\uparrow \\ ["redshift factor"]}} \quad (33.20)$$

Exercise 33.3. LOCALLY NONROTATING OBSERVERS (Bardeen 1970b)

(a) Place a rigid, circular mirror ("ring mirror") at fixed (r, θ) around a black hole. Let an observer at (r, θ) with angular velocity Ω emit a flash of light. Some of the photons will get caught by the mirror and will skim along its surface, circumnavigating the black hole in the positive- ϕ direction. Others will get caught and will skim along in the negative- ϕ direction. Show that the observer will receive back the photons from both directions simultaneously only if his angular velocity is

$$\Omega = \omega(r, \theta) = \text{expression (33.16).}$$

Thus in this case, and only in this case, can the observer regard the $+ \phi$ and $- \phi$ directions as equivalent in terms of local geometry. Put differently, in this case and only in this case is the observer "nonrotating relative to the local spacetime geometry." Thus, it is appropriate to use the name "locally nonrotating observer" for an observer who moves with the angular velocity $\Omega = \omega(r, \theta)$.

(b) Associated with the axial symmetry of a black hole is a conserved quantity, $p_\phi \equiv \mathbf{p} \cdot \xi_{(\phi)}$, for geodesic motion. This quantity for any particle—whether it is moving along a geodesic or not—is called the "component of angular momentum along the black hole's spin axis," or simply the particle's "angular momentum." (See §33.5 below.) Show that of all stationary observers at fixed (r, θ) , only the "locally nonrotating observer" has zero angular momentum. [Note: Bardeen, Press, and Teukolsky (1972) have shown that the "locally nonrotating observer" can be a powerful tool in the analysis of physical processes near a black hole.]

Exercise 33.4. ORTHONORMAL FRAMES OF LOCALLY NONROTATING OBSERVERS

(a) Let spacetime be filled with world lines of locally nonrotating observers, and let each such observer carry an orthonormal frame with himself. Show that the spatial orientations of these frames can be so chosen that their basis 1-forms are

$$\begin{aligned}\omega^{\hat{t}} &= |g_{tt} - \omega^2 g_{\phi\phi}|^{1/2} dt, & \omega^{\hat{\phi}} &= (g_{\phi\phi})^{1/2} (d\phi - \omega dt), \\ \omega^{\hat{r}} &= (\rho/\Delta^{1/2}) dr, & \omega^{\hat{\theta}} &= \rho d\theta.\end{aligned}\quad (33.21)$$

More specifically, show that these 1-forms are orthonormal and that the dual basis has

$$\partial/\partial\hat{t} = u \equiv 4\text{-velocity of locally nonrotating observer.} \quad (33.22)$$

Show that $u = -\omega^{\hat{t}}$ is a rotation-free field of 1-forms [$d\omega^{\hat{t}} \wedge \omega^{\hat{t}} = 0$; exercise 4.4].

(b) One sometimes meets the mistaken notion that a “locally nonrotating observer” is in some sense locally inertial. To destroy this false impression, verify that: (i) such an observer has nonzero 4-acceleration,

$$a = \Gamma_{\hat{j}\hat{i}} e_j = \frac{1}{2} \nabla \ln |g_{tt} - \omega^2 g_{\phi\phi}|; \quad (33.23)$$

(ii) if such an observer carries gyroscopes with himself, applying the necessary accelerations at the gyroscope centers of mass, he sees the gyroscopes precess relative to his orthonormal frame (33.21) with angular velocity

$$\begin{aligned}\Omega^{(\text{precess})} &= \Gamma_{\hat{\theta}\hat{\phi}\hat{t}} e_{\hat{r}} + \Gamma_{\hat{\phi}\hat{r}\hat{t}} e_{\hat{\theta}} \\ &= \frac{1}{2} \frac{g_{\phi\phi}^{-1/2}}{|g_{tt} - \omega^2 g_{\phi\phi}|^{1/2}} \left[\frac{\omega_{,\theta}}{\rho} e_{\hat{r}} - \frac{\Delta^{1/2} \omega_{,r}}{\rho} e_{\hat{\theta}} \right].\end{aligned}\quad (33.24)$$

[Hints: See exercise 19.2, equation (13.69), and associated discussions. The calculation of the connection coefficients is performed most easily using the methods of differential forms; see §14.6.]

Exercise 33.5. LOCAL LIGHT CONES

Calculate the shapes of the light cones depicted in the Kerr diagram for an uncharged ($Q = 0$) Kerr black hole (part II.F of Box 33.2). In particular, introduce a new time coordinate

$$\tilde{t} \equiv \tilde{V} - r \quad (33.25)$$

for which the slices of constant \tilde{t} are horizontal surfaces in the Kerr diagram. Then the Kerr diagram plots \tilde{t} vertically, r radially, and $\tilde{\phi}$ azimuthally, while holding $\theta = \pi/2$ (“equatorial slice through black hole”).

(a) Show that the light cone emanating from given $\tilde{t}, r, \tilde{\phi}$ has the form

$$\frac{dr}{d\tilde{t}} = a \left(\frac{d\tilde{\phi}}{d\tilde{t}} \right) - \frac{2M/r}{1 + 2M/r} \pm \sqrt{\frac{1}{(1 + 2M/r)^2} - \frac{r^2(d\tilde{\phi}/d\tilde{t})^2}{1 + 2M/r}}.$$

(b) Show that the light cone slices through the surface of constant radius along the curves

$$dr/d\tilde{t} = 0, \quad d\tilde{\phi}/d\tilde{t} = \Omega_{\min} \text{ and } \Omega_{\max}, \quad (33.26b)$$

where Ω_{\min} and Ω_{\max} are given by expressions (33.15a,b) (minimum and maximum allowed angular velocities for stationary observers).

(c) Show that at the static limit, $r = r_0(\pi/2)$, the light cone is tangent to a curve of constant $r, \theta, \tilde{\phi}$.

(d) Show that the light cone slices the surface of constant $\tilde{\phi}$ along the curves

$$\frac{d\tilde{\phi}}{d\tilde{t}} = 0, \quad \frac{dr}{d\tilde{t}} = -1 \text{ and } \frac{1 - 2M/r}{1 + 2M/r}. \quad (33.26c)$$

(e) Show that the light cone is tangent to the horizon.

(f) Make pictures of the shapes of the light cone as a function of radius.

(g) Describe qualitatively how the light cone must look near the horizon in Boyer-Lindquist coordinates. (Note: it will look “crazy” because the coordinates are singular at the horizon.)

§33.5. EQUATIONS OF MOTION FOR TEST PARTICLES [Carter (1968a)]

Let a test particle with electric charge e and rest mass μ move in the external fields of a black hole. Were there no charge down the black hole, the test particle would move along a geodesic (zero 4-acceleration). But the charge produces an electromagnetic field, which in turn produces a Lorentz force on the particle: $\mu\mathbf{a} = e\mathbf{F} \cdot \mathbf{u}$. (Here \mathbf{u} is the particle’s 4-velocity, and $\mathbf{a} \equiv \nabla_{\mathbf{u}}\mathbf{u}$ is its 4-acceleration.)

The geodesic equation, $\mathbf{a} = 0$, for the uncharged case is equivalent to Hamilton’s equations

$$dx^\mu/d\lambda = \partial\mathcal{K}/\partial p_\mu, \quad dp_\mu/d\lambda = -\partial\mathcal{K}/\partial x^\mu, \quad (33.27a)$$

where λ is an affine parameter so normalized that

$$d/d\lambda = \mathbf{p} = 4\text{-momentum}, \quad (33.27b)$$

and where

$$\mathcal{K} \equiv \text{“super-Hamiltonian”} = \frac{1}{2} g^{\mu\nu} p_\mu p_\nu \quad (33.27c)$$

(see exercise 25.2). Similarly (see exercise 33.6) the Lorentz-force equation, $\mu\mathbf{a} = e\mathbf{F} \cdot \mathbf{u}$, for the charged case is equivalent to Hamilton’s equations written in terms of position x^μ and “generalized momentum” π_μ :

$$dx^\mu/d\lambda = \partial\mathcal{K}/\partial\pi_\mu, \quad d\pi_\mu/d\lambda = -\partial\mathcal{K}/\partial x^\mu. \quad (33.28a)$$

The form of the superhamiltonian \mathcal{K} , in terms of the metric coefficients at the particle’s location, $g^{\mu\nu}(x^\alpha)$, and the particle’s charge e and generalized momentum π_μ , is

$$\mathcal{K} = \frac{1}{2} g^{\mu\nu} (\pi_\mu - eA_\mu)(\pi_\nu - eA_\nu). \quad (33.28b)$$

Superhamiltonian for a charged test particle in any electromagnetic field in curved spacetime

[See §7.3 of Goldstein (1959) for the analogous superhamiltonian in flat spacetime.]

The first of Hamilton's equations for this superhamiltonian reduces to

$$p^\mu \equiv (\text{4-momentum}) \equiv dx^\mu/d\lambda = \pi^\mu - eA^\mu \quad (33.29a)$$

(value of π^μ in terms of p^μ , e , and A^μ); the second, when combined with the first, reduces to the Lorentz-force equation

$$\frac{dp^\mu}{d\lambda} + \Gamma^\mu_{\alpha\beta} p^\alpha p^\beta = eF^{\mu\nu} p_\nu \quad (33.29b)$$

$$\left[\begin{array}{l} p_\nu, \text{ not } u_\nu \text{ because} \\ \lambda = \tau/\mu \end{array} \right]$$

For a Kerr-Newman black hole, the vector potential in Boyer-Lindquist coordinates can be put in the form

Vector potential for a charged black hole

$$\mathbf{A} = -\frac{Qr}{\rho^2}(\mathbf{dt} - a \sin^2\theta \mathbf{d}\phi), \quad (33.30)$$

as one verifies by checking that

$$\mathbf{dA} = \frac{1}{2}(A_{\beta,\alpha} - A_{\alpha,\beta}) \mathbf{dx}^\alpha \wedge \mathbf{dx}^\beta$$

reduces to the Faraday 2-form of equation (33.5).

There is good reason for going through all this formalism, rather than tackling head-on the Lorentz-force equation in its most elementary coordinate version,

$$\frac{d^2x^\alpha}{d\lambda^2} + \Gamma^\alpha_{\beta\gamma} \frac{dx^\beta}{d\lambda} \frac{dx^\gamma}{d\lambda} = eF^\alpha_\beta \frac{dx^\beta}{d\lambda}.$$

“Constants of motion” for a charged test particle moving around a charged black hole:

The Hamiltonian formalism enables one to discover immediately two constants of the motion; the elementary Lorentz-force equation does not. The key point is that the components A_μ of \mathbf{A} [equation (33.30)] and the components $g^{\mu\nu}$ of the metric [inverse of $g_{\mu\nu}$ of equation (33.2); see (33.35)] are independent of t and ϕ (stationarity and axial symmetry of both the electromagnetic field and the spacetime geometry). Consequently, the superhamiltonian is also independent of t and ϕ ; and therefore Hamilton's equation

$$d\pi_\alpha/d\lambda = -\partial\mathcal{H}/\partial x^\alpha$$

guarantees that π_t and π_ϕ are constants of the motion.

Far from the black hole, where the vector potential vanishes and the metric becomes

$$ds^2 = -dt^2 + dr^2 + r^2(d\theta^2 + \sin^2\theta d\phi^2),$$

the constants of the motion become

$$\begin{aligned} \pi_t &= p_t = -p^t = -\text{energy}, \\ \pi_\phi &= p_\phi = rp^\phi = \left(\begin{array}{l} \text{projection of angular momentum} \\ \text{along black hole's rotation axis} \end{array} \right). \end{aligned}$$

Thus it is appropriate to adopt the names and notation

$$E \equiv (\text{"energy at infinity"}) \equiv -\pi_t = -(p_t + eA_t), \quad (33.31a)$$

$$L_z \equiv \begin{pmatrix} \text{"axial component of angular momentum", or simply} \\ \text{"angular momentum"} \end{pmatrix} \equiv \pi_\phi = p_\phi + eA_\phi \quad (33.31b)$$

for the constants of the motion $-\pi_t$ and π_ϕ .

A third constant of the motion is the particle's rest mass

(3) rest mass μ

$$\mu = |\mathbf{p}| = (-g^{\alpha\beta}p_\alpha p_\beta)^{1/2}. \quad (33.31c)$$

In general, four constants of the motion are needed to determine uniquely the orbit of a particle through four-dimensional spacetime. If the black hole were to possess an additional symmetry—e.g., if it were spherical, rather than merely axially symmetric—then automatically there would be a fourth constant of the motion. But in general, black holes are not spherical; so test-particle motion around a black hole possesses only three *obvious* constants. It is rather remarkable, then, that a constant turns out to exist. It was discovered by Carter (1968a), using Hamilton-Jacobi methods. As of 1973, nobody has given a cogent geometric explanation of why this fourth constant should exist—although hints of an explanation may be found in Carter (1968c) and Walker and Penrose (1970).

Carter's "fourth constant" of the motion, as derived in exercise 33.7, is

(4) " \mathcal{Q} "

$$\mathcal{Q} = p_\theta^2 + \cos^2\theta[a^2(\mu^2 - E^2) + \sin^{-2}\theta L_z^2]. \quad (33.31d)$$

The constant of the motion

$$\mathcal{K} \equiv \mathcal{Q} + (L_z - aE)^2, \quad (33.31e)$$

obtained by combining \mathcal{Q} , L_z , and E , is often used in place of \mathcal{Q} . Whereas \mathcal{Q} can be negative, \mathcal{K} is always nonnegative:

$$\begin{aligned} \mathcal{K} &= p_\theta^2 + (L_z - aE \sin^2\theta)^2/\sin^2\theta + a^2\mu^2 \cos^2\theta \\ &\geq 0 \text{ everywhere} \\ &= 0 \text{ only for case of photon } (\mu = 0) \text{ moving along polar axis } (\theta = 0, \pi). \end{aligned}$$

The contravariant components of the test particle's 4-momentum, $p^\alpha = dx^\alpha/d\lambda$, are readily expressed in terms of the constants E , L_z , μ , \mathcal{Q} , by combining equations (33.31) with the metric coefficients (33.2) and the components of the vector potential (33.30). The result is

$$\rho^2 d\theta/d\lambda = \sqrt{\Theta}, \quad (33.32a)$$

$$\rho^2 dr/d\lambda = \sqrt{R}, \quad (33.32b)$$

$$\rho^2 d\phi/d\lambda = -(aE - L_z/\sin^2\theta) + (a/\Delta)P, \quad (33.32c)$$

$$\rho^2 dt/d\lambda = -a(aE \sin^2\theta - L_z) + (r^2 + a^2)\Delta^{-1}P. \quad (33.32d)$$

Equations of motion for charged test particles

Here $\rho^2 = r^2 + a^2 \cos^2\theta$ as defined in equation (33.3b), and the functions Θ , R , P are defined by

$$\Theta = \mathcal{Q} - \cos^2\theta [a^2(\mu^2 - E^2) + L_z^2/\sin^2\theta], \quad (33.33a)$$

$$P = E(r^2 + a^2) - L_z a - e Q r, \quad (33.33b)$$

$$R = P^2 - \Delta [\mu^2 r^2 + (L_z - aE)^2 + \mathcal{Q}]. \quad (33.33c)$$

When working in Kerr coordinates (to avoid the coordinate singularity at the horizon), one must replace equations (33.32c) and (33.32d) by

$$\rho^2 d\tilde{V}/d\lambda = -a(aE \sin^2\theta - L_z) + (r^2 + a^2)\Delta^{-1}(\sqrt{R} + P), \quad (33.32c')$$

$$\rho^2 d\tilde{\phi}/d\lambda = -(aE - L_z/\sin^2\theta) + a\Delta^{-1}(\sqrt{R} + P). \quad (33.32d')$$

[These follow from (33.32) and the transformation between the two coordinate systems—see equations (4) of Box 33.2.] In the above equations, the signs of \sqrt{R} and $\sqrt{\Theta}$ can be chosen independently; but once chosen, they must be used consistently everywhere.

Applications of these equations of motion will play a key role in the rest of this chapter.

EXERCISES

Exercise 33.6. SUPERHAMILTONIAN FOR CHARGED-PARTICLE MOTION

Show that Hamilton's equations (33.28a) for the Hamiltonian (33.28b) reduce to equation (33.29a) for the value of the generalized momentum, and to the Lorentz force equation (33.29b). [*Hint:* Use the relation $(g^{\alpha\beta} g_{\beta\gamma})_{,\mu} = 0$.]

Exercise 33.7. HAMILTON-JACOBI DERIVATION OF EQUATIONS OF MOTION [Based on Carter (1968a)]

Derive the first-order equations of motion (33.32) for a charged particle moving in the external fields of a Kerr-Newman black hole. Use the Hamilton-Jacobi method [Boxes 25.3 and 25.4 of this book; also Chapter 9 of Goldstein (1959)], as follows.

(a) Throughout the superhamiltonian \mathcal{K} of equation (33.28b), replace the generalized momentum π_α by the gradient $\partial S/\partial x^\alpha$ of the Hamilton-Jacobi function.

(b) Write down the Hamilton-Jacobi equation [generalization of equation (2) of Box 25.4] in the form

$$-\frac{\partial S}{\partial \lambda} = \mathcal{K} \left[x^\alpha, \frac{\partial S}{\partial x^\beta} \right] = \frac{1}{2} g^{\alpha\beta} \left(\frac{\partial S}{\partial x^\alpha} - e A_\alpha \right) \left(\frac{\partial S}{\partial x^\beta} - e A_\beta \right). \quad (33.34a)$$

(c) Show that the metric components $g^{\alpha\beta}$ for a Kerr-Newman black hole in Boyer-Lindquist coordinates are given by

$$\begin{aligned} \mathbf{g} \equiv g^{\alpha\beta} \frac{\partial}{\partial x^\alpha} \frac{\partial}{\partial x^\beta} &= -\frac{1}{\Delta \rho^2} \left[(r^2 + a^2) \frac{\partial}{\partial t} + a \frac{\partial}{\partial \phi} \right]^2 + \frac{1}{\rho^2 \sin^2\theta} \left[\frac{\partial}{\partial \phi} + a \sin^2\theta \frac{\partial}{\partial t} \right]^2 \\ &+ \frac{\Delta}{\rho^2} \left(\frac{\partial}{\partial r} \right)^2 + \frac{1}{\rho^2} \left(\frac{\partial}{\partial \theta} \right)^2. \end{aligned} \quad (33.35)$$

(d) Use these metric components and the components (33.30) of the vector potential to bring the Hamilton-Jacobi equation (33.33) into the concrete form

$$\begin{aligned} -\frac{\partial S}{\partial \lambda} = & -\frac{1}{2} \frac{1}{\Delta \rho^2} \left[(r^2 + a^2) \frac{\partial S}{\partial t} + a \frac{\partial S}{\partial \phi} - eQr \right]^2 \\ & + \frac{1}{2} \frac{1}{\rho^2 \sin^2 \theta} \left[\frac{\partial S}{\partial \phi} + a \sin^2 \theta \frac{\partial S}{\partial t} \right]^2 + \frac{1}{2} \frac{\Delta}{\rho^2} \left(\frac{\partial S}{\partial r} \right)^2 + \frac{1}{2} \frac{1}{\rho^2} \left(\frac{\partial S}{\partial \theta} \right)^2. \end{aligned} \quad (33.34b)$$

(e) Solve this Hamilton-Jacobi equation by separation of variables. [Hint: Because the equation has no explicit dependence on λ , ϕ , or t , the solution must take the form

$$S = \frac{1}{2} \mu^2 \lambda - Et + L_z \phi + S_r(r) + S_\theta(\theta), \quad (33.36a)$$

where the values of the “integration constants” follow from $\partial S / \partial \lambda = -\mathcal{K}$, $\partial S / \partial t = \pi_t$, $\partial S / \partial \phi = \pi_\phi$. Insert this assumed form into (33.35) and solve for $S_r(r)$ and $S_\theta(\theta)$ to obtain

$$S_r = \int \Delta^{-1} \sqrt{R} dr, \quad S_\theta = \int \sqrt{\Theta} d\theta, \quad (33.36b)$$

where $R(r)$ and $\Theta(\theta)$ are the functions defined in equation (33.33). Notice that the constant \mathcal{Q} arises naturally as a “separation-of-variables constant” in this procedure. It was in this way that Carter originally discovered \mathcal{Q} , following Misner’s suggestion that he seek analogies to a constant in Newtonian dipole fields (Corben and Stehle, 1960, p. 209).]

(f) By successively setting $\partial S / \partial [\mathcal{Q} + (L_z - aE)^2]$, $\partial S / \partial \mu^2$, $\partial S / \partial E$, and $\partial S / \partial L_z$ to zero, obtain the following equations describing the test-particle orbits:

$$\int^\theta \frac{d\theta}{\sqrt{\Theta}} = \int^r \frac{dr}{\sqrt{R}}, \quad (33.37a)$$

$$\lambda = \int^\theta \frac{a^2 \cos^2 \theta}{\sqrt{\Theta}} d\theta + \int^r \frac{r^2}{\sqrt{R}} dr, \quad (33.37b)$$

$$t = \int^\theta \frac{-a(aE \sin^2 \theta - L_z)}{\sqrt{\Theta}} d\theta + \int^r \frac{(r^2 + a^2)P}{\Delta \sqrt{R}} dr, \quad (33.37c)$$

$$\phi = \int \frac{-(aE \sin^2 \theta - L_z)}{\sin^2 \theta \sqrt{\Theta}} d\theta + \int \frac{aP}{\Delta \sqrt{R}} dr. \quad (33.37d)$$

(g) By differentiating these equations and combining them, obtain the equations of motion (33.32) cited in the text.

(h) Derive equations (33.31) for E , L_z , μ , and \mathcal{Q} by setting $\partial S / \partial x^\alpha = \pi_\alpha = p_\alpha + eA_\alpha$.

§33.6. PRINCIPAL NULL CONGRUENCES

Two special families of *photon* trajectories “mold themselves into” the Kerr-Newman geometry in an especially harmonious way. They are called the “*principal null congruences*” of the geometry. (“Congruence” is an elegant word that means “space-

Principal null congruences for the spacetime geometry of a black hole

filling family of curves.”) These congruences are the solutions to the test-particle equations of motion (33.32) with

$$\mu = 0 \text{ (zero rest mass; photon),} \quad (33.38a)$$

$$e = 0 \text{ (zero charge on photon),} \quad (33.38b)$$

$$L_z = aE \sin^2\theta \quad \begin{cases} \text{a permissible value for } L_z \\ \text{only because } d\theta/d\lambda \text{ turns} \\ \text{out to be zero} \end{cases}, \quad (33.38c)$$

$$\mathcal{Q} = -(L_z - aE)^2 = -a^2 E^2 \cos^4\theta. \quad (33.38d)$$

For these values of the constants of motion, the equations of motion (33.32) reduce to

$$k^\theta \equiv d\theta/d\lambda = 0, \quad (33.39a)$$

$$k^r \equiv dr/d\lambda = \pm E \quad (\text{“+” for outgoing photons,} \\ \text{“-” for ingoing}), \quad (33.39b)$$

$$k^\phi \equiv d\phi/d\lambda = aE/\Delta, \quad (33.39c)$$

$$k^t \equiv dt/d\lambda = (r^2 + a^2)E/\Delta. \quad (33.39d)$$

Significance of the principal null congruences

In what sense are these photon trajectories more interesting than others? (1) They mold themselves to the spacetime curvature in such a way that, if $C_{\alpha\beta\gamma\delta}$ is the Weyl conformal tensor (§13.5), and ${}^*C_{\alpha\beta\gamma\delta} = \epsilon_{\alpha\beta\mu\nu} C^{\{\mu\nu\}}{}_{\gamma\delta}$ is its dual, then

$$C_{\alpha\beta\gamma[\delta} k_{\epsilon]\gamma} k^\beta k^\gamma = 0, \quad {}^*C_{\alpha\beta\gamma[\delta} k_{\epsilon]\gamma} k^\beta k^\gamma = 0. \quad (33.40)$$

[This relationship implies that the Kerr-Newman geometry is of “Petrov-Pirani type D” and that these photon trajectories are “doubly degenerate, principal null congruences.” For details of the meanings and implications of these terms see, e.g., §8 of Sachs (1964), or Ehlers and Kundt (1962), or the original papers by Petrov (1954, 1969) and Pirani (1957).] (2) By suitable changes of coordinates (exercise 33.8), one can bring the Kerr-Newman metric into the form

$$ds^2 = (\eta_{\alpha\beta} + 2Hk_\alpha k_\beta) dx^\alpha dx^\beta, \quad (33.41)$$

where H is a scalar field and k_α are the components of the wave vector for one of the principal null congruences (either one; but not both!). [This was the property of the Kerr-Newman metric that led to its original discovery (Kerr, 1963). For further detail on metrics of this form, see Kerr and Schild (1965).] (3) In Kerr coordinates (Box 33.2), the ingoing principal null congruence is

$$r = -E\lambda, \quad \theta = \text{const}, \quad \tilde{\phi} = \text{const}, \quad \tilde{V} = \text{const}. \quad (33.42a)$$

arbitrary normalization factor; can be removed by redefinition of λ

These ingoing photon world lines are the generators of the conical surface $\tilde{V} = \text{const.}$ in the Kerr diagram of Box 33.2. (4) The only kind of particle that can remain forever at the horizon is a photon with world line in the outgoing principal null congruence (exercise 33.9). Such photon world lines are “generators” of the horizon (dotted curves with a “barber-pole twist” in Kerr diagram of Box 33.2). They have angular velocity

$$\Omega = \frac{d\phi}{dt} = \frac{d\tilde{\phi}}{d\tilde{V}} = \frac{a}{r_+^2 + a^2} = \frac{a}{2M^2 - Q^2 + 2M(M^2 - a^2 - Q^2)^{1/2}}. \quad (33.42b)$$

Exercise 33.8. KERR-SCHILD COORDINATES

EXERCISES

(a) Show that in Kerr coordinates the ingoing null congruence (33.39) has the form (33.42a). Also show that the covariant components of the wave vector—after changing to a new affine parameter $\lambda_{\text{new}} = \lambda_{\text{old}}E$ —are

$$k_r^{(\text{in})} = 0, \quad k_\theta^{(\text{in})} = 0, \quad k_{\tilde{\phi}}^{(\text{in})} = a \sin^2\theta, \quad k_{\tilde{V}}^{(\text{in})} = -1. \quad (33.43)$$

(b) Introduce new coordinates \tilde{t}, x, y, z , defined by

$$x + iy = (r + ia)e^{i\tilde{\phi}} \sin\theta, \quad z = r \cos\theta, \quad \tilde{t} = \tilde{V} - r; \quad (33.44a)$$

and show that in this “Kerr-Schild coordinate system” the metric takes the form

$$ds^2 = (\eta_{\alpha\beta} + 2Hk_\alpha^{(\text{in})}k_\beta^{(\text{in})}) dx^\alpha dx^\beta, \quad (33.44b)$$

where

$$H = \frac{Mr - \frac{1}{2}Q^2}{r^2 + a^2(z/r)^2}, \quad (33.44c)$$

$$k_\alpha^{(\text{in})} dx^\alpha = -\frac{r(x dx + y dy) - a(x dy - y dx)}{r^2 + a^2} - \frac{z dz}{r} - d\tilde{t}. \quad (33.44d)$$

For the transformation to analogous coordinates in which

$$ds^2 = (\eta_{\alpha\beta} + 2Hk_\alpha^{(\text{out})}k_\beta^{(\text{out})}) dx^\alpha dx^\beta.$$

see, e.g., Boyer and Lindquist (1967).

Exercise 33.9. NULL GENERATORS OF HORIZON

(a) Show that in Kerr coordinates the outgoing principle null congruence is described by the tangent vector

$$\frac{d\theta}{d\lambda} = 0, \quad \frac{dr}{d\lambda} = E, \quad \frac{d\tilde{\phi}}{d\lambda} = 2a \frac{E}{\Delta}, \quad \frac{d\tilde{V}}{d\lambda} = 2(r^2 + a^2) \frac{E}{\Delta}. \quad (33.45)$$

(b) These components of the wave vector become singular at the horizon ($\Delta = 0$), not because of a singularity in the coordinate system—the coordinates are well-behaved!—but because of poor normalization of the affine parameter. For each outgoing geodesic, let Δ_0

be a constant, defined as the value of Δ at the event where the geodesic slices the hypersurface $\tilde{V} = 0$. Then renormalize the affine parameter for each geodesic

$$\lambda_{\text{new}} = (E/\Delta_0)\lambda_{\text{old}}. \quad (33.46)$$

Show that the resulting wave vectors

$$\frac{d\theta}{d\lambda} = 0, \quad \frac{dr}{d\lambda} = \Delta_0, \quad \frac{d\tilde{\phi}}{d\lambda} = 2a \frac{\Delta_0}{\Delta}, \quad \frac{d\tilde{V}}{d\lambda} = 2(r^2 + a^2) \frac{\Delta_0}{\Delta} \quad (33.45')$$

are well-behaved as one approaches the horizon; and show that the geodesics on the horizon have the form

$$\theta = \text{const.}, \quad r = r_+ = \text{const.}, \quad \tilde{\phi} = 2a\lambda, \quad \tilde{V} = 2(r_+^2 + a^2)\lambda. \quad (33.47)$$

(c) Show that these are the only test-particle trajectories that remain forever on the horizon. [Hint: Examine the light cone.]

§33.7. STORAGE AND REMOVAL OF ENERGY FROM BLACK HOLES [Penrose (1969)]

When a small object falls down a large hole:

(1) energy radiated is negligible compared to object's rest mass

When an object falls into a black hole, it changes the hole's mass, charge, and intrinsic angular momentum (first law of black-hole dynamics; Box 33.4). If the infalling object is large, its fall produces much gravitational and electromagnetic radiation. To calculate the radiation emitted, and the energy and angular momentum it carries away—which are prerequisites to any calculation of the final state of the black hole—is an enormously difficult task. But if the object is very small (size of object \ll size of horizon; mass of object \ll mass of hole), and has sufficiently small charge, the radiation it emits in each circuit around the hole is negligible. For example, for gravitational radiation

$$\frac{(\text{energy emitted per circuit})}{(\text{rest mass of object})} \sim \frac{(\text{rest mass of object})}{(\text{mass of hole})} \quad (33.48)$$

[see §36.5; also Bardeen, Press, and Teukolsky (1972)]. Because the energy emitted is negligible, radiation reaction is also negligible, and the object moves very nearly along a test-particle trajectory. In this case, application of the first law of black-hole dynamics is simple and straightforward.

Consider, initially, a small object that falls directly into the black hole from far away. According to the first law, it produces the following changes in the mass, charge, and angular momentum of the black hole:

$$\Delta M = E = (\text{"energy at infinity" of infalling object}), \quad (33.49a)$$

$$\Delta Q = e = (\text{charge of infalling object}), \quad (33.49b)$$

$$\Delta S \equiv \Delta |\mathbf{S}| = L_z = \left(\begin{array}{l} \text{component of object's angular momentum} \\ \text{on black hole's rotation axis} \end{array} \right). \quad (33.49c)$$

(2) hole's mass, charge, and angular momentum change by $\Delta M = E$, $\Delta Q = e$, $\Delta S = L_z$

The infalling object will also change the direction of \mathbf{S} . In the black hole's original asymptotic Lorentz frame, its initial angular momentum vector points in the z -direction,

$$(S_z)_{\text{initial}} = S, \quad (S_x)_{\text{initial}} = 0, \quad (S_y)_{\text{initial}} = 0.$$

Consequently, only the z -component of angular momentum of the infalling object can produce any significant change in the magnitude of \mathbf{S} . But the x - and y -components, L_x and L_y , can change the direction of \mathbf{S} . If the object has negligible speed at infinity, then it produces the changes (exercise 33.10):

$$\Delta S_x = L_x = -(\sin \phi_\infty) \sqrt{\Theta_\infty} - (\cot \theta_\infty \cos \phi_\infty) L_z, \quad (33.49\text{d})$$

$$\Delta S_y = L_y = (\cos \phi_\infty) \sqrt{\Theta_\infty} - (\cot \theta_\infty \sin \phi_\infty) L_z, \quad (33.49\text{e})$$

$$\Delta(S_x^2 + S_y^2)^{1/2} = \sqrt{2} = (L^2 - L_z^2)^{1/2}. \quad (33.49\text{f})$$

Here a subscript “ ∞ ” means the value of a quantity at a point on the orbit far from the black hole (at “infinity”).

Consider, next, a more complicated process, first conceived of by Penrose (1969): (1) Shoot a small object A into the black hole from outside with energy-at-infinity E_A , charge e_A , and axial component of angular momentum L_{zA} . (2) When the object is deep down near the horizon, let it explode into two parts, B and C , each of which subsequently moves along a new test-particle trajectory, with new constants of the motion e_B and e_C , E_B and E_C , L_{zB} and L_{zc} . (3) So design the explosion that object B falls down the hole and gets captured, but object C escapes back to radial infinity. What will be the changes in mass, charge, and angular momentum of the black hole? According to the first law of black-hole dynamics,

$$\begin{aligned} \Delta M &= \left(\begin{array}{l} \text{total energy that distant observers see} \\ \text{fall inward past themselves minus} \\ \text{total energy that they see reemerge} \end{array} \right) \\ &= E_A - E_C. \end{aligned}$$

Similarly, $\Delta Q = e_A - e_C$ and $\Delta S = L_{zA} - L_{zc}$. Not unexpectedly, these changes can be written more simply in terms of the constants of motion for object B , which went down the hole. View the explosion “ $A \rightarrow B + C$ ” in a local Lorentz frame down near the hole, which is centered on the explosive event. As viewed in that frame, the explosion must satisfy the special relativistic laws of physics (equivalence principle!). In particular, it must obey charge conservation

$$e_A = e_B + e_C \quad (33.50\text{a})$$

and conservation of total 4-momentum

$$(\mathbf{p}_A)_{\text{immediately before explosion}} = (\mathbf{p}_B + \mathbf{p}_C)_{\text{immediately after explosion}}.$$

Moreover, conservation of 4-momentum \mathbf{p} and charge e implies also conservation of generalized momentum $\mathbf{n} \equiv \mathbf{p} - e\mathbf{A}$,

$$\mathbf{n}_A = \mathbf{p}_A - e_A \mathbf{A} = \mathbf{p}_B + \mathbf{p}_C - (e_B + e_C) \mathbf{A} = \mathbf{n}_B + \mathbf{n}_C;$$

and hence also conservation of the components of generalized momentum along the vectors $\partial/\partial t$ and $\partial/\partial\phi$,

$$E_A \equiv -\pi_{tA} = -\pi_{tB} - \pi_{tC} = E_B + E_C, \quad (33.50b)$$

$$L_{zA} \equiv \pi_{\phi B} + \pi_{\phi C} = L_{zB} + L_{zC}, \quad (33.50c)$$

(conservation of “energy-at-infinity” and “axial component of angular momentum” in explosion). Combining these conservation laws with the expressions

$$\Delta M = E_A - E_C, \quad \Delta Q = e_A - e_C, \quad \text{and } \Delta S = L_{zA} - L_{zC},$$

one obtains

$$\Delta M = E_B, \quad \Delta Q = e_B, \quad \Delta S = L_{zB}. \quad (33.51)$$

This result restated in words: the changes in mass, charge, and angular momentum are equal to the “energy-at-infinity,” charge, and “axial component of angular momentum” that object B carries inward across the horizon, *even though B may have ended up on a test-particle orbit that does not extend back to radial infinity!*

Straightforward extensions of the above thought experiment produce this generalization: *In any complicated black-hole process that involves infalling, colliding, and exploding pieces of matter that emit negligible gravitational radiation, the total changes in mass, charge, and angular momentum of the black hole are*

$$\Delta M = \left(\begin{array}{l} \text{sum of values of energy-at-infinity, } E, \\ \text{for all objects which cross the horizon—with} \\ E \text{ evaluated for each object at event of crossing} \end{array} \right), \quad (33.52a)$$

$$\Delta Q = \left(\begin{array}{l} \text{similar sum, of charges, } e, \text{ for} \\ \text{all objects crossing horizon} \end{array} \right), \quad (33.52b)$$

$$\Delta S = \left(\begin{array}{l} \text{similar sum of axial components of angular} \\ \text{momentum, } L_z, \text{ for all objects crossing horizon} \end{array} \right). \quad (33.52c)$$

Changes in M , Q , S for any nonradiative black-hole process

Extraction of energy from a black hole by processes in the ergosphere

This result is not at all surprising. It is precisely what one might expect from the most naive of viewpoints. Not so expected, however, is the following consequence [Penrose (1969)]: *By injecting matter into a black hole in a carefully chosen way, one can decrease the total mass-energy of the black hole—i.e., one can extract energy from the hole.*

For *uncharged* infalling objects, the key to energy extraction is the ergosphere [hence its name, coined by Ruffini and Wheeler (1971a) from the Greek word “ $\epsilon\rho\gamma\sigma\nu$ ” for “work”]. Outside the ergosphere, the Killing vector $\xi_{(t)} \equiv \partial/\partial t$ is timelike, as is the 4-momentum \mathbf{p} of every test particle; and therefore $E = -\mathbf{p} \cdot \xi_{(t)}$ is necessarily positive. But inside the ergosphere (between the horizon and the static limit), $\xi_{(t)}$

is spacelike, so for certain choices of timelike momentum vector (certain orbits of uncharged test particles), $E = -\mathbf{p} \cdot \boldsymbol{\xi}_{(t)}$ is negative, whereas for others it is positive. The orbits of negative E are confined entirely to the ergosphere. Thus, to inject an uncharged object with negative E into the black hole—and thereby to extract energy from the hole—one must always change its E from positive to negative and therefore also change its orbit, after it penetrates into the ergosphere. Of course, this is not difficult in principle—and perhaps not even in practice; see Figure 33.2.

For a charged object, electromagnetic forces alter the region where there exist orbits of negative energy-at-infinity. If the charges of object and hole have opposite sign, then the hole's electromagnetic field pulls inward on the object, giving it more kinetic energy when near the hole than one would otherwise expect. Thus, $-\mathbf{p} \cdot \boldsymbol{\xi}_{(t)}$ becomes an overestimate of E ,

$$E = -(\mathbf{p} - e\mathbf{A}) \cdot \boldsymbol{\xi}_{(t)} = -\mathbf{p} \cdot \boldsymbol{\xi}_{(t)} + \underbrace{eQr/p^2}_{\uparrow [< 0 \text{ if } eQ < 0]}; \quad (33.53)$$

and orbits with $E < 0$ exist in a region somewhat larger than the ergosphere. If, on the other hand, e and Q have the same sign, then orbits with $E < 0$ are confined to a region smaller than the ergosphere. For given values e , Q , and rest mass μ , the region where there exist orbits with $E < 0$ is called the “*effective ergosphere*.”

The “*effective ergosphere*”
for charged-particle processes

Exercise 33.10. ANGULAR MOMENTUM VECTOR FOR INFALLING PARTICLE

EXERCISE

Derive equations (33.49d,e,f) for the components L_x and L_y of the orbital angular momentum of a particle falling into a black hole. Assume negligible initial speed, $E^2 - \mu^2 \approx 0$.

§33.8. REVERSIBLE AND IRREVERSIBLE TRANSFORMATIONS [Christodoulou (1970), Christodoulou and Ruffini (1971)]

Take a black hole of given mass M , charge Q , and angular momentum S . By injection of small objects, make a variety of changes in M , Q , and S . Can one pick an arbitrary desired change, ΔM , ΔQ , and ΔS , and devise a process that achieves it? Or are there limitations?

The second law of black-hole dynamics (nondecreasing surface area of black hole; Box 33.4; proof in §34.5 of next chapter) provides a strict limitation.

Then can all values within that limitation be achieved—and can that limitation be discovered by a direct examination of test-particle orbits?

The answer is yes; and, in fact, the limitation was discovered by Christodoulou (1970) and Christodoulou and Ruffini (1971) from an examination of test-particle orbits, independently of and simultaneously with Hawking's (1971) discovery of the second law of black-hole dynamics.

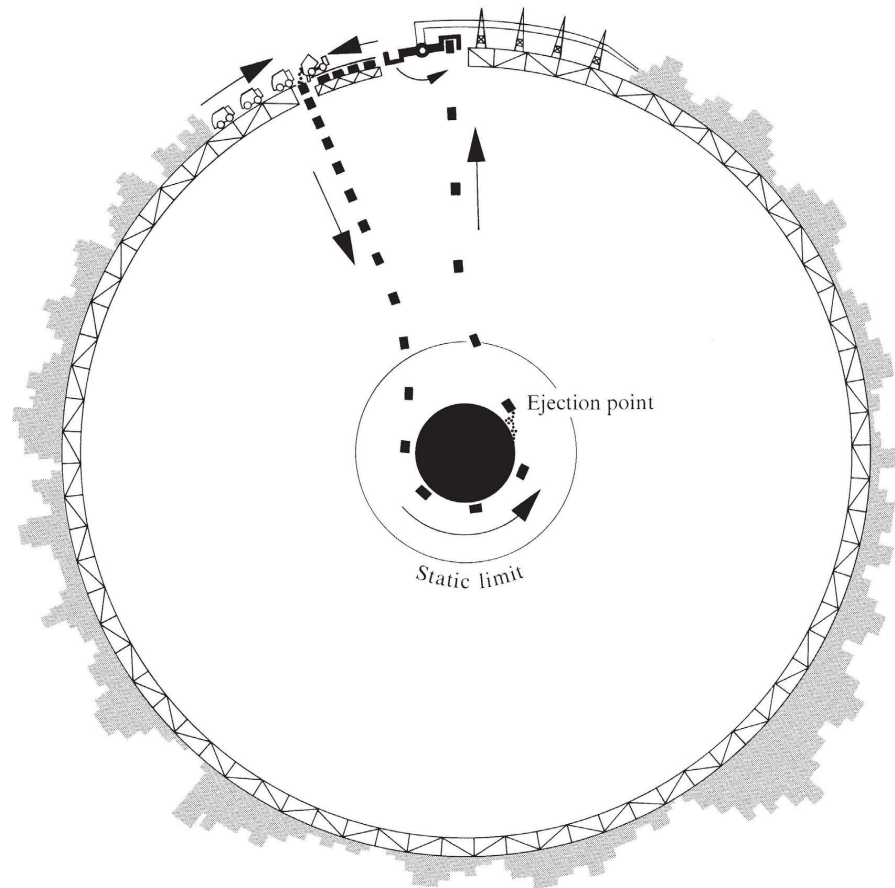


Figure 33.2.

An advanced civilization has constructed a rigid framework around a black hole, and has built a huge city on that framework. Each day trucks carry one million tons of garbage out of the city to the garbage dump. At the dump the garbage is shoveled into shuttle vehicles which are then, one after another, dropped toward the center of the black hole. Dragging of inertial frames whips each shuttle vehicle into a circling, inward-spiraling orbit near the horizon. When it reaches a certain “ejection point,” the vehicle ejects its load of garbage into an orbit of negative energy-at-infinity, $E_{\text{garbage}} < 0$. As the garbage flies down the hole, changing the hole’s total mass-energy by $\Delta M = E_{\text{garbage ejected}} < 0$, the shuttle vehicle recoils from the ejection and goes flying back out with more energy-at-infinity than it took down

$$\begin{aligned} E_{\text{vehicle out}} &= E_{\text{vehicle + garbage down}} - E_{\text{garbage ejected}} \\ &> E_{\text{vehicle + garbage down}} \end{aligned}$$

The vehicle deposits its huge kinetic energy in a giant flywheel adjacent to the garbage dump; and the flywheel turns a generator, producing electricity for the city, while the shuttle vehicle goes back for another load of garbage. The total electrical energy generated with each round trip of the shuttle vehicle is

$$\begin{aligned} (\text{Energy per trip}) &= E_{\text{vehicle out}} - (\text{rest mass of vehicle}) \\ &= (E_{\text{vehicle + garbage down}} - E_{\text{garbage ejected}}) - (\text{rest mass of vehicle}) \\ &= (\text{rest mass of vehicle} + \text{rest mass of garbage} - \Delta M) - (\text{rest mass of vehicle}) \\ &= (\text{rest mass of garbage}) + (\text{amount}, - \Delta M, \text{by which hole's mass decreases}). \end{aligned}$$

Thus, not only can the inhabitants of the city use the black hole to convert the entire rest mass of their garbage into kinetic energy of the vehicle, and thence into electrical power, but they can also convert some of the mass of the black hole into electrical power!

To derive the limitation of nondecreasing surface area from properties of test-particle orbits, one must examine what values of energy-at-infinity, E , are allowed at a given location (r, θ) outside a black hole. Equations (33.32a,b), when combined, yield the value of E in terms of a test particle's location (r, θ) , rest mass μ , charge e , axial component of angular momentum L_z , and momenta $p^r = dr/d\lambda, p^\theta = d\theta/d\lambda$ in the r and θ directions:

$$\alpha E^2 - 2\beta E + \gamma = 0; \quad E = \frac{\beta + \sqrt{\beta^2 - \alpha\gamma}}{\alpha}, \quad (33.54a) \quad \begin{array}{l} (1) \text{ } E \text{ as function of } \mu, e, L_z, \\ r, \theta, p^r \end{array}$$

where

$$\alpha = (r^2 + a^2)^2 - \Delta a^2 \sin^2\theta > 0 \text{ everywhere outside horizon,} \quad (33.54b)$$

$$\beta = (L_z a + e Q r)(r^2 + a^2) - L_z a \Delta, \quad (33.54c)$$

$$\gamma = (L_z a + e Q r)^2 - \Delta (L_z / \sin \theta)^2 - \mu^2 \Delta p^2 - \rho^4 [(p^r)^2 + \Delta (p^\theta)^2]. \quad (33.54d)$$

(One must take the positive square root, $+\sqrt{\beta^2 - \alpha\gamma}$, rather than the negative square root; positive square root corresponds to 4-momentum pointing toward future; while negative square root corresponds to past-pointing 4-momentum; see Figure 33.3.)

Several features of the energy equation (33.54) are noteworthy. (1) For orbits in the equatorial “plane,” $\theta = \pi/2$ and $p^\theta \equiv 0$, the energy equation yields an effective potential for radial motion (Box 33.5). (2) Orbits of negative E must have $\beta < 0$ and $\gamma > 0$ —which can be achieved only if $L_z a < 0$ and/or $e Q < 0$. Thus, *one cannot decrease the mass of a black hole without simultaneously decreasing the magnitude of its charge or angular momentum or both.* (3) For an orbit at given (r, θ) , with given e and L_z , E is a minimum if $p^r = p^\theta = \mu = 0$. *Put differently, the rest mass and the r - and θ -components of momentum always contribute positively to E .*

By injecting an object into a black hole, produce small changes

$$\delta M = E, \quad \delta Q = e, \quad \delta S = L_z,$$

in its mass, charge, and angular momentum. For given changes in Q and S , what range of changes in M is possible? Clearly δM can be made as large as one wishes by making the rest mass μ sufficiently large. But there will be a lower limit on δM . That limit corresponds to the minimum value of E for given e and L_z . The orbit of minimum E crosses the horizon (otherwise no changes in M, Q, S would occur!), so one can evaluate E there. At the horizon, as anywhere, a minimum for E is achieved if $\mu = p^r = p^\theta = 0$. Inserting these values and $r = r_+$ (so $\Delta = 0$) into equations (33.54), one finds

$$E_{\min} = \frac{L_z a + e Q r_+}{r_+^2 + a^2}, \quad (33.55)$$

Properties of test-particle orbits:

(2) effective potential

(3) negative E requires
 $L_z a < 0$ and/or $e Q < 0$

Changes in black-hole properties due to injection of particles:

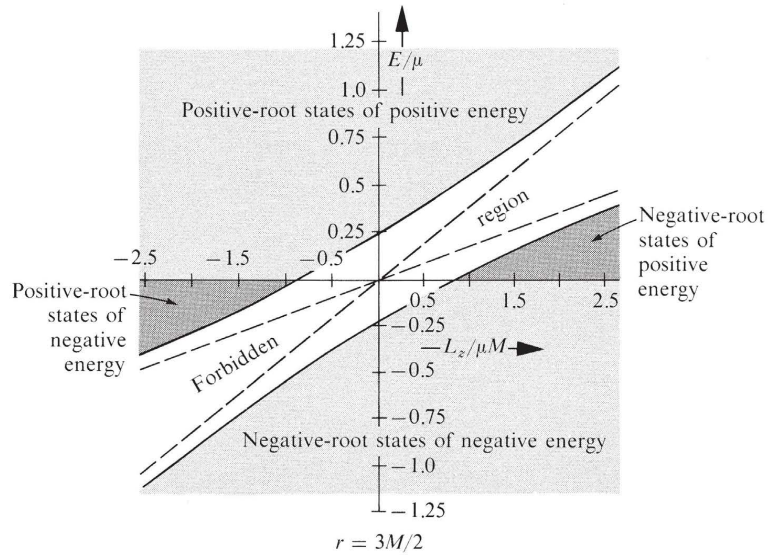


Figure 33.3.

Energy-at-infinity E allowed for a particle of angular momentum L_z and rest mass μ , which is (1) in the “equatorial plane” $\theta = \pi/2$, (2) at radius $r = 3M/2$, (3) of an uncharged ($Q = 0$) extreme-Kerr ($S = M^2$) black hole. E is here plotted against L_z . “Seas” of “positive and negative root” states are shown. The positive root states have energies-at-infinity given by equations (33.54)

$$E = \frac{\beta + \sqrt{\beta^2 - \alpha\gamma}}{\alpha}$$

and have 4-momentum vectors pointing into the future light cone. The negative root states (states of Dirac’s “negative energy sea”) have energies at infinity given by

$$E = \frac{\beta - \sqrt{\beta^2 - \alpha\gamma}}{\alpha},$$

and have 4-momentum vectors pointing into the past light cone. In the gap between the “seas” no orbits exist (forbidden region). The gap vanishes at the horizon $r = M$ (infinite redshift of local energy gap, 2μ , gives zero gap in energy-at-infinity). [Figure adapted from Christodoulou (1971).]

corresponding to changes in the black-hole properties of

- (1) limit on δM for given δQ and δS

$$\delta M \geq \frac{a \delta S + r_+ Q \delta Q}{r_+^2 + a^2} \quad \left(\begin{array}{l} \text{absolute minimum value of} \\ \delta M \text{ for given } \delta S \text{ and } \delta Q \end{array} \right). \quad (33.56)$$

Notice an important consequence [Bardeen (1970a)]: if the black hole is initially of the “extreme Kerr-Newman” variety, with $M^2 = a^2 + Q^2$, so that one might fear a change which makes $M^2 < a^2 + Q^2$ and thereby destroys the horizon, one’s fears are unfounded. Equation (33.56) then demands (since $r_+ = M$ and $S = Ma$)

$$M \delta M \geq a \delta a + Q \delta Q;$$

- (2) preservation of the horizon

so M^2 remains greater than or equal to $a^2 + Q^2$, and the horizon is preserved.

Box 33.5 ORBITS OF TEST PARTICLE IN “EQUATORIAL PLANE” OF KERR-NEWMAN BLACK HOLE

Radial motion is governed by energy equation (33.54) with $\theta = p^\theta = 0$:

$$\alpha E^2 - 2\beta E + \gamma_0 - r^4(p^r)^2 = 0; \quad E = \frac{\beta + \sqrt{\beta^2 - \alpha\gamma_0 + \alpha r^4(p^r)^2}}{\alpha}; \quad (1)$$

α, β, γ_0 are functions of r and of constants of motion,

$$\alpha = (r^2 + a^2)^2 - \Delta a^2 > 0, \quad (2a)$$

$$\beta = (L_z a + eQr)(r^2 + a^2) - L_z a \Delta, \quad (2b)$$

$$\gamma_0 = (L_z a + eQr)^2 - \Delta L_z^2 - \mu^2 r^2 \Delta; \quad (2c)$$

p^r = (radial momentum) is

$$p^r = dr/d\lambda. \quad (3)$$

Thus, equation (1) is an ordinary differential equation for $dr/d\lambda$.

Qualitative features of the radial motion can be read off an effective-potential diagram. The effective potential $V(r)$ is the minimum allowed value of E at radius r :

$$V(r) = \frac{\beta + \sqrt{\beta^2 - \alpha\gamma_0}}{\alpha}.$$

As in the Schwarzschild case (Figure 25.2), the allowed regions for a particle of energy-at-infinity E are the regions with $V(r) \leq E$; and the turning points ($p^r = dr/d\lambda = 0$) occur where $V(r) = E$.

Stable circular orbits occur at the minima of $V(r)$. By examining $V(r)$ closely, one finds that for uncharged black holes the innermost stable circular orbit (most tightly bound orbit) has the characteristics here tabulated [table adapted from Ruffini and Wheeler (1971b)].

Characteristic	Newtonian (Figure 25.2)	Schwarzschild ($a = Q = 0$) (Figure 25.2)	Extreme Kerr ($a^2 = M^2, Q = 0$) (see figure)	
			[Bardeen (1970a)] if $L_z a > 0$	[Bardeen (1970a)] if $L_z a < 0$
r/M	0	6	1	9
E/μ	$-\infty$	$2\sqrt{2}/3$	$1/\sqrt{3}$	$5/(3\sqrt{3})$
$(\mu - E)/\mu =$ “fractional binding”	$+\infty$	0.0572	0.4226	0.0377
$ L_z /\mu M$	0	$2\sqrt{3}$	$2/\sqrt{3}$	$22/(3\sqrt{3})$

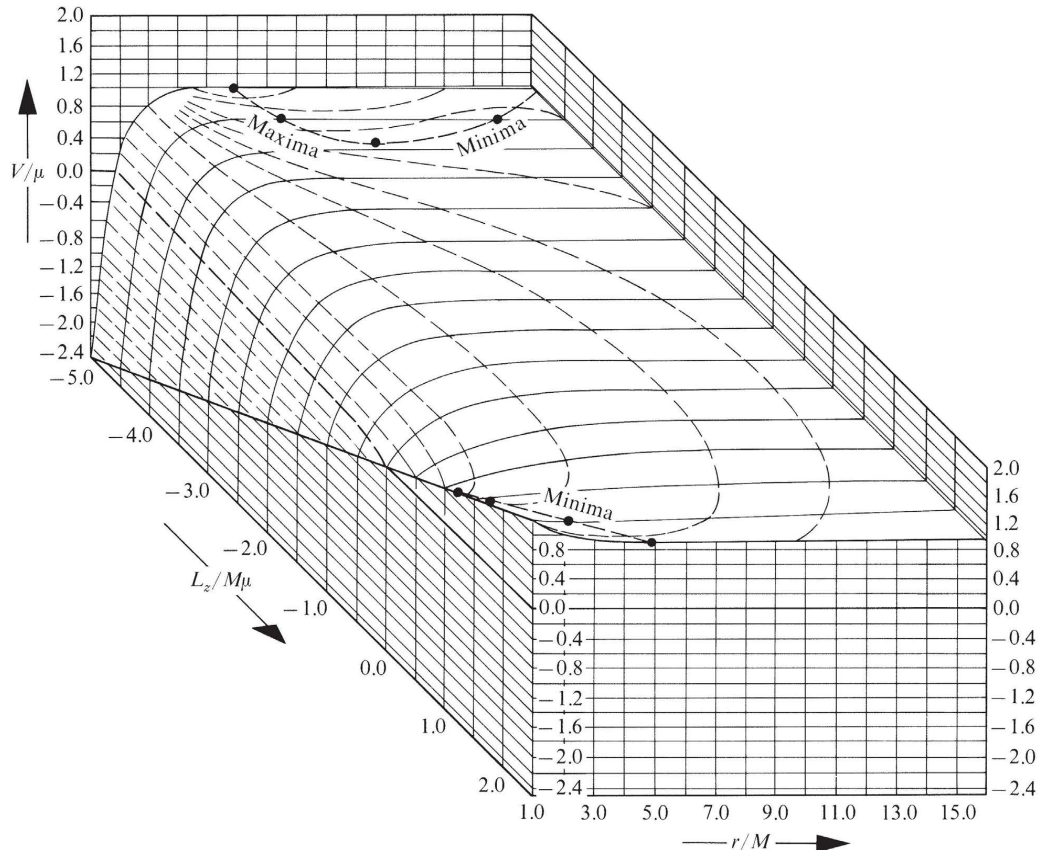
Box 33.5 (continued)

For a charged extreme Kerr-Newman black hole ($M^2 = Q^2 + a^2$, $Q \neq 0$ and $a \neq 0$) stable circular orbits with 100 per cent binding ($E = 0$) are achieved in the limit

$$\frac{e}{\mu} \rightarrow -\infty, \quad \frac{Q}{M} \rightarrow 0 \text{ (so } a \rightarrow M\text{)}, \quad \text{and } \left(\frac{e}{\mu}\right) \cdot \left(\frac{Q}{M}\right) \rightarrow -\infty.$$

[Christodoulou and Ruffini (1971)].

The effective potential for an uncharged, extreme Kerr black hole ($a = M$) is shown in the figure [figure adapted from Ruffini and Wheeler (1971b)]. For detailed diagrams of orbits in the equatorial plane, see de Felice (1968). For many interesting properties of orbits that are not confined to the equatorial plane, see Wilkins (1972).



The general limit (33.56) on the change in mass can be rewritten in an alternative form [Christodoulou (1970), Christodoulou and Ruffini (1971)]:

$$\delta M_{\text{ir}} \geq 0, \quad (33.57)$$

where

$$M_{\text{ir}} \equiv \frac{1}{2} \sqrt{r_+^2 + a^2} = \frac{1}{2} [(M + \sqrt{M^2 - Q^2 - a^2})^2 + a^2]^{1/2} \quad (33.58) \quad (3) \text{ irreducible mass}$$

is the “irreducible mass” of the black hole. *Equation (33.57) states that no black-hole transformation produced by the injection of small lumps of matter can ever reduce the irreducible mass of a black hole.* This result is actually a special case of the second law of black-hole dynamics, since the surface area of a black hole is

$$A = 16\pi M_{\text{ir}}^2 \quad (33.59)$$

(Exercise 33.12).

Equation (33.58) can be combined with $a = S/M$ and inverted to yield

$$M^2 = \left(M_{\text{ir}} + \frac{Q^2}{4 M_{\text{ir}}} \right)^2 + \frac{S^2}{4 M_{\text{ir}}^2}. \quad (33.60)$$

↓ ↓ ↓
 [irreducible con- [electromagnetic con- [rotational con-
 tribution to mass] tribution to mass] tribution to mass]

A black-hole transformation that holds fixed the irreducible mass is *reversible*; one that increases it is *irreversible*. The derivation of equation (33.56) revealed that the only injection processes that actually achieve the minimum possible value for δM (and thus make $\delta M_{\text{ir}} = 0$) are those with $\mu = p^r = p^\theta = 0$ at the horizon, $r = r_+$. Restated in words: To produce a reversible transformation by injecting an object into a black hole, one must (1) give the object a rest mass μ extremely small compared to its charge e or axial component of angular momentum L_z ,

$$\mu/e \ll 1 \text{ and/or } \mu^2/L_z^2 \ll 1;$$

and (2) set the object down “extremely gently” ($p^r = p^\theta = 0$), extremely close to the horizon ($r = r_+$). This does not sound too difficult until one recalls that objects with $p^r = p^\theta = 0$ at the horizon must be moving outward with the speed of light, and that the nearer one approaches the horizon as one sets down the object, the greater one’s danger of “slipping” and getting swallowed!

Clearly, any actual injection process will depart somewhat from irreversibility. Reversibility is an idealized limit, approachable but not attainable.

(4) reversible and irreversible transformations

EXERCISES**Exercise 33.11. IRREDUCIBLE MASS IS IRREDUCIBLE**

Show that condition (33.56) is equivalent to $\delta M_{\text{ir}} \geq 0$.

Exercise 33.12. SURFACE AREA OF A BLACK HOLE

Show that the surface area of the horizon of the Kerr-Newman geometry [area of surface $r = r_+$ and $t = \text{const}$ (Boyer-Lindquist coordinates) or $\tilde{V} = \text{const}$ (Kerr coordinates)] is $16\pi M_{\text{ir}}^2$.

Exercise 33.13. ANGULAR VELOCITY OF A BLACK HOLE

A general theorem [Hartle (1970) for relativistic case; Ostriker and Gunn (1969) for nonrelativistic case] says that, if one injects angular momentum into a rotating star while holding fixed all other contributions to its total mass-energy (contributions from entropy and from baryonic rest mass), then the injection produces a change in total mass-energy given by

$$\delta(\text{mass-energy}) = \left(\begin{array}{l} \text{angular velocity of star} \\ \text{at point of injection} \end{array} \right) \delta(\text{angular momentum}). \quad (33.61)$$

By analogy, if one injects an angular momentum δS into a rotating black hole while holding fixed all other contributions to its total mass-energy (contributions from irreducible mass and from charge), one identifies the coefficient Ω_h in the equation

$$\delta M = \Omega_h \delta S$$

as the angular velocity of the hole:

$$\Omega_h = (\partial M / \partial S)_{Q, M_{\text{ir}}}. \quad (33.62)$$

- (a) Show that the angular velocity of a black hole is equal to

$$\Omega_h = \frac{a}{r_+^2 + a^2}. \quad (33.63)$$

Notice that this is precisely the angular velocity of photons that live forever on the horizon [equation (33.42b); “barber-pole twist” of null generators of horizon].

(b) Show that *any* object falling into a black hole acquires an angular velocity (relative to Boyer-Lindquist coordinates) of $\Omega = d\phi/dt = \Omega_h$ in the late stages, as it approaches the horizon. (Recall that the horizon is a singularity of the Boyer-Lindquist coordinates. This is the reason that every object, regardless of its $L_z, E, e, \mu, \mathcal{Q}$, can approach and does approach $\Omega = \Omega_h$.)

Exercise 33.14. SEPARATION OF VARIABLES FOR WAVE EQUATIONS

This chapter has studied extensively the motion of small objects in the external fields of black holes. Of almost equal importance, but not so well-understood yet because of its complexity, is the evolution of weak electromagnetic and gravitational perturbations (“waves”) in the Kerr-Newman geometry. Just as one had no *a priori* reason to expect a “fourth constant” for test-particle motion in the Kerr-Newman geometry, so one had no reason to expect separability for Maxwell’s equations, or for the wave equations describing gravitational perturbations—or even for the scalar wave equation $\square\psi \equiv -\psi_{,\alpha}^\alpha = 0$. Thus it came as a great surprise when Carter (1968c) proved separability for the scalar wave equation, and later when Teukolsky (1972, 1973) separated both Maxwell’s equations and the wave equations for gravitational perturbations.

Show that separation of variables for the scalar-wave equation in the (uncharged) Kerr geometry yields solutions of the form

$$\psi = (r^2 + a^2)^{-1/2} u_{lm}(r) S_{ml}(-i\omega a, \cos \theta) e^{i(m\phi - \omega t)}, \quad (33.64a)$$

where m and l are integers with $0 \leq |m| \leq l$; S_{ml} is a spheroidal harmonic [see Meixner and Schärfke (1954)]; and u_{lm} satisfies the differential equation

$$-d^2u/dr^{*2} + Vu = 0. \quad (33.64b)$$

In order to put the equation in this form, define a Regge-Wheeler (1957) “tortoise”-type radial coordinate r^* by

$$dr^* = \Delta^{-1}(r^2 + a^2) dr, \quad (33.64c)$$

and find an effective potential $V(r^*)$ given by

$$\begin{aligned} V = & - \left(\omega - \frac{ma}{r^2 + a^2} \right)^2 + [(m - \omega a)^2 + \mathcal{Q}] (r^2 + a^2)^{-2} \Delta \\ & + 2(Mr - a^2)(r^2 + a^2)^{-3} \Delta + 3a^2(r^2 + a^2)^{-4} \Delta^2. \end{aligned} \quad (33.64d)$$

In this radial equation \mathcal{Q} is a constant (analog of Carter’s constant for particle motion), given in terms of m and l by

$$\mathcal{Q} \equiv \lambda_{ml} - m^2; \lambda_{ml} = \begin{bmatrix} \text{eigenfunction of spheroidal harmonic;} \\ \text{see Meixner and Schärfke (1954)} \end{bmatrix}. \quad (33.64e)$$

[These details of the separated solution were derived by Brill *et al.* (1972). For studies of the interaction between fields and Kerr black holes—studies performed using the above solution, and using analogous solutions to the electromagnetic and gravitational wave equations—see Bardeen, Press, and Teukolsky (1972), Misner (1972b), Teukolsky (1972), Ipser (1971), Press and Teukolsky (1973), and Chrzanowski and Misner (1973).]

CHAPTER 34

GLOBAL TECHNIQUES, HORIZONS, AND SINGULARITY THEOREMS

This chapter is entirely Track 2. §22.5 (geometric optics) and the Track-2 portions of Chapters 32 and 33 (collapse and black holes) are necessary preparation for it. It is not needed as preparation for any later chapter.

Local techniques of analyzing spacetime physics contrasted with global techniques

§34.1. GLOBAL TECHNIQUES VERSUS LOCAL TECHNIQUES

Until the 1960's, computations in gravitation theory used *local* techniques almost exclusively: the Einstein field equation describes how the stress-energy tensor \mathbf{T} at a given event generates curvature \mathbf{G} at that same event (*local* physics). When reduced to differential equations for the metric coefficients, $\mathbf{G} = 8\pi\mathbf{T}$ relates $g_{\alpha\beta}$, $\partial g_{\alpha\beta}/\partial x^\mu$, and $\partial^2 g_{\alpha\beta}/\partial x^\mu \partial x^\nu$ at each given event to $T_{\gamma\delta}$ at that same event (*local* equation). The solution of these differential equations is effected, on a computer or in any initial-value-type analysis, by integrating forward in time from event to event to event (*local* integration). The nongravitational laws of physics are obtained by invoking the equivalence principle in a *local* Lorentz frame at each individual event in spacetime. To build up an understanding of the global structure of spacetime, one performs *local* computations near each event, and then patches the local results together to form a global picture. Why this great reliance on local analyses? Because the laws of gravitation physics take on particularly simple forms when stated locally.

That gravitation physics is also subject to powerful and simple *global* laws, physicists did not realize until the mid 1960's. But since 1963, studies of black holes and of singularities have revealed global laws and global properties of spacetime that rival in their simplicity and elegance even the (local) equivalence principle. An example is the second law of black-hole dynamics: "In an isolated system, the sum of the surface areas of all black holes can never decrease." As a result, there has developed a powerful body of knowledge and techniques for analyzing *directly* the global properties of spacetime.

To give a full treatment of global techniques would require many chapters. Fortunately, a full treatment is being published, almost simultaneously with this book, by Hawking and Ellis (1973). Because Hawking and Ellis are much better qualified to write on this subject than are we (Misner, Thorne, and Wheeler), we have chosen to not write a "competitive" treatment. Instead, we give in this chapter only a brief taste of the subject—enough of a taste to make the reader acquainted with the types of techniques involved and several of the most important results, but

not enough to give him a working knowledge of the subject. The topics we have chosen to treat are those that contact most closely the rest of this book: properties of "infinity" in an asymptotically flat spacetime (§34.2); causality and horizons (§§34.3 and 34.4); a proof of the second law of black-hole dynamics (§34.5); and theorems about the evolution of singularities in spacetime (§34.6). For greater detail on global techniques, one can consult not only the book of Hawking and Ellis (1973), but also review articles by Geroch (1971), by Penrose (1968a, 1972), and by Hawking (1973), the thesis of Godfrey (1970b), and the more specialized papers cited in the body of this chapter.

§34.2. "INFINITY" IN ASYMPTOTICALLY FLAT SPACETIMES

When performing calculations in asymptotically flat spacetime, one often must examine the asymptotic forms of fields (e.g., the metric, or the curvature tensor, or the electromagnetic field) "at infinity." For example, the mass and angular momentum of an isolated system are determined by the asymptotic form of the metric (Chapter 19). It is rarely sufficient to examine asymptotic forms near "spatial infinity." For example, if one wishes to learn how much mass was carried away by gravitational and electromagnetic waves during a supernova explosion, one must examine the asymptotic form of the metric not just at "spatial infinity," but at "future null infinity" (see Figure 34.1).

Penrose (1964, 1965a) has developed a powerful body of mathematical technique for studying asymptotic properties of spacetime near "infinity." The key to his technique is a "conformal transformation" of spacetime, which brings "infinity" in to a finite radius and thereby converts asymptotic calculations into calculations at "finite points." Penrose's technique also provides rigorous definitions of several types of "infinity" that one encounters in asymptotically flat spacetimes.

The details of Penrose's technique are not of importance to the rest of this chapter. However, this chapter will refer frequently to the various types of "infinity" defined by Penrose. In heuristic terms, they are as follows (see Figure 34.2a).

References on global techniques

Motivation for studying properties of spacetime near infinity

Specific regions of infinity:
 I^+ , I^0 , I^- , \mathcal{I}^+ , \mathcal{I}^-

$I^+ \equiv$ "future timelike infinity":

the region $t \rightarrow +\infty$ at finite radius r
 (region toward which timelike lines extend).

$I^- \equiv$ "past timelike infinity":

the region $t \rightarrow -\infty$ at finite radius r
 (region from which timelike lines come).

$I^0 \equiv$ "spacelike infinity":

the region $r \rightarrow \infty$ at finite time t
 (region toward which spacelike slices extend).

$\mathcal{I}^+ \equiv$ "future null infinity":

the region $t + r \rightarrow \infty$ at finite $t - r$
 (region toward which outgoing null lines extend).

$\mathcal{I}^- \equiv$ "past null infinity":

the region $t - r \rightarrow -\infty$ at finite $t + r$
 (region from which ingoing null lines come).

Note: \mathcal{I} is a script I , and is sometimes given the name "scri."

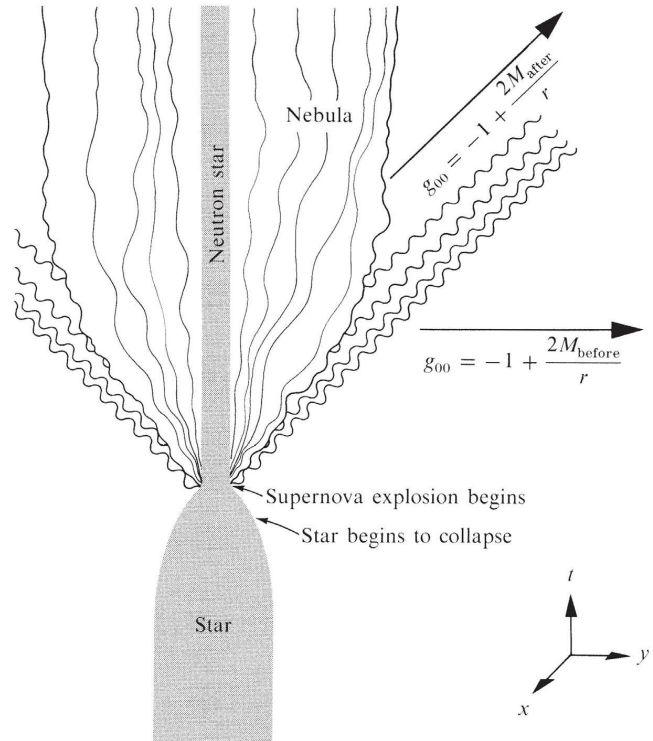


Figure 34.1.

Measurement of the mass-energy radiated as gravitational and electromagnetic waves by a supernova explosion in asymptotically flat spacetime. The mass-energy radiated equals the mass (M_{before}) of the presupernova star, minus the mass (M_{after}) of the neutron star and nebula after the explosion:

$$M_{\text{radiated}} = M_{\text{before}} - M_{\text{after}}.$$

To measure M_{before} , one can examine the asymptotic form (in suitable coordinates) of g_{00} at spatial infinity

$$g_{00} = -1 + \frac{2M_{\text{before}}}{r} + O\left(\frac{1}{r^2}\right) \quad \text{as } r \rightarrow \infty, t = \text{constant}.$$

But to measure M_{after} in the same way, one must wait, at any fixed r , until the radiation has flowed entirely past that point:

$$g_{00} = -1 + \frac{2M_{\text{after}}}{r} + O\left(\frac{1}{r^2}\right) \quad \text{as } r \rightarrow \infty \text{ with } t - r = \begin{cases} \text{(constant value sufficiently large)} \\ \text{(to be inside the burst of waves).} \end{cases}$$

Put differently, to measure M_{after} one must examine the asymptotic form of g_{00} *not* at “spatial infinity,” but rather at “future null infinity.”

Coordinate diagrams for exhibiting structure of infinity

It is often useful, in visualizing the asymptotic structure of spacetime, to introduce coordinates that attribute finite coordinate values to infinity. For example, in flat spacetime one can transform from the usual spherical coordinates t, r, θ, ϕ , with

$$ds^2 = -dt^2 + dr^2 + r^2(d\theta^2 + \sin^2\theta d\phi^2), \quad (34.1)$$

to new spherical coordinates ψ, ξ, θ, ϕ , with

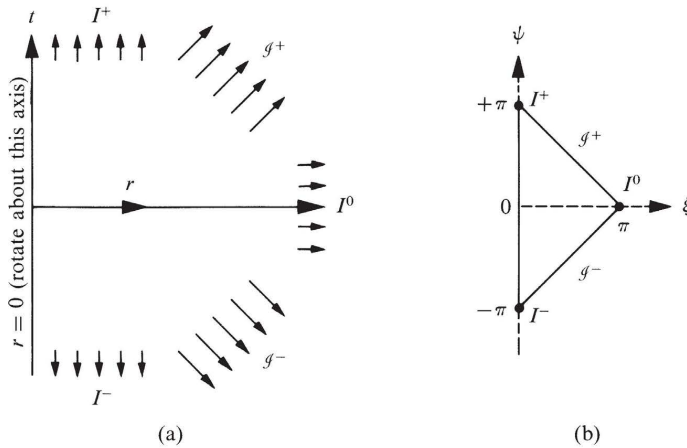


Figure 34.2.

Flat, “Minkowski” spacetime as depicted (a) in the usual spherical coordinates t , r , θ , ϕ of a global Lorentz frame, and (b) in the spherical coordinates of equations (34.2). The five regions of infinity— I^+ , I^- , I^0 , \mathcal{I}^+ , \mathcal{I}^- —are shown in each coordinate diagram. In both coordinate systems, radial null lines make angles of 45° with the vertical axis, and nonradial null lines make angles less than 45° [see equations (34.1) and (34.2c)]. See exercise 34.1 for further detail.

$$t + r = \tan \frac{1}{2}(\psi + \xi), \quad (34.2a)$$

$$t - r = \tan \frac{1}{2}(\psi - \xi), \quad (34.2b)$$

$$ds^2 = \frac{-d\psi + d\xi^2}{4 \cos^2 \frac{1}{2}(\psi + \xi) \cos^2 \frac{1}{2}(\psi - \xi)} + r^2(d\theta^2 + \sin^2\theta d\phi^2). \quad (34.2c)$$

The resulting ψ, ξ coordinate diagram (Figure 34.2b) depicts $I^+, I^-, I^0, \mathcal{I}^+, \mathcal{I}^-$ more clearly than does the usual t, r , coordinate diagram.

As another example, replace the Kruskal-Szekeres coordinates v, u, θ, ϕ for Schwarzschild spacetime by new coordinates ψ, ξ, θ, ϕ :

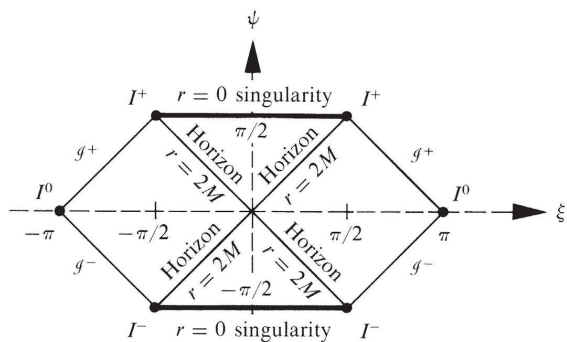
$$v + u = \tan \frac{1}{2}(\psi + \xi), \quad (34.3a)$$

$$v - u = \tan \frac{1}{2}(\psi - \xi), \quad (34.3b)$$

$$(1 - r/2M)e^{r/2M} = v^2 - u^2 = \tan \frac{1}{2}(\psi + \xi) \tan \frac{1}{2}(\psi - \xi), \quad (34.3c)$$

$$ds^2 = \frac{32M^3}{r} \frac{e^{-r/2M}(-d\psi^2 + d\xi^2)}{4 \cos^2 \frac{1}{2}(\psi + \xi) \cos^2 \frac{1}{2}(\psi - \xi)} + r^2(d\theta^2 + \sin^2\theta d\phi^2). \quad (34.3d)$$

The resulting coordinate diagram (Figure 34.3) depicts clearly the causal connections between the horizons, the singularities, and the various regions of infinity.

**Figure 34.3.**

Schwarzschild spacetime as depicted in the ψ , ξ , θ , ϕ coordinates of equations (34.3). This coordinate diagram should be compared with the Kruskal-Szekeres coordinate diagram (Figure 31.3). In both diagrams, radial null geodesics are 45° lines. Each of the asymptotically flat regions (one on each side of the “wormhole” of Figure 31.5a) has its own set of infinities I^+ , I^- , I^0 , \mathcal{I}^+ , and \mathcal{I}^- . See exercise 34.2 for justification of this diagram.

EXERCISES

Exercise 34.1. FLAT SPACETIME IN ψ , ξ , θ , ϕ COORDINATES

- (a) Derive equation (34.2c) from (34.1) and (34.2a,b).
 (b) Show that the regions I^+ , I^- , I^0 , \mathcal{I}^+ , and \mathcal{I}^- of flat spacetime are located at

$$\begin{aligned} I^+ &: \psi = \pi, \xi = 0, \\ I^- &: \psi = -\pi, \xi = 0, \\ I^0 &: \psi = 0, \xi = \pi, \\ \mathcal{I}^+ &: \psi + \xi = \pi, -\pi < \psi - \xi < \pi, \\ \mathcal{I}^- &: \psi - \xi = -\pi, -\pi < \psi + \xi < \pi. \end{aligned} \tag{34.4}$$

[see equations (34.2)]. These are the regions depicted in Figure 34.2.

- (c) Show that in flat spacetime, in a ψ , ξ coordinate diagram (Figure 34.2), radial null lines make angles of 45° with the vertical axis, and nonradial null lines make angles of less than 45° .

Exercise 34.2. SCHWARZSCHILD SPACETIME IN ψ , ξ , θ , ϕ COORDINATES

- (a) Derive equations (34.3c,d) from (34.3a,b) and the Kruskal-Szekeres equations (31.14).
 (b) Use equations (34.3) to justify the precise form of the coordinate diagram in Figure 34.3.

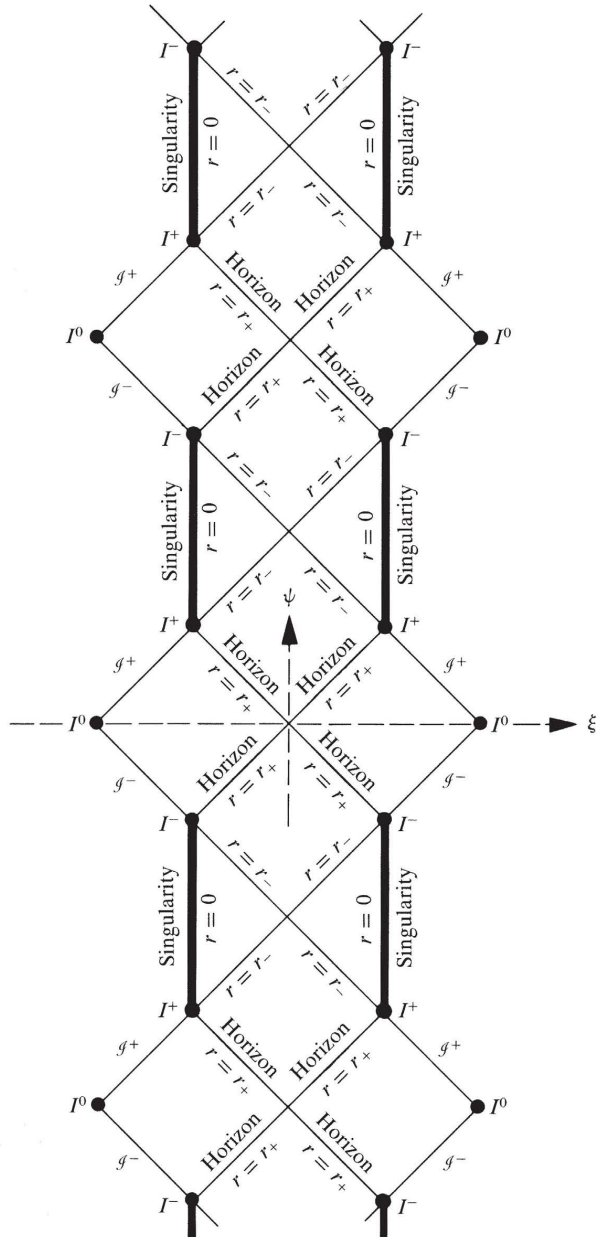
Exercise 34.3. REISSNER-NORDSTROM SPACETIME

- (a) Show that there exists a coordinate system in which the Reissner-Nordström geometry with $0 < |Q| < M$ (exercises 31.8 and 32.1) has the form

$$\begin{aligned} ds^2 &= F^2(-d\psi^2 + d\xi^2) + r^2(d\theta^2 + \sin^2\theta d\phi^2), \\ F &= F(\psi, \xi), \quad r = r(\psi, \xi), \end{aligned} \tag{34.5}$$

and in which the horizons and infinities are as shown in Figure 34.4. [Note: This is a very difficult exercise unless one has in hand the solution to exercise 31.8(d). For solution, see Carter (1966b).]

- (b) Use Figure 34.4 to deduce that the Reissner-Nordström geometry describes a “wormhole” or bridge, connecting two asymptotically flat spacetimes, which: (i) expands to a state of maximum circumference; (ii) recontracts toward a state of minimum circumference, and in the process disconnects its outer regions from the two I^0 's (spatial infinity) and reconnects them to a pair of $r = 0$ singularities; (iii) bounces; (iv) reexpands, and in the process

**Figure 34.4.**

Reissner-Nordström spacetime

$$ds^2 = -\left(1 - \frac{2M}{r} + \frac{Q^2}{r^2}\right)dt^2 + \frac{dr^2}{1 - 2M/r + Q^2/r^2} + r^2(d\theta^2 + \sin^2\theta d\phi^2)$$

with $0 < |Q| < M$, as depicted in a new $(\psi, \xi, \theta, \phi)$ coordinate system where the line element has the form

$$ds^2 = F^2(-d\psi^2 + d\xi^2) + r^2(d\theta^2 + \sin^2\theta d\phi^2).$$

(see exercise 34.3.) This coordinate diagram reveals the global structure of the geometry, including its singularities at $r = 0$, its horizons at

$$r = r_+ = M + \sqrt{M^2 - Q^2}$$

(which limit communication with \mathcal{J}^+ and \mathcal{J}^-), the null surfaces at

$$r = r_- = M - \sqrt{M^2 - Q^2}$$

(which limit communication with the singularities), and the various asymptotically flat infinities, I^+ , I^- , I^0 , \mathcal{J}^+ , and \mathcal{J}^- . From this diagram one can read off the “causal structure” of the geometry—i.e., the abilities of various regions to communicate with each other. For detailed discussion of the geometry, see Graves and Brill (1960) and Carter (1966b). For discussions of collapsing charged stars, for which this geometry is the external gravitational field, see Novikov (1966a,b), de la Cruz and Israel (1967), and Bardeen (1968).

disconnects its “outer regions” from the two singularities and reconnects them to a pair of I^0 ’s in two new asymptotically flat universes; (v) slows its expansion to a halt; (vi) recontracts toward a state of minimum circumference, and in the process disconnects its outer regions from the two I^0 ’s and reconnects them to a new pair of $r = 0$ singularities; etc. *ad infinitum*.

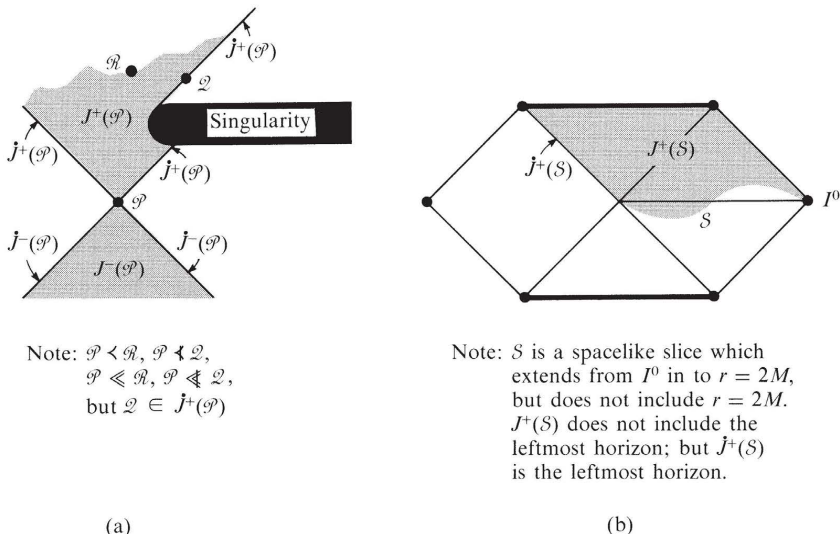


Figure 34.5.

Spacetime diagrams illustrating various causal relationships. Diagram (a) is a hypothetical spacetime; diagram (b) is Schwarzschild spacetime (see Figure 34.3). In both diagrams, null lines have slopes of 45° .

§34.3. CAUSALITY AND HORIZONS

Turn now to global* techniques for analyzing black holes. The goals of the discussion will be (1) to define the concept of horizon (this section), (2) to deduce global geometric properties of horizons (next section), and (3) to prove the second law of black-hole dynamics (following section). The entire discussion will be confined to spacetime manifolds that (1) contain at least one asymptotically flat region (“the external universe”; region “outside black holes”), and (2) are “time-oriented.” By “*time-oriented*” one means that at each event in spacetime a distinct choice has been made as to which light cone is the future cone and which is the past, and moreover that this choice is continuous from event to event throughout spacetime.

The discussion begins with definitions of a variety of causal relationships between events and regions of spacetime (see Figure 34.5).

Restriction of discussion to asymptotically flat, time-oriented manifolds

Definitions of several causality concepts

Definition: $\mathcal{P} \ll \mathcal{Q}$ or equivalently $\mathcal{Q} \gg \mathcal{P}$ (“the event \mathcal{P} precedes the event \mathcal{Q} ”; “the event \mathcal{Q} follows the event \mathcal{P} ”) means that there exists at least one smooth, future-directed timelike curve that extends from \mathcal{P} to \mathcal{Q} .

Definition: A *causal curve* $\mathcal{C}(\lambda)$ is any smooth curve that is nowhere spacelike—i.e., that is timelike or null or “zero” [$\mathcal{C}(\lambda) = \text{some fixed } \mathcal{P}$, for all λ] or some admixture thereof.

Definition: $\mathcal{P} \prec \mathcal{Q}$ or equivalently $\mathcal{Q} \succ \mathcal{P}$ (“the event \mathcal{P} causally precedes the event

*Global, but not fully global; the “universe” of §§34.3–34.5 is asymptotically flat; no account is taken here of possible closure or collapse of the universe or of their consequences.

\mathcal{Q}'' ; the event \mathcal{Q} causally follows the event \mathcal{P}'') means that there exists at least one future-directed causal curve that extends from \mathcal{P} to \mathcal{Q} .

Definition: $J^-(\mathcal{P})$, called *the causal past of \mathcal{P}* , is the set of all events that causally precede \mathcal{P} —i.e., $J^-(\mathcal{P}) = \{\mathcal{Q} | \mathcal{Q} < \mathcal{P}\}$.

Definition: $J^+(\mathcal{P})$, called *the causal future of \mathcal{P}* , is the set of all events that causally follow \mathcal{P} —i.e., $J^+(\mathcal{P}) = \{\mathcal{Q} | \mathcal{Q} > \mathcal{P}\}$.

Definition: If S is a region of spacetime—e.g., a segment of a spacelike hypersurface—then $J^-(S)$ (*the causal past of S*) is the set of all events that causally precede at least one event in S —i.e.,

$$J^-(S) = \{\mathcal{Q} | \mathcal{Q} < \mathcal{P} \text{ for at least one } \mathcal{P} \in S\}.$$

Definition: Similarly, $J^+(S)$ (*the causal future of S*) is the set of all events that causally follow at least one event in S —i.e.,

$$J^+(S) = \{\mathcal{Q} | \mathcal{Q} > \mathcal{P} \text{ for at least one } \mathcal{P} \in S\}.$$

Definition: $J^+(S)$ is the *boundary of $J^+(S)$* ,
 $J^-(S)$ is the *boundary of $J^-(S)$* .

Definition: One defines *the future of \mathcal{P}* , $I^+(\mathcal{P})$; *the past of \mathcal{P}* , $I^-(\mathcal{P})$; *the future of S* , $I^+(S)$; *the past of S* , $I^-(S)$; *the boundary of the future of S* , $I^+(S)$; and *the boundary of the past of S* , $I^-(S)$ in precisely the same manner as above, except that the phrase “causally precede” is replaced by “precede,” and “causally follow” is replaced by “follow.” Example:

$$I^+(S) = \{\mathcal{Q} | \mathcal{Q} \gg \mathcal{P} \text{ for at least one } \mathcal{P} \in S\}.$$

Not all these definitions are needed in the following discussion; but the literature on global methods uses these concepts so extensively that the reader should be familiar with them.

Focus attention on a specific spacetime manifold, and in that manifold select out a specific asymptotically flat region. [In the external field of a star, there is but one asymptotically flat region. In the vacuum Schwarzschild geometry without source (Figure 34.3), there are two. In the Reissner-Nordstrøm geometry without source (Figure 34.4), there are infinitely many different asymptotically flat regions.] The selected asymptotically flat region (“external universe”) has one future timelike infinity I^+ , one past timelike infinity I^- , one spacelike infinity I^0 , one future null infinity \mathcal{I}^+ , and one past null infinity \mathcal{I}^- . It may also possess black holes, which form by stellar collapse, and which collide, coalesce, accrete matter, and generally wreak havoc in their immediate vicinities. The surfaces of all black holes (“future horizons”) separate the external universe, which can send signals out to \mathcal{I}^+ , from the black-hole interiors, which cannot. One thus has the definition:

Definition: The *totality (or “union”) of all future horizons* (surfaces of all black holes) is the region $J^-(\mathcal{I}^+)$ —i.e., it is the boundary of the domain $J^-(\mathcal{I}^+)$ that can send future-directed causal curves out to future null infinity.

Definition: surfaces of black holes; future horizons— $J^-(\mathcal{I}^+)$

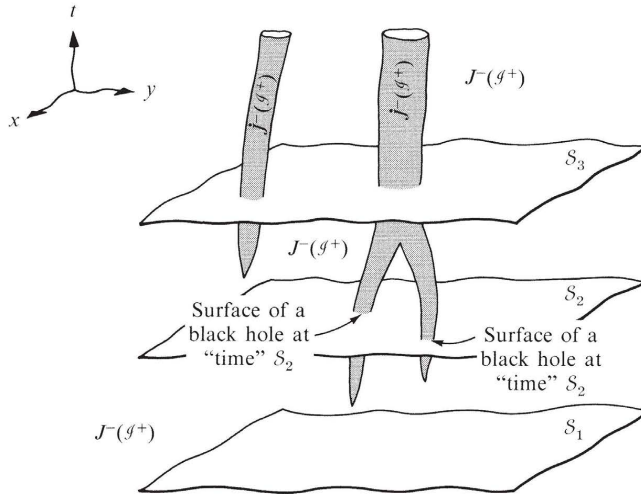


Figure 34.6.

Black holes in an asymptotically flat spacetime (schematic spacetime diagram). $J^-(\mathcal{I}^+)$ is the “external universe”—i.e., the region which can send causal curves to future null infinity. $\hat{J}^-(\mathcal{I}^+)$, the greyish region, is the boundary of the “external universe”—i.e., it is the union of all future horizons. At the “time” of spacelike slice S_1 , there are no black holes in the universe. Between S_1 and S_2 , two stars collapse to form black holes. The two closed 2-surfaces, in which S_2 intersects $\hat{J}^-(\mathcal{I}^+)$ are the horizons of those black holes at “time” S_2 . Between S_2 and S_3 , the two original black holes collide and coalesce, while a third black hole is being formed by stellar collapse.

[Similarly, one can define the totality of all past horizons to be $\hat{J}^+(\mathcal{I}^-)$. But past horizons are of little interest for astrophysics. Whereas gravitational collapse produces future horizons in a quite natural manner, past horizons must be primordial in origin—i.e., they must be postulated as initial structure in the origin of the universe [Novikov (1964), Ne’eman (1965)]. There is no good reason to believe that the universe began with or should have begun with such strange initial structure.]

Any given spacelike slice S through spacetime will intersect $\hat{J}^-(\mathcal{I}^+)$ in a number of disjoint, closed, two-dimensional surfaces. Each such 2-surface is the horizon of a single black hole at the “moment of time” S . See Figure 34.6.

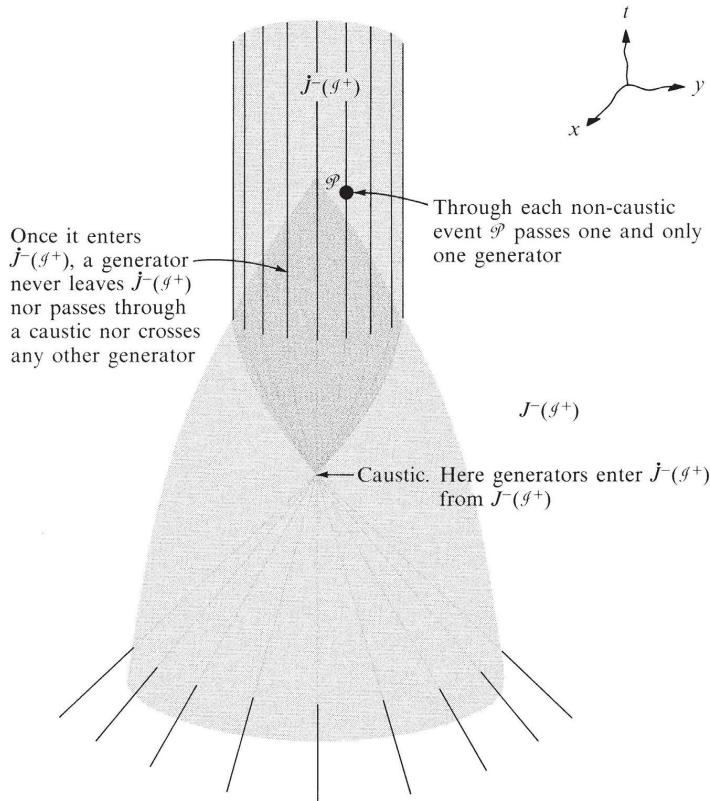
§34.4. GLOBAL STRUCTURE OF HORIZONS

The union of all future horizons, $\hat{J}^-(\mathcal{I}^+)$, has an especially simple global geometric structure, as follows.

Penrose’s theorem on the structure of $\hat{J}^-(\mathcal{I}^+)$ (future horizons)

THEOREM [Penrose (1968a)]: $\hat{J}^-(\mathcal{I}^+)$ is generated by null geodesics that have no future end points. Stated more precisely (see Figure 34.7):

- (1) Definition: The “generators” of $\hat{J}^-(\mathcal{I}^+)$ are null geodesics which (at least for some finite lapse of affine parameter) lie in $\hat{J}^-(\mathcal{I}^+)$.

**Figure 34.7.**

The future horizon $J^-(\mathcal{I}^+)$ produced by the spherical gravitational collapse of a star. This horizon illustrates the global geometric structure of $J^-(\mathcal{I}^+)$ as spelled out in Penrose's theorem (§34.4 of text). In this special case, there is only one caustic. In general there will be many.

- (2) Theorem: When followed into the past, a generator may (but does not have to!) leave $J^-(\mathcal{I}^+)$. Each event at which a generator leaves is called a “caustic” of $J^-(\mathcal{I}^+)$. When a generator leaves, it goes into $J^-(\mathcal{I}^+)$.
- (3) Once a generator, being followed into the future, enters $J^-(\mathcal{I}^+)$ from $J^-(\mathcal{I}^+)$ at a caustic, it can never thereafter leave $J^-(\mathcal{I}^+)$, nor can it ever intersect another generator. [Generators can intersect only at the “caustics,” where they enter $J^-(\mathcal{I}^+)$.]
- (4) Through each noncaustic event of $J^-(\mathcal{I}^+)$ there passes one and (aside from normalization of affine parameter) only one generator.

This theorem is proved in Box 34.1.

For a Schwarzschild black hole, the generators of $J^-(\mathcal{I}^+)$ are the world lines of radially outgoing photons at the gravitational radius [$r = 2M$, θ and ϕ constant,

$u = +v$; dotted line on horizon in Figure 32.1(c)]. For a Kerr-Newman black hole, the generators of $\hat{J}^-(\mathcal{I}^+)$ are the “barber-pole-twist” null geodesics of Box 33.2(F)—i.e., they are those members of the outgoing principal null congruence that lie on the horizon, $r = r_+$ (§33.6; exercise 33.9). But the theorem is more general. It refers to any black hole—dynamic or static; accreting matter, or coalescing with a neighboring black hole, or existing alone in isolation—in any time-oriented, asymptotically flat spacetime.

(continued on page 931)

Box 34.1 HORIZONS ARE GENERATED BY NONTERMINATING NULL GEODESICS (Penrose 1968a)

A. *Lemma:* If (1) $\mathcal{C}_1(\lambda)$ is a causal, future-directed curve from event \mathcal{P} to event \mathcal{Q} , (2) $\mathcal{C}_2(\lambda)$ is a causal, future-directed curve from event \mathcal{Q} to event \mathcal{R} , and (3) $\mathcal{P} \ll \mathcal{R}$ (\mathcal{P} is not in the past of \mathcal{R}), then \mathcal{C}_1 and \mathcal{C}_2 are null geodesics, and their tangent vectors coincide (aside from normalization) at event \mathcal{Q} .

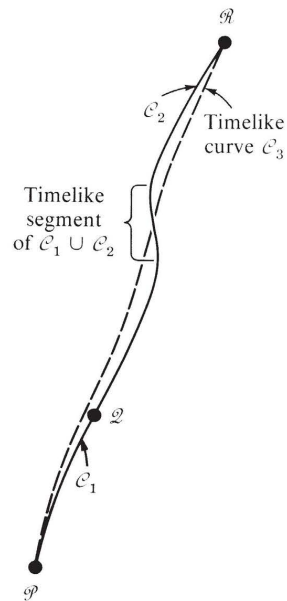
Proof:*

1. Suppose that \mathcal{C}_1 were not a null geodesic, or \mathcal{C}_2 were not a null geodesic, or both. Then somewhere along $\mathcal{C}_1 \cup \mathcal{C}_2$ there would be a timelike segment, or a nongeodesic null segment, or both.
 - a. If $\mathcal{C}_1 \cup \mathcal{C}_2$ contained a timelike segment, then a slight deformation[†] of $\mathcal{C}_1 \cup \mathcal{C}_2$ would produce a smooth curve \mathcal{C}_3 from \mathcal{P} to \mathcal{R} which is everywhere timelike[‡]—contradicting the assumption $\mathcal{P} \ll \mathcal{R}$.

*The proof utilizes some elementary concepts of point-set topology; see, e.g., Wallace (1963) or Kelley (1955).

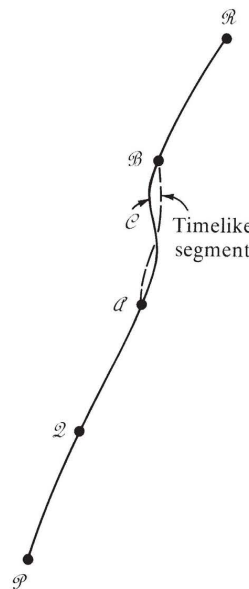
[†]One can always deform any curve in any spacetime manifold by a small amount in any direction one wishes, without running into singularities or into other boundaries of the manifold. This is possible because a manifold by definition is *open*. In physical terms, spacetime is open because each event in spacetime must possess a local Lorentz neighborhood which also lies in spacetime.

[‡]One can convince oneself of this, and of similar claims made later in the proof, by arguments using local Lorentz frames. In the literature on global geometry, claims such as this are rarely substantiated—though each author is always convinced that he could do so if forced to by a skeptic. Unfortunately, to substantiate such claims with rigorous arguments would lengthen and complicate the discussion enormously and would tend to obscure the simplicity of the underlying ideas.

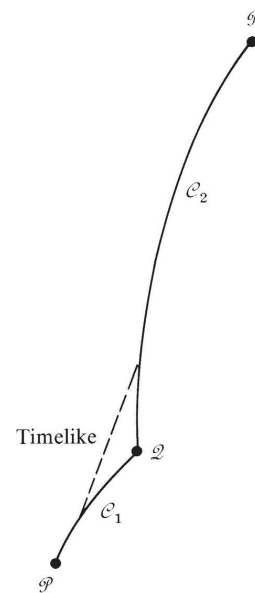


- b. If $\mathcal{C}_1 \cup \mathcal{C}_2$ contained a nongeodesic null segment \mathcal{C} reaching from event \mathcal{A} to event \mathcal{B} , then, when compared to neighboring curves between \mathcal{A} and \mathcal{B} , \mathcal{C} would not have stationary length. This means that some curves from \mathcal{A} to \mathcal{B} would have larger squared length—i.e., would be spacelike—while others would have smaller squared length—i.e., would be timelike. Thus, a slight deformation of \mathcal{C} would produce a timelike segment from \mathcal{A} to \mathcal{B} . Then a further deformation of $\mathcal{C}_1 \cup \mathcal{C}_2$, as described in (a) above, would produce a smooth timelike curve from \mathcal{P} to \mathcal{R} , contradicting $\mathcal{P} \ll \mathcal{R}$.

Thus, the supposition is wrong; i.e., both \mathcal{C}_1 and \mathcal{C}_2 must be null geodesics.



2. Suppose that the tangent vectors of \mathcal{C}_1 and \mathcal{C}_2 did not agree at their join point, \mathcal{Q} . Then one could “round off the corner” at \mathcal{Q} , producing a timelike segment there. One could then further deform $\mathcal{C}_1 \cup \mathcal{C}_2$ as in (1a) above, to produce a smooth timelike curve from \mathcal{P} to \mathcal{R} —contradicting $\mathcal{P} \ll \mathcal{R}$. Thus, the supposition is wrong; i.e., the tangent vectors must agree at \mathcal{Q} . Q.E.D.



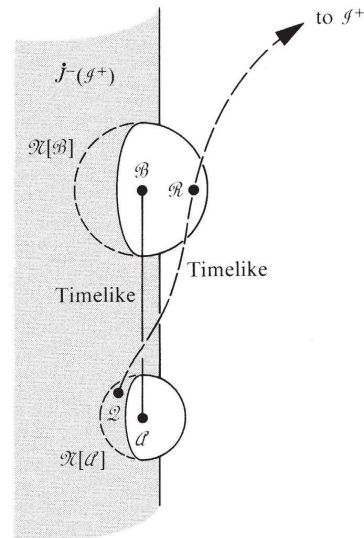
Box 34.1 (continued)

B. *Lemma:* If $\mathcal{A} \in J^-(\mathcal{I}^+)$ and $\mathcal{B} \in J^-(\mathcal{I}^+)$, then $\mathcal{A} \ll \mathcal{B}$.

Proof: Assume $\mathcal{A} \ll \mathcal{B}$.

1. Then there exists a timelike curve from \mathcal{A} to \mathcal{B} .
2. A slight deformation of that curve which keeps it still timelike will make it link an arbitrary event \mathcal{Q} in some sufficiently small neighborhood $\mathcal{N}[\mathcal{A}]$ to an arbitrary event \mathcal{R} in some small $\mathcal{N}[\mathcal{B}]$.
3. Pick \mathcal{R} to lie in $J^-(\mathcal{I}^+)$. Then join the timelike curve from \mathcal{Q} to \mathcal{R} onto a causal curve from \mathcal{R} to \mathcal{I}^+ . The resulting curve, when smoothed in a neighborhood of the join, becomes a causal curve from any arbitrary $\mathcal{Q} \in \mathcal{N}[\mathcal{A}]$ to \mathcal{I}^+ .
4. The existence of such curves implies that $\mathcal{N}[\mathcal{A}] \subset J^-(\mathcal{I}^+)$, and hence that $\mathcal{A} \notin J^-(\mathcal{I}^+)$ —in contradiction to the original hypotheses.

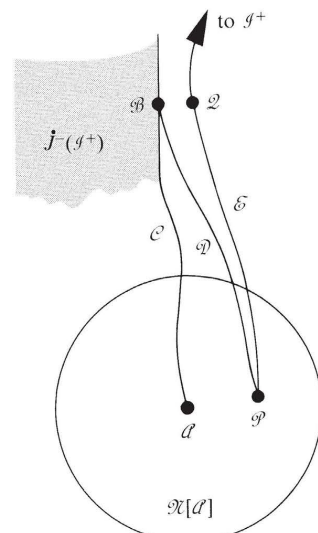
Conclusion: $\mathcal{A} \ll \mathcal{B}$. Q.E.D.



C. *Lemma:* Let $\mathcal{C}(\lambda)$ be a causal curve that intersects $J^-(\mathcal{I}^+)$ at some event \mathcal{B} . Then when followed into the past from \mathcal{B} , $\mathcal{C}(\lambda)$ forever lies in $J^-(\mathcal{I}^+) \cup J^-(\mathcal{I}^+)$.

Proof:

1. Pick an arbitrary event \mathcal{A} on $\mathcal{C}(\lambda)$, with $\mathcal{A} \prec \mathcal{B}$.
2. Construct an arbitrarily small neighborhood $\mathcal{N}[\mathcal{A}]$.
3. A small deformation of \mathcal{C} , between \mathcal{A} and \mathcal{B} , produces a timelike curve \mathcal{D} from some event $\mathcal{P} \in \mathcal{N}[\mathcal{A}]$ to \mathcal{B} .
4. Since $\mathcal{B} \in J^-(\mathcal{I}^+)$, a slight deformation of \mathcal{D} , keeping it still timelike, produces a curve \mathcal{E} from \mathcal{P} to some event $\mathcal{Q} \in J^-(\mathcal{I}^+)$. \mathcal{E} can then be prolonged, remaining causal, until it reaches \mathcal{I}^+ . The result is a causal curve from \mathcal{P} to \mathcal{I}^+ . Hence, $\mathcal{P} \in J^-(\mathcal{I}^+)$.
5. But \mathcal{P} was in an arbitrarily small neighborhood $\mathcal{N}[\mathcal{A}]$. Hence, \mathcal{A} must also be in $J^-(\mathcal{I}^+)$ or else in its boundary, $J^-(\mathcal{I}^+)$. Q.E.D.

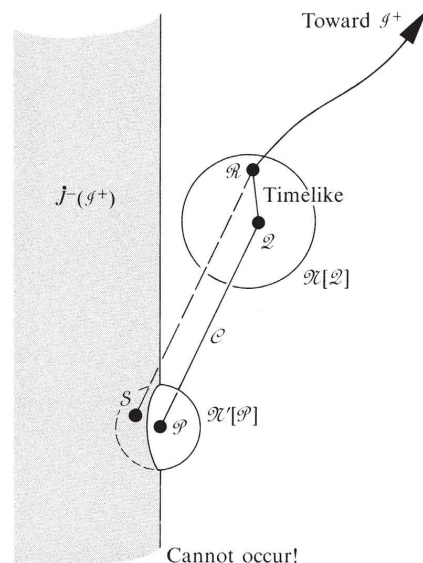
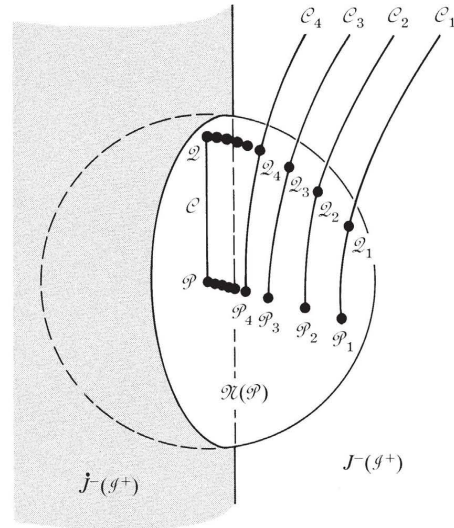


D. *Theorem [Penrose (1968a)]:* $\dot{J}^-(\mathcal{I}^+)$ is generated by null geodesics which have no future endpoints. [See text of §34.4 for more detailed statement of theorem.]

Proof:

1. Pick an arbitrary event \mathcal{P} in $\dot{J}^-(\mathcal{I}^+)$. Prove as follows that through \mathcal{P} there passes a future-directed null geodesic which lies in $\dot{J}^-(\mathcal{I}^+)$:
 - a. Construct an arbitrary neighborhood $\mathcal{N}[\mathcal{P}]$. [If $\dot{J}^-(\mathcal{I}^+)$ happens somewhere to encounter a singularity of spacetime, then $\mathcal{N}[\mathcal{P}]$ must be chosen small enough to keep the singularity outside it.]
 - b. In $\mathcal{N}[\mathcal{P}] \cap J^-(\mathcal{I}^+)$, construct a sequence of events $\{\mathcal{P}_i\}$ which converges to the event \mathcal{P} .
 - c. For each i , construct a causal curve \mathcal{C}_i extending from \mathcal{P}_i to \mathcal{I}^+ .
 - d. Let \mathcal{Q}_i be the intersection of \mathcal{C}_i with $\mathcal{N}[\mathcal{P}]$, the boundary of $\mathcal{N}[\mathcal{P}]$. Since $\mathcal{N}[\mathcal{P}]$ is a compact set, the sequence \mathcal{Q}_i must have a limit point, \mathcal{Q} .
 - e. Because there exist causal curves from events \mathcal{P}_i arbitrarily near \mathcal{P} to events \mathcal{Q}_i arbitrarily near \mathcal{Q} , there must be a causal curve from \mathcal{P} to \mathcal{Q} . Call that curve \mathcal{C} .
 - f. Since \mathcal{Q} is a limit point of a sequence of events in $J^-(\mathcal{I}^+)$, \mathcal{Q} either lies in $J^-(\mathcal{I}^+)$, or else lies on its boundary $\dot{J}^-(\mathcal{I}^+)$, or both. Suppose $\mathcal{Q} \notin \dot{J}^-(\mathcal{I}^+)$.
 - i. Then some small neighborhood $\mathcal{N}[\mathcal{Q}]$ is contained entirely in $J^-(\mathcal{I}^+)$.
 - ii. Construct a causal curve from \mathcal{P} to \mathcal{I}^+ by going from \mathcal{P} to \mathcal{Q} along the causal curve \mathcal{C} , then from \mathcal{Q} along a timelike curve to some event $\mathcal{R} \in \mathcal{N}[\mathcal{Q}]$, and then from \mathcal{R} to \mathcal{I}^+ along a causal curve—and by smoothing at the join points \mathcal{Q} and \mathcal{R} .
 - iii. Since this curve from \mathcal{P} to \mathcal{I}^+ has a timelike segment, it can be deformed smoothly, while being kept causal, so that it reaches any desired event \mathcal{S} in some small neighborhood $\mathcal{N}[\mathcal{P}]$. But this means that $\mathcal{N}[\mathcal{P}] \subset J^-(\mathcal{I}^+)$, hence that $\mathcal{P} \notin \dot{J}^-(\mathcal{I}^+)$ —which contradicts the original definition of \mathcal{P} .

Conclusion: $\mathcal{Q} \in \dot{J}^-(\mathcal{I}^+)$.



Box 34.1 (continued)

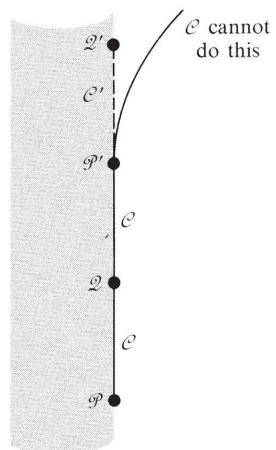
- g. By Lemma B, since $\mathcal{P} \in J^-(\mathcal{I}^+)$ and $\mathcal{Q} \in J^-(\mathcal{I}^+)$, then $\mathcal{P} \ll \mathcal{Q}$. But \mathcal{C} is a future-directed causal curve from \mathcal{P} to \mathcal{Q} . Consequently, by Lemma A, \mathcal{C} is a null geodesic.
- h. Since the curve \mathcal{C} intersects $J^-(\mathcal{I}^+)$ at \mathcal{Q} , between \mathcal{P} and \mathcal{Q} it must everywhere lie in $J^-(\mathcal{I}^+) \cup J^+(\mathcal{I}^+)$ [Lemma C]. Apply the reasoning of (f) above, with \mathcal{Q} replaced by an arbitrary point on \mathcal{C} between \mathcal{P} and \mathcal{Q} . Thereby conclude that, everywhere between \mathcal{P} and \mathcal{Q} , \mathcal{C} lies in $J^-(\mathcal{I}^+)$.

Summary: Through every event $\mathcal{P} \in J^-(\mathcal{I}^+)$ there passes a null geodesic \mathcal{C} which, when followed into the future from \mathcal{P} , lies in $J^-(\mathcal{I}^+)$. This null geodesic is called a “generator” of $J^-(\mathcal{I}^+)$.

2. Follow the generator \mathcal{C} from \mathcal{P} to \mathcal{Q} and then onward still further. Can it ever leave $J^-(\mathcal{I}^+)$? No! For suppose it did leave, at some event $\mathcal{P}' \in J^-(\mathcal{I}^+)$.
 - a. Repeat the entire construction of step 1, with \mathcal{P}' replacing \mathcal{P} , to conclude that there is a null geodesic $\mathcal{C}' \subset J^-(\mathcal{I}^+)$ extending into the causal future from \mathcal{P}' to some event \mathcal{Q}' .
 - b. By Lemma B, since $\mathcal{P} \in J^-(\mathcal{I}^+)$ and $\mathcal{Q}' \in J^-(\mathcal{I}^+)$, $\mathcal{P} \ll \mathcal{Q}'$.
 - c. Then by Lemma A the null geodesic \mathcal{C} from \mathcal{P} to \mathcal{P}' and the null geodesic \mathcal{C}' from \mathcal{P}' to \mathcal{Q}' have tangents that coincide at \mathcal{P}' (aside from normalization). Thus, with a renormalization of affine parameter, \mathcal{C}' becomes the prolongation of \mathcal{C} —which means that \mathcal{C} does not leave $J^-(\mathcal{I}^+)$ at \mathcal{P}' .

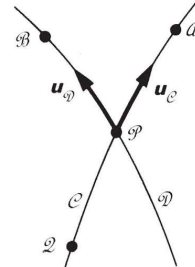
Conclusion: Once a generator, being followed into the future, enters $J^-(\mathcal{I}^+)$, it can never thereafter leave $J^-(\mathcal{I}^+)$.

3. Figure 34.7 provides an example of how a null geodesic, being following into the future, can enter $J^-(\mathcal{I}^+)$ and become a generator. Lemma C guarantees that, when a null geodesic enters $J^-(\mathcal{I}^+)$, it enters from $J^-(\mathcal{I}^+)$.



4. As indicated by the example of Fig. 34.7, at a “caustic” [entry point of generators onto $J^-(\mathcal{I}^+)$] generators can cross each other. Follow a generator \mathcal{C} to the causal future from its entry point onto $J^-(\mathcal{I}^+)$. Can it ever again cross another generator? No. For suppose that at an event \mathcal{P} the generator \mathcal{C} were to cross another generator \mathcal{D} .
- To the causal future of \mathcal{P} , both generators always lie in $J^-(\mathcal{I}^+)$. Thus, events \mathcal{A} and \mathcal{B} of the picture are in $J^-(\mathcal{I}^+)$.
 - Since \mathcal{P} is to the causal future of the caustic where \mathcal{C} enters $J^-(\mathcal{I}^+)$, there exists an event $\mathcal{Q} \in J^-(\mathcal{I}^+) \cap \mathcal{C}$ to the causal past of \mathcal{P} .
 - Since $\mathcal{Q} \in J^-(\mathcal{I}^+)$ and $\mathcal{B} \in J^-(\mathcal{I}^+)$, $\mathcal{Q} \ll \mathcal{B}$ [Lemma B].
 - Lemma A, applied to the curves \mathcal{C} from \mathcal{Q} to \mathcal{P} , and \mathcal{D} from \mathcal{P} to \mathcal{B} , then guarantees that the tangent vectors $\mathbf{u}_\mathcal{C}$ and $\mathbf{u}_\mathcal{D}$ coincide at \mathcal{P} (aside from normalization), and that therefore (aside from normalization) the geodesics \mathcal{C} and \mathcal{D} are identical. This contradicts the supposition that \mathcal{C} and \mathcal{D} are different generators which cross at \mathcal{P} .

Conclusion: Once a generator has entered $J^-(\mathcal{I}^+)$, it can never thereafter cross any other generator.

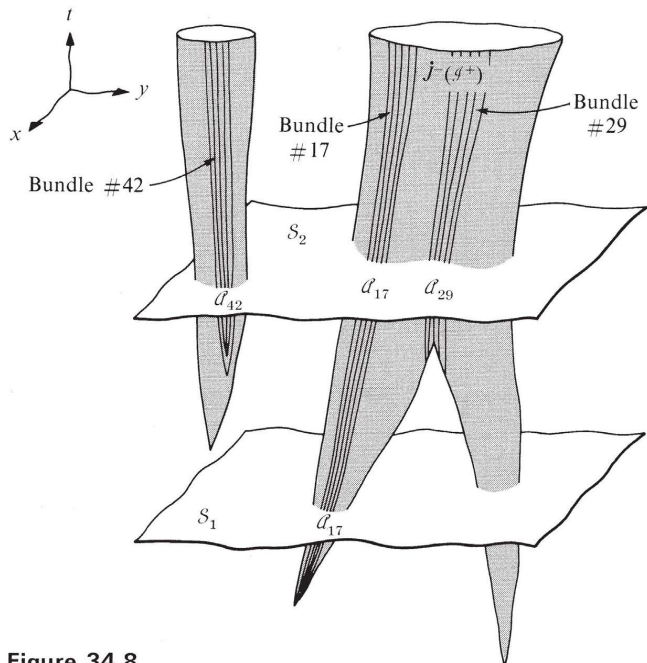


§34.5. PROOF OF SECOND LAW OF BLACK-HOLE DYNAMICS [Hawking (1971b, 1972a, 1973)]

All the tools are now in hand for a proof of the second law of black-hole dynamics.

Consider the union of all future horizons, $J^-(\mathcal{I}^+)$, in an asymptotically flat space-time, as depicted in Figure 34.8. Divide up the null-geodesic generators of $J^-(\mathcal{I}^+)$ into a large number of infinitesimal bundles, and give each bundle an identifying number, K . As one moves from past toward future along $J^-(\mathcal{I}^+)$, one occasionally sees new bundles of generators created in “caustics” of the 3-surface $J^-(\mathcal{I}^+)$. The caustic sources of new generators are created by such processes as the infall of matter through the horizon (example: bundle #42 in Figure 34.8), and the collision and coalescence of two black holes (example: bundle #29). But each bundle, once created, can never be destroyed (no termination of null generators as one moves from past toward future).

Proof of second law of black-hole dynamics:

**Figure 34.8.**

Schematic spacetime diagram used in proving the second law of black-hole dynamics. See text for details of the proof, and see Figure 34.6 for physical interpretation of the diagram.

Focus attention on a specific bundle of generators—bundle $\# K$. At a specific event \mathcal{P} along that bundle, let various observers, moving with various velocities, measure its (two-dimensional) cross-sectional area $\alpha_K(\mathcal{P})$. As shown in Figure 22.1, exercise 22.13, and exercise 22.14: (1) the cross-sectional area $\alpha_K(\mathcal{P})$ is independent of the velocity of the observer who measures it—i.e., $\alpha_K(\mathcal{P})$ depends only on location \mathcal{P} along the bundle; and (2) α_K changes from event to event along the bundle in a manner governed by the “focusing theorem”

$$\frac{d^2\alpha_K^{1/2}}{d\lambda_K^2} \leq 0 \quad \begin{array}{l} \text{if the energy density } T_{\hat{0}\hat{0}}, \text{ as measured} \\ \text{by all observers along the bundle, is} \\ \text{nonnegative.} \end{array} \quad (34.6)$$

Proof assumes nonnegative energy density

Here λ_K is affine parameter along the bundle. *Assume*—in accord with all physical experience and the best assessments of modern physics—that energy density $T_{\hat{0}\hat{0}}$ can never be negative. (This assumption underlies the second law of black-hole dynamics. If it were ever found to be invalid, then one would have to abandon the second law.)

Suppose that $d\alpha_K^{1/2}/d\lambda_K$ were negative at some event \mathcal{P} along the bundle. Then, according to the focusing theorem, $d\alpha_K^{1/2}/d\lambda_K$ would always remain at least as

negative as its value at \mathcal{P} —and, hence, after a lapse of affine parameter given by

$$\Delta\lambda_K \leq \left(\frac{\mathcal{A}_K^{1/2}}{-d\mathcal{A}_K^{1/2}/d\lambda_K} \right)_{\text{at } \mathcal{P}}, \quad (34.7)$$

$\mathcal{A}_K^{1/2}$ would go to zero. At the point where $\mathcal{A}_K^{1/2}$ reaches zero, adjacent null geodesics in the bundle cross each other, giving rise to events in $J^-(\mathcal{I}^+)$ through which pass more than one null geodesic generator. But this violates Penrose's theorem on the global structure of horizons (§34.4).

Thus either the supposition of negative $d\mathcal{A}_K^{1/2}/d\lambda_K$ is wrong; or else $d\mathcal{A}_K^{1/2}/d\lambda_K$ goes negative, but then, before the generators get a chance to cross [before the finite lapse (34.7) of affine parameter], the generators hit a singularity and cease to exist. *To prove the second law of black-hole dynamics, one must assume that no singularity is hit by the horizon, and thereby conclude that $d\mathcal{A}_K^{1/2}/d\lambda_K$ never goes negative.* Hawking (1971b, 1972a) makes an alternative assumption which implies $d\mathcal{A}_K^{1/2}/d\lambda_K \geq 0$: Hawking assumes that spacetime is “future asymptotically predictable.” In essence this means that spacetime possesses no “naked singularities”—i.e., no singularities visible from \mathcal{I}^+ . (Naked singularities could influence the evolution of the external universe; and, therefore, unless one knew the laws of physics governing singularities—which one does not—they would prevent one from predicting the future in the external universe.)

Under either assumption (no naked singularities; or horizon never hits a singularity), one concludes that

$$d\mathcal{A}_K^{1/2}/d\lambda_K \text{ is nonnegative everywhere along bundle } K. \quad (34.8)$$

This result says that the cross-sectional area \mathcal{A}_K of each bundle can never decrease as one moves toward the future along $J^-(\mathcal{I}^+)$. Since new bundles can be created, but old ones can never be destroyed as one moves toward the future, *the total cross-sectional area of $J^-(\mathcal{I}^+)$ cannot decrease toward the future*. Equivalently, (see Figure 34.8), if \mathcal{S}_1 and \mathcal{S}_2 are spacelike hypersurfaces with \mathcal{S}_2 everywhere to the future of \mathcal{S}_1 , then the cross-sectional area of $J^-(\mathcal{I}^+)$ at its intersection with \mathcal{S}_2 , $\mathcal{A}(\mathcal{S}_2)$, cannot be less than the cross-sectional area at \mathcal{S}_1 , $\mathcal{A}(\mathcal{S}_1)$. This is the second law of black-hole dynamics, reformulated in more precise language than that of Chapter 33, and finally proved.

Proof assumes that horizon never hits a singularity (no naked singularities)

Precise formulation of second law

Exercise 34.4. A BLACK HOLE CAN NEVER BIFURCATE [Hawking (1972a)]

Make plausible the theorem that no matter how hard one “zaps” a black hole, and no matter what one “zaps” it with, one can never make it bifurcate into two black holes. [Hint: By drawing pictures, make it plausible that, at any bifurcation point, some null geodesic generators of $J^-(\mathcal{I}^+)$ must leave $J^-(\mathcal{I}^+)$ as one follows them into the *future*—in violation of Penrose’s theorem (§34.4). Assume that the surface of each hole is topologically a 2-sphere. Note: The same argument, time-reversed, shows that if two black holes coalesce, generators enter $J^-(\mathcal{I}^+)$ from $J^-(\mathcal{I}^+)$ at the coalescence point; and the surface area of the horizon increases.]

EXERCISE

§34.6. THEOREMS ON SINGULARITIES, AND THE “ISSUE OF THE FINAL STATE”

Overview of theorems on singularities

Just as global techniques are powerful tools in the analysis of horizons, so they also are powerful in the analysis of spacetime singularities. In fact, it was the proof of Penrose's (1965b) pioneering theorem on singularities that gave birth to global techniques for studying spacetime.

For a detailed introduction to the global analysis of singularities, one can read the book of Hawking and Ellis (1973). Now that the reader has had a taste of global techniques, attention here will focus on a qualitative description of results:

How does gravitational collapse terminate? Is the singularity at the end point of spherical collapse typical, or can asymmetries remove it? That singularities are very general phenomena, and cannot be wished away, has been known since 1965, thanks to theorems on singularities proved by Penrose, Hawking, and Geroch. [For a full list of references, see Hawking and Penrose (1969) or Hawking and Ellis (1973).]

Singularity defined

Before examining the theorems on singularities, one must make precise the concept of a *singularity*. This is not easy, as Geroch (1968) has emphasized in a long treatise on the wide variety of pathologies that can occur in spacetime manifolds. However, after vigorous efforts by many people, Schmidt (1970) finally produced a definition that appears to be satisfactory. Put in heuristic terms, Schmidt's highly technical definition goes something like this. In a spacetime manifold, consider all spacelike geodesics (paths of “tachyons”), all null geodesics (paths of photons), all timelike geodesics (paths of freely falling observers), and all timelike curves with bounded acceleration (paths along which observers are able, in principle, to move). Suppose that one of these curves terminates after the lapse of finite proper length (or finite affine parameter in the null-geodesic case). Suppose, further, that it is impossible to extend the spacetime manifold beyond that termination point—e.g., because of infinite curvature there. Then that termination point, together with all adjacent termination points, is called a “singularity.” (What could be more singular than the cessation of existence for the poor tachyon, photon, or observer who moves along the terminated curve?)

Trapped surface defined

Another concept needed in the singularity theorems is that of a *trapped surface*. This concept, devised by Penrose (1965b), is motivated by a close examination of the two-dimensional, spherical surfaces $(r, t) = \text{const.}$ inside the horizon of the Schwarzschild geometry. These surfaces signal the nearness of a singularity ($r = 0$) by this property: light rays emitted from one of these surfaces in the perpendicular outward direction (i.e., outgoing, orthogonal, null geodesics) converge toward each other as they propagate; and inward light rays perpendicular to the 2-surface also converge. Penrose gives the name “trapped surface” to any closed 2-surface, spherical or not, that has this property. In Schwarzschild spacetime, the convergence of light rays, both outgoing and ingoing, can be attributed to the “intense pull of gravity,” which sucks the photons into the singularity. That this might also be true in asymmetric spacetimes is suggested by the Hawking-Penrose (1969) theorem [the most powerful of a wide class; see Hawking and Penrose (1969) for references to others; and see Boxes 34.2 and 34.3 for introductions to Hawking and Penrose]:

A spacetime M necessarily contains incomplete, inextendable timelike or null geodesics (and is thus singular in the Schmidt sense) if, in addition to Einstein's equations, the following four conditions hold: (1) M contains no closed timelike curves (reasonable causality condition); (2) at each event in M and for each unit timelike vector \mathbf{u} , the stress-energy tensor satisfies

$$\left(T_{\alpha\beta} - \frac{1}{2} g_{\alpha\beta} T \right) u^\alpha u^\beta \geq 0$$

(reasonable energy condition); (3) the manifold is “general” (i.e., not too highly symmetric) in the sense that every timelike or null geodesic with unit tangent \mathbf{u} passes through at least one event where the curvature is not lined up with it in a specific way:

$$u_{[\alpha} R_{\beta]\gamma\delta[\epsilon} u_{\rho]} u^\gamma u^\delta \neq 0 \text{ at some point on the geodesic.}$$

(4) the manifold contains a trapped surface.

All these conditions, except the trapped surface, seem eminently reasonable for any physically realistic spacetime! Note, especially, that the energy condition can be violated only if, as measured by some local observer in his proper frame, the total energy density E is negative or the principal pressures (eigenvalues of stress tensor) P_i are so negative that

$$\sum_i P_i < -E.$$

The relevance of the Hawking-Penrose theorem for collapse follows from the general expectation that, in the real universe, trapped surfaces will always exist just below all future horizons, $J^-(\mathcal{I}^+)$. (Exceptions, such as the Kerr metric with $a = M$, are probably a “set of measure zero.”) Since horizons and accompanying trapped surfaces are necessarily produced by slightly nonspherical collapse (Box 32.2), and since they probably also result from moderately deformed collapse (§32.7), such collapse presumably produces singularities—or a violation of causality, which is also a rather singular occurrence!

If the singularities are really such a general feature of collapse, then the exact nature of the singularity is of life-and-death importance to anyone who falls through a horizon! Here one is on very shaky ground. Although the main results and conjectures described up to now in this section will probably survive all future research, opinions about the nature of the singularities are likely to change several times more before the whole story is in. Hence, it is safe only to describe the possibilities, not to attempt to judge them.

Possibility 1

The singularity at the endpoint of a realistic collapse is a region of infinite tidal gravitational forces (infinite curvature), which crushes the collapsing matter to infinite density. Examples: the very special, homogeneous crushing of the Oppenheimer-Snyder (1939) spherical collapse (§32.4); also the very special inhomogeneous but spherical crushing described by Podurets (1966); also the special inhomogeneous,

The Hawking-Penrose theorem on singularities

Relevance of the Hawking-Penrose theorem for gravitational collapse

The nature of the singularity at the endpoint of realistic collapse: 4 possibilities

(continued on page 940)

Box 34.2 ROGER PENROSE: Born August 8, 1931, Colchester, Essex, England

Roger Penrose started out as an algebraic geometer. However, while at Cambridge from 1952–55 and again from 1957–60, his interest in general relativity was aroused by Hermann Bondi and Dennis Sciama. Because of his pure mathematical background, his approach to the subject was different from those which had been adopted hitherto. He was particularly interested in the global light-cone structure of spacetime and in the equations of zero rest-mass fields, both of which are preserved under conformal transformations. He exploited this conformal invariance to give an elegant and powerful treatment of gravitational radiation in terms of a null surface \mathcal{I}^+ at infinity. More recently this interest has led him to develop the theory of twistors, which are the spinors corresponding to the conformal group of Minkowski space. These offer a new and very promising approach to the quantization of spacetime.

His interest in conformal geometry also led him to study the properties of the causality relationships between points of spacetime. These in turn led him to the theorems on the occurrence of sin-



gularities in spacetime, which are probably the most important predictions of general relativity, since they seem to imply that spacetime has a beginning or an end.

"If spacetime is considered from the point of view of its conformal structure only, points at infinity can be treated on the same basis as finite points"

[PENROSE, IN INFELD (1964)]

"The argument will be to show that the existence of a trapped surface implies—irrespective of symmetry—that singularities necessarily develop"

[PENROSE (1965b)]

"While the quantum effects of gravitation are normally thought to be significant only when curvatures approach 10^{33} cm^{-1} , all our local physics is based on the Poincaré group being a good approximation of a local symmetry group at dimensions greater than 10^{-13} cm . Thus, if curvatures ever even approach 10^{13} cm^{-1} , there can be little doubt but that extraordinary local effects are likely to take place"

[HAWKING AND PENROSE (1969)]

"We are thus presented with what is perhaps the most fundamental unanswered question of general-relativistic collapse theory, namely: does there exist a "cosmic censor" who forbids the appearance of naked singularities, clothing each one in an absolute event horizon?"

[PENROSE (1969)]

"Under normal circumstances, general relativity can, for practical purposes, remain remarkably apart—almost aloof—from the rest of physics. At a space-time singularity, the very reverse must surely be the case!"

"I do not believe that a real understanding of the nature of elementary particles can ever be achieved without a simultaneous deeper understanding of the nature of spacetime itself. But if we are concerned with a level of phenomena for which such an understanding is not necessary—and this will cover almost all of present-day physics—then the smooth manifold picture presents an (unreasonably!) excellent framework for the discussion of phenomena."

"The most important single lesson of relativity theory is, perhaps, that space and time are not concepts that can be considered independently of one another but must be combined together to give a four-dimensional picture of phenomena: the description in terms of spacetime"

[PENROSE (1968a)]

"If a formalism enables one to treat myriads of non-existent types of universe, then (effectively) it contains 'arbitrary parameters,' only special values of which will correspond to the world as it actually is. In the ordinary approach to spacetime as a pseudo-Riemannian differentiable manifold, the dimension of the manifold and the signature of the metric are two such arbitrary parameters."

"As we localize the position of a particle, it jumps essentially along the null cone. Other particles are produced, which leap backward and forward essentially along null directions, without apparent regard for continuity, heeding only the positions of the null cones themselves and "topology" only in the respect in which this term is applied to the structure of graphs"

[PENROSE (1966)]

"My own view is that ultimately physical laws should find their most natural expression in terms of essentially combinatorial principles, that is to say, in terms of finite processes such as counting or other basically simple manipulative procedures. Thus, in accordance with such a view, should emerge some form of discrete or combinatorial spacetime"

[PENROSE, IN KLAUDER (1972)]

"Complex numbers are . . . a very important constituent of the structure of physical laws. The twistor theory carries this further in suggesting that complex numbers may also be very basically involved in defining the nature of spacetime itself."

[PENROSE AND MACCALLUM (1973)]

"It is thus very tempting to believe that a link between spacetime curvature and quantum processes may be supplied by the use of twistors. Then, roughly speaking, it is the continual slight 'shifting' of the interpretations of the quantum (twistor) operators which results in the curvature of spacetime"

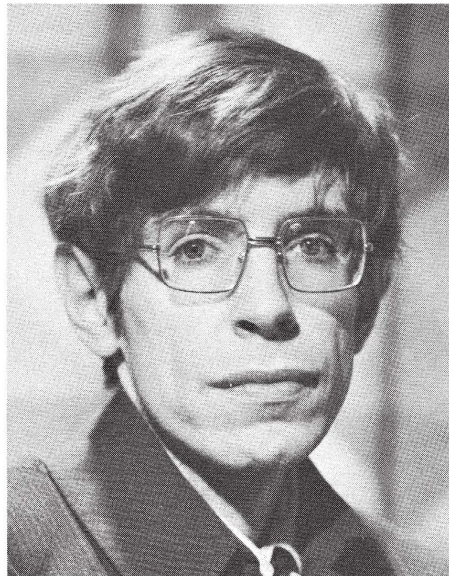
[PENROSE (1968b)]

Box 34.3 STEPHEN W. HAWKING: Born January 8, 1942, Oxford, England

As a research student of Dennis Sciama's in Cambridge, Stephen Hawking's early interest in relativity theory centered mainly on the question of spacetime singularities. With Ellis, he showed that a large class of homogeneous cosmological models must be singular. Then, encouraged by work of Penrose on the singularities arising in gravitational collapse, he developed new techniques which, in a series of papers in the Royal Society of London during 1966-67, established the important result that any plausible general-relativistic cosmology must be singular.

The major portion of his later research has been concerned with black holes. He devised a series of arguments of great ingenuity which, together with the work of Israel and Carter, established to all intents and purposes the result that (vacuum) black holes in general relativity are described by Kerr metrics, that topologies other than spherical cannot occur, and that a certain limit on the energy emitted when two black holes congeal into one must be satisfied.

Some of this work has had substantial pure mathematical interest (e.g., singularity theorems), some of it is concerned with astrophysics (e.g., work with Taylor on helium production in the big bang), some with observations (work with Gibbons on the possibility of black holes in binary star



systems) and even experimental developments (with Gibbons on gravitational-wave detectors). In such scope is exhibited not only a considerable insight, depth, and versatility, but also the gift of an extraordinary determination to overcome severe physical handicaps, to seek out and comprehend the truth.

"The observed isotropy of the microwave background indicates that the universe is rotating very little if at all. . . . This could possibly be regarded as an experimental verification of Mach's Principle"

[HAWKING (1969)]

"Undoubtedly, the most important results are the theorems . . . on the occurrence of singularities. These seem to imply either that the general theory of relativity breaks down or that there could be particles whose histories did not exist before (or after) a certain time. The author's own opinion is that the theory probably does break down but only when quantum gravitational effects become important."

"Although we have omitted the singular points from the definition of spacetime, we can still recognize the 'holes' left where they have been cut out by the existence of incomplete geodesics."

"A good physical theory should not only correctly describe the currently experimental knowledge, but should also predict new results which can be tested by experiment, the further the predictions from the original experiments, the greater the credit to the theory if they are found to be correct. Thus observations of whether or not singularities actually occurred, would provide a powerful test of the general theory of relativity in strong fields"

[HAWKING (1966a)]

"The construction of gravitational radiation detectors may open up a whole new field of 'gravitational astronomy' which could be as fruitful as radio astronomy has been in the last two decades. . . . Black hole collisions . . . would be much more effective in converting rest-mass energy into radiation than nuclear reactions, which can release only about 1 per cent of the rest-mass energy. In addition, black holes formed by collisions of smaller black holes can undergo further collisions, releasing more energy, whereas matter that has been fully processed by nuclear reactions cannot yield any more energy by the same means. . . . we are witnessing something really cataclysmic at the centre of our galaxy"

[HAWKING (1972b)]

"One might suggest that prior to the present expansion there was a collapsing phase. In this, local inhomogeneities grew large and isolated singularities occurred. Most of the matter avoided the singularities and reexpanded to give the present observed universe."

"It seems that we should draw a surface around regions where the radius of curvature is less than, say, 10^{-16} cm. On our side of this surface, a manifold picture of spacetime would be appropriate, but we have no idea what structure spacetime would have on the other side"

[HAWKING AND ELLIS (1968)]

"Presumably it would be necessary to consider quantum effects in very strong fields. However, these would not become important until the radius of curvature became of the order of 10^{-14} cm, which for practical purposes is pretty singular."

"The view has been expressed that singularities are so objectionable that if the Einstein equations were to predict their occurrence, this would be a compulsive reason for modifying them. However, the real test of a physical theory is not whether its predicted results are aesthetically attractive but whether they agree with observation. So far there are no observations which would show that singularities do not occur"

[HAWKING (1966b)]

"It is shown that a stationary black hole must have a topologically spherical boundary and must be axisymmetric if it is rotating. These results, together with those of Israel and Carter, go most of the way toward establishing the conjecture that any stationary black hole is a Kerr solution"

[HAWKING (1972a)]

"The fact that we have observed the universe to be isotropic is only a consequence of our existence."

[COLLINS AND HAWKING (1973)]

“Kasner-like” crushing of Lifschitz and Khalatnikov (1963a,b); also, most importantly, the very general “mixmaster” crushing (Chapter 30), discovered in the homogeneous case by Misner (1969b) and by Belinsky and Khalatnikov (1969a), and analyzed in the inhomogeneous case by Belinsky and Khalatnikov (1969b, 1970) and by Khalatnikov and Lifschitz (1970). The mixmaster singularities—and only they among all explicitly known singularities—appear to be generic in this sense: if one perturbs slightly but arbitrarily the initial conditions of a spacetime that evolves a mixmaster singularity, then the resultant perturbed spacetime will also evolve a mixmaster singularity. Because of this, the prevalent opinion today (1973) is that realistic collapse probably produces, inside the horizon, a mixmaster singularity. But that opinion might change tomorrow.

Possibility 2

The singularity is a region of spacetime in which timelike or null geodesics terminate, not because of infinite tidal gravitational forces or infinite crushing, but because of other, more subtle pathologies. Example: “Taub-NUT space” [see Misner and Taub (1968)]. For other examples created specially to exhibit various pathologies, see Geroch (1968).

Possibility 3

The singularity may be sufficiently limited in “size” and influence that all or most of the collapsing matter successfully avoids it. The matter cannot then explode back outward through the horizon that it went down; the horizon is a one-way membrane and will not let anything back out. Instead, the matter may reach a stage of maximum but finite contraction, and then reexplode into some other region of spacetime (multiply connected spacetime topology; “wormhole”). Analytical solutions for collapsing, charged spheres do reexplode in this manner [Novikov (1966); de la Cruz and Israel (1967); Bardeen (1968); see Figure 34.4]. Such a process requires that the “exploding” end of the wormhole be built into the initial conditions of the universe, with mass and angular momentum (as measured by Keplerian orbits and frame dragging) precisely equal to those that go down the black-hole end. This seems physically implausible. So does the “explosion.”

Other Possibilities

Various combinations of the above.

Will quantization of
spacetime save the universe
from singularities?

If, as one suspects today, the singularities are of a very physical, infinite-curvature type, then one must face up to John Wheeler’s (1964a) “issue of the final state” in its most raw and disturbing form. Wheeler, when faced with the issue, argues that infinite-curvature singularities signal a breakdown in classical general relativity—a breakdown forced by the onset of quantum gravitational phenomena (see Chapter 44). Whether quantization of gravity will actually save spacetime from such singularities one cannot know until the “fiery marriage of general relativity with quantum physics has been consummated” [Wheeler (1964a); see also Misner (1969c), and the last section of Box 30.1].

PART **VIII**

GRAVITATIONAL WAVES

*Wherein the reader voyages on stormy seas of curvature ripples,
searching for the ripple-generating storm gods, and battles
through an electromagnetic and thermal fog that allows only
uncertain visibility upon those seas.*

CHAPTER 35

PROPAGATION OF GRAVITATIONAL WAVES

Born: "*I should like to put to Herr Einstein a question, namely, how quickly the action of gravitation is propagated in your theory. That it happens with the speed of light does not elucidate it to me. There must be a very complicated connection between these ideas.*"

Einstein: "*It is extremely simple to write down the equations for the case when the perturbations that one introduces in the field are infinitely small. Then the g's differ only infinitesimally from those that would be present without the perturbation. The perturbations then propagate with the same velocity as light.*"

Born: "*But for great perturbations things are surely very complicated?*"

Einstein: "*Yes, it is a mathematically complicated problem. It is especially difficult to find exact solutions of the equations, as the equations are nonlinear.*"

Excerpts from discussion after Einstein's Fall 1913 lecture in Vienna on "The present position of the problem of gravitation," already two years before he had the final field equations [EINSTEIN, 1913a]

§35.1. VIEWPOINTS

Study one idealization after another. Build a catalog of idealizations, of their properties, of techniques for analyzing them. This is the only way to come to grips with so complicated a subject as general relativity!

Spherical symmetry is the idealization that has dominated most of the last 12 chapters. Together with the idealization of matter as a perfect fluid, and of the universe as homogeneous, it has yielded insight into stars, into cosmology, into gravitational collapse.

Turn attention now to an idealization of an entirely different type, one independent of any symmetry considerations at all: the idealization of a "gravitational wave."

Just as one identifies as "water waves" small ripples rolling across the ocean, so one gives the name "gravitational waves" to small ripples rolling across spacetime.

We are deeply indebted to Mr. James M. Nester, who found and corrected many errors in the equations of this chapter and of a dozen others throughout the book.

Gravitational waves
compared to water waves on
ocean:

(1) approximate nature of a wave

(2) local viewpoint vs. large-scale viewpoint

Ripples of what? Ripples in the shape of the ocean's surface; ripples in the shape (i.e., curvature) of spacetime. Both types of waves are idealizations. One cannot, with infinite accuracy, delineate at any moment which drops of water are in the waves and which are in the underlying ocean: Similarly, one cannot delineate precisely which parts of the spacetime curvature are in the ripples and which are in the cosmological background. But one can almost do so; otherwise one would not speak of "waves"!

Look at the ocean from a rowboat. Waves dominate the seascape. Changes in angle and level of the surface occur every 30 feet or less. These changes propagate. They obey a simple wave equation

$$\left(\frac{1}{g^2} \frac{\partial^4}{\partial t^4} + \frac{\partial^2}{\partial y^2} + \frac{\partial^2}{\partial x^2} \right) (\text{height of surface}) = 0.$$

Now get more sophisticated. Notice from a spaceship the large-scale curvature of the ocean's surface—curvature because the Earth is round, curvature because the sun and the moon pull on the water. As waves propagate long distances, this curvature bends their fronts and changes slightly their simple wave equation. Also important over large distance are nonlinear interactions between waves, interaction with the wind, Coriolis forces due to the Earth's rotation, etc.

Spacetime is similar. Propagating through the universe, according to Einstein's theory, must be a complex pattern of small-scale ripples in the spacetime curvature, ripples produced by binary stars, by supernovae, by gravitational collapse, by explosions in galactic nuclei. Locally ("rowboat viewpoint") one can ignore the interaction of these ripples with the large-scale curvature of spacetime and their nonlinear interaction with each other. One can pretend the waves propagate in flat spacetime; and one can write down a simple wave equation for them. But globally one cannot. The large-scale curvature due to quiescent stars and galaxies will produce redshifts and will deform wave fronts; and the energy carried by the waves themselves will help to produce the large-scale curvature. This chapter treats both viewpoints, the local (§§35.2–6), and the global (§§35.7–15).

§35.2. REVIEW OF "LINEARIZED THEORY" IN VACUUM

Linearized theory of gravitational waves:

Idealize, for awhile, the gravitational waves of our universe as propagating through flat, empty spacetime (local viewpoint). Then they can be analyzed using the "linearized theory of gravity," which was introduced in Chapter 18.

Linearized theory, one recalls, is a weak-field approximation to general relativity. The equations of linearized theory are written and solved as though spacetime were flat (special-relativity viewpoint); but the connection to experiment is made through the curved-space formalism of general relativity.

More specifically, linearized theory describes gravity by a symmetric, second-rank tensor field $\bar{h}_{\mu\nu}$. In the standard ("Lorentz," or Hilbert) gauge, this field satisfies the "gauge" or "subsidiary" conditions (coordinate conditions)

$$\bar{h}^{\mu\alpha}_{,\alpha} = 0. \quad (35.1a)$$

(1) Lorentz gauge condition

(Here, and throughout linearized theory, indices of $\bar{h}_{\mu\nu}$ are raised and lowered with the Minkowski metric $\eta_{\alpha\beta}$.) In this gauge the *propagation equations* for vacuum gravitational fields are the familiar wave equations

$$\square \bar{h}_{\mu\nu} \equiv \bar{h}_{\mu\nu,\alpha}{}^\alpha = 0. \quad (35.1b) \quad (2) \text{ propagation equation}$$

Spacetime is really curved in linearized theory, although equations (35.1) are written and solved as though it were not. The global inertial frames of equations (35.1) are only *almost* inertial. In them the metric components are actually

$$g_{\mu\nu} = \eta_{\mu\nu} + h_{\mu\nu} + O([h_{\mu\nu}]^2); \quad (35.2a)^* \quad (3) \text{ metric}$$

and the “metric perturbation” $h_{\mu\nu}$ is related to the “gravitational field” $\bar{h}_{\mu\nu}$ by

$$\begin{aligned} h_{\mu\nu} &= \bar{h}_{\mu\nu} - \frac{1}{2}\bar{h}\eta_{\mu\nu}, & \bar{h}_{\mu\nu} &= h_{\mu\nu} - \frac{1}{2}h\eta_{\mu\nu}, \\ h &\equiv h_\alpha{}^\alpha = -\bar{h} = -\bar{h}_\alpha{}^\alpha. \end{aligned} \quad (35.2b)$$

The metric (35.2a) governs the motion of test particles, the propagation of light, etc., in the usual general-relativistic manner.

Recall the origin of the equations (35.1) that govern $\bar{h}_{\mu\nu}$. The subsidiary conditions $\bar{h}_{\mu,\alpha}{}^\alpha = 0$ were imposed by specializing the coordinate system; and the Einstein field equations in vacuum then reduced to $\square \bar{h}_{\mu\nu} = 0$.

Actually, as was shown in Box 18.2, the coordinates of linearized theory are not fully fixed by the conditions $\bar{h}_{\mu,\alpha}{}^\alpha = 0$. There remains an ambiguity embodied in further “gauge changes” (infinitesimal coordinate transformations), ξ_μ , which satisfy a restrictive condition

$$\xi_{\mu,\alpha}{}^\alpha = 0 \quad (35.3a)$$

in order to preserve conditions (35.1a). Then

$$x^\mu_{\text{new}} = x^\mu_{\text{old}} + \xi^\mu \quad (35.3b)$$

is the coordinate transformation and

$$\bar{h}_{\mu\nu \text{ new}} = \bar{h}_{\mu\nu \text{ old}} - \xi_{\mu,\nu} - \xi_{\nu,\mu} + \eta_{\mu\nu}\xi^\alpha{}_{,\alpha} \quad (35.3c)$$

is the gauge change. All this was derived and discussed in Chapter 18.

§35.3. PLANE-WAVE SOLUTIONS IN LINEARIZED THEORY

The simplest of all solutions to the linearized equations $\bar{h}_{\mu\nu,\alpha}{}^\alpha = \bar{h}_{\mu,\alpha}{}^\alpha = 0$ is the monochromatic, plane-wave solution,

Monochromatic, plane wave

$$\bar{h}_{\mu\nu} = \Re[A_{\mu\nu} \exp(ik_\alpha x^\alpha)]. \quad (35.4a)$$

*A more nearly rigorous treatment defines $h_{\mu\nu} \equiv g_{\mu\nu} - \eta_{\mu\nu}$, and puts the small corrections $O([h_{\mu\nu}]^2)$ into the field equations:

$$\bar{h}_{\mu,\alpha}{}^\alpha = O([h_{\mu\nu}]^2, \alpha), \quad \bar{h}_{\mu\nu,\alpha}{}^\alpha = O([h_{\mu\nu}]^2, \alpha, \beta).$$

Here $\Re[\dots]$ means that one must take the real part of the expression in brackets; while $A_{\mu\nu}$ (*amplitude*) and k_μ (*wave vector*) are constants satisfying

$$k_\alpha k^\alpha = 0 \quad (\mathbf{k} \text{ a null vector}), \quad (35.4b)$$

$$A_{\mu\alpha} k^\alpha = 0 \quad (\mathbf{A} \text{ orthogonal to } \mathbf{k}) \quad (35.4c)$$

[consequences of $\bar{h}_{\mu\nu,\alpha}^\alpha = 0$ and $\bar{h}_{\mu,\alpha}^\alpha = 0$, respectively; see (35.10) below for the true physics associated with this wave, the curvature tensor]. Clearly, this solution describes a wave with frequency

$$\omega \equiv k^0 = (k_x^2 + k_y^2 + k_z^2)^{1/2}, \quad (35.5)$$

which propagates with the speed of light in the direction $(1/k^0)(k_x, k_y, k_z)$.

At first sight the amplitude $A_{\mu\nu}$ of this plane wave appears to have six independent components (ten, less the four orthogonality constraints $A_{\mu\alpha} k^\alpha = 0$). But this cannot be right! As Track-2 readers have learned in Chapter 21, the gravitational field in general relativity has two dynamic degrees of freedom, not six. Where has the analysis gone astray?

One went astray by forgetting the arbitrariness tied up in the gauge freedom (35.3). The plane-wave vector

$$\xi^\mu \equiv -iC^\mu \exp(ik_\alpha x^\alpha), \quad (35.6)$$

with four arbitrary constants C^μ , generates a gauge transformation that can change arbitrarily four of the six independent components of $A_{\mu\nu}$. One gets rid of this arbitrariness by choosing a specific gauge.

Plane wave has two degrees of freedom in amplitude (two polarizations)

Transverse-traceless (TT)
gauge:
(1) for plane wave

§35.4. THE TRANSVERSE TRACELESS (TT) GAUGE

Select a 4-velocity \mathbf{u} —not at just one event, but the same \mathbf{u} throughout all of spacetime (special-relativistic viewpoint!). By a specific gauge transformation (exercise 35.1), impose the conditions

$$A_{\mu\nu} u^\nu = 0. \quad (35.7a)$$

These are only three constraints on $A_{\mu\nu}$, not four, because one of them— $k^\mu(A_{\mu\nu} u^\nu) = 0$ —is already satisfied (35.4c). As a fourth constraint, use a gauge transformation (exercise 35.1) to set

$$A_{\mu\alpha} u^\alpha = 0. \quad (35.7b)$$

One now has eight constraints in all, $A_{\mu\alpha} u^\alpha = A_{\mu\alpha} k^\alpha = A_\alpha^\alpha = 0$, on the ten components of the amplitude; and the coordinate system (gauge) is now fixed rigidly. Thus, the two remaining free components of $A_{\mu\nu}$ represent the two degrees of freedom (two polarizations) in the plane gravitational wave.

It is useful to restate the eight constraints $A_{\mu\alpha}u^\alpha = A_{\mu\alpha}k^\alpha = A^\mu_\mu = 0$ in a Lorentz frame where $u^0 = 1$, $u^j = 0$, and in a form where k^α does not appear explicitly:

$$h_{\mu 0} = 0, \quad \begin{array}{l} \text{i.e., only the spatial components} \\ h_{jk} \text{ are nonzero;} \end{array} \quad (35.8a)$$

$$h_{kj,j} = 0, \quad \begin{array}{l} \text{i.e., the spatial components are} \\ \text{divergence-free;} \end{array} \quad (35.8b)$$

$$h_{kk} = 0, \quad \begin{array}{l} \text{i.e., the spatial components are} \\ \text{trace-free.} \end{array} \quad (35.8c)$$

(Here and henceforth repeated spatial indices are to be summed, even if both are down; e.g., $h_{kk} \equiv \sum_{k=1}^3 h_{kk}$.) Notice that, since $h = h^\mu_\mu = h_{kk} = 0$, *there is no distinction between $h_{\mu\nu}$ and $\bar{h}_{\mu\nu}$ in this gauge.*

Turn attention now away from plane waves to arbitrary gravitational waves in linearized theory. Any electromagnetic wave can be resolved into a superposition of plane waves, and so can any gravitational wave. For each plane wave in the superposition, introduce the special gauge (35.8). Note that the gauge conditions are all linear in $h_{\mu\nu}$. Therefore the arbitrary wave will also satisfy conditions (35.8). Thus arises the theorem: *Pick a specific global Lorentz frame of linearized theory (i.e., pick a specific 4-velocity \mathbf{u}). In that frame (where $u^\alpha = \delta^\alpha_0$), examine a specific gravitational wave of arbitrary form. One can always find a gauge in which $h_{\mu\nu}$ satisfies the constraints (35.8).* Moreover, in this gauge only the h_{jk} are nonzero. Therefore, one need only impose the six wave equations

$$\square h_{jk} = h_{jk,\alpha}{}^\alpha = 0. \quad (35.9)$$

Any symmetric tensor satisfying constraints (35.8) [but not necessarily the wave equations (35.9)] is called a *transverse-traceless (TT) tensor*—transverse because it is purely spatial ($h_{0\mu} = 0$) and, if thought of as a wave, is transverse to its own direction of propagation ($h_{ij,j} = h_{ij}k_j = 0$); traceless because $h_{kk} = 0$. The most general purely spatial tensor S_{ij} can be decomposed [see Arnowitt, Deser, and Misner (1962) or Box 35.1] into a part S_{ij}^{TT} , which is “transverse and traceless”; a part $S_{ij}^T = \frac{1}{2}(\delta_{ij}f_{kk} - f_{,ij})$, which is “transverse” ($S_{ij}^T = 0$) but is determined entirely by one function f giving the trace of S ($S_{kk}^T = \nabla^2 f$); and a part $S_{ij}^L = S_{i,j}^L + S_{j,i}^L$, which is “longitudinal” and is determined by the vector field S_i^L . In linearized theory h_{ij}^L is a purely gauge part of $h_{\mu\nu}$, whereas h_{ij}^T and h_{ij}^{TT} are gauge-invariant parts of $h_{\mu\nu}$. The special gauge in which $h_{\mu\nu}$ reduces to its transverse-traceless part is called the *TT* or transverse-traceless gauge. The conditions (35.8) defining this gauge can be summarized as

$$h_{\mu\nu} = h_{\mu\nu}^{TT}. \quad (35.8d)$$

As exercise 35.2 illustrates, only pure waves (and not more general solutions of the linearized field equations with source, $\square h_{\mu\nu} = -16\pi T_{\mu\nu}$) can be reduced to *TT* gauge.

(2) for any wave

Decomposition of spatial tensors

Curvature tensor in TT gauge

In the *TT* gauge, the time-space components

$$R_{j0k0} = R_{0j0k} = -R_{j00k} = -R_{0jk0}$$

of the Riemann curvature tensor have an especially simple form [see equation (18.9) and exercise 18.4]:

$$R_{j0k0} = -\frac{1}{2} h_{jk,00}^{TT}. \quad (35.10)$$

Recall that the curvature tensor is gauge-invariant (exercise 18.1). It follows that $h_{\mu\nu}$ cannot be reduced to still fewer components than it has in the *TT* gauge.

Box 35.1 describes methods to calculate $h_{\mu\nu}^{TT}$ from a knowledge of $h_{\mu\nu}$ in some other gauge.

Box 35.1 METHODS TO CALCULATE "TRANSVERSE-TRACELESS PART" OF A WAVE

Problem: Let a gravitational wave $h_{\mu\nu}(t, x^j)$ in an arbitrary gauge of linearized theory be known. How can one calculate the metric perturbation $h_{\mu\nu}^{TT}(t, x^j)$ for this wave in the transverse-traceless gauge?

Solution 1 (valid only for waves; i.e., when $\square \bar{h}_{\mu\nu} = 0$). Calculate the components R_{j0k0} of **Riemann** in the initial gauge; then integrate equation (35.10)

$$h_{jk,00}^{TT} = -2R_{j0k0} \quad (1)$$

to obtain h_{jk}^{TT} . When the wave is monochromatic, $h_{\mu\nu} = h_{\mu\nu}(x^i)e^{-i\omega t}$; then the solution of (1) has the simple form

$$h_{jk}^{TT} = 2\omega^{-2}R_{j0k0}. \quad (2)$$

Solution 2 (valid only for plane waves). "Project out" the *TT* components in an algebraic manner using the operator

$$P_{jk} = \delta_{jk} - n_j n_k. \quad (3)$$

Here

$$n_k = k_k / |\mathbf{k}|$$

is the unit vector in the direction of propagation. Verify that P_{jk} is a projection operator onto the transverse plane:

$$P_{jl}P_{lk} = P_{jk}, \quad P_{jk}n_k = 0, \quad P_{kk} = 2.$$

Then the transverse part of h_{jk} is $P_{jl}h_{lm}P_{mk}$ (or in matrix notation, PhP); and the *TT* part is this quantity diminished by its trace:

$$h_{jk}^{TT} = P_{jl}P_{mk}h_{lm} - \frac{1}{2}P_{jk}(P_{ml}h_{lm}) \quad (4)$$

(index notation),

$$h^{TT} = PhP - \frac{1}{2}P \operatorname{Tr}(Ph) \quad (matrix \text{ notation}). \quad (4')$$

The sequence of operations that gives h_{ij}^{TT} cuts two parts out of h_{ij} . The first part cut out is

$$h_{jk}^T = \frac{1}{2}P_{jk}(P_{lm}h_{lm}), \quad (5)$$

which is transverse but is built from its own trace,

$$h^T \equiv \operatorname{Tr}(PhP) = \operatorname{Tr}(Ph) = P_{lm}h_{ml}.$$

Exercise 35.1. TRANSFORMATION OF PLANE WAVE TO TT GAUGE

Let a plane wave of the form (35.4) be given, in some arbitrary gauge of linearized theory. Exhibit explicitly the transformation that puts it into the *TT* gauge. [Hint: Work in a Lorentz frame where the 4-velocity u^μ of the *TT* gauge is $u^0 = 1, u^j = 0$. Solve for the four constants C^μ of the generating function (35.6) by demanding that $\bar{h}_{\mu\nu}$ satisfy the *TT* constraints (35.7).]

EXERCISES**Exercise 35.2. LIMITATION ON EXISTENCE OF TT GAUGE**

Although the metric perturbation $h_{\mu\nu}$ for any *gravitational wave* in linearized theory can be put into the *TT* form (35.8), nonradiative $h_{\mu\nu}$'s cannot. Consider, for example, the external field of a rotating, spherical star, which cannot be written as a superposition of plane waves:

The second part cut out of h_{ij} is the longitudinal part

$$\begin{aligned} h^L_{jk} &= h_{jk} - P_{jl}P_{mk}h_{lm} \\ &= n_l n_k h_{jl} + n_j n_l h_{lk} - n_j n_k (n_l n_m h_{lm}); \end{aligned} \quad (6)$$

or

$$h^L = h - PhP \quad (6')$$

Solution 3 (general case). Fourier analyze any symmetric array $h_{ij} = f h_{ij}(k, t) \exp(ik_m x^m) d^3 k$, and apply the formulas (4) from solution 2 to each Fourier component individually. But note that in this case one can write the projection operator in the direction-independent form

$$P_{jk} = \delta_{jk} - \frac{1}{\nabla^2} \partial_j \partial_k \quad (7)$$

or

$$n_l n_m = \frac{1}{\nabla^2} \partial_l \partial_m \quad (8)$$

(provided the formulas are written with all h 's standing on the right), since $\partial_\ell = ik_\ell$ under the Fourier integral. Of course the operation $1/\nabla^2$ can be evaluated by other methods, e.g., by Green's functions, as well as by Fourier analysis. [The

quantity $\psi \equiv \nabla^{-2}f$ stands for the solution ψ of the Poisson equation $\nabla^2\psi = f$.] The advantage of this method is its power in certain analytic computations (see, e.g., below).

Gauge Transformations. The change in $h_{\mu\nu}$ due to a gauge transformation is

$$\delta h_{\mu\nu} = -(\partial_\nu \xi_\mu + \partial_\mu \xi_\nu). \quad (9)$$

The transverse part of this change is

$$P_{jl}P_{km}(\delta h_{lm}) = -P_{jl}P_{km}(\partial_l \xi_m + \partial_m \xi_l) = 0. \quad (10)$$

To verify this formula for a plane wave (solution 2), note that $\partial_\ell = i|\mathbf{k}|n_\ell$ and $P_{jl}n_\ell = 0$. To verify the same result in general, use equation (7) to give the result

$$P_{jl} \partial_\ell = 0. \quad (11)$$

Thus both h_{ij}^{TT} of equation (4), and h_{ij}^T of equation (5) are gauge-invariant:

$$\delta h_{ij}^{TT} = \delta h_{ij}^T = 0. \quad (12)$$

In empty space ($T_{\mu\nu} = 0$), both h_{ij}^T and another gauge-invariant quantity \tilde{h}_{0k} (discussed in exercise 35.4) vanish, by virtue of the field equations.

$$h_{00} = \frac{2M}{r}, \quad h_{jk} = \frac{2M}{r} \delta_{jk}, \quad h_{0k} = -2\epsilon_{klm} \frac{S^l x^m}{r^3},$$

$$r = (x^2 + y^2 + z^2)^{1/2}$$

[see equation (19.5)]. Here M is the star's mass and \mathbf{S} is its angular momentum. Show that this *cannot* be put into TT gauge. [Hint: Calculate R_{j0k0} and from it, by means of (35.10), infer h_{jk}^{TT} . Then calculate R_{0xyz} in both the original gauge and the new gauge, and discover that they disagree—not only by virtue of the mass term, but also by virtue of the angular-momentum term.]

Exercise 35.3. A CYLINDRICAL GRAVITATIONAL WAVE

To restore one's faith, which may have been shaken by exercise 35.2, one can consider the radiative solution whose only nonvanishing component $h_{\mu\nu}$ is

$$\bar{h}_{zz} = 4A \cos(\omega t) J_0(\omega \sqrt{x^2 + y^2}),$$

where J_0 is the Bessel function. This solution represents a superposition of ingoing and outgoing cylindrical gravitational waves. For this gravitational field calculate R_{j0k0} , and from it infer h_{jk}^{TT} . Then calculate several other components of $R_{\alpha\beta\gamma\delta}$ (e.g., R_{xyxy}) in the original gauge and in TT gauge, and verify that the answers are the same.

Exercise 35.4. NON-TT PARTS OF METRIC PERTURBATION [Track 2]

From Box 35.1 establish the formula $h^T = \nabla^{-2}(h_{kk,tt} - h_{kt,kt})$; then verify the gauge invariance of h^T directly, by showing that $h_{kk,tt} - h_{kt,kt}$ is gauge-invariant. Use $\delta h_{ij} = \xi_{i,j} + \xi_{j,i}$. Show similarly that the quantities \tilde{h}_{0k} defined by

$$\tilde{h}_{0k} = \bar{h}_{0k} - \nabla^{-2}(\bar{h}_{0,\mu k}^\mu + \bar{h}_{k,\ell 0}^\ell)$$

are gauge-invariant. Show from the gauge-invariant linearized field equations (18.5) that

$$\nabla^2 h^T = -16\pi T^{00},$$

$$\nabla^2 \tilde{h}_{0k} = -16\pi T_{0k},$$

so h^T and \tilde{h}_{0k} must vanish for waves in empty space.

§35.5. GEODESIC DEVIATION IN A LINEARIZED GRAVITATIONAL WAVE

Action of a gravitational wave on separation of two test particles

The oscillating curvature tensor of a gravitational wave produces oscillations in the separation between two neighboring test particles, A and B . Examine the oscillations from the viewpoint of A . Use a coordinate system (“proper reference frame of A ”), with spatial origin $x^{\hat{j}} = 0$, attached to A 's world line (comoving coordinates); with coordinate time equal to A 's proper time ($x^{\hat{0}} = \tau$ on world line $x^{\hat{j}} = 0$); and with orthonormal spatial axes attached to gyroscopes carried by A (“nonrotating frame”). This coordinate system, appropriately specialized, is a local Lorentz frame not just at one event \mathcal{P}_0 on A 's geodesic world line, but all along A 's world line:

$$ds^2 = -dx^{\hat{0}2} + \delta_{\hat{j}\hat{k}} dx^{\hat{j}} dx^{\hat{k}} + O(|x^{\hat{j}}|^2) dx^{\hat{\alpha}} dx^{\hat{\beta}}. \quad (35.11)$$

[Proof: such a “proper reference frame” was set up for accelerated particles in Track 2’s §13.6. The line element (13.71) derived there, when specialized to particle A ($a_j = 0$ because A falls freely; $\omega^{\hat{l}} = 0$ because the spatial axes are attached to gyroscopes) reduces to the above form, as in equation (13.73).]

As the gravitational wave passes, it produces an oscillating curvature tensor, which wiggles the separation vector \mathbf{n} reaching from particle A to particle B :

$$D^2 n^{\hat{j}} / d\tau^2 = -R_{\hat{j}\hat{0}\hat{k}\hat{l}}^{\hat{j}} n^{\hat{k}} = -R_{\hat{j}\hat{0}\hat{k}\hat{0}}^{\hat{j}} n^{\hat{k}}. \quad (35.12)$$

The components of the separation vector are nothing but the coordinates of particle B , since particle A is at the origin of its own proper reference frame; thus,

$$n^{\hat{j}} = x_B^{\hat{j}} - x_A^{\hat{j}} = x_B^{\hat{j}}.$$

Moreover, at $x^{\hat{j}} = 0$ [where the calculation (35.12) is being performed], the $\Gamma^{\hat{\mu}}_{\hat{\alpha}\hat{\beta}}$ vanish for all $x^{\hat{0}}$; so $d\Gamma^{\hat{\mu}}_{\hat{\alpha}\hat{\beta}}/d\tau$ also vanish. This eliminates all Christoffel-symbol corrections in $D^2 n^{\hat{j}} / D\tau^2$. Hence, equation (35.12) reduces to

$$d^2 x_B^{\hat{j}} / d\tau^2 = -R_{\hat{j}\hat{0}\hat{k}\hat{l}}^{\hat{j}} x_B^{\hat{k}}. \quad (35.13)$$

There is a TT coordinate system that, to first order in the metric perturbation h_{jk}^{TT} , moves with particle A and with its proper reference frame. To first order in h_{jk}^{TT} , the TT coordinate time t is the same as proper time τ , and $R_{\hat{j}\hat{0}\hat{k}\hat{0}}^{TT} = R_{\hat{j}\hat{0}\hat{k}\hat{0}}^{\hat{j}}$. Hence, equation (35.13) can be rewritten

$$d^2 x_B^{\hat{j}} / dt^2 = -R_{\hat{j}\hat{0}\hat{k}\hat{0}}^{TT} x_B^{\hat{k}} = \frac{1}{2} (\partial^2 h_{jk}^{TT} / \partial t^2) x_B^{\hat{k}}. \quad (35.14)$$

Suppose, for concreteness, that the particles are at rest relative to each other before the wave arrives ($x_B^{\hat{j}} = x_{B(0)}^{\hat{j}}$ when $h_{jk}^{TT} = 0$). Then the equation of motion (35.14) can be integrated to yield

$$x_B^{\hat{j}}(\tau) = x_{B(0)}^{\hat{k}} \left[\delta_{jk} + \frac{1}{2} h_{jk}^{TT} \right]_{\text{at position of } A}. \quad (35.15)$$

This equation describes the wave-induced oscillations of B ’s location, as measured in the proper reference frame of A .

Turn to the special case of a plane wave. Suppose the test-particle separation lies in the direction of propagation of the wave. Then the wave cannot affect the separation; there is no oscillation:

$$h_{jk}^{TT} x_{B(0)}^{\hat{k}} \propto h_{jk}^{TT} k_k = 0.$$

Only separations in the transverse direction oscillate; *the wave is transverse not only in its mathematical description (h_{jk}^{TT}), but also in its physical effects (geodesic deviation)!*

Transverse character of relative accelerations

EXERCISE**Exercise 35.5. ALTERNATIVE CALCULATION OF RELATIVE OSCILLATIONS**

Introduce a TT coordinate system in which, at time $t = 0$, the two particles are both at rest. Use the geodesic equation to show that subsequently they both always remain at rest in the TT coordinates, despite the action of the wave. This means that the contravariant components of the separation vector are always constant in the TT coordinate frame:

$$n^j = x_B^j - x_A^j = \text{const.}$$

Call this constant $x_{B(0)}^j$. Transform these components to the comoving orthonormal frame; the answer should be equation (35.15).

§35.6. POLARIZATION OF A PLANE WAVE

Polarization of gravitational waves:

- (1) States of linear polarization, “+” and “ \times ”

Geodesic deviation in the transverse direction provides a means for studying and characterizing the polarizations of plane waves.

Consider a plane, monochromatic wave propagating in the z direction. In the TT gauge the constraints $h_{0\mu}^{TT} = 0$, $h_{ij,j}^{TT} \equiv ik_j h_{ij}^{TT} = 0$, and $h_{kk}^{TT} = 0$ reveal that the only nonvanishing components of $h_{\mu\nu}^{TT}$ are

$$\begin{aligned} h_{xx}^{TT} &= -h_{yy}^{TT} = \Re\{A_+ e^{-i\omega(t-z)}\}, \\ h_{xy}^{TT} &= h_{yx}^{TT} = \Re\{A_\times e^{-i\omega(t-z)}\}. \end{aligned} \quad (35.16)$$

The amplitudes A_+ and A_\times represent two independent modes of polarization.

As for electromagnetic plane waves (Figure 35.1), so also for gravitational plane waves (Figure 35.2), one can resolve a given wave into two linearly polarized components, or, alternatively, into two circularly polarized components.

$\omega(t-z)$	Displacement, δx , for polarization			
	e_x	e_y	e_R	e_L
$2n\pi$	•	•	↑	↓
$(2n + \frac{1}{2})\pi$	↔	↓	↔	↔
$(2n + 1)\pi$	•	•	↓	↑
$(2n + \frac{3}{2})\pi$	↔	↑	↔	↔

Figure 35.1.
Plane Electromagnetic Waves.
Polarization vector: e_p
Vector Potential

$$\begin{aligned} A &= \Re\{A_0 e^{-i\omega(t-z)} e_p\} \\ \text{Acceleration of a test charge:} \\ \mathbf{a} &= (q/m)\mathbf{E} = (q/m)(-\partial A/\partial t) \\ &= \Re[i\omega(q/m)A_0 e^{-i\omega(t-z)} e_p] \end{aligned}$$

Displacement of charge relative to inertial frame:

$$\delta x = \Re\left[\frac{q/m}{i\omega} A_0 e^{-i\omega(t-z)} e_p\right]$$

For *linearly polarized waves*, the unit polarization vectors of electromagnetic theory are e_x and e_y . A test charge hit by a plane wave with polarization vector e_x oscillates in the x -direction relative to an inertial frame; and similarly for e_y . By analogy, the *unit linear-polarization tensors* for gravitational waves are

$$\mathbf{e}_+ \equiv \mathbf{e}_x \otimes \mathbf{e}_x - \mathbf{e}_y \otimes \mathbf{e}_y, \quad (35.17a)$$

$$\boldsymbol{e}_\times \equiv \boldsymbol{e}_x \otimes \boldsymbol{e}_y + \boldsymbol{e}_y \otimes \boldsymbol{e}_x. \quad (35.17b)$$

The plane wave (35.16), when $A_x = 0$, has polarization \mathbf{e}_+ and can be rewritten

$$h_{jk} = \Re\{A_+ e^{-i\omega(t-z)} e_{+jk}\}. \quad (35.18)$$

Its effect in altering the geodesic separation between two test particles depends on the direction of their separation. To see the effect in all directions at once, consider a circular ring of test particles in the transverse (x, y) plane, surrounding a central particle (Figure 35.2). As the plane wave (35.18) (polarization \mathbf{e}_+) passes, it deforms what was a ring as measured in the proper reference frame of the central particle into an ellipse with axes in the x and y directions that pulsate in and out:

etc. By contrast (Figure 35.2), a wave of polarization e_x deforms the ring at a 45-degree angle to the x and y directions: $\circ \circ \circ \circ \circ \circ \circ \circ \circ \circ$ etc.

For circularly polarized waves, the unit polarization vectors of electromagnetic theory are

$$\mathbf{e}_R = \frac{1}{\sqrt{2}}(\mathbf{e}_x + i\mathbf{e}_y), \quad \mathbf{e}_L = \frac{1}{\sqrt{2}}(\mathbf{e}_x - i\mathbf{e}_y) \quad (35.19)$$

(2) States of circular polarization

$\omega(t - z)$	Deformation of a ring of test particles			
	e_+	e_\times	e_R	e_L
$2n\pi$				
$(2n + \frac{1}{2})\pi$				
$(2n + 1)\pi$				
$(2n + \frac{3}{2})\pi$				

Figure 35.2.

Plane Gravitational Waves. Polarization tensor:

e_p

Metric perturbation:

$$h_{jk} = \Re [A_0 e^{-i\omega(t-z)} e_{Pjk}]$$

Tidal acceleration between two test particles:

$$\frac{D^2 n_j}{D\tau^2} = -R_{j0k0}n_k = \frac{1}{2}\frac{\partial^2 h_{jk}}{\partial t^2} n_k$$

$$= \Re \left[-\frac{1}{2} \omega^2 A_0 e^{-i\omega(t-z)} e_{P_{jk}} n_k \right]$$

Separation between two test particles:

$$n_{\hat{j}} = n_{\hat{j}}^{(0)} + \Re \left[\frac{1}{2} A_0 e^{-i\omega(t-z)} e_{Pjk} n_{\hat{k}}^{(0)} \right]$$

Position of test particle B in proper reference frame of test particle A . (In drawing, A is the central particle and B is any peripheral particle):

$$x_B^{\hat{j}} = x_{B(0)}^{\hat{j}} + \Re \left[\frac{1}{2} A_0 e^{-i\omega(t-z)} e_{Pjk} x_{B(0)}^{\hat{k}} \right]$$

Similarly, the *unit circular polarization tensors* of gravitation theory are

$$\mathbf{e}_R = \frac{1}{\sqrt{2}}(\mathbf{e}_+ + i\mathbf{e}_x), \quad \mathbf{e}_L = \frac{1}{\sqrt{2}}(\mathbf{e}_+ - i\mathbf{e}_x). \quad (35.20)$$

A test charge hit by an electromagnetic wave of polarization \mathbf{e}_R moves around and around in a circle in the righthanded direction (counterclockwise for a wave propagating toward the reader); for \mathbf{e}_L it circles in the lefthanded (clockwise) direction (see Figure 35.1). Similarly (Figure 35.2), a gravitational wave of polarization \mathbf{e}_R rotates the deformation of a test-particle ring in the righthanded direction,



while a wave of \mathbf{e}_L rotates it in the lefthanded direction. The individual test particles in the ring rotate in small circles relative to the central particle. However, just as the drops in an ocean wave do not move along with the wave, so the particles on the ring do not move *around* the central particle with the rotating ellipse.

Notice from Figure 35.2 that, at any moment of time, a gravitational wave is invariant under a rotation of 180° about its direction of propagation. The analogous angle for electromagnetic waves (Figure 35.1) is 360° , and for neutrino waves it is 720° . This behavior is intimately related to the spin of the zero-mass particles associated with the quantum-mechanical versions of these waves: gravitons have spin 2, photons spin 1, and neutrinos spin 1/2. The classical radiation field of a spin- S particle is always invariant under a rotation of $360^\circ/S$ about its propagation direction.

A radiation field of any spin S has precisely two orthogonal states of linear polarization. They are inclined to each other at an angle of $90^\circ/S$; thus, for a neutrino field, with $S = \frac{1}{2}$, the two states are distinguished as $|\uparrow\rangle$ and $|\downarrow\rangle$ (spin up and spin down; 180° angle). For an electromagnetic wave $S = 1$ and two orthogonal states of polarization are \mathbf{e}_x and \mathbf{e}_y (90° angle). For a gravitational wave $S = 2$, and two orthogonal states are \mathbf{e}_+ and \mathbf{e}_x (45° angle).

Spin-2 character of gravitational field and its relation to symmetries of waves

EXERCISES

Exercise 35.6. ROTATIONAL TRANSFORMATIONS FOR POLARIZATION STATES

Consider two Lorentz coordinate systems, one rotated by an angle θ about the z direction relative to the other:

$$t' = t, \quad x' = x \cos \theta + y \sin \theta, \quad y' = y \cos \theta - x \sin \theta, \quad z' = z. \quad (35.21)$$

Let $|\uparrow\rangle$ and $|\downarrow\rangle$ be quantum-mechanical states of a neutrino with spin-up and spin-down relative to the x direction; and similarly for $|\uparrow'\rangle$ and $|\downarrow'\rangle$. Let \mathbf{e}_x , \mathbf{e}_y , \mathbf{e}'_x , \mathbf{e}'_y be the unit polarization vectors in the two coordinate systems for an electromagnetic wave traveling in the z -direction; and similarly \mathbf{e}_+ , \mathbf{e}_x , \mathbf{e}_+ , \mathbf{e}_x for a gravitational wave in linearized theory. Derive the following transformation laws:

$$\begin{aligned} |\uparrow'\rangle &= |\uparrow\rangle \cos \frac{1}{2}\theta + |\downarrow\rangle \sin \frac{1}{2}\theta; & |\downarrow'\rangle &= -|\uparrow\rangle \sin \frac{1}{2}\theta + |\downarrow\rangle \cos \frac{1}{2}\theta; \\ \mathbf{e}'_x &= \mathbf{e}_x \cos \theta + \mathbf{e}_y \sin \theta; & \mathbf{e}'_y &= -\mathbf{e}_x \sin \theta + \mathbf{e}_y \cos \theta; \\ \mathbf{e}'_+ &= \mathbf{e}_+ \cos 2\theta + \mathbf{e}_x \sin 2\theta; & \mathbf{e}'_x &= -\mathbf{e}_+ \sin 2\theta + \mathbf{e}_x \cos 2\theta. \end{aligned} \quad (35.22)$$

What is the generalization to the linear-polarization basis states for a radiation field of arbitrary spin S ?

Exercise 35.7. ELLIPTICAL POLARIZATION

Discuss elliptically polarized gravitational waves in a manner analogous to the discussion of linearly and circularly polarized waves in Figure 35.2.

§35.7. THE STRESS-ENERGY CARRIED BY A GRAVITATIONAL WAVE

Exercise 18.5 showed that in principle one can build detectors which extract energy from gravitational waves. Hence, it is clear that the waves must carry energy.

Unfortunately, to derive and justify an expression for their energy requires a somewhat more sophisticated viewpoint than linearized theory. Such a viewpoint will be developed later in this chapter (§§35.13 and 35.15). But for the benefit of Track-1 readers, the key result is stated here.

In accordance with the discussions in §§19.4 and 20.4, the stress-energy carried by gravitational waves cannot be localized inside a wavelength. One cannot say whether the energy is carried by the crest of a wave, by its trough, or by its “walls.” However, one *can* say that a certain amount of stress-energy is contained in a given “macroscopic” region (region of several wavelengths’ size), and one can thus talk about a tensor for an *effective* smeared-out stress-energy of gravitational waves, $T_{\mu\nu}^{(\text{GW})}$. In a (nearly) inertial frame of linearized theory, $T_{\mu\nu}^{(\text{GW})}$ is given by

$$T_{\mu\nu}^{(\text{GW})} = \frac{1}{32\pi} \langle h_{jk,\mu}^{TT} h_{jk,\nu}^{TT} \rangle, \quad (35.23)$$

Approximate localization of energy in a gravitational wave

Effective stress-energy tensor for gravitational waves:

(1) expressed in terms of metric perturbations

where $\langle \rangle$ denotes an average over several wavelengths and h_{jk}^{TT} means the (gauge-invariant) transverse-traceless part of $h_{\mu\nu}$, which is simply \bar{h}_{jk} in the TT gauge. Another formula for $T_{\mu\nu}^{(\text{GW})}$, valid in any arbitrary gauge, with $\bar{h} \neq 0$, $\bar{h}_{\mu,\alpha} \neq 0$, and $\bar{h}_{0\mu} \neq 0$ is

$$T_{\mu\nu}^{(\text{GW})} = \frac{1}{32\pi} \left(\bar{h}_{\alpha\beta,\mu} \bar{h}^{\alpha\beta,\nu} - \frac{1}{2} \bar{h}_{,\mu} \bar{h}_{,\nu} - \bar{h}^{\alpha\beta,\beta} \bar{h}_{\alpha\mu,\nu} - \bar{h}^{\alpha\beta,\beta} \bar{h}_{\alpha\nu,\mu} \right) \quad (35.23')$$

This stress-energy tensor, like any other, is divergence-free in vacuum

$$T_{\mu,\nu}^{(\text{GW})} = 0; \quad (35.24)$$

(2) subject to conservation law

and it contributes to the large-scale background curvature (which linearized theory ignores) just as any other stress-energy does:

$$G_{\mu\nu}^{(\text{B})} = 8\pi(T_{\mu\nu}^{(\text{GW})} + T_{\mu\nu}^{(\text{matter})} + T_{\mu\nu}^{(\text{other fields})}). \quad (35.25)$$

(3) role as source of background curvature

In writing here the term $T_{\mu\nu}^{(\text{GW})}$ for the effective smeared-out energy density of the gravitational wave, one is foregoing any further insertion of the gravitational wave into the Einstein equation. Otherwise one might end up counting twice over the

(4) for a plane, monochromatic wave

contribution of the same wave to the background curvature of space, even though expressed in very different formalisms.

According to equation (35.23), the stress-energy tensor for the plane wave,

$$h_{\mu\nu} = \Re \{(A_+ e_{+\mu\nu} + A_\times e_{\times\mu\nu}) e^{-i\omega(t-z)}\}, \quad (35.26)$$

is

$$T_{tt}^{(\text{GW})} = T_{zz}^{(\text{GW})} = -T_{tz}^{(\text{GW})} = \frac{1}{32\pi} \omega^2 (|A_+|^2 + |A_\times|^2). \quad (35.27)$$

Notice that the background radius of curvature \mathcal{R} (ignored by linearized theory), and the mean reduced wavelength λ (= wavelength/2π) and amplitude \mathcal{A} of the gravitational waves satisfy

$$\begin{aligned} \mathcal{R}^{-2} &\sim \text{typical magnitude of components of } R_{\alpha\beta\gamma\delta}^{(\text{B})} \\ &\sim T_{\mu\nu}^{(\text{GW})} \sim \mathcal{A}^2/\lambda^2 \text{ if } T_{\mu\nu}^{(\text{GW})} \text{ is chief source of background curvature,} \\ &\gg T_{\mu\nu}^{(\text{GW})} \sim \mathcal{A}^2/\lambda^2 \text{ if } T_{\mu\nu}^{(\text{GW})} \text{ is not chief source.} \end{aligned}$$

Consequently, the dimensionless numbers \mathcal{A} and λ/\mathcal{R} are related by

$$\mathcal{A} \lesssim \lambda/\mathcal{R}. \quad (35.28)$$

Conditions for validity of gravitational-wave formalism

Thus, the whole concept of a small-scale ripple propagating in a background of large-scale curvature breaks down, and the whole formalism of this chapter becomes meaningless, if the dimensionless amplitude of the wave approaches unity. One must always have $\mathcal{A} \ll 1$ as well as $\lambda \ll \mathcal{R}$ if the concept of a gravitational wave is to make any sense!

§35.8. GRAVITATIONAL WAVES IN THE FULL THEORY OF GENERAL RELATIVITY

Nonlinear effects in gravitational waves:

(1) radiation damping

Curving up of the background spacetime by the energy of the waves is but one of many new effects that enter, when one passes from linearized theory to the full, nonlinear general theory of relativity.

In linearized theory one can consider a localized source of gravitational waves (e.g., a vibrating bar) in steady oscillation, radiating a strictly periodic wave. But the exact theory insists that the energy of the source decrease secularly, to counterbalance the energy carried off by the radiation (energy conservation; gravitational radiation damping; see §§36.8 and 36.11). This makes an exactly periodic wave impossible, though a very nearly periodic one can certainly be emitted [Papapetrou (1958); Arnowitt, Deser, and Misner as reported by Misner (1964b)].

(2) refraction

In the real universe there are spacetime curvatures due not only to the energy of gravitational waves, but also, and more importantly, to the material content of the universe (planets, stars, gas, galaxies). As a gravitational wave propagates through these curvatures, its wave fronts change shape (“refraction”), its wavelength changes

(gravitational redshift), and it backscatters off the curvatures to some extent. If the wave is a pulse, the backscatter will cause its shape and polarization to keep changing and will produce “tails” that spread out behind the moving pulse, traveling slower than light [see exercise 32.10; also Riesz (1949), DeWitt and Brehme (1960), DeWitt and DeWitt (1964a), Kundt and Newman (1968), Couch *et. al.* (1968)]. However, so long as $\mathcal{A} \ll 1$ and $\lambda/\mathcal{R} \ll 1$, these effects will be extremely small locally. They can only build up over distances of the order of \mathcal{R} —and sometimes not even then. Thus, locally, linearized theory will remain highly accurate.

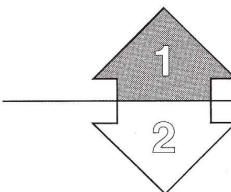
Even in an idealized universe containing nothing but gravitational waves, backscatter and tails are produced by the interaction of the waves with the background curvature that they themselves produce.

If the reduced wavelength $\lambda = \lambda/2\pi$ and the mass-energy m of a pulse of waves satisfy $\lambda \ll m$, it is possible (in principle) to focus the pulse into a region of size $r < m$, whereupon a part of the energy of the pulse will undergo gravitational collapse to a singularity, leaving behind a black hole [see Ruffini and Wheeler (1970), and pp. 7–24 of Christodoulou (1971)]. Short of a certain critical strength, no part of the pulse undergoes such a collapse. But it does undergo a time delay before reexpanding. This time delay is definable and measurable in the asymptotically flat space, far from the domain where the energy a little earlier underwent temporary focusing into dimensions of order λ .

All these effects can be analyzed in general relativity theory using approximation schemes which, in first order, are similar to or identical to linearized theory. Later in this chapter (§§35.13–35.15), one such approximation scheme will be developed. But first it is helpful to study an exact solution that exhibits some of these effects.

- (3) redshift
- (4) backscatter
- (5) tails

- (6) self-gravitational attraction



§35.9. AN EXACT PLANE-WAVE SOLUTION

Any exact gravitational-wave solution that can be given in closed mathematical form must be highly idealized; otherwise it could not begin to cope with the complexities outlined above. Consequently, mathematically exact solutions are useful for pedagogical purposes only. However, pedagogy should not be condemned: it is needed not only by students, but also by veteran workers in the field of relativity, who even today are only beginning to develop intuition into the nonlinear regime of geometrodynamics!

From the extensive literature on exact solutions, we have chosen, as a compromise between realism and complexity, the following plane wave [Bondi *et. al.* (1959), Ehlers and Kundt (1962)]:

$$\begin{aligned} ds^2 &= L^2(e^{2\beta} dx^2 + e^{-2\beta} dy^2) + dz^2 - dt^2 \\ &= L^2(e^{2\beta} dx^2 + e^{-2\beta} dy^2) - du dv. \end{aligned} \tag{35.29a}$$

(1) form of metric

Here

$$u = t - z, \quad v = t + z, \quad L = L(u), \quad \beta = \beta(u). \tag{35.29b}$$

The rest of this chapter is Track 2. No earlier Track-2 material is needed as preparation for it, but Chapter 20 (conservation laws) and §22.5 (geometric optics) will be found to be helpful. It is not needed as preparation for any later chapter.

Exact plane-wave solution of vacuum field equation:

The forms that the functions $L(u)$ (“background factor”) and $\beta(u)$ (“wave factor”) can take are determined by the vacuum field equations. In the null coordinate system u, v, x, y , the only component of the Ricci tensor that does not vanish identically is (see Box 14.4, allowing for the difference in coordinates, $2v_{\text{there}} = v_{\text{here}}$)

$$R_{uu} = -2L^{-1}[L'' + (\beta')^2 L], \quad (35.30)$$

where the prime denotes d/du . Thus, Einstein’s equations in vacuum read

- (2) generation of
“background factor” L
by “wave factor” β

- (3) linearized limit

- (4) special case: a
plane-wave pulse

$$L'' + (\beta')^2 L = 0. \quad (35.31)$$

(“effect of wave factor on background factor”)

The linearized version of this equation is $L'' = 0$, since $(\beta')^2$ is a second-order quantity. Therefore the solution corresponding to linearized theory is

$$L = 1, \quad \beta(u) \text{ arbitrary but small.}$$

The corresponding metric is

$$ds^2 = (1 + 2\beta) dx^2 + (1 - 2\beta) dy^2 + dz^2 - dt^2, \quad \beta = \beta(t - z). \quad (35.32)$$

Notice that this is a plane wave of polarization \mathbf{e}_+ propagating in the z -direction. (See exercise 35.10 at end of §35.12 for the extension to a wave possessing both polarizations, \mathbf{e}_+ and \mathbf{e}_\times .)

Return attention to the exact plane wave, and focus on the case where the “wave factor” $\beta(u)$ is a pulse of duration $2T$, and $|\beta'| \ll 1/T$ throughout the pulse. Then the exact solution (Figure 35.3) is: (1) for $u < -T$ (flat spacetime; pulse has not yet arrived),

$$\beta = 0, \quad L = 1; \quad (35.33a)$$

(2) for $-T < u < +T$ (interior of pulse),

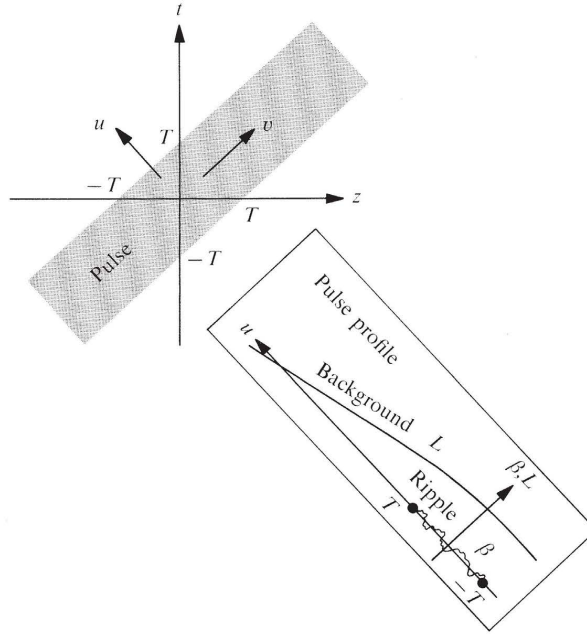
$$\beta = \beta(u) \text{ is arbitrary, except that } |\beta'| \ll 1/T,$$

$$L(u) = 1 - \int_{-T}^u \left\{ \int_{-T}^{\bar{u}} [\beta'(\bar{u})]^2 d\bar{u} \right\} d\bar{u} + O([\beta'T]^4); \quad (35.33b)$$

(3) for $u > T$ (after the pulse has passed),

$$\beta = 0, \quad L = 1 - \frac{u}{a}, \quad a \equiv \frac{1}{\int_{-T}^T (\beta')^2 du} + \frac{O([\beta'T]^2)}{\int_{-T}^T (\beta')^2 du}. \quad (35.33c)$$

Before discussing the physical interpretation of this exact solution, one must come to grips with the singularity in the metric coefficients at $u = a \gg T$. (There $L = 0$, so $g_{xx} = g_{yy} = 0$.) Is this a physical singularity like the region $r = 0$ of the Schwarzschild geometry, or is it merely a coordinate singularity as $r = 2M$ is in Schwarzschild coordinates (Chapters 31, 32, and 33)? The only nonzero components of the Riemann tensor for the metric (35.29) are (see Box 14.4)

**Figure 35.3.**

Spacetime diagram and pulse profile for an exact plane-wave solution to Einstein's vacuum field equations. The metric has the form

$$ds^2 = L^2(e^{2\beta} dx^2 + e^{-2\beta} dy^2) + dz^2 - dt^2.$$

The “wave factor” $\beta(u) \equiv \beta(t - z)$ (short-scale ripples) and the “background factor” $L(u) \equiv L(t - z)$ (large-scale bending of the background geometry by the effective mass-energy of the “ripply” gravitational wave) are shown in the drawing and are given analytically by equations (35.33).

$$R_{uxu}^x = \frac{1}{2} R_{uu} - \beta'' - 2(L'/L)\beta', \quad (35.34)$$

$$R_{uyu}^y = \frac{1}{2} R_{uu} + \beta'' + 2(L'/L)\beta'.$$

Moreover, these components both vanish in any extended region where $\beta = 0$. Thus, *spacetime is completely flat in regions where the “wave factor” vanishes—which is everywhere outside the pulse!* In particular, spacetime is flat near $u = a$, so the singularity there must be a coordinate singularity, not a physical singularity. To eliminate this singularity, one can perform the coordinate transformation

$$x = \frac{X}{1 - U/a}, \quad y = \frac{Y}{1 - U/a}, \quad u = U, \quad v = V + \frac{X^2 + Y^2}{a - U} \quad (35.35)$$

throughout the region to the future of the pulse ($u > T$), where

$$ds^2 = (1 - u/a)^2(dx^2 + dy^2) - du dv. \quad (35.36a)$$

(5) spacetime is flat outside the pulse

In the new X, Y, U, V , coordinates the metric has the explicitly flat form

$$ds^2 = dX^2 + dY^2 - dUdV \quad \text{for } U = u > T. \quad (35.36b)$$

EXERCISES

Exercise 35.8. GLOBALLY WELL-BEHAVED COORDINATES FOR PLANE WAVE [based on Ehlers and Kundt (1962)]

Find a coordinate transformation similar to (35.35), which puts the exact plane-wave solution (35.29a), (35.31), into the form

$$ds^2 = dX^2 + dY^2 - dUdV + (X^2 - Y^2)F dU^2, \quad (35.37)$$

$F = F(U)$ completely arbitrary.

This coordinate system has the advantage of no coordinate singularities anywhere; while the original coordinate system has the advantages of an easy transition to linearized theory, and easy interpretation of the action of the wave on test particles.

Exercise 35.9. GEODESIC COMPLETENESS FOR PLANE-WAVE MANIFOLD [based on Ehlers and Kundt (1962)]

Prove that the coordinate system (X, Y, U, V) of exercise 35.8 completely covers its spacetime manifold. More specifically, show that every geodesic can be extended in both directions for an arbitrarily large affine-parameter length without leaving the X, Y, U, V coordinate system. (This property is called *geodesic completeness*.) [Hint: Choose an arbitrary event and an arbitrary tangent vector $d/d\lambda$ there. They determine an arbitrary geodesic. Perform a coordinate transformation that leaves the form of the metric unchanged and puts $d/d\lambda$ either in the $(\tilde{U}, \tilde{V}) = \text{constant}$ 2-surface, or in the $(\tilde{X}, \tilde{Y}) = \text{constant}$ 2-surface. Verify that the two coordinate systems cover the same region of spacetime. Then analyze completeness of $d/d\lambda$'s geodesic in $(\tilde{X}, \tilde{Y}, \tilde{U}, \tilde{V})$ coordinates.]

§35.10. PHYSICAL PROPERTIES OF THE EXACT PLANE WAVE

Flatness outside gravitational-wave pulses is unusual

Action of exact gravitational-wave pulse on test particles:

Spacetime is completely flat both before the arrival of the plane-wave pulse ($u < -T$) and after it has passed ($u > T$). This is the message of the last paragraph.

Complete flatness outside the pulse is very atypical for gravitational waves in the full, nonlinear general theory of relativity. It occurs in this example only because the wave fronts (surfaces of constant u and v , i.e., constant z and t) are perfectly flat 2-surfaces. If the wave fronts were bent (e.g., spherical), the energy carried by the pulse would produce spacetime curvature outside it.

To see nonlinear effects in action, turn from the flat geometry outside the pulse to the action of the pulse on freely falling test particles. Consider a family of particles that are all at rest in the original t, x, y, z coordinate system (world lines: $[x, y, z] = \text{constant}$) before the pulse arrives. Then even while the pulse is passing, and after it has gone, the particles remain at rest in the coordinate system. (This is true for any metric, such as (35.29a), with $g_{0\mu} = -\delta^0_\mu$, for then $\Gamma^\mu_{00} = 0$, so $x^\mu = \delta^\mu_0 \tau + \text{const.}$ satisfies the geodesic equation.)

Two particles whose separation is in the direction of propagation of the pulse (z -direction) have not only constant coordinate separation, $\Delta x = \Delta y = 0$ and $\Delta z \neq 0$; they also have constant proper separation, $\Delta s = g_{zz}^{1/2} \Delta z = \Delta z$. Hence, the exact plane wave is completely transverse, like a plane wave of linearized theory.

Neighboring particles transverse to the propagation direction, ($\Delta x \neq 0$, $\Delta y \neq 0$, $\Delta z = 0$) have a proper separation that wiggles as the pulse passes:

$$\begin{aligned}\Delta s &= L(t - z)[e^{2\beta(t-z)}(\Delta x)^2 + e^{-2\beta(t-z)}(\Delta y)^2]^{1/2} \\ &\approx L[(1 + 2\beta)(\Delta x)^2 + (1 - 2\beta)(\Delta y)^2]^{1/2}.\end{aligned}\quad (35.38)$$

Superimposed on the usual linearized-theory type of wiggling, due to the “wave factor” β , is a very small net acceleration of the particles toward each other, due to the “background factor” L [note the form of $L(u)$ in Figure 35.3]. This is an acceleration of almost Newtonian type, caused by the gravitational attraction of the energy that the gravitational wave carries between the two particles. The total effect of all the energy that passes is to convert the particles from an initial state of relative rest, to a final state of relative motion with speed

$$v_{\text{final}} = d\Delta s/dt = d(L\Delta s_i)/dt = -\Delta s_i/a,\quad (35.39)$$

where

$$\Delta s_i = [(\Delta x)^2 + (\Delta y)^2]^{1/2} = (\text{initial particle separation}).$$

[Recall: $L_{\text{initial}} = 1$, $L_{\text{final}} = 1 - u/a = 1 - (t - z)/a$; equation (35.33).]

Precisely the same effect can be produced by a pulse of electromagnetic waves (§35.11).

§35.11. COMPARISON OF AN EXACT ELECTROMAGNETIC PLANE WAVE WITH THE GRAVITATIONAL PLANE WAVE

Consider the metric

$$ds^2 = L^2(u)(dx^2 + dy^2) - du dv, \quad \begin{cases} u = t - z \\ v = t + z \end{cases}, \quad (35.40)$$

which is always flat if it satisfies the vacuum Einstein equations ($R_{\mu\nu} = 0$ or $L'' = 0$), and therefore cannot represent a gravitational wave. In this metric the electromagnetic potential

$$\mathbf{A} = A_\mu \mathbf{d}x^\mu = \mathcal{A}(u) \mathbf{d}x \quad (35.41)$$

satisfies Maxwell's equations for arbitrary $\mathcal{A}(u)$. It represents an electromagnetic plane wave analogous to the gravitational plane wave of the last few sections. The only nonzero field components of this wave are

$$F_{ux} = \mathcal{A}', \text{ i.e., } F_{tx} = -F_{zx} = \mathcal{A}'; \quad (35.42)$$

(1) transverse character of relative accelerations

(2) gravitational attraction due to energy in pulse

An electromagnetic plane-wave pulse

so the electric vector oscillates back and forth in the x -direction, the magnetic vector oscillates in the y -direction, and the wave propagates in the z -direction. The stress-energy tensor in x, y, u, v , coordinates has only

$$T_{uu} = (4\pi L^2)^{-1}(\mathcal{A}')^2 \quad (35.43)$$

nonzero.

The Maxwell equations are already satisfied by the potential (35.41) in the background metric (35.40), as the reader can verify. In order to make that metric itself equally acceptable, one need only impose the Einstein equations $G_{\mu\nu} = 8\pi T_{\mu\nu}$. They read [see equation (35.30) with $\beta = 0$]

$$L'' + (4\pi T_{uu})L = 0. \quad (35.44)$$

Electromagnetic plane wave and gravitational plane wave produce same gravitational attractions

This has exactly the form of the equation $L'' + (\beta')^2 L = 0$ for the gravitational plane wave. Consequently, the relative motions of uncharged test particles produced by the “background factor” $L(u)$ are the same whether $L(u) \neq 1$ is produced by the stress-energy of an electromagnetic wave, or by a corresponding gravitational wave with

$$[(\beta')^2/4\pi]_{\text{grav wave}} = [T_{uu}]_{\text{em wave}} = (\mathcal{A}')^2/4\pi L^2. \quad (35.45)$$

The analogy can be made even closer. Decrease the wavelength of the waves, while holding $(\beta')^2/4\pi$ and $(\mathcal{A}')^2/4\pi L^2$ fixed:

$$\langle(\beta')^2/4\pi\rangle = \langle(\mathcal{A}')^2/4\pi L^2\rangle = \text{const}; \quad \lambda \rightarrow 0.$$

In the limit of very small wavelength (i.e., from a viewpoint whose characteristic length is $\gg \lambda$), the two solutions are completely indistinguishable. Their metrics are identical ($\lambda \rightarrow 0$ and $\langle(\beta')^2\rangle = \text{const.}$ imply $\beta \rightarrow 0$), and their jigglings of test particles are too small to be seen. Only their curving up of spacetime ($L \neq 1$) and the associated gravitational pull of their energy are detectable.

§35.12. A NEW VIEWPOINT ON THE EXACT PLANE WAVE

Exact gravitational plane waves reexamined in the language of “short-wave approximation”:

(1) ripples vs. background

The above comparison suggests a viewpoint that was sketched briefly in the introduction to this chapter and in §35.8. Think of the exact gravitational plane-wave solution [Figure 35.3; equations (35.29) and (35.33)] as ripples in the spacetime curvature, described by $\beta(u)$, propagating on a very slightly curved background spacetime, characterized by $L(u)$. The most striking difference between the background and the ripples is not in the magnitude of their spacetime curvatures, but in their characteristic lengths. The ripples have characteristic length

$$\lambda \equiv (\text{typical reduced wavelength, } \lambda/2\pi, \text{ of waves}); \quad (35.46)$$

the background has characteristic length (“radius of curvature of background geometry”)

$$\mathcal{R} \sim |L/L''|^{1/2} \text{inside wave} \sim 1/|\beta'|. \quad (35.47)$$

Recall that λ is somewhat smaller than the pulse length, $2T$. Recall also that $|\beta' T| \ll 1$. Conclude that the characteristic lengths of the “wave factor” and the “background factor” differ greatly:

$$\lambda \ll \mathcal{R}. \quad (35.48)$$

This difference in scales enables one to separate out the background from the ripples.

The ripples are very much smaller in scale ($\lambda \ll \mathcal{R}$) than the background. Nevertheless the local curvature in a ripple is correspondingly larger than the background curvature [equations (35.30), (35.34)]; thus,

$$\begin{aligned} (R^x_{uxu})_{\text{background}} &= (R^y_{uyu})_{\text{background}} = -L''/L \sim 1/\mathcal{R}^2, \\ (R^x_{uxu})_{\text{waves}} &= -(R^y_{uyu})_{\text{waves}} = -\beta'' \sim |\beta'|/\lambda \sim 1/(\lambda\mathcal{R}) \\ &\sim (\mathcal{R}/\lambda)(R^x_{uxu})_{\text{background}}. \end{aligned} \quad (35.49)$$

One is reminded of the mottled surface of an orange!

The metric for the background of the gravitational plane wave is the same as for the electromagnetic one [equation (35.40)]:

$$ds^2 = g_{\mu\nu}^{(B)} dx^\mu dx^\nu = L^2(dx^2 + dy^2) - du dv. \quad (35.50)$$

By comparison with equation (35.29a), one sees that the metric for the full spacetime (background plus ripple) is

$$ds^2 = (g_{\mu\nu}^{(B)} + h_{\mu\nu}) dx^\mu dx^\nu, \quad (35.51)$$

$$h_{xx} = -h_{yy} = 2\beta, \text{ all other } h_{\mu\nu} = 0. \quad (35.52)$$

(Recall, in the region where $\beta \neq 0$, L is very nearly 1.) One can think of the ripples as a transverse, traceless, symmetric tensor field $h_{\mu\nu}$ analogous to the electromagnetic field A_μ , propagating in the background geometry. Just as the electromagnetic field produces the background curvature via

$$G_{uu} = -2L''/L = 8\pi T_{uu},$$

so the gravitational-wave ripples $h_{\mu\nu}$ produce the background curvature via equation (35.31), which one can rewrite as

$$G_{uu}^{(B)} = -2L''/L = 8\pi T_{uu}^{(\text{EFF})}. \quad (35.53)$$

Here

$$T_{uu}^{(\text{EFF})} \equiv \frac{1}{4\pi}(\beta')^2 = \frac{1}{32\pi} h_{jk,u} h_{jk,u} \quad (35.54) \quad (3) \text{ effective stress-energy tensor for ripples}$$

is the “effective stress-energy tensor” for the gravitational waves. Notice that it agrees, except for averaging, with the expression (35.23) that was written down without justification in §35.7.

EXERCISE**Exercise 35.10. PLANE WAVE WITH TWO POLARIZATIONS PRESENT**

The exact plane-wave solution (35.29) has polarization \mathbf{e}_+ . Construct a similar solution, containing two arbitrary amplitudes, $\beta(u)$ and $\gamma(u)$, for polarizations \mathbf{e}_+ and \mathbf{e}_\times . Extend the discussions of §§35.9–35.12 to this solution.

§35.13. THE SHORTWAVE APPROXIMATION

The remainder of this chapter extends the above viewpoint in a rigorous manner to very general gravitational-wave solutions. This extension is called the “shortwave formalism”; it was largely devised by Isaacson (1968a,b), though it was built on foundations laid by Wheeler (1964a) and by Brill and Hartle (1964). Versions that are even more rigorous have been given in the W.K.B. or geometric-optics limit by Choquet-Bruhat (1969), and by MacCallum and Taub (1973).

Foundations for shortwave formalism:

- (1) \mathcal{R} , λ , and \mathcal{A} defined
- (2) demand that $\mathcal{A} \ll 1$ and $\lambda/\mathcal{R} \ll 1$
- (3) split of metric into background plus perturbation; “steady coordinates”

Consider gravitational waves propagating through a *vacuum* background spacetime. As in §35.7, let \mathcal{R} be the typical radius of curvature of the background; let λ and \mathcal{A} be the typical reduced wavelength ($\lambda/2\pi$) and amplitude of the waves; and demand both $\mathcal{A} \ll 1$ and $\lambda/\mathcal{R} \ll 1$. The background curvature might be due entirely to the waves, or partly to waves and partly to nearby matter and nongravitational fields.

The analysis uses a coordinate system closely “tuned” to spacetime in the sense that the metric coefficients can be split into “background” coefficients plus perturbations

$$g_{\mu\nu} = g_{\mu\nu}^{(B)} + h_{\mu\nu} \quad (35.55)$$

with these properties: (1) the amplitude of the perturbation is \mathcal{A}

$$h_{\mu\nu} \lesssim (\text{typical value of } g_{\mu\nu}^{(B)}) \cdot \mathcal{A}; \quad (35.56a)$$

(2) the scale on which $g_{\mu\nu}^{(B)}$ varies is $\gtrsim \mathcal{R}$

$$g_{\mu\nu,\alpha}^{(B)} \lesssim (\text{typical value of } g_{\mu\nu}^{(B)})/\mathcal{R}; \quad (35.56b)$$

(3) the scale on which $h_{\mu\nu}$ varies is $\sim \lambda$

$$h_{\mu\nu,\alpha} \sim (\text{typical value of } h_{\mu\nu})/\lambda. \quad (35.56c)$$

Such coordinates are called “*steady*.”

A rather long computation (exercise 35.11) shows that the Ricci tensor for an expanded metric of the form (35.55) is

$$R_{\mu\nu} = R_{\mu\nu}^{(B)} + R_{\mu\nu}^{(1)}(h) + R_{\mu\nu}^{(2)}(h) + \text{error.} \quad (35.57)$$

$$\text{?} \quad \mathcal{A}/\lambda^2 \quad \mathcal{A}^2/\lambda^2 \quad \mathcal{A}^3/\lambda^2$$

- (4) Split of Ricci curvature tensor

Here a marker (\mathcal{A}/λ^2 , etc.) has been placed under each term to show its typical order of magnitude; $R_{\mu\nu}^{(B)}$ is the Ricci tensor for the background metric $g_{\mu\nu}^{(B)}$; and $R_{\mu\nu}^{(1)}$ and $R_{\mu\nu}^{(2)}$ are expressions defined by

$$R_{\mu\nu}^{(1)}(h) \equiv \frac{1}{2}(-h_{|\mu\nu} - h_{\mu\nu|\alpha}^\alpha + h_{\alpha\mu|\nu}^\alpha + h_{\alpha\nu|\mu}^\alpha), \quad (35.58a)$$

$$\begin{aligned} R_{\mu\nu}^{(2)}(h) \equiv & \frac{1}{2}\left[\frac{1}{2}h_{\alpha\beta|\mu}h^{\alpha\beta|_\nu} + h^{\alpha\beta}(h_{\alpha\beta|\mu\nu} + h_{\mu\nu|\alpha\beta} - h_{\alpha\mu|\nu\beta} - h_{\alpha\nu|\mu\beta})\right. \\ & \left.+ h_{\nu}^{\alpha|\beta}(h_{\alpha\mu|\beta} - h_{\beta\mu|\alpha}) - \left(h^{\alpha\beta|_\beta} - \frac{1}{2}h^{|\alpha}\right)(h_{\alpha\mu|\nu} + h_{\alpha\nu|\mu} - h_{\mu\nu|\alpha})\right]. \end{aligned} \quad (35.58b)$$

In these expressions and everywhere below, indices are raised and lowered with $g_{\mu\nu}^{(B)}$, and an upright line denotes a covariant derivative with respect to $g_{\mu\nu}^{(B)}$ (whereas in Chapter 21 it denoted covariant derivative with respect to 3-geometry).

At the heart of the shortwave formalism is its method for solving the vacuum field equations $R_{\mu\nu} = 0$. One begins by selecting out of expression (35.57) the part linear in the amplitude of the wave \mathcal{A} , and setting it equal to zero. The action of the waves to curve up the background is a nonlinear phenomenon (linearized theory shows no sign of it); so $R_{\mu\nu}^{(B)}$ cannot be linear in \mathcal{A} . Hence, in expression (35.57), $R_{\mu\nu}^{(1)}(h)$ is the only linear term, and it must vanish by itself

$$R_{\mu\nu}^{(1)}(h) = 0. \quad (35.59a)$$

[Of course $h_{\mu\nu}$ may contain nonlinear correction terms—call them $j_{\mu\nu}$ —of order \mathcal{A}^2 , which must not be constrained by this linear equation. They will be determined by (35.59c), below.]

One next splits the remainder of $R_{\mu\nu}$ into a part that is free of ripples—i.e., that varies only on scales far larger than λ (“coarse-grain viewpoint”), and a second part that contains the fluctuations. This split can be accomplished by averaging over several wavelengths (see exercise 35.14 for a precise treatment of the averaging process, also see Choquet-Bruhat (1969) for a class of solutions where such averaging is not required):

$$R_{\mu\nu}^{(B)} + \langle R_{\mu\nu}^{(2)}(h) \rangle + \text{error} = 0 \quad \begin{array}{l} \text{smooth} \\ \text{part} \end{array} \quad (35.59b)$$

$$\begin{array}{ccc} ? & \mathcal{A}^2/\lambda^2 & \mathcal{A}^3/\lambda^2 \\ \nearrow \mathcal{A}^2/\lambda^2 & \mathcal{A}^2/\lambda^2 & \mathcal{A}^3/\lambda^2 \\ R_{\mu\nu}^{(1)}(j) + R_{\mu\nu}^{(2)}(h) - \langle R_{\mu\nu}^{(2)}(h) \rangle + \text{error} = 0 & \begin{array}{l} \text{fluctuating} \\ \text{part} \end{array} \end{array} \quad (35.59c)$$

$\boxed{\text{nonlinear cor-}} \\ \text{rection to } h$

That's all there is to it!—except for reducing the equations to manageable form, and a fuller interpretation of the physics.

Begin with the interpretation.

Split of vacuum field equations into “wave part” ($\propto \mathcal{A}$) plus “coarse-grain part” ($\propto \mathcal{A}^2$ and smooth on scale λ) plus “fluctuational corrections” ($\propto \mathcal{A}^2$ and ripply on scale λ)

Physical interpretation of the three parts of field equations:

- (1) propagation of waves
- (2) production of background curvature by energy of waves; $T_{\mu\nu}^{(\text{GW})}$ defined
- (3) nonlinear self-interaction of waves

Equation (35.59a) is an equation for the propagation of the gravitational waves $h_{\mu\nu}$.

Equation (35.59b) shows how the stress-energy in the waves creates the background curvature. It can be rewritten in the more suggestive form

$$G_{\mu\nu}^{(\text{B})} \equiv R_{\mu\nu}^{(\text{B})} - \frac{1}{2} R^{(\text{B})} g_{\mu\nu}^{(\text{B})} = 8\pi T_{\mu\nu}^{(\text{GW})} \text{ in vacuum,} \quad (35.60)$$

where

$$T_{\mu\nu}^{(\text{GW})} \equiv -\frac{1}{8\pi} \left\{ \langle R_{\mu\nu}^{(2)}(h) \rangle - \frac{1}{2} g_{\mu\nu}^{(\text{B})} \langle R^{(2)}(h) \rangle \right\} \quad (35.61)$$

is the stress-energy tensor for the gravitational waves. Now one sees the origin of the statement in §35.7, that the stress-energy of gravitational waves is well-defined only in a smeared-out sense.

Finally, equation (35.59c) shows how the gravitational waves h generate nonlinear corrections j to themselves (wave-wave scattering, harmonics of the fundamental frequency, etc.). These higher-order effects will not be investigated in this chapter.

EXERCISE

Exercise 35.11. CONNECTION COEFFICIENTS AND CURVATURE TENSORS FOR A PERTURBED METRIC

In a specific coordinate frame of an arbitrary spacetime, write the metric coefficients in covariant representation in the form

$$g_{\mu\nu} = g_{\mu\nu}^{(\text{B})} + h_{\mu\nu}. \quad (35.62a)$$

(At the end of the calculation, one can split $h_{\mu\nu}$ into two parts, $h_{\mu\nu} \rightarrow h_{\mu\nu} + j_{\mu\nu}$; and out of this split obtain the formulas used in the text.) Assume that the typical components of $h_{\mu\nu}$ are much less than those of $g_{\mu\nu}^{(\text{B})}$; so one can expand Christoffel symbols and curvature tensors in $h_{\mu\nu}$. Raise and lower indices of $h_{\mu\nu}$ with $g_{\mu\nu}^{(\text{B})}$; and denote by a “ \parallel ” covariant derivatives relative to $g_{\mu\nu}^{(\text{B})}$ and by a “ $\parallel;$ ” covariant derivatives relative to $g_{\mu\nu}$.

(a) Here $g_{\mu\nu}$ and $g_{\mu\nu}^{(\text{B})}$ can be thought of as two different metrics coexisting in the spacetime manifold. Show that the difference between the corresponding covariant derivatives, $\nabla - \nabla^{(\text{B})} \equiv \mathbf{S}$ —indeed, the difference between any two covariant derivatives!—is a tensor with components

$$S^\mu_{\beta\gamma} = \Gamma^\mu_{\beta\gamma} - \Gamma^{(\text{B})\mu}_{\beta\gamma} \quad (35.62b)$$

[Hint: See part B of Box 10.3.]

(b) Show that

$$g^{\mu\nu} = g^{(\text{B})\mu\nu} - h^{\mu\nu} + h^{\mu\alpha} h_\alpha^\nu - h^{\mu\alpha} h_\alpha^\beta h_\beta^\nu + \dots, \quad (35.62c)$$

and also that

$$g^{\mu\nu} = g^{(\text{B})\mu\nu} - h^{\mu\nu} + h^{\mu\alpha} h_\alpha^\nu - h^{\mu\alpha} h_\alpha^\beta h_{\beta\gamma} g^{\gamma\nu}. \quad (35.62c')$$

(c) By calculating in a local Lorentz frame of $g_{\mu\nu}^{(B)}$ and then transforming back to the original frame, show that

$$S^\mu_{\beta\gamma} = \frac{1}{2} g^{\mu\alpha} (h_{\alpha\beta|\gamma} + h_{\alpha\gamma|\beta} - h_{\beta\gamma|\alpha}), \quad (35.62d)$$

$$R^\alpha_{\beta\gamma\delta} - R^{(B)\alpha}_{\beta\gamma\delta} = S^\alpha_{\beta\gamma|\delta} - S^\alpha_{\beta\gamma|\delta} + S^\alpha_{\mu\gamma} S^\mu_{\beta\delta} - S^\alpha_{\mu\delta} S^\mu_{\beta\gamma}, \quad (35.62e)$$

$$R_{\beta\delta} - R^{(B)}_{\beta\delta} = S^\alpha_{\beta\delta|\alpha} - S^\alpha_{\beta\delta|\alpha} + S^\alpha_{\mu\alpha} S^\mu_{\beta\delta} - S^\alpha_{\mu\delta} S^\mu_{\beta\alpha}. \quad (35.62f)$$

(d) Show that expression (35.62f) reduces to

$$R_{\beta\delta} = R^{(B)}_{\beta\delta} + R^{(1)}_{\beta\delta}(h) + R^{(2)}_{\beta\delta}(h) + \dots \quad (35.62g)$$

where $R^{(1)}$ and $R^{(2)}$ are defined by equations (35.58).

§35.14. EFFECT OF BACKGROUND CURVATURE ON WAVE PROPAGATION

Focus attention on the propagation equation $R_{\mu\nu}^{(1)}(h) = 0$. As in linearized theory, so also here, the propagation is studied more simply in terms of

$$\bar{h}_{\mu\nu} \equiv h_{\mu\nu} - \frac{1}{2} h g_{\mu\nu}^{(B)}, \quad (35.63) \quad \bar{h}_{\mu\nu} \text{ defined}$$

than in terms of $h_{\mu\nu}$. Rewritten in terms of $\bar{h}_{\mu\nu}$, $R_{\mu\nu}^{(1)}(h) = 0$ says

$$\bar{h}_{\mu\nu|\alpha}^\alpha + g_{\mu\nu}^{(B)} \bar{h}_{|\beta\alpha}^\alpha - 2 \bar{h}_{\alpha(\mu}^\alpha \bar{h}_{\nu)\beta} + 2 R_{\alpha\mu\beta\nu}^{(B)} \bar{h}^{\alpha\beta} - 2 R_{\alpha(\mu}^{(B)} \bar{h}_{\nu)\alpha} = 0. \quad (35.64)$$

[To obtain this, invert equation (35.63) obtaining $h_{\mu\nu} = \bar{h}_{\mu\nu} - \frac{1}{2} g_{\mu\nu}^{(B)} \bar{h}$; insert this into (35.58a) and equate to zero; then commute covariant derivatives using the identity (16.6b); finally contract to obtain an expression for $\bar{h}_{|\alpha}^\alpha$ and substitute that back in.]

The propagation equation (35.64) can be simplified by a special choice of gauge. An infinitesimal coordinate transformation

$$x^\mu_{\text{new}}(\mathcal{P}) = x^\mu_{\text{old}}(\mathcal{P}) + \xi^\mu(\mathcal{P}) \quad (35.65a)$$

induces a first-order change in the functional forms of the metric coefficients given by

$$h_{\mu\nu\text{new}}(x^\alpha_{\text{new}}) = h_{\mu\nu\text{old}}(x^\alpha_{\text{new}}) - 2\xi_{(\mu|\nu)} \quad (35.65b)$$

[analog of the gauge transformation of linearized theory, equation (35.3c); see exercise 35.12]. By an appropriate choice of the four functions ξ^μ , one can enforce the four “Lorentz gauge conditions”

$$\bar{h}_{\mu}^{\alpha}{}_{|\alpha} = 0 \quad (35.66)$$

Propagation equation for waves on curved background

Specialization to “Lorentz gauge”

Coupling of waves to Ricci tensor can be ignored

in the new coordinate system (exercise 35.13). This choice of gauge is analogous to that of linearized theory. It makes the second and third terms in the propagation equation vanish. (For additional gauge conditions of the “TT” type, see exercise 35.13.)

The last term of the propagation equation, $-2R_{\alpha(\mu}^{(B)}\bar{h}_{\nu)}^{\alpha}$, vanishes to within the precision of the analysis, for this reason: attention has been confined to vacuum; so the only source of a nonvanishing Ricci tensor is the stress-energy carried by the gravitational waves themselves [equation (35.60)]; hence $R_{\alpha\beta}^{(B)} \sim \mathcal{Q}^2/\lambda^2$ and

$$R_{\alpha(\mu}^{(B)}\bar{h}_{\nu)}^{\alpha} \sim \mathcal{Q}^3/\lambda^2. \quad (35.67)$$

This is of the same order as $R_{\mu\nu}^{(3)}(h)$, the third-order correction to the Ricci tensor, which is far below the precision of the analysis. For consistency in the analysis it will therefore be neglected.

Summary of this section thus far: by choosing a gauge where $\bar{h}_{\mu}^{\alpha}{}_{|\alpha} = 0$, and by discarding terms of higher order than the precision of the analysis, one obtains the vacuum propagation equation

$$\bar{h}_{\mu\nu}{}_{|\alpha}^{\alpha} + 2R_{\alpha\mu\beta\nu}^{(B)}\bar{h}^{\alpha\beta} = 0, \quad (35.68)$$

subject to the Lorentz gauge condition

$$\bar{h}_{\mu\alpha}{}^{|\alpha} = 0.$$

Equation (35.68) is accurate to first order in the amplitude [corrections $\propto \mathcal{Q}^2$ are embodied in equation (35.59c)]; and its accuracy is independent of the ratio λ/\mathcal{R} , as one sees from equations (35.59). Thus, *it can be applied whenever the waves are weak, even if the wavelength is large!*

Lists of effects absent from and contained in propagation equation

All nonlinear interactions of the wave with itself are neglected in this first-order propagation equation. Absent is the mechanism for waves to scatter off each other and off the background curvature that they themselves produce. Also absent are any hints of a change in shape of pulse due to self-interaction as a pulse of waves propagates. There are no signs of the gravitational collapse that one knows must occur when a mass-energy m of gravitational waves gets compressed into a region of size $\lesssim m$. To see all these effects, one must turn to corrections of second order in \mathcal{Q} and higher [e.g., equations (35.59c) and (35.60)].

Actually contained in the propagation equation are all effects due to the linear action of the background curvature on the propagating wave. These effects are explored, for short wavelengths ($\lambda/\mathcal{R} \ll 1$) and for nearly flat wave fronts, in exercises 35.15–35.17 at the end of the chapter. The effects considered include a gravitational redshift of gravitational radiation and gravitational deflection of the direction of propagation of gravitational radiation, identical to those for light; and also a rotation of the polarization tensor. When the wavelength is not small (λ/\mathcal{R} not $\ll 1$), the propagation equation includes a back-scatter of the gravitational waves off the background curvature and a resultant pattern of wave “tails” analogous to that explored in exercise 32.10 [see, e.g., Couch *et al.* (1968), Price (1971a), Bardeen and Press (1972), Unt and Keres (1972)].